ISSN 0021-9673

VOL. 654 NO. 2 NOVEMBER 19, 1993

THIS ISSUE COMPLETES VOL. 654

JOURNAL OF CHROMATOGRAPHY A

INCLUDING ELECTROPHORESIS AND OTHER SEPARATION METHODS

EDITORS
U.A.Th. Brinkman (Amsterdam)
R.W. Giese (Boston, MA)
J.K. Haken (Kensington, N.S.W.)
K. Macek (Prague)
L.R. Snyder (Orinda, CA)

EDITORS, SYMPOSIUM VOLUMES,
E. Heftmann (Orinda, CA), Z. Deyl (Prague)

EDITORIAL BOARD
D.W. Armstrong (Rolla, MO)
W.A. Aue (Halifax)
P. Boček (Brno)
A.A. Boulton (Saskatoon)
P.W. Carr (Minneapolis, MN)
N.H.C. Cooke (San Ramon, CA)
V.A. Davankov (Moscow)
G.J. de Jong (Weesp)
Z. Deyl (Prague)
S. Dilli (Kensington, N.S.W.)
H. Engelhardt (Saarbrücken)
F. Erni (Basle)
M.B. Evans (Hatfield)
J.L. Glajch (N. Billerica, MA)
G.A. Guiochon (Knoxville, TN)
P.R. Haddad (Hobart, Tasmania)
I.M. Hais (Hradec Králové)
W.S. Hancock (San Francisco, CA)
S. Hjertén (Uppsala)
S. Honda (Higashi-Osaka)
Cs. Horváth (New Haven, CT)
J.F.K. Huber (Vienna)
K.-P. Hupe (Waldbronn)
T.W. Hutchens (Houston, TX)
J. Janák (Brno)
P. Jandera (Pardubice)
B.L. Karger (Boston, MA)
J.J. Kirkland (Newport, DE)
E. sz. Kováts (Lausanne)
A.J.P. Martin (Cambridge)
L.W. McLaughlin (Chestnut Hill, MA)
E.D. Morgan (Keele)
J.D. Pearson (Kalamazoo, MI)
H. Poppe (Amsterdam)
F.E. Regnier (West Lafayette, IN)
P.G. Righetti (Milan)
P. Schoenmakers (Eindhoven)
R. Schwarzenbach (Dübendorf)
R.E. Shoup (West Lafayette, IN)
R.P. Singhal (Wichita, KS)
A.M. Siouffi (Marseille)
D.J. Strydom (Boston, MA)
N. Tanaka (Kyoto)
S. Terabe (Hyogo)
K.K. Unger (Mainz)
R. Verpoorte (Leiden)
Gy. Vigh (College Station, TX)
J.T. Watson (East Lansing, MI)
B.D. Westerlund (Uppsala)

EDITORS, BIBLIOGRAPHY SECTION
Z. Deyl (Prague), J. Janák (Brno), V. Schwarz (Prague)

ELSEVIER

JOURNAL OF CHROMATOGRAPHY A

INCLUDING ELECTROPHORESIS AND OTHER SEPARATION METHODS

Scope. The *Journal of Chromatography A* publishes papers on all aspects of **chromatography, electrophoresis** and related methods. Contributions consist mainly of research papers dealing with chromatographic theory, instrumental developments and their applications. In the *Symposium volumes*, which are under separate editorship, proceedings of symposia on chromatography, electrophoresis and related methods are published. *Journal of Chromatography B: Biomedical Applications* —This journal, which is under separate editorship, deals with the following aspects: developments in and applications of chromatographic and electrophoretic techniques related to clinical diagnosis or alterations during medical treatment; screening and profiling of body fluids or tissues related to the analysis of active substances and to metabolic disorders; drug level monitoring and pharmacokinetic studies; clinical toxicology; forensic medicine; veterinary medicine; occupational medicine; results from basic medical research with direct consequences in clinical practice.

Submission of Papers. The preferred medium of submission is on disk with accompanying manuscript (see *Electronic manuscripts* in the Instructions to Authors, which can be obtained from the publisher, Elsevier Science Publishers B.V., P.O. Box 330, 1000 AH Amsterdam, Netherlands). Manuscripts (in English; *four* copies are required) should be submitted to: Editorial Office of *Journal of Chromatography A*, P.O. Box 681, 1000 AR Amsterdam, Netherlands, Telefax (+31-20) 5862 304, or to: The Editor of *Journal of Chromatography B: Biomedical Applications*, P.O. Box 681, 1000 AR Amsterdam, Netherlands. Review articles are invited or proposed in writing to the Editors who welcome suggestions for subjects. An outline of the proposed review should first be forwarded to the Editors for preliminary discussion prior to preparation. Submission of an article is understood to imply that the article is original and unpublished and is not being considered for publication elsewhere. For copyright regulations, see below.

Publication information. *Journal of Chromatography A* (ISSN 0021-9673): for 1994 Vols. 652–682 are scheduled for publication. *Journal of Chromatography B: Biomedical Applications* (ISSN 0378-4347): for 1994 Vols. 652–662 are scheduled for publication. Subscription prices for *Journal of Chromatography A*, *Journal of Chromatography B: Biomedical Applications* or a combined subscription are available upon request from the publisher. Subscriptions are accepted on a prepaid basis only and are entered on a calendar year basis. Issues are sent by surface mail except to the following countries where air delivery via SAL is ensured: Argentina, Australia, Brazil, Canada, China, Hong Kong, India, Israel, Japan, Malaysia, Mexico, New Zealand, Pakistan, Singapore, South Africa, South Korea, Taiwan, Thailand, USA. For all other countries airmail rates are available upon request. Claims for missing issues must be made within six months of our publication (mailing) date. Please address all your requests regarding orders and subscription queries to: Elsevier Science Publishers, Journal Department, P.O. Box 211, 1000 AE Amsterdam, Netherlands. Tel.: (+31-20) 5803 642; Fax: (+31-20) 5803 598. Customers in the USA and Canada wishing information on this and other Elsevier journals, please contact Journal Information Center, Elsevier Science Publishing Co. Inc., 655 Avenue of the Americas, New York, NY 10010, USA, Tel. (+1-212) 633 3750, Telefax (+1-212) 633 3764.

Abstracts/Contents Lists published in Analytical Abstracts, Biochemical Abstracts, Biological Abstracts, Chemical Abstracts, Chemical Titles, Chromatography Abstracts, Current Awareness in Biological Sciences (CABS), Current Contents/Life Sciences, Current Contents/Physical, Chemical & Earth Sciences, Deep-Sea Research/Part B: Oceanographic Literature Review, Excerpta Medica, Index Medicus, Mass Spectrometry Bulletin, PASCAL-CNRS, Referativnyi Zhurnal, Research Alert and Science Citation Index.

US Mailing Notice. *Journal of Chromatography A* (ISSN 0021-9673) is published weekly (total 52 issues) by Elsevier Science Publishers (Sara Burgerhartstraat 25, P.O. Box 211, 1000 AE Amsterdam, Netherlands). Annual subscription price in the USA US$ 5132.25 (US$ price valid in North, Central and South America only) including air speed delivery. Second class postage paid at Jamaica, NY 11431. **USA POSTMASTERS**: Send address changes to *Journal of Chromatography A*, Publications Expediting, Inc., 200 Meacham Avenue, Elmont, NY 11003. Airfreight and mailing in the USA by Publications Expediting.

See inside back cover for Publication Schedule, Information for Authors and information on Advertisements.

© 1993 ELSEVIER SCIENCE PUBLISHERS B.V. All rights reserved.

0021-9673/93/$06.00

No part of this publication may be reproduced, stored in a retrieval system or transmitted in any form or by any means, electronic, mechanical, photocopying, recording or otherwise, without the prior written permission of the publisher, Elsevier Science Publishers B.V., Copyright and Permissions Department, P.O. Box 521, 1000 AM Amsterdam, Netherlands.

Upon acceptance of an article by the journal, the author(s) will be asked to transfer copyright of the article to the publisher. The transfer will ensure the widest possible dissemination of information.

Special regulations for readers in the USA. This journal has been registered with the Copyright Clearance Center, Inc. Consent is given for copying of articles for personal or internal use, or for the personal use of specific clients. This consent is given on the condition that the copier pays through the Center the per-copy fee stated in the code on the first page of each article for copying beyond that permitted by Sections 107 or 108 of the US Copyright Law. The appropriate fee should be forwarded with a copy of the first page of the article to the Copyright Clearance Center, Inc., 27 Congress Street, Salem, MA 01970, USA. If no code appears in an article, the author has not given broad consent to copy and permission to copy must be obtained directly from the author. All articles published prior to 1980 may be copied for a per-copy fee of US$ 2.25, also payable through the Center. This consent does not extend to other kinds of copying, such as for general distribution, resale, advertising and promotion purposes, or for creating new collective works. Special written permission must be obtained from the publisher for such copying.

No responsibility is assumed by the Publisher for any injury and/or damage to persons or property as a matter of products liability, negligence or otherwise, or from any use or operation of any methods, products, instructions or ideas contained in the materials herein. Because of rapid advances in the medical sciences, the Publisher recommends that independent verification of diagnoses and drug dosages should be made.

Although all advertising material is expected to conform to ethical (medical) standards, inclusion in this publication does not constitute a guarantee or endorsement of the quality or value of such product or of the claims made of it by its manufacturer.

This issue is printed on acid-free paper.

Printed in the Netherlands

VOL. 654, NO. 2 JOURNAL OF CHROMATOGRAPHY A NOVEMBER 19, 1993

CONTENTS

(Abstracts/Contents Lists published in Analytical Abstracts, Biochemical Abstracts, Biological Abstracts, Chemical Abstracts, Chemical Titles, Chromatography Abstracts, Current Awareness in Biological Sciences (CABS), Current Contents/Life Sciences, Current Contents/Physical, Chemical & Earth Sciences, Deep-Sea Research/Part B: Oceanographic Literature Review, Excerpta Medica, Index Medicus, Mass Spectrometry Bulletin, PASCAL-CNRS, Referativnyi Zhurnal, Research Alert and Science Citation Index)

REGULAR PAPERS

Column Liquid Chromatography

Gas Chromatography

(Continued overleaf)

ห้องสมุดกรมวิทยาศาสตร์บริการ
14 S.A. 2536

Contents (continued)

SHORT COMMUNICATIONS

Column Liquid Chromatography

Gas Chromatography

Journal of Chromatography A, 654 (1993) 197–205
Elsevier Science Publishers B.V., Amsterdam

CHROMSYMP. 2923

Model for the mixed ion-exclusion–adsorption retention mechanism in ion-exclusion chromatography☆

Bronisław K. Głód* and Janusz Stafiej

Polish Academy of Sciences, Institute of Physical Chemistry, Kasprzaka 44/52, 01-224 Warsaw (Poland)

(Received September 20th, 1992)

ABSTRACT

The model elaborated in a previous paper for the retention mechanism in ion-exclusion chromatography was generalized to include adsorption of the solute. The computer modelling of the column performance by the Craig method was used in the case of an unbuffered mobile phase. The retention process in the case of a sufficiently buffered mobile phase turned out to be governed by a linear partition isotherm and can be described globally by simple equations. The adsorption constants of several compounds were calculated from the data available in the literature.

INTRODUCTION

Ion-exclusion chromatography (IEC) is an efficient method for the separation of partially ionized species [1–12]. The ion-exclusion mechanism of solute retention is based on the phenomenon that neutral molecules penetrate the ion-exchange resin while the counter ions with respect to the exchanged ion are repulsed or, in other words, excluded from it [1]. Therefore, by this mechanism acidic compounds can be separated on cation-exchange resins and basic compounds on anion-exchange resins. This is the opposite situation to ion-exchange chromatography, where an anion-exchange resin is used to separate anions and a cation-exchange resin to separate cations.

Tanaka *et al.* [13] have shown for a cation-exchange resin that the dependence of the distribution coefficient, K_d, on the pK_a values of various acidic compounds is analogous to the dependence of K_d on the logarithm of the molecular mass in size-exclusion chromatography. They interpreted this as evidence for an ion-exclusion mechanism of acidic solutes separated on a cation-exchange resin.

A more quantitative description of these findings was attempted in a previous paper [14], where the following equation was derived:

$$K_d = \frac{1 + 2c/K_a - \sqrt{1 + 8c/K_a}}{2c/K_a - 2} \quad (1)$$

This equation expresses the distribution coefficient as a function of the solute acidic dissociation constant and the solute concentration at the peak maximum, c.

Eqn. 1 is inconvenient from the analytical point of view because the solute concentration at the peak maxium is not easy to determine and one would prefer the analytical solute concentration instead [14]. Also, the simplifications involved in eqn. 1 are not generally justifiable [15].

The improved approach in ref. 15 removes the inconvenience and some of the simplifications. The price to pay for the improvements is that the

* Corresponding author.

☆ Presented at the *International Ion Chromatography Symposium 1992, Linz, September 21–24, 1992.* The majority of the papers presented at this symposium were published in *J. Chromatogr.*, Vol. 640 (1993).

0021-9673/93/$06.00 © 1993 Elsevier Science Publishers B.V. All rights reserved

distribution coefficient can only be evaluated numerically from a non-linear set of equations as an implicit function of the parameters characterizing the system. In general, the solution of the equations cannot be obtained as explicit expressions in a closed form. The equations describe the partitioning of an amount of the solute between specified amounts of the mobile and the stationary phases. The set of equations can be applied locally to a small fragment of the column (corresponding to a theoretical plate) or globally to the peak volume of the solute. The global approach is unjustified for a non-linear partition isotherm. Then the local approach can be conveniently applied in the computer simulation using the Craig method.

Ion exclusion can seldom be considered as the sole retention mechanism even on an ion-exclusion resin [16,17]. Ion-exclusion chromatography, like other chromatographic techniques, is classified according to the primary mechanism of solute retention. The primary mechanism is the coulombic repulsion between the solute ions and the dissociated groups of the resin. However, the fact that there are secondary retention mechanisms is well known. This is especially true for neutral, large molecules, which include aromatic and long-chain aliphatic compounds [18]. Non-ionized solutes cannot be ion excluded and other interactions of the solute with the stationary phase [16–18] have to be considered. The completely non-ionized solutes are just a limiting case for the weakest electrolytes where these interactions co-exist with the ion-exclusion mechanism. Referring to the interactions causing an increase in the solute retention as compared with the ion-exclusion mechanism, we shall tentatively use the term adsorption. We should like to avoid speculation on the nature of this adsorption and focus attention on a tentative phenomenological description instead. It is worth noting, however, that the hydrophobic nature of this interaction for long-chain aliphatic compounds finds support in the literature [18,19]. It has also been found [18] that aromatic compounds are characterized by especially large adsorption, probably caused by their π-electron interaction with the network of the polystyrene–divinylbenzene resin.

The retention of partially ionized organic compounds with a mixed ion-exclusion–adsorption mechanism is expected to be involved in most practical applications of ion-exclusion chromatography. Therefore, in this paper we attempt to include adsorption phenomena in the framework of the models devised initially to describe a pure ion-exclusion mechanism.

Similar attempts can be found in the recent literature [20,21], but the different volumes of the stationary and the mobile phases were not taken into account and also the predictions of the models were applied to dicarboxylic acids. In our option, dicarboxylic acids are an unfortunate choice for a test of a model for an ion-exclusion mechanism owing to the additional complications in their retention mechanism such as size-exclusion and shielding effects [18].

THEORY

Model formulation

The chromatographic column will be considered as a uniform, homogeneous mixture of the eluent and the support. The mobile phase flow-rate is assumed to be constant and also uniformly distributed within the column.

The ion-exclusion mechanism is ruled by the Donnan membrane equilibrium as described previously [14,15]. The partitioning of the solute due to this mechanism takes place between the stationary and mobile phases. Both phases contain solvents with identical physico-chemical parameters, including dielectric constants. The stationary phase is regarded as a solution of resin functional groups immobilized by the resin network. The immobilized functional groups cannot enter the mobile phase. We shall also assume that the resin functional groups are completely dissociated and their concentration is much higher than that of the solute. These are reasonable assumptions for typical analytical conditions. As found previously [15], they make the parameters describing the chromatographic peak independent of the resin functional group concentration and their dissociation constant.

Under the above assumptions, only undissociated forms of the solutes exist in the stationary phase and can be adsorbed from there into

what we call the adsorption volume. The existence of an adsorption phase filling the adsorption volume is postulated. A linear isotherm is assumed to govern the adsorption mechanism. The adsorption volume, the stationary phase volume and the mobile phase volume are assumed to add up to the geometrical volume of the column. The stationary phase and the mobile phase volumes are identified with the inner and the dead column volumes, respectively.

The equilibration after the repartitioning of the analyte solute is assumed to be fast enough to be able to neglect kinetic effects, diffusion, temperature changes and other non-equilibrium effects.

A buffered mobile phase is also considered in the case of complete buffer dissociation and its concentration is much higher than that of the solute compound.

Equations describing the system

The assumptions outlined above lead to a set of equations analogous to eqns. 2–10 in ref. [15] for the case of a pure aqueous mobile phase. The first equation in the set expresses the thermodynamic equilibrium condition for the case of solute concentrations low enough to substitute concentrations for activities:

$$[H^+]_M[R^-]_M[HR]_M = [H^+]_S[R^-]_S[HR]_S \quad (2)$$

The definition of the acidic dissociation constant is

$$K_a = [H^+]_M[R^-]_M/[HR]_M \quad (3)$$

The mobile and stationary phases are characterized by equal concentrations of the neutral form of the solute:

$$[HR]_M = [HR]_S \quad (4)$$

The mobile and stationary phases are electrically neutral. It follows that

$$[H^+]_M = [R^-]_M \quad (5)$$

$$[H^+]_S = [F^-]_S + [R^-]_S \quad (6)$$

As the resin functional groups are completely dissociated, their concentration in the stationary phase can be expressed as follows:

$$c_f = [F^-]_S \quad (7)$$

The mass conservation equation for the amount m of the acidic compound on a theoretical plate distributed in the mobile, the stationary and the adsorption phase volumes is

$$m = ([R^-]_M + [HR]_M)v_M + ([R^-]_S + [HR]_S)v_S + [HR]_A v_A \quad (8)$$

From now on we shall assume that $[R^-]_S = 0$, which follows from the already assumed excess of functional group concentration with respect to the concentration of the solute.

The neutral form of the solute is assumed to be partitioned between the stationary and the adsorption phases according to the Nernstian law or, equivalently, according to the linear Henry isotherm. This is expressed as

$$[HR]_A = K_H[HR]_S \quad (9)$$

where K_H is a constant.

Solution method

Eqns. 2–9, after some algebra, yield the following set of equations:

$$[R^-]_M = \frac{\sqrt{[K_a^2V_M^2 + 4K_am(V_M + V_S + K_HV_A)]}}{2(V_M + V_S + K_HV_A)} \quad (10)$$

$$[HR]_M = [R^-]_M^2/K_a \quad (11)$$

$$[HR]_A = K_H[HR]_M \quad (12)$$

The above equations express the three concentrations $[R^-]_M$, $[HR]_M$ and $[HR]_A$ as functions of the parameters K_a, m, V_M, V_S and the product K_HV_A in an explicit form. Eqn. 11 is analogous to the set of eqns. 19–21 in ref. 15. The set of equations in ref. 15 cannot be solved in so simple a way and require a time-consuming recurrent numerical procedure to calculate $[R^-]_M$ as an implicit function of the parameters. The closed form of eqn. 10 yields a significant time decrease in the computer simulation described below and it is based on the assumption that $[R^-]_S = 0$, which is reasonable under analytical conditions.

Numerical modelling of column performance with unbuffered mobile phase

We use the Craig method in a fashion fully analogous to that in our previous paper [15]. The Craig method turns out to yield improved results with respect to K_d values as compared with the global approach [15]. It also yields correct predictions with regard to the peak shape [15]. We use it in the case of an unbuffered mobile phase when the non-linear partition isotherm invalidates the use of the global approach.

Let us briefly recall that in this method the partitioning of the solute is calculated using eqns. 10–12 for a small fragment of the column corresponding to a theoretical plate. The portion of the mobile phase at the plate is then "moved" to the next plate, simulating the passage of the solute. The mass conservation balance requires that the amount of solute at the plate is composed of what remains in the stationary and the adsorption phases plus what is brought by the incoming portion of the mobile phase. The solute amount is then repartitioned again, closing the cycle. The procedure implies that the equation

$$m(i, j) = ([R^-]_M^{(i-1,j-1)} + [HR]_M^{(i-1,j-1)})v_M + [HR]_S^{(i-1,j)}v_S + [HR]_A^{(i-1,j)}v_A \quad (13)$$

is solved at the ith time step and the jth plate with the following initial and boundary conditions:

$$[HR]_S^{0,j)} = [HR]_A^{(0,j)} = [HR]_M^{(0,j)} = [R^-]_M^{(0,j)} = 0 \quad \text{for } i = 1, \ldots, N \quad (14)$$

$$([R^-]_M^{(i,0)} + [HR]_M^{(i,0)}) = c_i \quad \text{for } i = 1, \ldots, V_i/v_m \quad (15)$$

$$([R^-]_M^{(i,0)} + [HR]_M^{(i,0)}) = 0 \quad \text{for } i > V_i/v_m \quad (16)$$

Buffered mobile phase

The consideration of the buffered mobile phase in our previous paper [15] led to considerable complication of the equations. However, the buffered mobile phase turns out to be particularly interesting and simple to analyse when the buffer concentration is much higher than that of the solute. Then eqn. 3 assumes the form

$$K_a = c_b[R^-]_M/[HR]_M \quad (17)$$

where c_b is the buffer concentration. This leads to the linear distribution isotherm and the distribution coefficient K_d is given by

$$K_d = \frac{[HR]_S V_S + [HR]_A V_A}{([HR]_M + [R^-]_M)V_M} = \frac{V_S + K_H V_A}{(1 + K_a/c_b)V_S} \quad (18)$$

When there is no adsorption ($K_H V_A = 0$) then the above equation assumes a simpler form:

$$K_d = \frac{c_b}{c_b + K_a} \quad (19)$$

It is worth noting that the peak shape remains unchanged during elution when the partition isotherm is linear, as in the considered case of excess of buffer with respect to the solute compound in IEC. The peak migrates down the column with the effective velocity U_a lower than the mobile phase velocity u:

$$U_a = u/(1 + V_S/V_M + K_H V_A/V_M + K_a/c_b) \quad (20)$$

RESULTS

Assessment of assumed simplifications

As mentioned in the previous section, the simple form of eqn. 11 used in the simulations is due to the assumed excess of dissociated resin functional groups when the dissociated form of the acid is practically excluded from the resin: $[R^-]_S = 0$. Mathematically, eqn. 11 is strict in the limit of infinite functional group concentration ($c_f \to \infty$) with an arbitrary non-vanishing dissociation constant for the groups ($K_f > 0$).

In order to assess the practical validity of the discussed assumption, computer simulations were performed for several pK_a values of the acidic solute excluding adsorption. The results are presented in the form of simulated peak profiles in Fig. 1. The simulated peak profiles are almost identical with those obtained previously [15] for the same set of pK_a values and for finite, reasonable values of c_f and K_f (see Fig. 9 in ref.

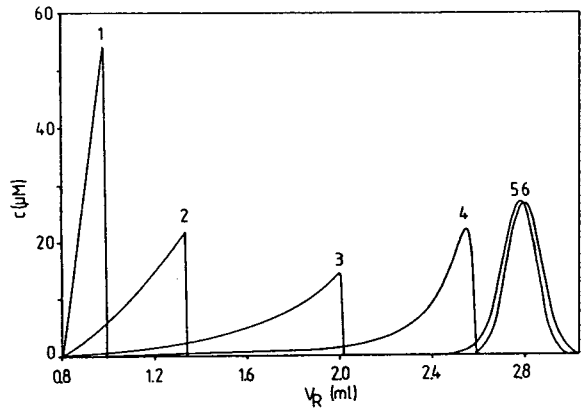

Fig. 1. Simulated chromatographic peaks of acidic compounds in an unbuffered mobile phase. The pK_a values of the compounds represented by peaks 1, 2, 3, 4, 5 and 6 are 3, 4, 5, 6, 8 and 12 respectively. The values of the other parameters are $c_i = 10^{-3}$ M, $V_M = 800$ μl, $V_S = 2000$ μl, $V_i = 5$ μl, $N = 1000$ and $K_H = 0$.

15). The assumption is therefore valid under working chromatographic conditions.

The validity of eqn. 20 can be assessed in a similar way for the dependences of the distribution coefficient on the acid dissociation constant and on the buffer concentration. These dependences are presented in Figs. 2 and 3, respectively. Again, it is worth noting that although based on a very simple, easy to use equation, the results in Figs. 2 and 3 are close to the analogous results obtained previously using a more general and therefore unduly complicated approach (see Figs. 4 and 8 in ref. 15).

Adsorption evaluation

Having shown the practical validity of the assumptions used when deriving eqns. 10 and 19, let us consider how they could be applied in chromatographic data evaluation. From eqn. 10, it follows that the solute retention depends on the product $K_H V_A$. The product can be resolved into the factors on the basis of some extra assumption such as additivity: $V_M + V_S + V_A = V$, where $V = \pi d_c^2 l_c$ is the geometrical volume of the column cavity calculated from its dimensions, *i.e.*, the inner column diameter d_c and the column length l_c.

An example of the dependence of V_R on $K_H V_A$ is presented in Fig. 4 for the pK_a value as for

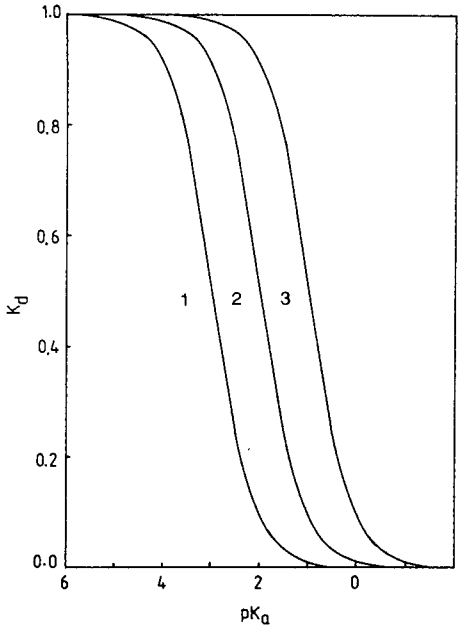

Fig. 2. Distribution coefficient K_d as a function of the solute pK_a value for the following mobile phase buffer concentrations: (1) $c_b = 10^{-3}$ M, (2) $c_b = 10^{-2}$ M and (3) $c_b = 10^{-1}$ M.

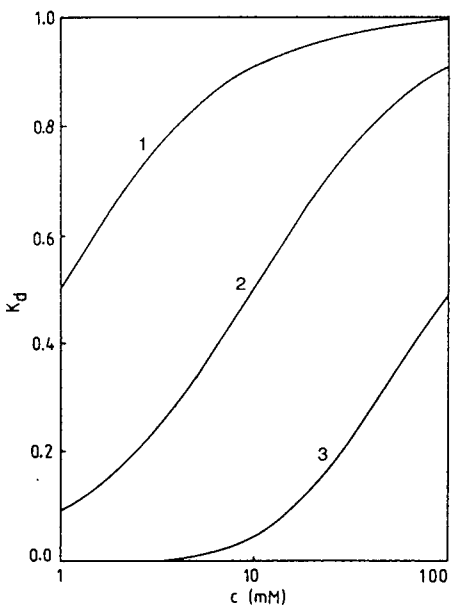

Fig. 3. Distribution coefficient K_d as a function of the buffer concentration for the following solute K_a values: (1) 10^{-3} M, (2) 10^{-2} M and (3) 10^{-1} M.

ห้องสมุด

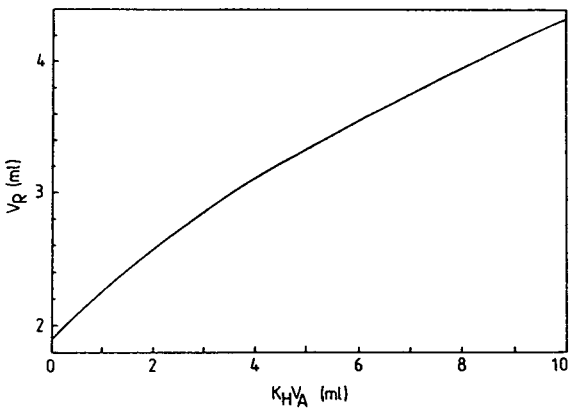

Fig. 4. Retention volume V_R as a function of the solute adsorption strength K_HV_A. $pK_a = 4.48$ is selected as for valeric acid. Other conditions as in Fig. 1.

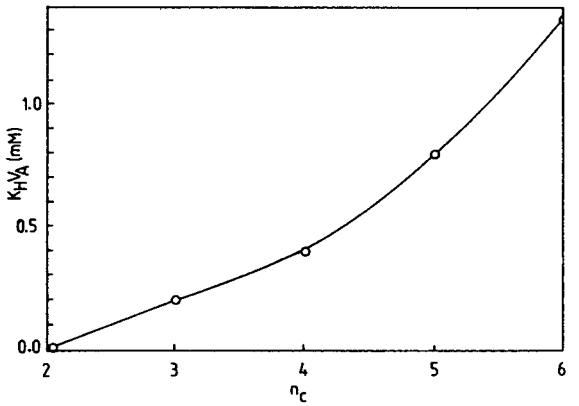

Fig. 5. Adsorption strength as expressed by K_HV_A for a number of aliphatic acids as a function of the number of carbon atoms n_c in the acid chain.

valeric acid. The dependence can be used conversely to determine the K_HV_A product from the experimentally determined retention volume V_R.

Table I presents adsorption constants calculated on the basis of our data [14] for a number of aliphatic acids using the Craig method. The retention volumes based on the calculations and obtained experimentally are also given in Table I. The data indicate an increase in adsorption with increasing chain length. This is illustrated in Fig. 5, where the adsorption strength as measured by K_HV_A is plotted as a function of the chain length. This behaviour of the aliphatic acids has been confirmed recently [18,19,22].

The results for the peak shapes presented in Fig. 6 indicate that the significant increase in the

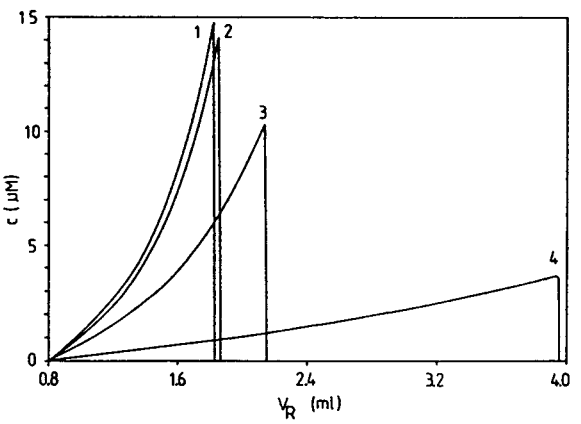

Fig. 6. Simulated peak shapes for K_HV_A values of (1) 0, (2) 10^{-7}, (3) 10^{-6} and (4) 10^{-5} ml. The pK_a value is 4.76; other conditions as in Fig. 1.

TABLE I

EXPERIMENTALLY DETERMINED RETENTION VOLUMES, $V_R^{exp.}$ [14], COMPARED WITH THOSE CALCULATED ASSUMING A PURE ION-EXCLUSION MECHANISM, $V_R^{calc.}$, AND THE ADSORPTION STRENGTH AS EXPRESSED BY K_HV_A CALCULATED USING CRAIG METHOD FOR SOME VOLATILE FATTY ACIDS

Acid	pK_a	$V_R^{exp.}$ (ml)	$V_R^{calc.}$ (ml)	K_HV_A (ml)
Acetic	4.76	1.51	1.51	0.0
Propionic	4.87	1.66	1.59	$2.0 \cdot 10^{-7}$
Butyric	4.81	1.66	1.55	$3.0 \cdot 10^{-7}$
Valeric	4.84	1.84	1.57	$8.0 \cdot 10^{-7}$
Caproic	4.88	2.09	1.60	$13.5 \cdot 10^{-7}$

TABLE II

ADSORPTION STRENGTH AS MEASURED BY $K_H V_A$ CALCULATED FROM THE DATA IN REF. 3 FOR SOME ALIPHATIC ALCOHOLS

Alcohol	$K_H V_A \times 10^3$ (ml)	Alcohol	$K_H V_A \times 10^3$ (ml)
Methanol	0.0	*n*-Butanol	57.0
Ethanol	3.6	*sec.*-Butanol	28.3
n-Propanol	15.0	*tert.*-Butanol	11.9
Isopropanol	8.16		

retention volume due to the strong adsorption coincides with an increased asymmetry of the peak shape. This effect has also been observed experimentally [17,23].

Analogous calculations were performed for the homologous series of aliphatic alcohols on the basis of the experimental data from ref. 3. Table II gives the estimated products $K_H V_A$. They turned out to be identical with those calculated using eqn. 18. The simulated peak shapes are presented in Fig. 7. Again, good agreement with the experimental data is found.

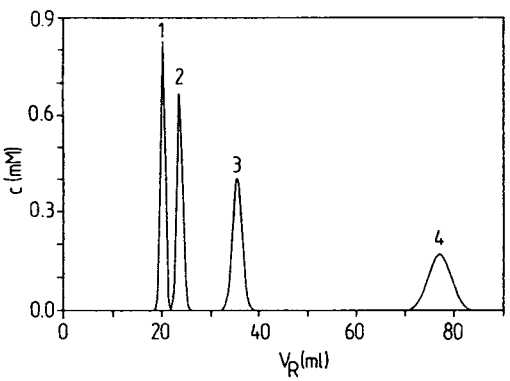

Fig. 7. Simulated chromatographic peaks of alcohols: (1) methanol; (2) ethanol; (3) propanol; (4) butanol. The chromatographic parameters are those given in ref. 3.

Tables III and IV give the experimental and calculated retention volumes and adsorption constants K_H based on recently collected data for a number of aromatic acids and amines, respectively, in buffered mobile phases [18,22]. The calculations of retention volumes and adsorption constants were based on eqns. 18 and 19. Aromatic compounds are characterized by very strong adsorption and it is the adsorption that governs the retention mechanism for these compounds rather than ion exclusion on ion-exchange resins.

CONCLUSIONS

Adsorption, although considered a secondary mechanism in ion-exclusion chromatography, in many instances plays the dominant role in the retention of the solutes. The retention mechanism of weakly dissociated organic compounds on an ion-exclusion resin has to be interpreted as a combination of ion exclusion and adsorption on the resin network. The adsorption contributes little to the retention of ions. However, it has a large effect on the retention of weakly ionized solutes. To describe this effect the model presented in this paper can be applied.

The computer simulations based on the model yield qualitatively correct peak shapes as in-

TABLE III

EXPERIMENTALLY DETERMINED RETENTION VOLUMES, $V_R^{exp.}$ [18], COMPARED WITH THOSE CALCULATED ASSUMING A PURE ION-EXCLUSION MECHANISM (EQN. 19), $V_R^{calc.}$, AND THE ADSORPTION STRENGTH AS MEASURED BY $K_H V_A$ CALCULATED USING THE GLOBAL APPROACH (EQN. 18) FOR SOME AROMATIC CARBOXYLIC ACIDS

Acid	K_a	$V_R^{exp.}$ (ml)	$V_R^{calc.}$ (ml)	$K_H V_A$ (ml)
Gallic	$3.89 \cdot 10^{-5}$	13.5	12.3	1.3
o-Nitrobenzoic	$6.76 \cdot 10^{-3}$	15.5	4.6	84.0
Acetylsalicylic	$2.69 \cdot 10^{-5}$	23.0	12.4	10.9
Salicylic	$1.00 \cdot 10^{-3}$	43.0	8.0	69.9
m-Nitrobenzoic	$3.24 \cdot 10^{-4}$	70.0	10.4	78.9

TABLE IV

EXPERIMENTALLY DETERMINED RETENTION VOLUMES, $V_R^{exp.}$ [18], COMPARED WITH THOSE CALCULATED ASSUMING A PURE ION-EXCLUSION MECHANISM (EQN. 19), $V_R^{calc.}$, AND THE ADSORPTION STRENGTH AS MEASURED BY $K_H V_A$ CALCULATED USING THE GLOBAL APPROACH (EQN. 18) FOR SOME AROMATIC AMINES

Compound	pK_b	$V_R^{exp.}$ (ml)	$V_R^{calc.}$ (ml)	$K_H V_A$ (ml)
Pyridine	8.75	22.4	13.4	11.4
3-Aminopyridine	8.00	27.4	13.4	17.7
α-Picoline	8.08	33.0	13.4	25.3
4-Aminopyridine	4.89	35.0	13.27	12.2
γ-Picoline	7.92	39.4	13.4	33.0
β-Picoline	8.48	41.8	13.4	35.6
2, 6-Lutidine	7.28	51.4	13.4	48.2
2, 4-Lutidine	7.01	66.4	13.4	67.3
2, 3-Lutidine	7.43	66.9	13.4	68.5
3, 4-Lutidine	7.51	81.8	13.4	86.2
3, 5-Lutidine	7.85	97.1	13.4	106.5
p-Aminoaniline	7.84	19.6	13.4	7.8
o-Aminoaniline	9.51	70.8	13.4	72.3
Aniline	9.39	114.0	13.4	126.8
p-Methylaniline	8.89	200.9	13.4	241.0
o-Methylaniline	9.56	206.7	13.4	241.0
m-Methylaniline	8.30	223.2	13.4	266.3
4, 6-Dimethylaniline	9.11	394.3	13.4	482.0
3, 5-Dimethylaniline	9.11	456.2	13.4	558.1
Benzylamine	4.67	49.1	13.2	46.9
2-Phenylethylbenzylamine	4.16	84.6	12.7	97.6
o-Benzylamine	4.81	87.1	13.2	95.1
p-Benzylamine	4.64	104.9	13.2	119.3

fluenced by the adsorption mechanism. It is worth emphasizing that the simplifications introduced in this paper are justifiable under working chromatographic conditions and lead to very simple equations describing the chromatographic process. They lead to a 20-fold decrease in computing time when applied to the computer simulations described previously [15]. The equations are particularly simple in the case of mobile phases with a sufficiently concentrated buffer where a linear partition isotherm obtains.

SYMBOLS

A as a subscript refers to the adsorption phase
c_b mobile phase buffer concentration
c_f functional group concentration in the support
c_i injected solute concentration
d_c column diameter
HF (F^-) functional group in undissociated (dissociated) form
HR (R^-) acidic solute in undissociated (dissociated) form
K_a solute acid dissociation constant
K_d distribution coefficient
K_f resin functional group dissociation constant
K_H Henry's isotherm adsorption constant
l_c column length
m solute mass on one theoretical plate
N column theoretical plate number
U_a effective linear velocity of the solute compound
u linear velocity of the mobile phase
V column volume
v_A $= V_A/N$
V_A volume of the adsorbed layer on one theoretical plate

V_i	injected solute volume
V_M	column dead volume, column mobile phase volume
v_M	$= V_M/N$
V_R	retention volume
V_S	column inner volume, column stationary phase volume
v_S	$= V_S/N$

REFERENCES

1 R.H. Wheaton and W.C Bauman, *Ind. Eng. Chem.*, 45 (1953) 238.
2 G.A. Harlow and D.H. Morman, *Anal. Chem.*, 36 (1964) 2438.
3 K. Tanaka and J.S. Fritz, *J. Chromatogr.*, 409 (1987) 271.
4 D.T. Gjerde and J.S. Fritz, *Ion Chromatography*, Hüthig, Heidelberg, 2nd ed., 1987, pp. 235–251.
5 W. Czerwinski, *Chem. Anal. (Warsaw)*, 12 (1967) 597.
6 S.L. Bafna, M.B. Patel, M.C. Dosni and S.S. Kazi, *J. Chromatogr.*, 201 (1980) 131.
7 E. Rajakyla, *J. Chromatogr.*, 218 (1981) 695.
8 K. Tanaka and J.S. Fritz, *Anal. Chem.*, 59 (1987) 708.
9 T. Okada and P.K. Dasgupta, *Anal. Chem.*, 61 (1989) 548.
10 P.E. Buell and J.E. Girard, in J.G. Tarter (Editor), *Ion Chromatography*, Marcel Dekker, New York, 1987, pp. 157–190.
11 F.C. Smith and R.C. Chang, *The Practice of Ion Chromatography*, Wiley, New York, 1983, pp. 34–35.
12 J. Chen and J.S. Fritz, *J. Chromatogr.*, 482 (1989) 279.
13 K. Tanaka, T. Ishizuka and H. Sunahara, *J. Chromatogr.*, 174 (1979) 153.
14 B.K. Głód and W. Kemula, *J. Chromatogr.*, 366 (1986) 39.
15 B.K. Głód, A. Piasecki and J. Stafiej, *J. Chromatogr.*, 457 (1988) 43.
16 B.K. Głód and P.R. Haddad, unpublished results.
17 K. Tanaka and J.S. Fritz, *J. Chromatogr.*, 361 (1987) 151.
18 F. Hao, P.R. Haddad and B.K. Głód, unpublished results.
19 E. Papp and P. Keresztes, *J. Chromatogr.*, 506 (1990) 157.
20 G.L. Zhao and L.N. Liu, *Chromatographia*, 32 (1991) 453.
21 G.L. Zhao, Z.G. Liu and Z.S. Zhang, *Yingyong Huaxue*, 6 (1989) 95; *C.A.*, 112 (1990) 12426n.
22 B.K. Głód, P.W. Alexander and R.R. Haddad, in preparation.
23 W. Rich, F. Smith, L. Maneil and T. Sidebottom, in P. Jandik and R.M. Cassidy (Editors), *Advances in Ion Chromatography*, Vol. 2, Ann Arbor Sci. Publ., Ann Arbor, MI, 1988, pp. 17–29.

Journal of Chromatography A, 654 (1993) 207–213
Elsevier Science Publishers B.V., Amsterdam

CHROM. 25 494

Chiral high-performance liquid chromatography of some related bicyclic lactams

Patrick Camilleri*
SmithKline Beecham, The Frythe, Welwyn, Hertfordshire AL6 9AR (UK)

Drake Eggleston
SmithKline Beecham, 709 Swedeland Road, King of Prussia, PA 19406-2799 (USA)

Carlo Farina☆
SB Farmaceutici SpA, Via Zambelletti, 20021 Baranzate, Milan (Italy)

Jose A. Murphy
SmithKline Beecham, The Frythe, Welwyn, Hertfordshire AL6 9AR (UK)

Ugo Pfeiffer and Mario Pinza☆☆
SB Farmaceutici SpA, Via Zambelletti, 20021 Baranzate, Milan (Italy)

Lesley A. Senior
SmithKline Beecham, The Frythe, Welwyn, Hertfordshire AL6 9AR (UK)

(First received May 14th, 1993; revised manuscript received August 16th, 1993)

ABSTRACT

Chromatographic methods utilising a Chiralcel OC cellulose-based column were developed for the chiral resolution of optical isomers of the cognition-enhancing ISF 4185 and related bicyclic lactams. These methods were scaled up for the preparation of purified samples of enantiomers, one pair of which was submitted to X-ray analysis. The resolution of the enantiomers derived from these compounds appears to be mainly dependent on their ability to hydrogen bond to the chiral stationary phase.

INTRODUCTION

2,5-Dioxohexahydro-1*H*-pyrrolo[1,2-*a*] imidazole (ISF 4185) (**1**) is currently being developed as Dimiracetam by ISF (Milan, Italy) because of its potency as a cognition enhancer [1]. The therapeutic efficacy of compounds of this class has been demonstrated [2] in the case of oxiracetam (**2**), a derivative of γ-amino-β-hydroxybutyric acid (GABOB). Both **1** and **2** contain an asymmetric centre (denoted by an asterisk) so that each molecule can exist in two enantiomeric forms.

* Corresponding author.
☆ Present address: F.lli Lamberti SpA, Via Piare 1, Albizzate, Varese, Italy.
☆☆ Present address: Istituto Ricerca F. Angelini SpA, Piazzole della Staziona, 00040 Pomezia, Rome, Italy.

0021-9673/93/$06.00 © 1993 Elsevier Science Publishers B.V. All rights reserved

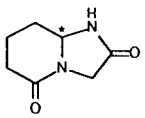

(1)

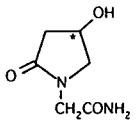

(2)

We reported previously the separation of the enantiomers of **2** using a Chiralcel OC column [3]. In this study, we analysed the chromatographic behaviour of **1** and a number of structurally related molecules. Pure samples of the enantiomers of one of the lactams were also chromatographically prepared for the determination of its absolute configuration by X-ray analysis.

EXPERIMENTAL

Materials and reagents

All compounds used were greater than 99% pure and were used without further purification. *n*-Hexane (Rathburn Chemicals), 2-propanol (BDH) and chloroform (May and Baker) were degassed with helium before use.

High-performance liquid chromatography

The HPLC pump system used was either a Gilson Model 303 or a Perkin-Elmer Series 3B or Series 4. Samples were injected with a Perkin-Elmer ISS-100 autoinjector or a Rheodyne Model 7125 manual injector and detected using a Gilson HM/Holochrome or a Perkin-Elmer LC90 variable-wavelength detector. Chromatographic peaks were injected using either the Perkin-Elmer LIMS 2000/CLAS or the Nelson 2600 data systems.

For the analytical separations a Chiralcel OC column (250 mm × 4.6 mm I.D.), supplied by Daicel, was used. Preparative separations were carried out on a Chiralcel OC column (250 mm × 10 mm I.D.). The mobile phase for chiral resolution consisted of various amounts of hexane and 2-propanol at flow-rates between 1 and 4 ml min^{-1}. Compounds were injected on to the column at a concentration of about 1 mg ml^{-1} in the mobile phase. The temperature for these chiral separations was ambient. UV detection was at 205 or 210 nm.

Polarimetry

In order to determine the enantiomeric composition of the separated enantiomers, their specific rotation, $[\alpha]_D^{25}$, was measured using a Perkin-Elmer Model 241 polarimeter set at a wavelength of 589 nm (sodium D-line). Optical rotation was determined in a cell of 100 mm path length. Compounds were dissolved in methanol at a concentration of 1 mg ml^{-1}.

X-Ray diffraction

Three-dimensional X-ray diffraction data were collected for each compound on an Enraf-Nonius CAD-4 diffractor equipped with incident beam graphite monochromated copper radiation. Preliminary crystal examination and the data collection set-up were the same for each sample. The crystal was mounted with epoxy on glass-fibre and centred optically on the goniostat of the diffractometer. Preliminary lattice parameters were obtained either through a random search of reciprocal space or by use of a rotation photograph from which diffraction spots were measured.

After attaining a preliminary cell the diffraction symmetry was checked and the crystal quality was assessed using a plot of intensities for several axial reflections in the plane of the scanning monitors θ and ω. A small shell of higher order data was then collected rapidly in order to assess the diffraction range and to select 25 reflections well distributed in reciprocal space which were accurately centred to provide the final lattice parameters. Intensity data were then collected using variable-speed $\omega - 2\theta$ scans with the final scan speed selected according to the diffraction of any given reflection based on a prescan. Final scans were extended in width 25% on both sides to allow for estimation of background intensity. Three intensity standards were monitored every 3 h of X-ray exposure time in order to account for any crystal decay or significant fluctuations in the cold stream temperature for those data sets in which cooling was employed. The crystal orientation was also monitored every 250 reflections and adjustments to the orientation matrix were made automatically whenever the scattering vectors of the monitor

reflections had moved by a preset amount from the angle calculated based on the orientation matrix. A unique octant of data along with the Friedel mate of each reflection was collected for each crystal data set.

Structure analysis, refinement and configuration assignment

The first structure was solved by direct methods using the MULTAN [4] program series. Subsequently, coordinates of this solution were used as a starting point for refinement of the others. After refinement with isotropic temperature factors the non-hydrogen atoms were assigned anisotropic parameters and refined to convergence. Hydrogen positions were suggested from difference Fourier maps in all instances. Hydrogen atoms were included as fixed contributions to the models at calculated positions based on geometric considerations and assuming a C–H or N–H bond length of 1.03 Å. Fixed isotropic temperature factors equal to 1.1 × B_{iso} of the attached non-hydrogen atom were assigned to each hydrogen. Values of the neutral atom scattering factors and for anomalous dispersion corrections were taken from ref. 5.

Absolute configuration assignment samples were based both on an analysis of the signs of the intensity ratios of Friedel mates and on the purely statistical basis of Hamilton's *R*-factor ratio test [6]. Results from both methods were in agreement for both the data sets. The signs of the differences in F_0 and F_c for all Friedel mates significantly affected by anomalous dispersion (6% or greater) were in agreement for the correct enantiomer in each case. For (R) ISF 4393 (determined from sample code LCA/1/NC2-3/1) the *R*-factor ratio was 1.259 and is significant at the 99.995% confidence level compared with the theoretical value of 1.003 for the refinement. Similarly, for (S)-ISF-4393 (determined from sample code UP-23-48) the *R*-factor ratio of 1.067 is statistically significant at the 99.995% confidence level as compared with the calculated value of 1.008. Our findings for this latter sample are in agreement with its preparation from (*S*)-pyroglutamic acid under non-racemizing conditions.

RESULTS AND DISCUSSION

Compound **1** is a relatively hydrophilic molecule containing few aliphatic and no aromatic residues, essential for hydrophobic interactions and important for the resolution of enantiomers on most commercial chiral stationary phases (CSPs). The absence of aromatic residues also precludes the occurrence of $\pi-\pi$ interactions, important for the formation of charge-transfer transient complexes. However, **1** contains two amide moieties which can be involved in hydrogen-bonding interactions between a CSP and the enantiomers of this molecule. Hydrogen bonding will be enhanced in non-polar solvents.

Because of the above limitations, the choice of the most suitable CSP for the resolution of the enantiomers of **1** was limited. The use of either a Pirkle-type [7] or a cyclodextrin [8] column was very doubtful as the chemical structure of **1** does not give any indication that it can be associated with either charge transfer or inclusion in the hydrophobic cavity of cyclodextrin. The use of a protein column [9] was thought not to be practical as such a CSP can be used only for analytical and not preparative purposes. Moreover, most of the analytes resolved on such a column contain aromatic groups [10].

From our experience on the chiral separation of the enantiomers of oxiracetam and closely related molecules [11], a Chiralcel OC column was chosen for the resolution of the optical isomers of **1** and other lactams. This CSP is made up of cellulose with the three hydroxy groups on each D-glucose unit replaced by phenylcarbamate residues. The Chiralcel OC column is especially effective for the chiral resolution of polar racemates as the carbamate residues can be involved in stereoselective hydrogen bonding with a substrate [11]. The chiral resolution of the enantiomers of **1** using a semi-preparative column of this type is shown in Fig. 1. About 20 mg of each enantiomer of **1** were obtained using this column with hexane–2-propanol (50:50) as the mobile phase at a flow-rate of 4 ml min^{-1}.

Fig. 2 shows the purity of the prepared samples. The peak areas of the (+)- and (−)-en-

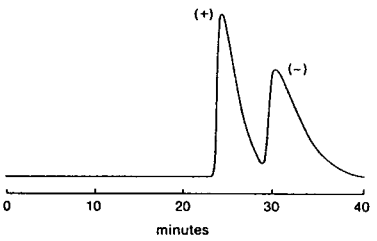

Fig. 1. Resolution of the enantiomers of **1** on a semi-preparative Chiralcel OC column. Column, Chiral OC (250 mm × 10 mm I.D.; 10 μm); mobile phase, hexane–2-propanol (50:50); flow-rate, 4 ml min^{-1}; temperature, ambient; detection at 205 nm.

antiomers integrated to 97% and 95%, respectively. The enantiomeric excess (ee) was calculated as 95 and 91% and the optical rotations, $[\alpha]_D^{25}$, were measured in methanol as +38.5 and −35.2. These values are in agreement with purity values for the individual enantiomers. The absolute configuration of the (+)- and (−)-enantiomers was *S* and *R*, respectively. The identity of the enantiomers was obtained by comparison of retention times with those of authentic samples of the separate enantiomers.

In order to evaluate the usefulness of the Chiralcel OC column for the chromatographic resolution of racemates closely related to **1**, several molecules were analysed using similar chromatographic conditions. Expanding one of the lactam rings of **1** to give the lactams **3** and **4** does not have much effect on either the resolution or the retention time of the enantiomers. Table I compares some of the properties of the three compounds. The separation factors for **3** and **4** are lower than that measure for **1**. Unlike

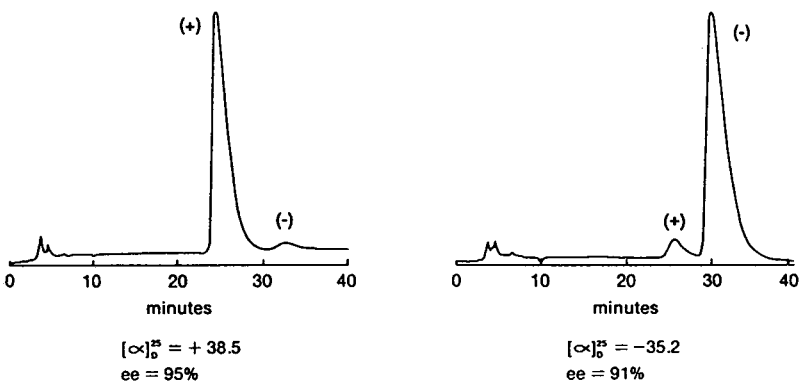

Fig. 2. Analysis of the separate enantiomers of **1**.

TABLE I

COMPARISON OF SOME PROPERTIES OF 1 AND CLOSELY RELATED COMPOUNDS

Compound	Separation factor	Mobile phase hexane–2-propanol	Specific rotation, $[\alpha]_D^{25}$ (°)	
			First-eluting enantiomer	Second-eluting enantiomer
1	1.38	50:50	+38.5	−35.2
3	1.28	50:50	−5.0	+4.0
4	1.35	50:50	+9.6	−9.3
5	1.26	60:40	–	–
6	1.29	60:40	–	–
7	1.17	80:20	+16.2	−15.7

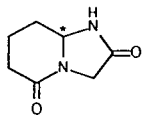

(3)

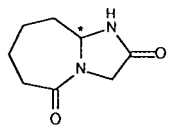

(4)

1 and **4**, the (−)-enantiomer of **3** elutes before the (+)-isomer.

Expansion of one of the lactam rings by the addition of one or two methylene groups would have been expected to increase the hydrophobicity of the resulting molecules so that under the conditions of elution described retention of the three molecules would normally be predicted to be in the order **1** > **3** > **4**. The apparent lack of sensitivity of retention to the size of one of the lactam rings is remarkable and may emphasize that the hydrogen bonding character of these molecules is the dominant mechanism both for their retention and for their stereoselective interaction with the CSP.

The chromatographic behaviour of two more derivatives of **1** was also studied to provide information on the influence of substituents on chiral resolution. The enantiomers of both **5** and **6** were resolved (see Table 1), showing that introduction of substituents that differ widely in their size and their electronic and hydrophobic characteristics [12] is tolerated at the chiral centre. No optical rotation studies were carried out on **5** and **6**.

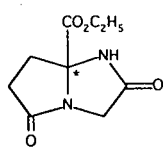

(5)

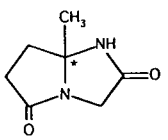

(6)

We finally analysed the chromatographic behaviour of the dithio derivative of **1**. The chromatographic resolution of the two optical isomers of this compound (**7**) on a semi-preparative Chiralcel column is shown in Fig. 3.

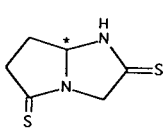

(7)

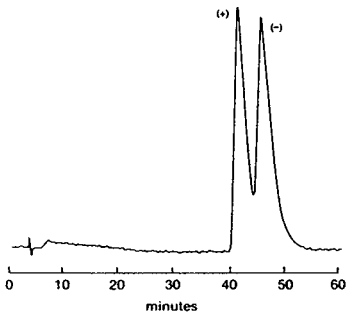

Fig. 3. Chiral resolution of the enantiomers of **7** on a semi-preparative column. Conditions as in Fig. 1 except hexane–2-propanol (80:20) and UV detection at 210 nm.

The enantiomers of **7** were not completely resolved over a wide range of hexane-to-2-propanol ratios. This may be due to the weaker hydrogen-bonding efficacy of sulphur compared with oxygen and to the larger atomic size of

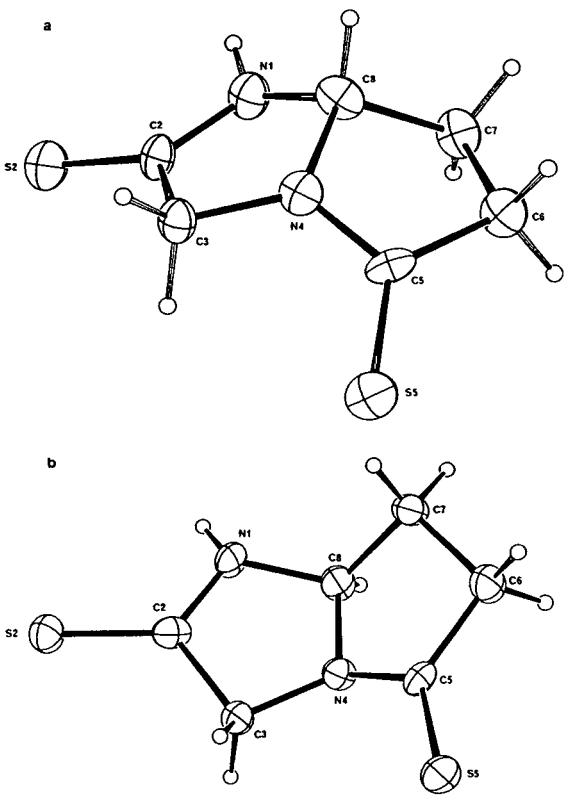

Fig. 4. X-Ray structures of (a) (*S*)-**7** and (b) (*R*)-**7**.

sulphur. These two effects may both contribute to a smaller energy difference associated with the transient diastereoisomers between each enantiomer and the CSP, although different mechanisms for enantiorecognition may also be involved. The two enantiomers of **7** were prepared with ee values greater than 98% for the (+)-isomer and 93% for the (−)-isomer. The $[\alpha]_D^{25}$ values for the respective enantiomers were measured as +16.2 and −15.7.

The purified enantiomers were submitted to X-ray crystallography in order to determine absolute configuration. Results from these studies are given in Fig. 4 and Table II.

X-Ray studies on **7** were done to relate the absolute configuration of the enantiomers of this compound to those of the antipodes of **1**. These studies showed that although that although the (+)- and (−)-enantiomers of the two compounds eluted in the same order, the absolute configuration was the reverse, that is, the (+)- and (−)-enantiomers had the *R* and *S* absolute configuration, respectively, as confirmed by comparison of the retention times of the two antipodes with those of authentic samples [13,14]. This result was surprising and the reverse order of elution of the antipodes of **7** compared with those of **1** on a Chiralcel OC column appears to indicate that one or more of the three points of interaction (necessary for chiral recognition) between these

TABLE II

CRYSTALLOGRAPHIC DATA FOR THE ENANTIOMERS OF **7**

Parameter	(*S*)-**7**	(*R*)-**7**
Formula	$C_6H_8N_2S_2$	$C_6H_8N_2S_2$
M_r	172.27	172.27
Crystal shape and dimensions (mm)	Ellipsoidal, 0.40 × 0.30 × 0.30	Tabloid, 0.35 × 0.15 × 0.30
Space group	$P2_12_12_1$	$P2_12_12_1$
Temperature (K)	173	145
Lattice parameters (Å):		
a	6.667(2)	6.650(4)
b	7.689(10)	7.675(3)
c	14.984(5)	14.982(5)
Volume (Å^3)	768.1(1)	764.6(7)
Z	4	4
P_{calc} (g cm^{-1})	1.490	1.496
μ (cm^{-1})	55.700	55.955
F(000)	360	360
Range of data	$20 \leq 135°$	$20 \leq 135°$
	$h \leq 7$	$h \leq 7$
	$k \leq 9$	$k \leq 9$
	$l \leq 19$	$l \leq 19$
Total observed data including Friedel mates	1259	1305
Unique data	774	818
Variables	92	92
R [a]	0.0584 (0.0635)	0.0386 (0.0478)
R_w [a]	0.0696 (0.730)	0.0504 (0.0653)
Goodness of fit	1.432	2.358
Extinction correction ($\times 10^{-6}$)	11.14	9.101
Absorbtion corrections:		
Max.	0.9986	0.9991
Min.	0.8399	0.7499
Decay corrections	–	–

[a] Values in parentheses are crystallographic residuals for the enantiomer of each data set.

substrates and the CSP are different; for example, a different extent of enolization would be expected for **7** than for **1**. This will be investigated by constructing chiral recognition models in the same way as has been done for oxiracetam [11].

In conclusion, we have shown that it is possible to isolate enough material chromatographically for structure determination by X-ray crystallography. Moreover, the influence of the structure of the bicyclic lactam **1** on the chiral resolution of its enantiomers has been investigated and it has been shown that resolution is not greatly dependent on hydrophobicity but on the ability of the molecule to hydrogen bond to the cellulose-based chiral stationary phase.

REFERENCES

1 M. Pinza, C. Farina, U. Pfeiffer, M.T. Riccaboni, R. Begetti, O. Pozzi and L. Dorigotti, presented at the *XIth International Symposium on Medicinal Chemistry, Jerusalem, 2–7 September, 1990.*

2 C. Villardita, J. Parini, S. Grioli, M. Quattropani, C. Lomeo and U. Scapagnini, *J. Neural Transm., Suppl.*, 24 (1987) 293.

3 P. Camilleri, J.A. Murphy and C.J. Thorpe, *J. Chromatogr.*, 508 (1990) 208.

4 P. Main, S.J. Fiske, S.E. Hull, L. Lessinger, G. Germain, J.P. Declercq and M.M. Woolfson, *MULTAN80 – a System of Programs for the Automatic Solution of Crystal Structures from X-Ray Diffraction Data*, Universities of York, UK, and Louvain, Belgium, 1980.

5 *International Tables for X-Ray Crystallography*, Vol. IV, Kynoch Press, Birmingham, 1974; present distributor, Reidel, Dordrecht.

6 W.C. Hamilton, *Acta Crystallogr.*, 18 (1965) 502.

7 W.H. Pirkle and C.J. Welch, *J. Org. Chem.*, 49 (1984) 148.

8 W.L. Hinze, T.E. Riehl, D.W. Armstrong, W. Demond, A. Alak and T. Ward, *Anal. Chem.*, 57 (1985) 237.

9 S. Allenmark, B. Bomgren and H. Boren, *J. Chromatogr.*, 316 (1984) 617.

10 S. Allenmark, in A.M. Krstulović (Editor), *Chiral Separations by HPLC*, Wiley, New York, 1989, p. 285.

11 P. Camilleri, J.A. Murphy, M.R. Saunders and C.J. Thorpe, *J. Comput.-Aided Mol. Des.*, 5 (1991) 277.

12 C. Hansch and A. Leo, *Substituent Constants for Correlation Analysis in Chemistry and Biology*, Wiley, New York, 1979.

13 SmithKline Beecham, *UK Pat. Appl.*, 9123641.4 (1991).

14 SmithKline Beecham, *UK Pat. Appl.*, 9206618.2 (1992).

Journal of Chromatography A, 654 (1993) 215–220
Elsevier Science Publishers B.V., Amsterdam

CHROM. 25 479

Determination of ascorbic acid and dehydroascorbic acid in juices by high-performance liquid chromatography with electrochemical detection using L-cysteine as precolumn reductant

Hiroshi Iwase* and Ichiro Ono

Ajinomoto Co., Inc., Central Research Laboratories, 1-1 Suzuki-cho, Kawasaki-ku, Kawasaki, 210 (Japan)

(First received March 30th, 1993; revised manuscript received August 2nd, 1993)

ABSTRACT

Determination of ascorbic acid (AA) and dehydroascorbic acid (DHAA) in juices was performed by high-performance liquid chromatography with electrochemical detection using L-cysteine as precolumn reductant. This method was suitable for the determination of AA and total AA (AA + DHAA) in juices. The mild reduction of DHAA to AA with L-cysteine took *ca.* 15 min, and the retention time of AA was *ca.* 15 min. The detection limit (signal-to-noise ratio = 2) was *ca.* 0.15 ng. The method was selective and reproducible (relative standard deviation 2.6–3.2% for AA and 2.1–3.2% for total AA). The calibration graph for AA was linear in the range 0.1–10 ng. The recovery of AA was over 90% by the standard addition method.

INTRODUCTION

A number of reports on the determination of ascorbic acid (AA) [1–11] have appeared in the last 10 years. Numerous efforts have been directed to the development of specific and sensitive detection systems in high-performance liquid chromatography (HPLC). HPLC with UV detection, electrochemical detection (ED) and fluorescence detection has proved useful for the determination of AA in foods such as juices, vegetables and potatoes [1–4] and in biological fluids [4–10]. HPLC with ED is valuable in the determination of trace compounds in complex matrices because of the excellent sensitivity and selectivity provided [12].

Usually, dehydroascorbic acid (DHAA) is determined as the difference between the total AA (AA + DHAA) after DHAA reduction and the AA content of the original sample. AA is easily oxidized to DHAA in the presence of reagents such as halogens, hydrogen peroxide and heavy metal ions, especially CU^{2+}, Ag^{+} and Fe^{3+} and at alkaline pH [13]. DHAA is electrochemically inactive and most DHAA assays involve preliminary reduction of DHAA to AA with homocysteine [1–6] and subsequent measurement of total AA by HPLC with UV detection or ED. The reduction reagent requires the rapid and mild reduction of DHAA to AA, no response to ED monitoring of the applied potential and low cost. Commercially available and cheap L-cysteine has not been used as a precolumn reductant for the reduction of DHAA to AA.

A simple, rapid, sensitive, highly selective and reproducible method for the determination of AA and DHAA in foods, drugs and biomedical samples is required for quality control purposes and in clinical chemistry. We reported previously [11] the routine determination of AA in complex

* Corresponding author.

0021-9673/93/$06.00 © 1993 Elsevier Science Publishers B.V. All rights reserved

sample matrices (elemental diets) by HPLC with ED without the use of an internal standard. This paper describes the selective and sensitive determination of AA and DHAA in juices by HPLC with ED using an internal standard and L-cysteine as pre-column reductant.

EXPERIMENTAL

Reagents and materials

AA was purchased from Tokyo Kasei (Tokyo, Japan), L-cysteine from Ajinomoto (Kawasaki, Japan) and α-methyl-L-dopa was from Nacalai Tesque (Kyoto, Japan). Other reagents were of analytical-reagent grade. Membrane filters (0.45 μm) were obtained from Millipore (Bedford MA, USA). Lemon and grape juices were freshly prepared prior to use. Other juices were commercially available.

Apparatus and conditions

A Model 655 A-11 high-performance liquid chromatograph (Hitachi, Tokyo, Japan) equipped with a Model Σ 875 electrochemical detector (Irica, Kyoto, Japan) was used. The applied potential was set at 300 mV *versus* an Ag/AgCl reference electrode. The samples were applied by a Rheodyn Model 7125 sample loop injector with an effective volume of 20 μl. HPLC was carried out on a 15 × 0.46 cm I.D. Inertsil ODS-2 (5 μm) reversed-phase column (GL Sciences, Tokyo, Japan) using as the mobile phase 100 m*M* KH_2PO_4 (pH 3, adjusted with phosphoric acid)–1 m*M* ethylenediaminetetraacetic acid disodium salt (EDTA·2Na). The flow-rate was 0.6 ml/min at room temperature.

Standard AA preparation

Standard AA solution (10 μg/ml) was freshly prepared prior to use. AA in this solution was stable for 30 min at 5°C. The AA peak-height ratio was constant for 30 min and subsequently decreased.

Standard DHAA preparation

Standard DHAA solution was freshly prepared by the addition of 0.1 *M* iodine solution (250 μl) to the standard AA solution (10 μg) prior to use [14,15]. DHAA in this solution was stable for 30 min at 5°C. The AA peak-height ratio after reduction of DHA to AA with L-cysteine was constant for 30 min and subsequently decreased periodically.

Sample preparation

Samples were preliminarily diluted to an estimated AA concentration of 10 μg/ml with deionized water, then the solution was filtered with a membrane filter (0.45 μm) and the filtrate was used for the two purposes of the determination of AA and of total AA. AA in this sample solution was stable for 30 min at 5°C. The AA peak-height ratio was constant for 30 min and subsequently decreased.

AA determination

To 20 μl of the above solution were added 10 μl of α-methyl-L-dopa (125 μg/ml) and 2% metaphosphoric acid solution (800 μl) for the determination of AA. AA in this solution was stable at room temperature for 30 min. The AA peak-height ratio was constant for 30 min and subsequently decreased. An aliquot (20 μl) was injected into the chromatograph.

DHAA determination

DHAA was determined as the difference between the total AA after DHAA reduction and the AA content of the original sample. To 20 μl of the above solution were added 10 μl of α-methyl-L-dopa (125 μg/ml) and L-cysteine (2.5 mg/ml) diluted in 10 m*M* phosphate buffer (pH 6.8) (800 μl) for a the determination of total AA. After this solution had been allowed to stand at room temperature for 15 min, an aliquot (20 μl) was injected into the chromatograph. AA in this solution was stable at room temperature for 30 min. The AA peak-height ratio was constant for 30 min and subsequently decreased periodically.

RESULTS AND DISCUSSION

Internal standard

At the beginning of the work, several internal standards were examined for the determination of AA in juices. Electrochemically active 4-hydroxy-3-methoxybenzoic acid, 2,5-dihydroxy

benzoic acid, N-acetyl-L-cysteine, N-acetyl-L-tyrosine, N-acetyl-L-tryptophan and α-methyl-L-dopa were examined. It was found that α-methyl-L-dopa was the most useful internal standard, because it has a suitable retention time (about 14 min) and shows excellent separation and applied potential (300 mV *versus* an Ag/AgCl reference electrode).

The relationship between applied potential and sensitivity of AA, α-methyl-L-dopa, cysteine, tyrosine and tryptophan was examined. A typical hydrodynamic voltammogram is illustrated in Fig. 1. The current (peak height) at each applied potential was divided by the current at the maximum possible potential to obtain the relative current ratio. This value was plotted against the applied potential. The detector gave a linear response up to 500 mV *versus* Ag/AgCl for α-methyl-L-dopa and 900 or 1000 mV *versus* Ag/AgCl for cysteine, tyrosine and tryptophan. When the applied potential was set at 400 mV or more *versus* Ag/AgCl AA could not be determined, because AA was present on the solvent front with a large shoulder and was not separated completely.

Based on the above, the applied potential was set at 300 mV *versus* Ag/AgCl for the selective determination of AA.

Reduction conditions

The effects of the pH of the solution, amount of L-cysteine and reaction time at room temperature on the reduction of DHAA to AA were examined by comparing the peak height of AA with that of α-methyl-L-dopa. It can be seen in Figs. 2–4 that all three parameters affect the reduction of DHAA to AA. The results that the optimum reduction pH was 6–7.5, amount of L-cysteine 2.5% and reaction time at room temperature about 15 min. Rapid and mild reduction was carried out as follows: DHAA (200 ng) diluted in 10 m*M* phosphate buffer (pH 6.8) (800 μl) containing L-cysteine (2.5 mg/ml) was allowed to stand at room temperature for 15 min. The reduction scheme is shown in Fig. 5.

Chromatography

The chromatograms obtained by HPLC with ED of AA and AA after reduction of DHAA using the proposed reduction conditions were examined.

The chromatograms in Fig. 6a and b of AA (200 ng) diluted in 800 μl of deionized water and 10 m*M* phosphate buffer (pH 6.8) containing 0.25% L-cysteine show that the standard AA used here did not contain DHAA, because both AA peak heights were almost identical. When

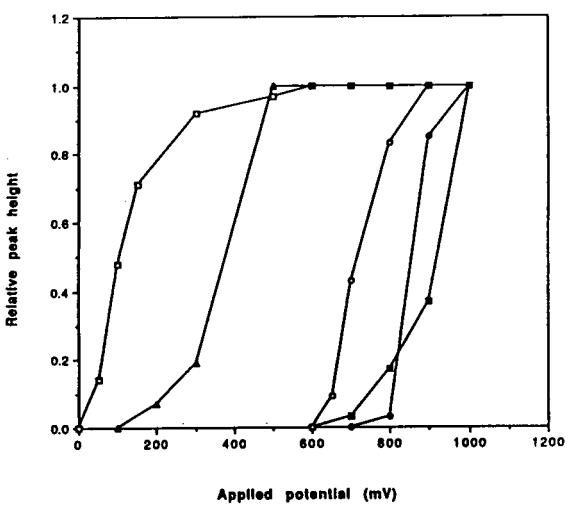

Fig. 1. Hydrodynamic voltammograms of AA, cysteine, tyrosine and tryptophan. ▲ = α-Methyl-L-dopa (internal standard); □ = AA; ■ = L-tryptophan; ○ = L-cysteine; ● = L-tyrosine.

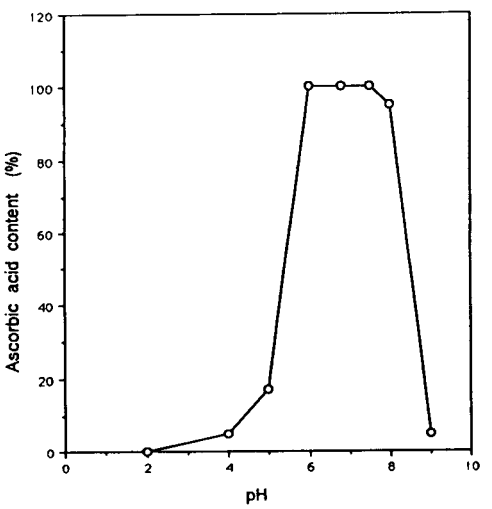

Fig. 2. Effect of pH on the reduction of DHAA to AA. Conditions: DHAA (200 ng) diluted in 10 m*M* phosphate buffer (800 μl) containing L-cysteine (2.5 mg/ml) was allowed to stand at room temperature for 15 min.

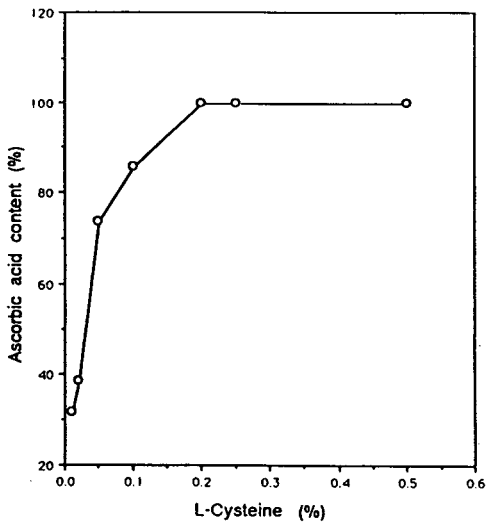

Fig. 3. Effect of amount of L-cysteine on the reduction of DHAA to AA. Conditions: DHAA (200 ng) diluted in 10 m*M* phosphate buffer (pH 6.8) (800 μl) containing L-cysteine was allowed to stand at room temperature for 15 min.

0.1 *M* iodine solution was added to AA (200 ng) in deionized solution, no AA peak was observed on the chromatogram (Fig. 6c) because of the oxidation of AA to DHAA by the iodine [14,15]. On the other hand, after further addition of L-cysteine to the above oxidized AA (Fig. 6c) an AA peak was observed on the chromatogram (Fig. 6d) because of the rapid reduction of DHAA to AA by the L-cysteine. The recovery in the reduction of DHAA to AA was over 95%.

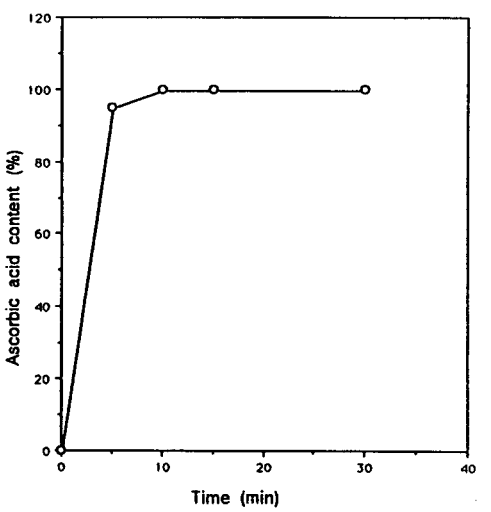

Fig. 4. Effect of reaction time on the reduction of DHAA to AA. Conditions: DHAA (200 ng) diluted in 10 m*M* phosphate buffer (pH 6.8) (800 μl) containing L-cysteine (2.5 mg/ml) was allowed to stand at room temperature.

Usually, AA in foods and biomedical samples is determined by HPLC with ED at +600 mV or more *versus* an Ag/AgCl reference electrode or HPLC with UV detection at 245 nm [1–6]. When the determination of AA was performed by HPLC with ED at ≥600 mV *versus* Ag/AgCl or by HPLC with UV detection at 245 nm, not only AA but also cysteine, tyrosine and tryptophan were detected, as described previously [11]. It took about 60 min after the retention time of AA for complete elution. On the other hand, the chromatography for AA can be highly selective with rapid detection (retention time *ca.* 15 min) in the presence of other compounds by ED at 300 mV *versus* Ag/AgCl. This allows analysis without the need for clean-up. This procedure was simple and suitable for routine work. A typical chromatogram of AA (detection limit *ca.* 0.15 ng at a signal-to-noise ratio of 2) in orange juice is shown in Fig. 7.

From the above results, it was concluded that the method established here was advantageous for the routine determination of AA and total AA in juices, because of the simple, rapid (reduction time of DHAA to AA *ca.* 15 min; retention time of AA *ca.* 15 min) and highly selective analysis without the need for clean-up.

Determination of AA

A calibration graph for AA was constructed by plotting the peak-height ratio against the amount of AA in the internal standard. Satisfactory linearity was obtained over the range 0.1–10 ng ($y = 0.3421x - 0.023$; y = peak-height ratio, x = amount of AA in ng).

A known amount of AA and DHAA was added to orange juices and the overall recoveries were calculated by the standard addition method. As shown in Table I, the AA recovery was over 90% and the DHAA recovery was *ca.* 80%.

Table II gives the analytical data for AA and DHAA in juices. The relative standard deviation (R.S.D.) was 2.6–3.2% for AA and 2.1–3.2% for total AA with no addition of AA and

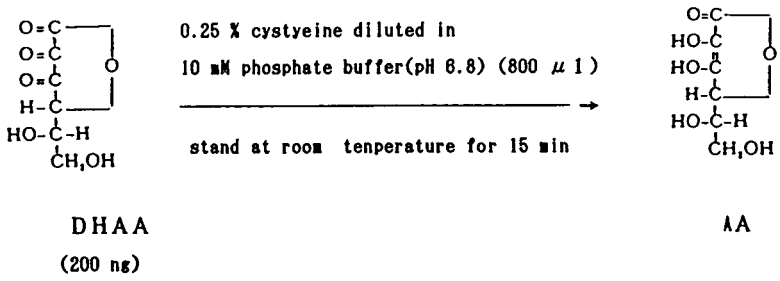

Fig. 5. Reduction scheme.

DHAA. Between-day R.S.D.s were not examined because AA and DHAA were unstable.

CONCLUSION

The use of commercially available and cheap L-cysteine for the rapid and mild reduction of DHAA to AA seems very useful for the determination of AA and total AA by HPLC with ED. The proposed method is satisfactory with respect to selectivity, rapidity and cost in comparison with published methods [1–6]. This method established here seems to be applicable to the routine analysis of AA and total AA in juices because of the simple, rapid (mild reduction time of DHAA to AA with L-cysteine *ca.* 15 min; retention time of AA *ca.* 15 min), sensitive [detection limit *ca.* 0.15 ng (signal-to-noise ratio = 2)], reproducible (R.S.D. = 2.6–3.2% for AA and 2.1–3.2% for total AA) and highly selective analysis without the need for clean-up and with recoveries of over 90% for AA and about 80% for DHAA. The application of the proposed method to the determination of AA and total AA in biological fluids is being studied.

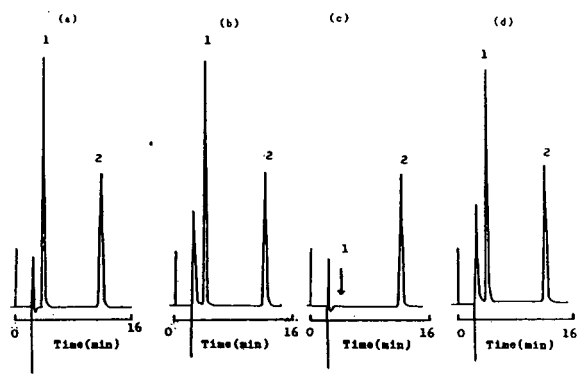

Fig. 6. Chromatograms of standard AA under various conditions obtained by HPLC with ED at 300 mV *versus* an Ag/AgCl reference electrode. AA concentration = 200 ng in 800 μl; internal standard (I.S.) concentration = 1.25 μg in 800 μl. (a) AA (200 ng) and I.S. (1.25 μg) diluted in deionized water (800 μl); (b) AA (200 ng) and I.S. (1.25 μg) diluted in 10 m*M* phosphate buffer (pH 6.8) containing 0.25% L-cysteine (800 μl); (c) AA (200 ng) and I.S. (1.25 μg) and 0.1 *M* I_2 solution (50 μjl); diluted in deionized water (800 μl); (d) AA (200 mg), I.S. (1.25 μg) and 0.1 *M* I_2 solution (50 μl) diluted in 10 mM phosphate buffer (pH 6.8) containing 0.25% L-cysteine (800 μl). Peaks: 1 = AA; 2 = I.S.

Fig. 7. Chromatogram of AA in orange juice obtained by HPLC with ED at 300 mV *versus* an Ag/AgCl reference electrode. Amount of AA injected, 6.33 ng in 20 μl. HPLC was carried out on a 15 × 0.46 cm I.D. column of Inertsil ODS-2 (5 μm) using 100 m*M* KH_2PO_4 (pH 3, adjusted with phosphoric acid)–1 m*M* EDTA·2Na as the mobile phase at a flow-rate of 0.6 ml/min at ambient conditions. Peaks: 1 = AA; 2 = I.S.

TABLE I

RECOVERIES OF AA AND DHAA ADDED TO ORANGE JUICE

Compound	Amount (mg per 100 ml)		R.S.D. (%)[a]	Recovery (%)
	Added	Found		
AA	0	25.3	3.2	–
	5	29.9	3.1	92
	10	35.0	2.9	97
	20	44.9	2.8	98
	40	65.5	2.9	100.5
Total AA (AA + DHAA)	0	28.1	3.3	–
	10	36.3	3.1	82

[a] $n = 3$.

TABLE II

CONTENTS OF AA AND DHAA IN JUICES

Sample	AA		DHAA concentration (mg per 100 ml)
	Concentration (mg per 100 ml)	R.S.D. (%)[a]	
Orange juice A	25.3	3.2	1.8
Orange juice B	15.3	3.1	16.4
Apple juice	27.9	2.9	5.8
Lemon juice	39.2	2.6	0
Japanese tea	5.2	3.2	0.3
Grape juice	0	–	2.2

[a] $n = 3$.

REFERENCES

1 D.B. Dennison, T.G. Brawley and G.L.K. Hunter, *J. Agric. Food Chem.*, 29 (1981) 927.
2 W.A. Behrens and R. Madere, *J. Liq. Chromatogr.*, 15 (1992) 753.
3 W.D. Grahham and D. Annette, *J. Chromatogr.*, 594 (1992) 187.
4 W.A. Behrens and R. Madere, *Anal. Biochem.*, 165 (1987) 102.
5 R.R. Howard, T. Peterson and P.R. Kastl, *J. Chromatogr.*, 414 (1987) 434.
6 L.S. Liau, B.L. Lee, A.L. New and C.N. Ong, *J. Chromatogr.*, 612 (1993) 63.
7 K. Iriyama, M. Yoshiura, T. Iwamoto and Y. Ozaki, *Anal. Biochem.*, 141 (1984) 238.
8 M. Yoshiura, T. Iwamoto and K. Iriyama, *Jikeiika Med. J.*, 32 (1985) 21.
9 M.A. Kotnink, J.H. Skala, H.E. Sauberlich and S.T. Omaye, *J. Liq. Chromatogr.*, 8 (1985) 31.
10 M. Yoshiura and K. Iriyama, *J. Liq. Chromatogr.*, 9 (1986) 177.
11 H. Iwase, *J. Chromatogr.*, 505 (1992) 277.
12 P.T. Kissinger, *Anal. Chem.*, 49 (1977) 477 A.
13 A.P. De Leenheer, W.E. Lambert and H.J. Nelis, *Modern Chromatographic Analysis of Vitamins*, Marcel Dekker, New York, 2nd ed., 1992, p. 235.
14 *The United States Pharmacopeia, XXII Revision*, US Pharmacopeial Convention, Rockville, MD, 1990, p. 109.
15 *The Pharmacopeia of Japan*, Hirokawa, Tokyo, 12th ed., 1992, p. C-37.

Journal of Chromatography A, 654 (1993) 221–228
Elsevier Science Publishers B.V., Amsterdam

CHROM. 25 453

Liquid chromatographic–atmospheric pressure chemical ionization mass spectral characterization of carboxylic acids and their glycine conjugates

F. Kasuya*, K. Igarashi and M. Fukui

Faculty of Pharmaceutical Sciences, Kobe-gakuin University, 518, Arise, Ikawadani, Nishiku, Kobe 651-21 (Japan)

(First received May 10th, 1993; revised manuscript received July 25th, 1993)

ABSTRACT

A series of substituted benzoic acids and their glycine conjugates were characterized by liquid chromatography–atmospheric pressure chemical ionization mass spectrometry. Each substituted benzoic acid and its glycine conjugate were separated with a Cosmosil 5 C_8 column using three mobile phases. All negative-ion mass spectra of the substituted benzoic acids gave abundant $[M-H]^-$ and $[M-COOH]^-$ ions. For acids with halogen, nitro, cyano, and acetylamino groups, fragmentations corresponding to losses equivalent to the mass of each functional group were also observed. In addition, the alkoxyl group gave a characteristic fragmentation representing loss of the alkyl moiety. The abundances of the fragment ions due to the functional groups gave information on the position of the ring substituents. All of the positive- and negative-ion mass spectra of the glycine conjugates gave abundant $[M+H]^+$ and $[M-H]^-$ ions with characteristic fragment ions, respectively. Fragmentations of the glycine conjugates obtained in the positive-ion mode were different from those in the negative-ion mode. Similar information on the substituents was obtained for the glycine conjugates.

INTRODUCTION

Xenobiotics containing carboxylic acid groups are very commonly encountered and are of great significance as drugs, herbicides, plant hormones and insecticides. The carboxylic acid group may also result from metabolism of a xenobiotic. Glycine conjugation is the most important route in the metabolism of carboxylic acids. Correlations between molecular structure and enzymatic activities are extremely important in order to understand detoxification mechanisms. Therefore, relationships between the chemical structure of acids and glycine conjugation have been investigated [1–4]. We have also studied a series of substituted benzoic acids as simple model compounds of carboxylic acids and have elucidated the influence of chemical structure on the extent of glycine conjugation [5–7].

For the determination of glycine conjugation activities, we developed a specific and simple high-performance liquid chromatographic (HPLC) method. Because only a few synthetic glycine conjugates are available, enzymatic activities were calculated from the decreasing rates of the substrates. However, it was confirmed that a decrease in the size of the peak of the substrate resulted in a concomitant increase in that of the glycine conjugate. When synthetic glycine conjugates were available, the glycine conjugates were tentatively identified by comparison with the chromatographic properties of the synthetic glycine conjugates. When no synthetic glycine conjugates are available, it is difficult to identify the glycine conjugates formed in mitochondria.

There have been no reports of investigations in which liquid chromatography–mass spec-

* Corresponding author.

0021-9673/93/$06.00 © 1993 Elsevier Science Publishers B.V. All rights reserved

trometry (LC–MS) has been used to identify various glycine conjugates produced from substituted benzoic acids in the liver mitochondria and to define their spectral characteristics. Further, it is useful for metabolism studies to elucidate the spectrometric features of a wide variety of acids. The conventional gas chromatographic–mass spectrometric (GC–MS) analysis for the identification of these compounds requires chemical derivatization such as methylation or silylation. Recently, LC–MS has played an increasingly important role in a variety of biochemical fields. One of the main advantages of LC–MS is that polar, non-volatile or thermally stable compounds do not require a derivatization step. This system seems to be very attractive for structural identification in metabolism studies.

This paper reports the determination of a series of benzoic acid derivatives and their glycine conjugates using liquid chromatography–atmospheric pressure chemical ionization mass spectrometry (LC–APCI-MS). The mass spectrometric fragmentation properties of the acids and their glycine conjugates are also described.

EXPERIMENTAL

Chemicals

Benzoic acid and 2-chloro-, 2-methoxy-, 2-nitro-, 3-amino-, 3-acetylamino-, 3-chloro-, 3-methoxy-, 3-methyl-, 3-nitro-, 4-amino-, 4-acetylamino-, 4-chloro-, 4-cyano-, 4-ethoxy-, 4-methoxy-, 4-methyl-, 4-nitro-, 4-dimethylamino- and 3-nitro-4-chlorobenzoic acid were purchased from Nacalai Tesque (Kyoto, Japan), 3-cyanobenzoic acid from Aldrich (Milwaukee, WI, USA) and hippuric acid and 4-aminohippuric acid from Wako (Osaka, Japan). All other chemicals were of analytical-reagent grade.

3-Butoxy-4-aminobenzoic acid, N-(3-butoxy-4-aminobenzoyl)glycine and N-(4-acetylaminobenzoyl)glycine were synthesized as described previously [5,6].

Preparation of mitochondria

The animals used were ddY strain male mice weighing about 25–30 g. Mitochondria were prepared by the method described previously [6]. Protein concentration was determined by the method of Lowry *et al.* [8].

Formation of glycine conjugates of a series of substituted benzoic acids

The formation of glycine conjugates was carried out by using the technique described previously [6,7].

Instrumentation

HPLC separation was performed with a Hitachi (Tokyo, Japan) L-6200 instrument equipped with a 5-μm Cosmosil C_8 reversed-phase column (150 mm × 4.5 mm I.D.) (Nacalai Tesque). The mobile phases were water–methanol–acetic acid systems as follows: (a) 49.8:50:0.2, (b) 61.3:38.5:0.2 and (c) 77.8:22:0.2 (v/v/v). The flow-rate was 1 ml/min. The mobile phases used for the separation of substituted benzoic acids and their glycine conjugates are given in Table I. The column effluent of each acid and its glycine conjugate was monitored at the wavelength described previously.

Positive- and negative-ion mass spectra were measured with a Hitachi M-2000 double-focusing mass spectrometer equipped with an atmospheric pressure ionization source. All mass spectral data were obtained by scanning the mass range from m/z 1 to 600 in 4 s, with a dwell time of 0.5 s. Sensitivity measurements were carried out with selected ion monitoring (SIM) by flow-injection analysis. The nebulizer temperature

TABLE I

MOBILE PHASES FOR SEPARATION OF SUBSTITUTED BENZOIC ACIDS AND THEIR GLYCINE CONJUGATES

Mobile phase (Water–methanol–acetic acid)	Substituted benzoic acids
(a) 49.8:50:0.2 (v/v/v)	4-Cl-, 4-CH_3-, 4-C_2H_5O-, 4-$(CH_3)_2N$-, 3-Cl-, 3-CH_3-, 3-C_4H_9O-4-NH_2-, 3-NO_2-4-Cl-
(b) 61.3:38.5:0.2 (v/v/v)	H-, 4-CN-, 4-NO_2-, 4-CH_3O-, 3-CN-, 3-NO_2-, 3-CH_3O-
(c) 77.8:22:0.2 (v/v/v)	4-NH_2-, 4-CH_3CONH-, 3-NH_2-, 3-CH_3CONH-

was set at 300 or 340°C. The drift voltage varied in the range 120–170 V.

RESULTS AND DISCUSSION

In a previous study, HPLC separation of a series of acids and their glycine conjugates, tentatively identified, was achieved by using water–methanol–acetic acid–0.5 *M* tetrabutylammonium hydroxide as the mobile phase [6]. However, the mobile phase is restricted in LC–MS methods. As the ion-pair reagent, tetrabutylammonium hydroxide, was not appropriate in the the mobile phase, it was omitted. Although a solvent system of water–methanol–acetic acid was used, an acid and its glycine conjugate, tentatively identified, could be well separated. Retention times (t_R) of the glycine conjugates were shorter than those obtained by using the previous mobile phase, whereas those of the substrates were longer. A decrease in the size of the peak of a substrate and a corresponding increase in that of the glycine conjugate, tentatively identified, were observed on the chromatogram. When authentic glycine conjugates were available, each glycine conjugate could be detected by comparing the retention time with that of the authentic glycine conjugate. However, there were only a few synthetic glycine conjugates available. Therefore, LC–APCI-MS was applied to identify each increasing peak as the glycine conjugate of each acid.

Fig. 1 shows UV detection and extracted ion profiles (full-scan mode) of the supernatant obtained after incubation with (A) 4-methoxybenzoic and (B) 3-chlorobenzoic acid in the mouse liver mitochondria. The UV traces each showed two peaks, respectively. Individual peaks were monitored by the $[M - H]^-$ ions of the acids or their glycine conjugates. Each increasing peak was identified as the glycine conjugate from the mass spectral fragmentation patterns. In addition, the chromatographic properties for a series of acids and their glycine conjugates were expressed as the relative t_R values (t_R of conjugate/t_R of parent acid). When various acids and their glycine conjugates could be separated using mobile phase (a) or (b), the relative t_R values were 0.36 ± 0.02 and were also constant. With mobile phase (c), the relative t_R values were 0.49 ± 0.03. These findings indicate that calculation of the relative t_R value will permit the provisional identification of an unknown conjugate.

The ionization mechanism in APCI is known to be very similar to that of CI, and therefore the molecular mass can be easily determined. However, it is necessary for identification of the metabolites to obtain structural information. The optimum analytical conditions were investigated to obtain some structural information.

The positive- and negative-ion mass spectra of benzoic acid derivatives were measured using water–methanol (50:50, v/v) as the mobile phase at a flow-rate of 1.0 ml/min in the flow-injection mode (no column). Benzoic acid reacts as a strong acid in the gas phase, resulting in the generation of negative ions in the APCI source.

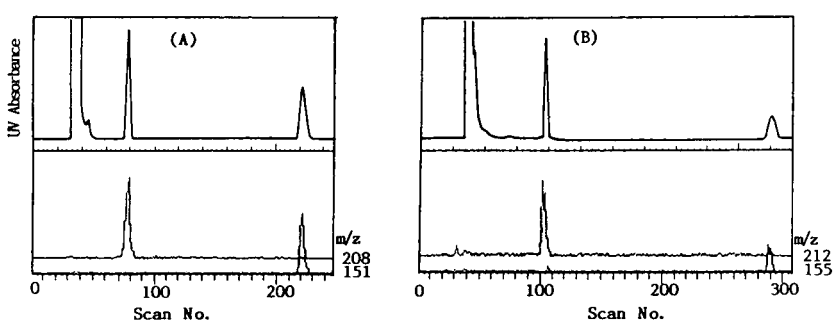

Fig. 1. Typical UV detection and extracted ion profiles of the supernatant obtained after incubation with (A) 4-methoxybenzoic acid and (B) 3-chlorobenzoic acid in mouse liver mitochondria. Detector wavelength, (A) 270 and (B) 235 nm; mobile phase, water–methanol–acetic acid, (A) 61.3:38.5:0.2 and (B) 49.8:50:0.2 (v/v/v).

Therefore, the mass spectra of the substituted benzoic acids could be achieved not in the positive- but in the negative-ion mode. Because of the background due to the mobile phase, it is difficult to obtain good mass spectra at low nebulizer temperatures, so the nebulizer temperature was set at >300°C. As acetic acid was required in the mobile phase for the HPLC separation of an acid and its glycine conjugate, the $[M-H]^-$ responses of the acids having an amino group decreased with 0.2% of acetic acid in water–methanol as the mobile phase. The negative-ion mass spectra obtained were relatively simple.

Fig. 2 shows effect of drift voltage on the negative-ion mass spectra of 4-chlorobenzoic acid. A drift voltage is necessary in order to increase the ionization efficiency and to dissociate cluster ions into a high-abundance deprotonated molecular ion. At a drift voltage of 120 V, the negative-ion mass spectrum of 4-chlorobenzoic acid gave a dominant $[M-H]^-$ ion with low-abundance cluster ions. At drift voltages >130 V, increases in the signals at m/z 111 ($[M-COOH]^-$) and 35 ($[Cl]^-$) occurred owing to collision-induced dissociation of the deprotonated molecular ion. Therefore, the drift voltage was kept at 150 V to obtain some structural information.

Figs. 3 and 4 show the negative-ion mass

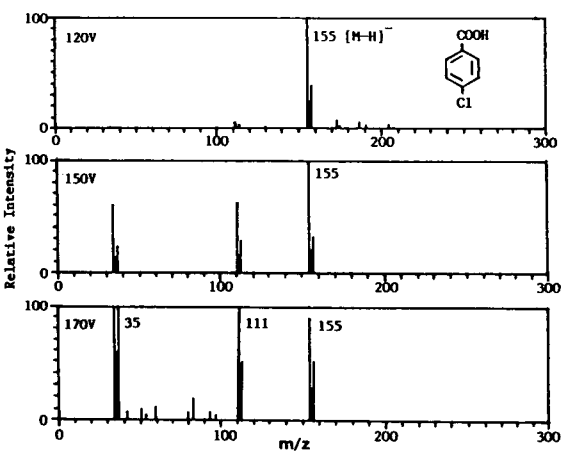

Fig. 2. Effect of drift voltage on the negative-ion mass spectra of 4-chlorobenzoic acid. Mobile phase, water–methanol (50:50, v/v); nebulizer temperature, 300°C; flow-rate, 1 ml/min; injection, flow-injection mode.

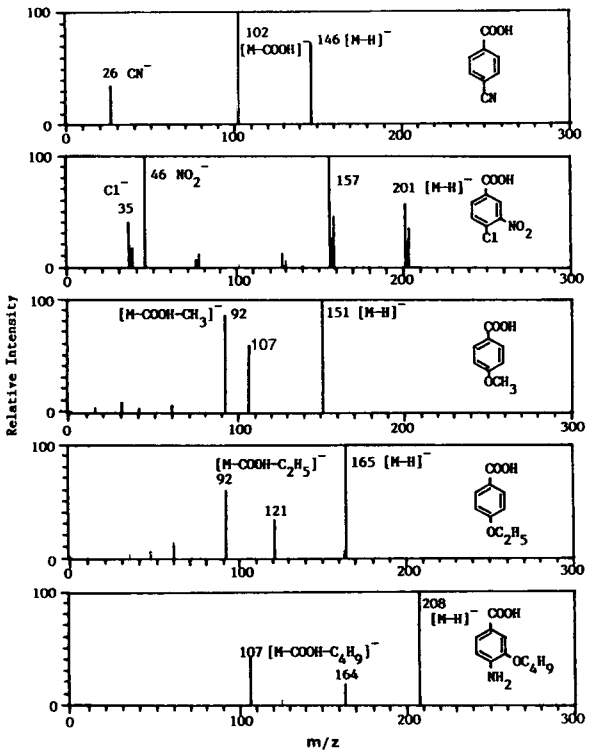

Fig. 3. Negative-ion mass spectra of 4-cyano-, 3-nitro-4-chloro-, 4-methoxy-, 4-ethoxy- and 3-butoxy-4-aminobenzoic acid. Mobile phase, water–methanol (50:50, v/v); nebulizer temperature, 300°C; flow-rate, 1 ml/min; injection, flow-injection mode.

spectra of 4-cyano-, 3-nitro-4-chloro-, 4-methoxy-, 4-ethoxy-, 3-butoxy-4-amino-, 4-acetylamino-, 4-methyl-, 4-amino- and 4-dimethylaminobenzoic acid. The same fragmentation tendency as for 4-chlorobenzoic acid was observed in the mass spectra of the acids with a cyano or a nitro group. The ions at m/z 46 and 26 indicated the possible presence of the nitro and cyano moieties, respectively. In the mass spectrum of 3-nitro-4-chlorobenzoic acid, two characteristic ions at m/z 35 and 46 were also observed. The mass spectrum of 4-methoxybenzoic acid gave $[M-H]^-$ at m/z 151, $[M-COOH]^-$ at m/z 107 and $[M-COOH-CH_3]^-$ at m/z 92. The mass spectra of 4-ethoxy- and 3-butoxy-4-aminobenzoic acid had important diagnostic ions, which were assigned to $[M-COOH-C_2H_5]^-$ at m/z 93 and $[M-COOH-C_4H_9]^-$ at m/z 107, respectively. The alkoxyl

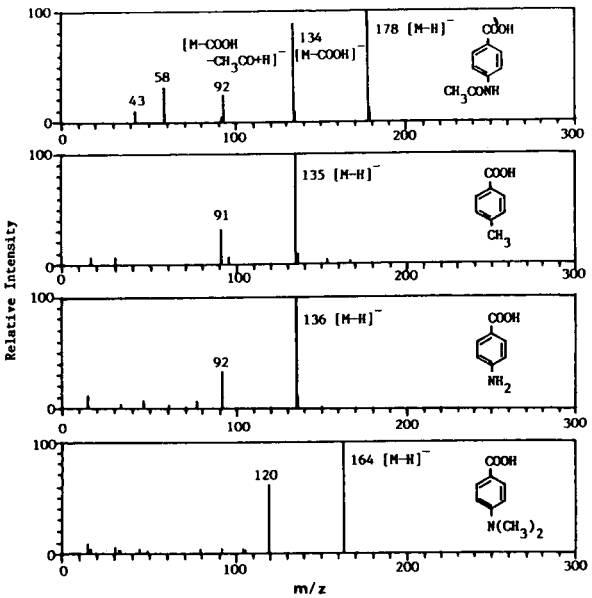

Fig. 4. Negative-ion mass spectra of 4-acetylamino-, 4-methyl-, 4-amino- and 4-dimethylaminobenzoic acid. Mobile phase, water–methanol (50:50, v/v); nebulizer temperature, 300°C; flow-rate, 1 ml/min; injection, flow-injection mode.

group gave a characteristic fragmentation representing loss of the alkyl moiety. Alkyl ions in the low-mass range did not appear. The mass spectrum of 4-acetylaminobenzoic acid gave an $[M-H]^-$ ion at m/z 178 and characteristic ions at m/z 134 ($[M-COOH]^-$), m/z 92 ($[M-COOH-CH_3CO+H]^-$), 58 ($[CH_3CONH]^-$) and 43 ($[CH_3CO]^-$). In contrast, the mass spectrum of 4-methylbenzoic acid was very simple, consisting primarily of $[M-H]^-$ and $[M-COOH]^-$ ions. At a high drift voltage of 170 V, an ion generated by cleavage of the bond between the methyl group and the benzene ring was not observed. In addition, the same observations were made for the mass spectra of the acids having an amino or a dimethylamino group.

The influence of the position of the ring substituent on the mass spectrum was also investigated. Fig. 5 shows the mass spectra of 2-, 3- and 4-nitrobenzoic acid. At a drift voltage of 150 V, no significant differences in the ion abundances at m/z 46 were observed. However, at a drift voltage of 140 V, the ion abundances at m/z 46 were increased in the order 4-position < 3-position < 2-position (on the benzene ring). On

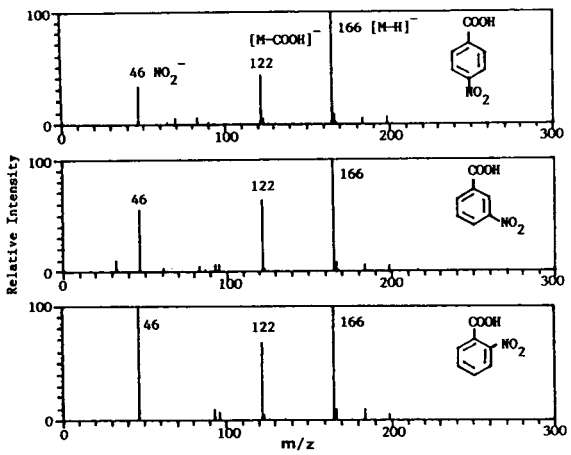

Fig. 5. Influence of the position of the nitro group on the negative-ion mass spectra of nitrobenzoic acid. Mobile phase, water–methanol (50:50, v/v); nebulizer temperature, 300°C; drift voltage, 140 V; flow-rate, 1 ml/min; injection, flow-injection mode.

the other hand, the mass spectra of methoxy-substituted benzoic acids showed different fragment ions depending on the position of the substituent. The negative-ion mass spectra of 2-, 3- and 4-methoxybenzoic acid taken at a drift voltage of 150 V are shown in Fig. 6. In the mass spectrum of 4-methoxybenzoic acid, a signal at m/z 92 corresponding to $[M-COOH-CH_3]^-$

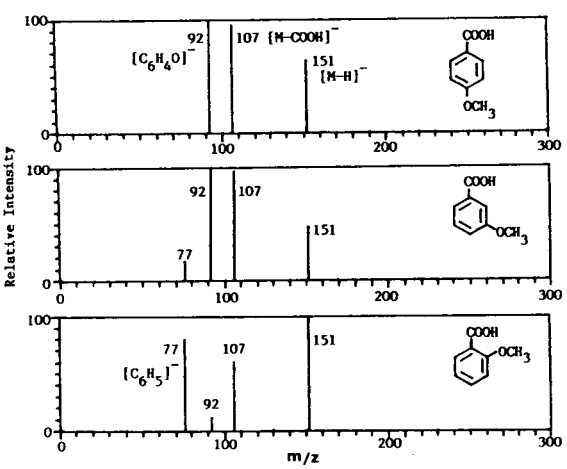

Fig. 6. Influence of the position of the methoxy group on the negative-ion mass spectra of methoxybenzoic acid. Mobile phase, water–methanol (50:50, v/v); nebulizer temperature, 300°C; drift voltage, 150 V; flow-rate, 1 ml/min; injection, flow-injection mode.

was observed. With the methoxy group in the 2-position, the signal at m/z 92 decreased, whereas that at m/z 77 corresponding to $[M - COOH - OCH_3 + H]^-$ increased compared with the 3- and 4-positions. The fragment ions due to elimination of the substituent help to identify the position of the substituent.

The mass spectra of eight glycine conjugates formed in the mouse liver mitochondria and three authentic glycine conjugates could be determined in both the positive- and negative-ion modes. HPLC separation was performed using three mobile phases at a flow-rate of 1.0 ml/min. The acids having the chloro, methyl, methoxy and ethoxy groups in either the *para-* or *meta*-position on the benzene ring showed substantial glycine conjugation. On the other hand, the acids with the cyano, nitro, amino, acetylamino and dimethylamino groups in the *para-* or *meta*-position resulted in decreases in glycine conjugation. However, the acids with the substituent at the *ortho*-position were conjugated with glycine to only a small extent or did not undergo glycine conjugation.

To obtain characteristic fragmentations of glycine conjugates, the mass spectra of 4-aminohippuric acid were taken at different drift voltages with a nebulizer temperature of 340°C. At a drift voltage of 120 V, the mass spectrum gave a dominant $[M - H]^-$ ion at m/z 193 with very low-abundant fragment ions. The mass spectrum at a drift voltage of 150 V gave an abundant $[M - H]^-$ ion with characteristic fragment ions at m/z 149 ($[M - COOH]^-$) and 92 ($[M - CONHCH_2COOH]^-$) (Table II). The drift voltage was kept at 150 V in order to promote specific fragmentations of glycine conjugates. The optimum drift voltage was constant for the nebulizer temperatures in the range 300–340°C.

The negative-ion mass spectra of glycine conjugates of 4-acetylamino-, 4-chloro-, 4-methyl- and 3-butoxy-4-aminobenzoic acid are shown in Fig. 7. All the negative-ion mass spectra gave characteristic ions of the glycine conjugates, consisting of $[M - H]^-$, $[M - COOH]^-$ and $[M - CONHCH_2COOH]^-$ ions. The mass spectra of 4-acetylamino- and 3-butoxy-4-aminohippuric acid showed more abundant additional signals at m/z 92 and 107, corresponding to characteristic losses of CH_2CO and C_4H_9 from $[M - CONHCH_2COOH]^-$ ions, respectively. In the presence of a chloro group, the chloride anion was observed in the low-mass region. The ions due to the cleavage of the substituents were also observed in the same fragmentation as with the acids.

Fig. 8 shows the positive-ion mass spectra of the glycine conjugates of 4-methyl-, 4-chloro-, 4-acetylamino- and 3-butoxy-4-aminobenzoic acid. In addition, characteristic ions of the positive-ion mass spectra of glycine conjugates are given in Table III. The positive-ion mass spectra of the glycine conjugates were different from their negative-ion mass spectra, the former

TABLE II

CHARACTERISTIC IONS IN THE NEGATIVE-ION MASS SPECTRA OF GLYCINE CONJUGATES

Values are m/z with relative intensities (%) in parentheses.

Substituent	Molecular mass	Characteristic ion			
		$[M - H]^-$	$[M - COOH]^-$	$[M - CONHCH_2COOH]^-$	Others
H	179	178 (100)	134 (9)	77 (35)	
3-Cl	213	212 (100)	168 (20)	111 (78)	35 (73)
3-CH_3	193	192 (100)	148 (10)	91 (33)	
3-CH_3O	209	208 (100)	164 (19)	107 (60)	92 (41)
4-CH_3O	209	208 (100)	164 (10)	107 (51)	92 (52)
4-NH_2	194	193 (100)	149 (4)	92 (21)	
4-C_2H_5O	223	222 (100)	178 (12)	121 (48)	92 (59)

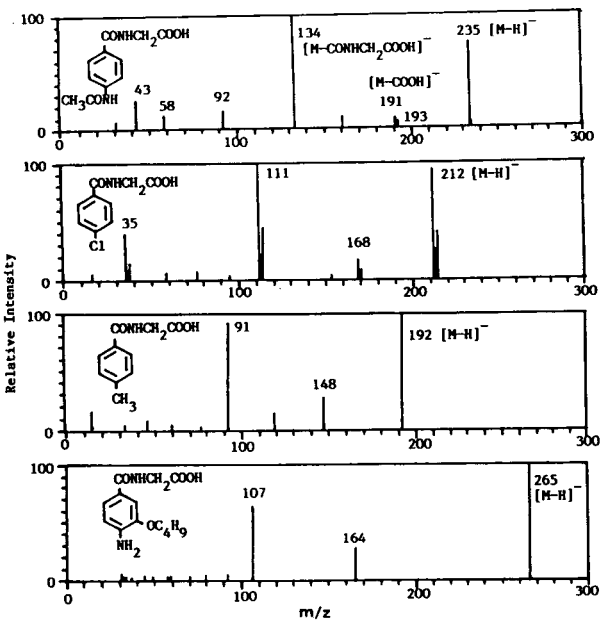

Fig. 7. Negative-ion mass spectra of the glycine conjugates of 4-acetylamino-, 4-chloro-, 4-methyl- and 3-butoxy-4-aminobenzoic acid. Column, Cosmosil $5C_8$; nebulizer temperature, 300–340°C; drift voltage, 150 V; flow-rate, 1 ml/min; mobile phase, see Table I.

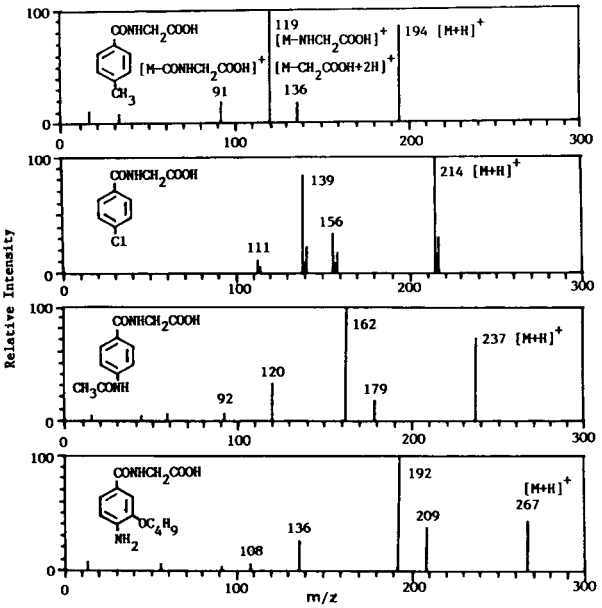

Fig. 8. Positive-ion mass spectra of the glycine conjugates of 4-methyl-, 4-chloro-, 4-acetylamino- and 3-butoxy-4-aminobenzoic acid. Column, Cosmosil $5C_8$; nebulizer temperature, 300–340°C; drift voltage, 150 V; flow-rate, 1 ml/min; mobile phase, see Table I.

providing more useful structural information for the presence of glycine. The mass spectrum of the glycine conjugate of 4-methylbenzoic acid taken at a drift voltage of 150 V gave a dominant $[M + H]^+$ ion at m/z 194 with fragment ions, which were assigned to $[M - CH_2COOH + 2H]^+$ at m/z 136, $[M - NHCH_2COOH]^+$ at m/z 119 and $[M - CONHCH_2COOH]^+$ at m/z 91. This fragmentations in the positive-ion mass spectra were characteristic for all glycine conjugates. Apart from these fragment ions, the mass spectrum of 4-acetylaminohippuric acid showed $[M - NHCH_2COOH - CH_3CO + H]^+$ at m/z 120 and $[M - CONHCH_2COOH - CH_3CO + H]^+$ at m/z 92. In the mass spectrum of 3-butoxy-4-aminohippuric acid, more abundant ions at m/z 136 and 108 were also seen, which correspond to loss of a C_4H_8 moiety from $[M - NHCH_2COOH]^+$ and $[M - CONHCH_2COOH]^+$ ions, respectively. The mass spectra of glycine conjugates having an alkoxyl group gave additional fragment ions generated by loss of an alkyl moiety from $[M - NHCH_2COOH]^+$ and $[M - CONHCH_2COOH]^+$ ions, respectively. In the presence of an alkyl or an amino group, no information on the substituents was obtained in either the positive- or negative-ion mode. The chloride anion was not observed in the low-mass region of the positive-ion mass spectra.

The detection limits for a series of substituted benzoic acids and three authentic glycine conjugates were obtained by measuring each deprotonated molecular ion in the SIM mode. The detection limits based on a signal-to-noise ratio of 3:1 were 3.2–36 pmol.

CONCLUSION

All negative-ion mass spectra of the substituted benzoic acids and their glycine conjugates gave dominant $[M - H]^-$ ions with little fragmentation. In addition, similar observations were made for the positive-ion mass spectra of glycine conjugates (the abundant $[M + H]^+$ ions in these cases). However, collision-induced dissociation caused structurally characteristic frag-

TABLE III

CHARACTERISTIC IONS IN THE POSITIVE-ION MASS SPECTRA OF GLYCINE CONJUGATES

Values are m/z with relative intensities (%) in parentheses.

Substituent	Molecular mass	Characteristic ion				
		$[M+H]^+$	$[M-CH_2COOH+2H]^+$	$[M-NHCH_2-COOH]^+$	$[M-CONHCH_2-COOH]^+$	Others
H	179	180 (100)	122 (15)	105 (90)	77 (16)	
3-Cl	213	214 (100)	156 (31)	139 (85)	111 (12)	
3-CH_3	193	194 (90)	136 (18)	119 (100)	91 (22)	
3-CH_3O	209	210 (89)	152 (19)	135 (100)		121 (15), 93 (2)
4-CH_3O	209	210 (91)	152 (10)	135 (100)		121 (21), 93 (3)
4-NH_2	194	195 (100)	137 (8)	120 (96)	92 (23)	
4-C_2H_5O	223	224 (100)	166 (12)	149 (100)		121 (19), 93 (2)

mentations. The negative-ion mass spectra of the substituted benzoic acids permitted provisional identification of the position and kind of the substituent. The negative- and positive-ion mass spectra of glycine conjugates revealed the presence of glycine and the kind of substituent from the characteristic fragmentation patterns. Mass spectral features of a variety of acids and their glycine conjugates are suitable for the detection and identification of metabolites in biological samples.

REFERENCES

1 J. Caldwell, in A. Aitio (Editor), *Conjugation Reactions in Drug Biotransformation*, Elsevier/North-Holland, Amsterdam, 1978, p. 111.
2 J. Caldwell, J.R. Idle and R.L. Smith, in T.E. Gram (Editor), *Extrahepatic Metabolism of Drugs and Other Foreign Compounds*, SP Medical and Scientific Books, New York, 1980, p. 453.
3 J. Caldwell, in W.B. Jakoby (Editor), *Metabolic Basis of Detoxication*, Academic Press, New York, 1982, p. 271.
4 H.V. de Waterbeemd, B. Testa and J. Caldwell, *J. Pharm. Pharmacol.*, 38 (1986) 14.
5 F. Kasuya, K. Igarashi and M. Fukui, *J. Pharm. Sci.*, 76 (1987) 303.
6 F. Kasuya, K. Igarashi and M. Fukui, *J. Pharmacobio-Dyn.*, 13 (1990) 432.
7 F. Kasuya, K. Igarashi and M. Fukui, *J. Pharmacobio-Dyn.*, 14 (1991) 671.
8 O.H. Lowry, N.J. Rosenbrough, A.L. Farr and R.J. Randall, *J. Biol. Chem.*, 193 (1951) 265.

Journal of Chromatography A, 654 (1993) 229–246
Elsevier Science Publishers B.V., Amsterdam

CHROM. 25 473

Universal calibration of size-exclusion chromatography for proteins in guanidinium hydrochloride including the high-molecular-mass proteins titin and nebulin

R. Nave[☆], K. Weber and M. Potschka*[☆☆]

Max Planck Institute for Biophysical Chemistry, Am Fassberg, D-3400 Göttingen (Germany)

(First received January 16th, 1992; revised manuscript received July 21st, 1993)

ABSTRACT

The chromatography of polypeptides in 6 *M* guanidinium hydrochloride (GuHCl) was studied with respect to the measurement of two ultra-large polypeptides, titin and nebulin. These proteins are integral constituents of the muscle structure, responsible for elasticity, and play an important role in muscle function. Both are outside the previously available range of calibration standards. This problem was circumvented by universal calibration in two different solvents, namely denaturing GuHCl conditions for the unknown polypeptides and buffered solutions of viruses under native assembly conditions. The accuracy of the approach was established. Two matrices were tested for their stability towards this solvent change without changing their calibration graphs. For Superose-6 the calibration changed by 10%. TSK-6000PW exhibited a congruent calibration graph for native and denaturing conditions. By extrapolation it was possible to estimate the chain molecular masses for nebulin to be 560 000 and that for T-II, the extractable form of titin, to be 2 000 000.

INTRODUCTION

The size-exclusion chromatography (SEC) of proteins under denaturing conditions is widely used to study polypeptide chain molecular masses. Sodium dodecul sulphate (SDS), urea and guanidinium hydrochloride (GuHCl) have been employed to this end [1]. GuHCl (6 *M*) under reducing conditions or with alkylated proteins seems to be the most successful [2–19]. GuHCl breaks multimeric enzymes apart, unfolds the proteins, binds to the peptide backbone and to aromatic residues [20] and induces an extended coiled conformation whose dimensions are virtually sequence independent if disulphide bonds are broken. Normally calibration of the chromatographic columns is done directly in terms of molecular mass with the aid of some reference peptides of known molecular mass. This strategy fails for large peptides for which no references exist. This paper is devoted to this case of ultra-large polypeptide chains. It attempts universal calibration valid for different solvent conditions. Native polymeric protein assemblies, which would dissociate and denature in GuHCl, were eluted at regular ionic strength and compared with denatured proteins in 6 *M* GuHCl on the same matrix. Two different matrices were tested.

Universal calibration of SEC in a broad sense is an attempt to define a unique parameter that accounts for the elution properties of all chemical substances and physical shapes. In a narrower sense it refers to the suggestion of Grubisic *et al.* [21] that this parameter is found in the hydro-

* Corresponding author.
☆ Present address: Byk Gulden Pharmaceuticals, Department of Molecular Biology, Gottlieberstrasse 25, D-7750 Konstanz, Germany.
☆☆ Present address: Porzellangasse 19/2/9, A-1090 Vienna, Austria.

0021-9673/93/$06.00 © 1993 Elsevier Science Publishers B.V. All rights reserved

dynamic volume, *viz.*, the cube of the viscosity radius, defined as [22]

$$R_\eta = \left(\frac{3}{10\pi N_L} \cdot [\eta]M\right)^{1/3} = 0.0541\ ([\eta]M)^{1/3} \quad (1)$$

where R_η is the viscosity radius (nm), $[\eta]$ is the intrinsic viscosity (ml g^{-1}), M is the molecular mass and N_L is Avogadro's number. Note that eqn. 1 is frequently misprinted [14,23]. Judgement is still empirical and lacks a profound theory. However, calibration by viscosity radii yields the best correlations and is in this regard superior to all other known measures such as diffusional Stokes radius, radius of gyration and mean linear extension, which is sometimes erroneously called contour length, and also plain molecular mass [23–29]. At present only two systems, namely schizophyllan and DNA [23,28,29], are not represented by viscosity radii or any other of the mentioned measures. A future theory that truly accounts for all data therefore will have to define a physical shape function that coincides with intrinsic viscosity under most but not all circumstances.

Universal calibration is an idealized concept that excludes adsorptive effects which often trouble real systems. In choosing a proper solvent and matrix for a given solute, ideal conditions may be approached. Universal calibration demands that in a given eluent all solutes elute by a common criterion as long as adsorption is lacking. This criterion must further be independent of the matrix chosen except for the excluded case of adsorption. It does not require that two eluents given identical calibrations. In fact, the early matrices for biological applications all changed their pore structures with changes in pH and ionic strength. Thus each eluent required its own calibration. Only the recent high-performance matrices are rigid enough to withstand simple solvent changes. It was therefore possible to extend the theory of universal calibration to a comparison of different solvent conditions. All ionic effects are now accounted by a single theory [23]. This theory further predicts that different chemical classes follow a unique calibration only if solvation is explicitly accounted for. This concept has also been extended to GuHCl solutions. It has been noted that the viscosity radius is the most appropriate measure [9,10,13,14,18]. Thus a common congruent calibration in terms of viscosity radii was constructed on the silicate TSK-SW matrix [10,14] and on Sepharose, a cross-linked agarose [18]. One study even included 8 *M* urea and SDS in their common congruent calibration [10]. On the other hand, Eriksson and Hjertén [16] found that a different cross-linked agarose is unstable towards chemical exposure to GuHCl and completely changes pore size.

According to theory, R_η and R_s are virtually identical for globular compact proteins. For spherical particles R_s is measured with greater precision that intrinsic viscosity and is thus substituted for R_η. For elongated shapes $R_\eta > R_s$, the exact value of which depends on quaternary structure and flexibility. For denatured coils R_η is greater than R_s typically by about 15% based on experimental figures. A simple theory predicts about a 30% difference [30]. Thus data for GuHCl conditions appear early on the basis of R_s. Horiike *et al.* [14] most explicitly demonstrated this fact chromatographically. They thus confirmed that congruent calibration fails for diffusional Stokes radii as a putative universal parameter. Excellent correlation is obtained, however, using viscosity radii. To complicate matters, native proteins show gradually decreasing elution volumes with increasing GuHCl concentration prior to denaturation [31–34]. One possible explanation calls for a premature elution of proteins in GuHCl and universal calibration fails even in terms of R_η.

Notwithstanding these difficulties, we were able to assign molecular masses of unknown polypeptides in 6 *M* GuHCl on TSK-6000PW by reference to native proteins and viruses and to calculate the chain molecular masses. This is a particularly intriguing task for titin, probably the largest single polypeptide chain every found. Titin, previously also called connectin, is a major component of the elastic filaments in sarcomeric muscles (for reviews see refs. 35–37). Direct solubilization of myofibrils by SDS yields a doublet on polyacrylamide gel electrophoresis (SDS-PAGE), T-I and T-II. In the sarcomer, the ends of the titin T-I molecules are attached to

the M band and the Z band, respectively, and titin keeps the acto-myosin filament system in register. It also provides an elastic component beyond the acto-myosin system. Titin I–II is a proteolytic derivative of the parent T-I molecule, as shown by monoclonal antibodies, and it stretches from the M band to very close to the Z line of the sarcomer [38]. It is the only titin species extractable under native conditions in a variety of protocols [39–42] and will be characterized here. Molecular mass estimates based on SDS-PAGE, chromatography, ultracentrifugation and electron microscopy range from 800 000 to 2 800 000 [17,39–45] (see Table I). With our method we obtain a molecular mass of 2 000 000 for titin T-II. Titin T-I is estimated to be 200 000 [44] to (more likely) 700 000 [39,46] larger than the 2 000 000 M_r titin T-II. Native titin T-II is a mixture of aggregates that separates into two peaks on chromatography on TSK-6000PW. Titin T-II_A, still a broad inhomogeneous band, contains two M-line associated proteins of M_r 165 000 and 190 000 by SDS-PAGE on overloaded gels. They are visualized by electron microscopy as globular beads on one end of the titin molecule. They help to associate titin molecules and several, mostly two, titin tails protrude from these knobs as judged by electron microscopy [42]. These proteins dissociate in 4 *M* GuHCl and are removed in SEC by virtue of their size. The titin band in 4 *M* GuHCl lacks these associated proteins as judged by SDS-PAGE. The present study identifies titin T-II_B as the native monomer. Mild trypsin treatment of either T-II_A or T-II_B removes the mentioned terminal head domain (knobs) and causes T-II_A to dissociate. The resulting tail domain elutes identically regardless of whether it originates from T-II_A or T-II_B and lacks the associated proteins. It elutes about 0.1 ml after the native T-II_B band, in line with the observation that inadvertent proteolysis enlarges the apparent T-II_B peak. This small retention difference implies that the head domain cannot be much larger than M_r *ca.* 50 000. Titin T-II and the tail are not distinguished by SDS-PAGE.

As a second large polypeptide, we studied another myofibrillar protein, nebulin, which is only present in skeletal muscle. Much less is known about this protein, with a molecular mass

TABLE I

DATA ON SIZE AND SHAPE OF TITIN

Type of titin	Method[a]	M_r (×1000)	s (S)	R_{SEC} (nm)	Ref.
Chicken, native T-II_A/T-II_B mixture[b]	Sedimentation equilibrium	2700	17		39
Chicken, native T-II_A	SEC		27–57	75–95	42
Chicken, native T-II_B	SEC		12.5	48	42
Native T-II_B enriched mixture	–		13		40
Native T-II_B	STEM[c]	2400 ± 500			45
Rabbit, denatured T-II	SDS-PAGE based on glutaraldehyde-cross-linked myosin-H	1200			44
Chicken, denatured T-II	SDS-PAGE based on bismaleimide-cross-linked myosin-H	2100			39
Denatured T-II	SEC in 6 *M* GuHCl	800–1600			17
Rabbit, denatured T-I/II mixture	Sedimentation equilibrium in 6 *M* GuHCl	2400–2600[d]	13[e]		97
Chicken, denatured T-II	SEC in 6 *M* GuHCl	2000		53	This study

[a] Methods other than sedimentation velocity.
[b] Judged to be a mixture by comparison with other entries in this table.
[c] Scanning transmission electron microscopy.
[d] Based on partial specific volume $v = 0.727$.
[e] Authors report 4.15 S, which apparently was not corrected to unit viscosity.

in the range 500 000–900 000 calculated on the basis of its mobility in gel electrophoresis [36,39,43,46,47]. Resistant to extraction under native conditions, its size and shape are not known. However, it has been suggested that nebulin could form a fourth filament system in skeletal muscle [47–49] and may be the length regulator of thin filaments [46]. In the sarcomer, nebulin is primarily located within the I-band. Here we estimate a molecular mass of 560 000 for the monomer unit by SEC in GuHCl.

EXPERIMENTAL

Size-exclusion chromatography

The chromatographic instrumentation has been described in detail previously [24,25]. The columns consisted of a Superose-6 cross-linked agarose matrix in a 30-cm glass cartridge (Pharmacia–LKB) and a TSK6000-PW 60-cm stainless-steel column (Toso Haas–Pharmacia). Both columns have been described previously [23–26]. Flow-rates were less than 0.3 ml min^{-1}, corresponding to shear rates below 300 s^{-1} for the present experimental set-up. Absence of shear degradation was verified by SDS-PAGE (for a general discussion of shear degradation, see ref. 50). Elution was monitored by measuring the absorbance at 280 nm. Sample concentrations were kept to a minimum, *e.g.*, not exceeding 0.2 mg ml^{-1} for titin, to avoid concentration artifacts. The 6 *M* GuHCl eluent contained 0.4 m*M* β-mercaptoethanol, 50 m*M* Tris–HCl (pH 7.3) and 1 m*M* EDTA.

Materials

Most of the samples used for calibration have been described previously [24]. Briefly, we used albumin from bovine serum (Sigma A8531), alcohol dehydrogenase from yeast (Sigma A8656), aldolase from rabbit muscle (Sigma A6253), alkaline phosphatase from yeast (Sigma P9761), apoferritin from horse spleen (Sigma A3660), β-galactosidase from *Escherichia coli* (Sigma G8511, G6008), carbonic anhydrase from bovine erythrocytes (Sigma C7025), catalase from bovine liver (Sigma C100, Pharmacia 17044101), cytochrome *c* from horse heart (Sigma C7150), bovine gamma-immunoglobulin (Sigma I5506, BioRad 1511901), myoglobin from horse heart (Sigma M1882, Bio-Rad 1511901), ovalbumin from hen egg white (Pharmacia 17044201, Bio-Rad 1511901), ovomucoic from hen egg white (Sigma T2011), phosphorylase B from rabbit muscle (Boehringer 108570), thyroglobulin from pig thyroid (Sigma T1126, Bio-Rad 1511901), human transferrin (Sigma T2252), bovine α-trypsin, urease from jack beans (Sigma U7752), ATP (grade II, Sigma A3377) and vitamin B_{12} (Bio-Rad 1511901). Tomato bushy stunt virus (TBSV) and turnip yellow mosaic virus (TYMV) were kindly provided by J. Witz, Strasbourg; bacteriophages Qβ and MS2 were a gift from C. Biebricher, Göttingen; rabbit muscle tropomyosin was a gift from A. Wegner, Bochum; chicken muscle actin was a gift from D.O. Fürst, Göttingen; human erythrocyte spectrin was provided by S. Eber, Göttingen, and the haemolymph of *Eurypelma californicum* obtained from H.J. Schneider, Munich, was used to study haemocyanin under oxidative conditions; bovine brain clathrin was a gift from E. Ungewickel, Munich; and pig neurofilament protein NF200 was a gift from N. Geisler, Göttingen. Tobacco mosaic virus (TMV) was prepared as described previously [51]. Titin, nebulin and myosin were prepared as follows.

Preparation of titin and nebulin

Native titin T-II was purified from chicken pectoralis muscle as described previously [42]. The final step was SEC through Superose-6. This material was then dialysed to buffered 6 *M* GuHCl (see above) and analysed. In addition, native titin T-II was fractionated in high-salt buffer [500 m*M* KCl, 50 m*M* Tris–HCl (pH 7.9), 2 m*M* EGTA, 1 m*M* β-mercaptoethanol] as described in detail previously [42]. The two bands $T\text{-}II_A$ and $T\text{-}II_B$ were separately dialysed to 4 *M* GuHCl and analysed.

Enriched fractions of nebulin were obtained by extraction of myofibrils from chicken breast muscle with 0.6 *M* KCl and 1 *M* KI to remove most of the actin, myosin and titin as described [38]. These "high-salt extracted myofibrils" were subsequently solubilized in 6 *M* GuHCl [50 m*M*

Tris–HCl (pH 8.6), 1 m*M* EDTA, 10 m*M* β-mercaptoethanol] and repeatedly applied to a Superose-6 SEC column equilibrated in 6 *M* GuHCl [20 m*M* Tris–HCl (pH 7.3), 1 m*M* EDTA, 0.4 m*M* β-mercaptoethanol]. Nebulin essentially eluted in the void fraction and all smaller peptides were removed. An amount of 100 μg of nebulin could be obtained per run, requiring 30 min. Fractions from repetitive runs containing nebulin were pooled. The entire preparation could be accomplished within 1 day, which minimizes the risk of proteolytic breakdown.

Titin and nebulin were detected by gel electrophoresis and immunoblotting with monoclonal antibodies as described [38].

Cross-linking of myosin

During the preparation of titin, fractions enriched in myosin were obtained [42]. A subsequent SEC step on Superose-6 in high-salt buffer [0.6 *M* NaCl, 50 m*M* Tris–HCl (pH 7.9), 1 m*M* EDTA] yielded pure myosin heavy chains. For chemical cross-linking, myosin was dialysed against a different high-salt buffer [0.6 *M* NaCl, 25 m*M* sodium borate buffer (pH 9.0)] and then treated with *p*-N,N′-phenylenedimaleimide (Sigma P3396) at room temperature [52]. The molar ratio of the reagent to myosin was 10:1 and the reaction was stopped after 30 min by adding an excess of β-mercaptoethanol. The extent of cross-linking was monitored by SDS-PAGE.

RESULTS

Reference data for denaturing conditions

It was demonstrated in the past that reduced proteins denatured in 6 *M* GuHCl are well characterized by a Mark–Houwink relationship establishing a correlation between molecular mass and intrinsic viscosity or, for that matter, viscosity radii R_η. Surprised by the small but notable lack of universal calibration mentioned in the Introduction, we decided to review all available primary reference data and recalculate the Mark–Houwink relationship. This equation is subsequently applied in Table IV to calculate calibration data for the materials actually studied and its validity is crucial. Table II lists all molecular masses, intrinsic viscosities and corresponding viscosity radii found in the literature for reduced proteins in 6 *M* GuHCl. Most of them were determined in Tanford's laboratory. Two observations (glucose oxidase [53], ovomucoid [54]) were omitted from the table and subsequent calculation because their data seemed in error [9]. Older data for myosin [55–57] were rejected. A former value for albumin [13,58] has been adjusted by new measurements [19]. Data obtained in 5 *M* GuHCl (glyceraldehyde-3-phosphate dehydrogenase [59], thyroglobulin [60], tropomyosin [61]) and 7.5 *M* GuHCl (paramyosin [1,22,61]) have not been considered. For cytochrome *c* the molecular mass for the apo-enzyme is listed in Table II. The haeme group (an extra 617 in molecular mass) is covalently attached and makes cytochrome *c* an unreliable reference. If available, molecular masses have been calculated from the protein's sequence. This explains differences between Table II and previous compilations. The data are shown in Fig. 1. The resulting correlation between viscosity radius (nm) and molecular mass is

$$R_\eta = 1.73_5 \cdot 10^{-2} M^{0.552} \quad (2)$$

with a correlation coefficient of $\bar{r} = 0.9997$. The mean accuracy, defined in the section *Accuracy of measurement* below, is $1.9 \pm 1.2\%$. This is slightly different from the coefficients normally quoted, $1.676 \cdot 10^{-2}$ and 0.555, respectively [22], but it makes no difference over the applicable data range. In conclusion, reference viscosity radii seem to be reliable.

Reference data for non-denaturing conditions

The proper definition of R_{SEC} as the ultimate ratio of universal calibration (see Discussion) is still unsettled and R_η values are currently substituted for it. For nearly spherical objects this reduces to the equality $R_\eta = R_s$. For native proteins we used the same hydrodynamic constants as previously [24]. The reference values for apoferritin and urease are debated and thus uncertain in the range 6.1–6.6 nm (discussed in ref. 62). As can be seen from the data in Table

TABLE II

INTRINSIC VISCOSITY REFERENCE DATA IN 6 *M* GuHCl

Name	Origin	M_r [a]	$[\eta]$ (ml g^{-1})	R_η (nm)	Ref.
Albumin	Bovine serum	66 463	50.1	8.08	19
Aldolase	Rabbit muscle	39 211	35.3	6.03	58
Carbonic anhydrase		29 000	29.6	5.14	22
α-Chymotrypsinogen A	Bovine pancreas	25 666	26.8	4.78	58
Cytochrome *c*	Horse heart	11 702	14.4	2.99	4
Haemoglobin (α + β) (apo)	Human	15 500	18.9	3.60	58
Insulin (A + B)	Bovine	2870	6.1	1.40	58
Lactate dehydrogenase	Bovine heart	36 500	32.4	5.72	98
β-Lactoglobulin		18 400	22.8	4.05	58
Lysozyme	Chicken	14 313	17.1	3.38	22, 99
Myoglobin (apo)	Horse	16 950	20.9	3.83	58
Myosin H-chain		224 000	107.5	15.62	22
Ovalbumin	Hen egg white	44 310[c]	34.6	6.22	98
Pepsinogen		40 000	31.5	5.84	58
ATP phosphoribosyltransferase	*Salmonella typhimurium*	33 211	31.9	5.51	100
Ribonuclease A	Bovine	13 690	16.6	3.30	58
Surface antigen 51A protein	*Paramecium aurelia*	301 500	133.4	18.54	101
Surface antigen 51B protein	*Paramecium aurelia*	260 000	115.2	16.80	101
Surface antigen 51D protein	*Paramecium aurelia*	270 000	123.0	17.39	101
Transferrin	Human	82 555[d]	50.8	8.72	4, 102
Uromodulin[b]	Human	86 000[e]	52.9	8.96	103

[a] Molecular masses are based on sequence data whenever they were available in the SWISSPROT data bank.
[b] Formerly called Tamm–Horsfall urinary glycoprotein.
[c] Based on M_r 1560 carbohydrate [104].
[d] Based on M_r 6200 carbohydrate [104].
[e] Based on 28% carbohydrate [9].

III, the assignment is ambiguous and their order of elution depends on the column used. The issue could not yet be settled. The Stokes radius for α-trypsin was taken from the diffusion coefficient [63]. The value for 27S-thyroglobulin, *i.e.*, dimers of the primary native species, is taken from interpolation of chromatographic elution on two different matrices (Superose-6 and TSK-5000PW) and should properly be called an R_{SEC} value only. The size of the spherical virus also is well established and previous values are used [24]. The calibration data for TMV are reviewed and insignificantly revised from previous choices as follows.

Depending on conditions, solutions of TMV easily aggregate or disassemble, which historically has resulted in tremendous efforts to establish proper physical constants. The now settled electron microscopic (EM) length of the virus monomer is 300 nm [64,65]; values of 280 nm [66,67] and 270 nm [68] were reported previously. EM specimen preparation may break the virus particles on drying and part of the size variation may be an artifact without correspondence to solution properties [69]. In line with this reasoning is a 270-nm preparation that was found to be infectious [70] and its solution may well have contained proper 300-nm particles. Further, the intrinsic viscosity of 270-nm preparations is identical with if not larger than that of well defined 300-nm preparations [68,71].

Based on a 300-nm EM length, the X-ray

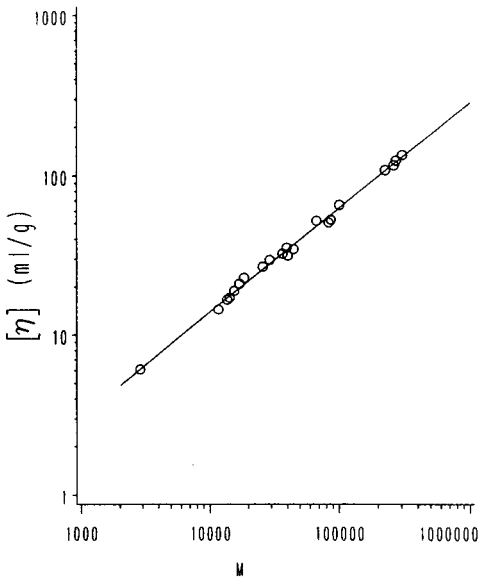

Fig. 1. Mark–Houwink relationship for proteins in 6 *M* GuHCl based on all available data given in Table II. The resulting correlation of intrinsic viscosity (ml g^{-1}) and molecular mass is $[\eta] = 3.16 \cdot 10^{-2} M^{0.66}$.

structure and the protein sequence, the molecular mass of the virus monomer is $39.4 \cdot 10^6$. This agrees well with light-scattering data of $39.0 \cdot 10^6$ [71] and $40.0 \cdot 10^6$ [72] and with values calculated from sedimentation and diffusion. At infinite dilution monomers sediment with $s^0_{20,w}$ values (in Svedberg units) of 185 S [68,73,74], 187 S [68], 188 S [71] or 198 S [69,75], albeit part of the latter data are equally represented by 190 S [69]. Sedimentation coefficients of rod-shaped objects primarily depend on the diameter and are insensitive to moderate length heterogeneity. The following diffusion coefficients, D^0_{20}, have been reported: $5.3 \cdot 10^{-8}$ cm^2 s^{-1} for a 270-nm preparation [68], $5.0 \cdot 10^{-8}$ cm^2 s^{-1} derived from the spreading sedimentation boundary extrapolated to the meniscus position to eliminate the effect of boundary sharpening [76], $4 \cdot 10^{-8}$ cm^2 s^{-1} as a crude determination [74], $4.4 \cdot 10^{-8}$ cm^2 s^{-1} (if the corresponding *s*-value truly were 198 S, a value of $4.6 \cdot 10^{-8}$ cm^2 s^{-1} would match the molecular mass better) [69] and $4.75 \cdot 10^{-8}$ cm^2 s^{-1} as the latest value [75]. The diffusion constant is very sensitive to length heterogeneity and measurements are less reliable than those for sedimentation coefficients. Stokes radii for TMV monomers based on diffusion measurements fall into the range 45–50 nm; larger values are undoubtedly aggregates and smaller ones fragments. Partial specific volumes (ν) have been given as 0.727, 0.730 and 0.743 ml g^{-1} [68,75]. Proper Stokes radii may also be calculated from molecular mass, *s* value and partial specific volume. Compared with diffusion measurements, the reproducibility of measured intrinsic viscosity is excellent even though it also depends heavily on the length of the rods. Values of $[\eta] = 36.7$ ml g^{-1} [71] for a 300-nm preparation [65], 39.0 ml g^{-1} for a 270-nm preparation [68], 36.5 ml g^{-1} [74], 37.0 ml g^{-1} [77] and 32.0 ml g^{-1} [78] have been reported. Together with the molecular mass the viscosity radius is $R_\eta = 62$ nm. Eqn. 3 in ref. 24 uniquely relates R_η and R_s and together with sedimentation coefficients sets the most likely value as $R_s = 49$ nm. This yields excellent agreement with the EM length using eqn. 2 of ref. 24. (Note that earlier equations based on ellipsoidal shapes give wrong results [24,71].) All the above parameters are interrelated by well established hydrodynamic relationships [24] and may be cross-checked. The following is an optimized balanced data set for TMV virus monomers: $M = 39.4 \cdot 10^6$, $s^0_{20,w} = 191$ S, $D^0_{20} = 4.4 \cdot 10^{-8}$ cm^2 s^{-1}, $[\eta] = 37$ ml g^{-1}, $\upsilon = 0.730$ ml g^{-1}, hydration $H = 0.7$ g H_2O g^{-1}, frictional ratio $f/f_0 = 2.2$, length $L = 300$ nm, 2130 subunits, $R_s = 49$ nm, $R_\eta = 62$ nm.

It is possible to prepare nearly pure preparations of virus monomers, but depending on solution conditions and age of the sample an additional sedimentation boundary may appear and physical parameters of such mixtures change. This extra boundary has a sedimentation coefficient of 220 S [73], 216 S [68] or 210 S [74], as would be expected for an axial dimer of the above-described monomeric virus particle. Disaggregation of virus proceeds in discrete steps owing to the preferential affinity of the RNA sequence to the coat protein [79] and yields what is called partially stripped viruses. The latter seem preferentially to induce aggregation [69] and a large fraction of the observed aggregates may therefore be shorter than proper dimers [68,80]. Like sedimentation, SEC also yields separate peaks but so far no preparative amounts

TABLE III

ELUTION VOLUMES OF NATIVE PROTEINS AND VIRUSES (NON-DENATURING CONDITIONS)

Sample	R_η [a] (nm)	V (ml)				
		Superose-6			TSK-6000PW	
		I = 100 mM, pH = 8.0 (40 mM borate, 98 mM NaF)	I = 214 mM, pH = 7.0 (100 mM Na phosphate)	I = 1214 mM, pH = 7.0 (100 mM Na phosphate, 1000 mM NaCl)	I = 60 mM, pH = 8.0 (40 mM borate, 58 mM NaF)	I = 202 mM, pH = 6.86 (6 mM Na_2HPO_4, 2 mM NaH_2PO_4, 1 mM EDTA-Na_2, 179 mM NaCl)
TMV dimer	(117)				13.30	13.21
TMV	62	7.01 (void)			15.08	14.85
Spectrin, tetramer	21.8	8.37			18.17	
TBSV	17.2[b]	9.33			18.7	
TYMV	15.1[b]	10.03			19.11	19.12
Spectrin, dimer	14.1	10.15			19.21	19.28
Qβ	14.3[b]	10.59			19.17	
MS2	13.9[b]	10.59			19.37	19.63
Thyroglobulin 27S[c]	12.1[d]	11.22	11.42	11.45		
Haemocyanin	10.8[b]	11.78	12.18		19.80	19.84
Thyroglobulin 19S[c]	8.6[b]	12.98	13.26	13.21	20.07	20.22
β-Galactosidase	6.86[b]	14.33				
Urease	6.34[b]	14.55			20.78	
Apoferritin	6.06[b]	14.85			20.60	
Catalase	5.23[b]	16.17			20.90	
Immunoglobulin G	5.23[b]	16.18	15.96	16.15		
Alcohol dehydrogenase	4.55[b]	16.34				
Albumin, bovine serum	3.62[b]	16.72			21.16	
Alkaline phosphatase	3.30[b]	16.99			21.35	21.65
Ovalbumin	2.83[b]	17.65	17.91	17.85		
Ovomucoid	2.75[b]	17.45				
Carbonic anhydrase	2.01[b]	18.50				
α-Trypsin	1.95[b]		18.67			
Myoglobin	1.91[b]	18.89	18.69	18.74		
ATP	–	20.30				
Cytochrome c	1.63[b]	21.08			22.5	
Vitamin B_{12} (V_{TOT})	–	21.72	21.78	22.35	23.0	22.90

[a] For asymmetric particles true R_η values are listed.
[b] For known spherical particles the R_s value has been used instead of proper values of intrinsic viscosity.
[c] 19S is the major species of 670 000 molecular mass.
[d] R_{SEC} value (see text).

of pure "dimers" have been isolated for detailed studies. A value of $[\eta]_{dimer} = 140$ ml g^{-1} may be calculated from a Mark–Houwink relationship [23]. Intrinsic viscosity measurement of a mixture of 61% monomer and 39% dimers (80.7 ml g^{-1}) is slightly larger than expected for true 600 nm dimers, which contradicts the lower apparent size of EM images [68]. This leads to $R_\eta = 117$ (±3) nm, with the upper bound for true dimers and the lower bound for worst case fragments. A value of 115 nm was obtained previously from SEC by extrapolating the calibration graph beyond the TMV monomer peak [24]. Even though the term "dimer" may be partly misleading, one is confronted with a well reproducible preparation. Mixtures have also been studied by

quasi-elastic light scattering [81] and by diffusion [82], but their composition remained unrecognized. Occasionally distinctly larger aggregates have also been observed.

In terms of hydrodynamics, TMV is probably the best characterized high-molecular-mass biopolymer. Of the few similar-sized viruses that are known, it is the only one readily available for routine analysis. The behaviour of DNA, albeit extensively studied, is not yet sufficiently understood. A limited number of synthetic flexible chain polymers, albeit heterogeneous in size, might be used in a future study to secure the present calibration graph in the ultra-high molecular mass region. Any SEC study calibrated by TMV, other viruses or chain polymers obviously depends on the reliability of the reference data and its results are subject to any revision of those.

Attempted universal calibration for Superose-6

We started our study on Superose-6, which has a convenient size range to compare native proteins with those denatured in GuHCl. Table III specifies the viscosity radii of native reference compounds and presents elution volumes. Note that these values depend on the actual filling volume of the column and may also suffer from batch-to-bach variability in matrix production. Hence these elution volumes are representative for the brand but may may differ slightly for different fillings. Earlier investigations have shown that elution volumes do in any case depend strongly on the ionic strength [23,25,27]. For repulsive interaction R varies at low ionic strength with $I^{-1/2}$ and normally levels off around $I = 100$–200 mM ionic strength. Table III shows that for Superose-6 there is little further difference for 1 M salt. Elution volumes were the same with and without 0.4 mM β-mercaptoethanol in the presence of a helium purge. Note that there is a significant drift of vitamin B_{12} elution volumes with increasing salt which is not paralleled by proteins. Similar observations have been made previously on TSK-5000PW [25] and TSK-6000PW [23].

The eluent was then switched to 6 M GuHCl (see Experimental) and the proper set of reference standards was measured (Table IV). This type is normally the sole set studied for GuHCl

TABLE IV

ELUTION VOLUMES OF DENATURED PROTEINS IN 6 M GuHCl

Sample	M_r (×1000)	R_η (nm)		V (ml)	
		Table II	Calc. with eqn. 2	Superose-6	TSK-6000PW
Blue dextran	2000		~25[a]	7.04	
Myosin, cross-linked H-chain dimer	448		22.85	7.86	18.24
Spectrin (monomer)	230		15.81		18.75
Myosin H-chain	224	15.62		9.22	18.93
Clathrin	190		14.23	9.85	
Neurofilament NF200	114[b]		10.79	10.75	
β-Galactosidase	116.4		10.86	11.60	19.93
Phosphorylase B	97.2		9.83	11.82	20.05
Transferrin	82.6	8.72		12.50	
Albumin, bovine serum	66.5	8.19		12.80	20.76
Immunoglobulin G, H-chain	49.5		6.77	13.82	20.90
Actin	41.8		6.17	14.15	21.27
Aldolase	39.2	6.03		14.20	
Immunoglobulin G, L-chain	23.5		4.49	15.65	
ATP	–			19.80	

[a] Estimated from eqn. 1 with $[\eta] \approx 50$ [83].

[b] Estimated from a sequence mass of 109.587 plus up to 4.750 bound phosphate [105].

conditions. Again calibration data are listed, some directly from Table II and others calculated via eqn. 2 from the known molecular mass. Blue dextran, which is included in the list, is a heterogeneous polysaccharide [83] which is at least partially included in the separation range of Superose-6 and thus is unsuitable to measure the void volume. In addition to the reference data, Table IV also presents the elution volumes for the particular columns employed in this study. Fig. 2 presents the data for Superose-6. Both data sets give log–linear relationships between R_η and V (ml) in the first 60% of the separation range and this is the range recommended for analysis, but the calibrations differ by 10% in R_η or 0.5 ml in elution volume. This means that the protein coils appear to be 10% larger than predicted from their intrinsic viscosities in 6 M GuHCl. However, even blue dextran and, more

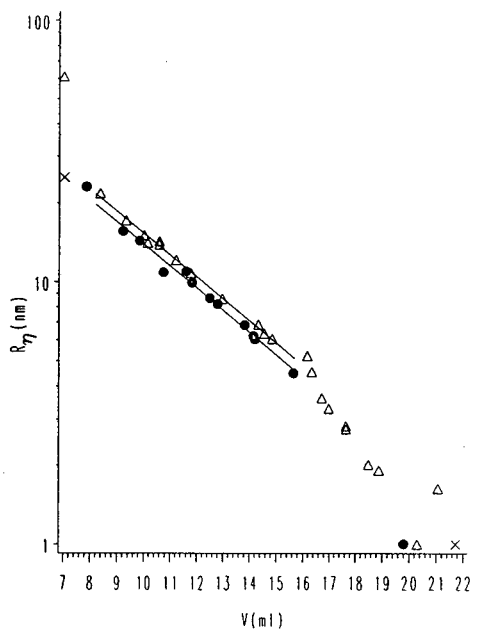

Fig. 2. Calibration of Superose-6. (△) Native proteins, viruses and ATP and (×) vitamin B_{12} at ionic strength $I = 100$ mM; data from Table III. (●) Denatured polypeptides and (×) blue dextran in 6 M GuHCl; data from Table IV. The log–linear calibration range extends from about 7.5 to 16 ml (solid lines); subsequently the calibration graph bends downwards. Cytochrome c is obviously somewhat adsorbed. Calibration of native and denatured conditions is virtually parallel but offset by about 0.5 ml in volume or 10% in R_η.

significantly, ATP are shifted by the same amount. Note that ATP, being charged, elutes differently from vitamin B_{12} and so will a number of small molecule markers. This illustrates the bias introduced in determining V_{TOT}.

The observed premature elution of proteins in GuHCl may have two reasons. The most likely is that the cross-linked agarose matrix changed conformation. Alternatively, elution simply would be premature and demonstrate once more that R_η is not the ultimate answer to universal calibration. However, if the latter were true, the effect had to be reproduced on a different matrix as universal calibration is assumed to be independent of the matrix.

Universal calibration for TSK-6000PW

We therefore repeated the measurement on a different matrix. The TSK-PW matrix is a hydrophilic polymer, albeit more hydrophobic than Superose, and TSK-6000PW is designed for the study of extremely large particles with viscosity radii above 10 nm up to at least 200 nm. Fig. 3 presents the data from Tables III and IV graphically and demonstrates a log–linear calibration in this size range which is only slightly dependent of ionic strength above 60 mM (up to at least 202 mM). This calibration is indirectly supported by a number of DNA standards that elute slightly differently but with a parallel calibration graph [23]. Some discrepancies do arise, however, in the last 40% of the separation range. This is the range after the bend of the calibration graph and is not recommended for analysis. In contrast to the range $R_\eta > 10$ nm there is a definite ionic strength dependence of these smaller native samples (difference between $I = 60$ and 202 mM) which predicts an even larger discrepancy of the GuHCl data ($I = 6$ M), as observed. It is difficult to judge whether in addition the matrix is also changing for this size range and TSK-PW may be less resistant to exposure to GuHCl than one would wish. However, for those peptides having a viscosity radius in the linear working range of the column, a congruent universal calibration between denatured proteins in 6 M GuHCl and native viruses is obtained. TSK-PW thus appears to be usable for dual solvent experiments like TSK-SW [14] supposedly is. The different pat-

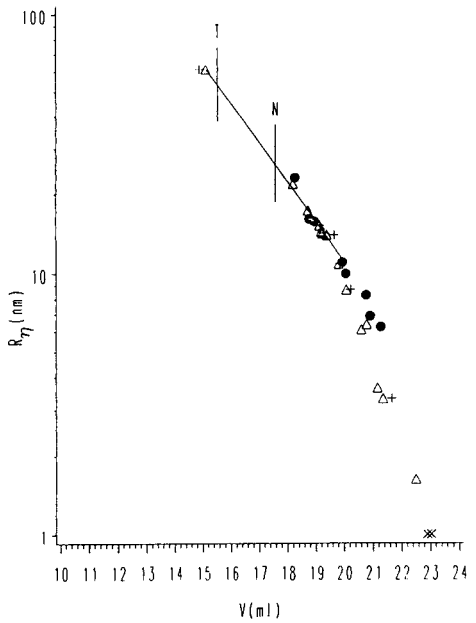

Fig. 3. Universal calibration of TSK-6000PW. Native proteins and viruses at ionic strength $I = (\triangle)$ 60 mM and (+) 202 mM. (×) Vitamin B_{12} in both conditions; data from Table III. (●) Denatured polypeptides in 6 M GuHCl; data from Table IV. Elution volume measured for titin (T) is 15.5 ml and for nebulin (N) 17.54 ml. The calibration graph was fitted for the linear range of the $I = 60$ mM data but is valid for all data in the range 10–62 nm (solid line).

terns observed with Superose-6 and TSK-6000PW clearly evade a common mechanism other than to assume that Superose is indeed unstable to exposure to GuHCl.

Cross-linked myosin

The cross-linked dimer of myosin heavy chain eluted slightly later in GuHCl than expected from eqn. 2. Cross-linked proteins are branched polymers and not strictly comparable to linear-chain polypeptides. In principle, such a deviation is therefore to be expected. The actual size of cross-linked proteins depends critically on the extent of cross-linking and also on the type of cross-linker. For example, studies of fibrinogen have amply demonstrated that glutaraldehyde completely contracts the chain. Our preparation of myosin seems fairly well behaved, but a heavy reliance on cross-linked samples may lead to erroneous results.

Neurofilament protein

Apart from the cross-linked myosin, only the largest of the neurofilament triplet proteins, NF200, deviated substantially from calibration in GuHCl. Designated "200" for its apparent molecular mass by SDS-PAGE, it elutes from the GuHCl column like an M_r 140 000 protein [84]. Its true sequence of M_r 110 000 is only slightly larger than that of the medium neurofilament protein NF145. It is heavily phosphorylated, which may be the reason for abnormal behaviour in GuHCl. Still, chromatography in GuHCl gives a smaller error than SDS-PAGE.

Accuracy of measurement

The partition radius R_{SEC} is the radius read off the mutual calibration graph. The bias is due to uncertainties in the calibration data themselves and due to interfacial interactions that are only present in the porous matrix and not in the bulk solvent where calibration data had been measured. Table V lists R_{SEC} values for two sets of conditions. Note that the values depend on the matrix used. Comparison with similar reports by other workers further indicates that they are certainly biased by the choice of reference compounds on which they are based. The mean accuracy was computed by omitting one sample at a time and calculating the percentage deviation from the residual calibration graph. These percentage deviations were then averaged. The mean accuracy for the native Superose-6 data is $3.2 \pm 2.2\%$ for the linear calibration range (see Fig. 2). That for the GuHCl data on Superose-6 is $3.1 \pm 2.6\%$. This is slightly worse than the accuracy of eqn. 2 itself. For TSK-6000PW, native conditions at $I = 60$ mM, the corresponding figure is $2.4 \pm 1.7\%$ for the linear calibration range (see Fig. 3). Merging all data obtained on TSK-6000PW in the linear range (both native and GuHCl), the figure is $4.6 \pm 4.1\%$. The dual solvent method is therefore clearly less accurate than single solvent calibrations. However, even the accuracy of matching R_η by R_{SEC} in the single solvent method is significantly lower than the precision of measurement, *i.e.*, the reproducibility in the determination of elution volumes, which is better than 1%. These discrepancies may in part be due to

TABLE V

PARTITION RADIUS R_{SEC} UNDER NON-DENATURING CONDITIONS

Sample	R_η (nm)	R_{SEC} (nm)	
		Superose-6 (I = 100 mM)	TSK-6000PW (I = 60 mM)
TMV	62		61.6
Spectrin, tetramer	21.8	21.0	20.8
TBSV	17.2	17.5	17.3
TYMV	15.1	15.3	15.0
Spectrin, dimer	14.1	14.9	14.5
Qβ	14.3	13.7	14.7
MS2	13.9	13.7	13.7
Thyroglobulin, dimer		12.1	
Haemocyanin	10.8	10.9	
Thyroglobin	8.6	8.67	
β-Galactosidase	6.86	6.69	
Urease	6.34	6.41	
Apoferritin	6.06	6.05	

inaccurate hydrodynamic reference data, but certainly also include minor systematic differences between R_η and R_{SEC} that have not previously been addressed.

Titin and nebulin

The theory presented and experimental data support the use of calibration graphs for TSK6000-PW outside the range accessible to monomeric polypeptides for both native and denatured GuHCl conditions. It is therefore straightforward to prepare unknown samples of titin or nebulin in 6 M GuHCl and to measure their elution volumes. Both native fractions of titin, T-II$_A$ and T-II$_B$, yielded identical elution volumes in GuHCl and lacked associated proteins as judged by SDS-PAGE. These elution volumes, 15.5 ml for titin T-II and 17.54 ml for nebulin, are then converted to viscosity radii via the universal calibration graph in Fig. 3. One obtains R_η = 53 nm for titin T-II and R_η = 26 nm for nebulin, each denatured in 6 M GuHCl. Subsequently the viscosity radius is converted into molecular mass via extrapolation of the Mark–Houwink relationship (eqn. 2), which strictly had only been obtained for the M_r range 2870–301 500. One obtains 2 000 000 for titin T-II and 560 000 for nebulin. Both proteins, in particular titin, are indeed extremely large.

DISCUSSION

Universal calibration

For isotropic random pore size distributions, theory predicts that the mean linear extension (L-measure) uniquely defines elution of all shapes [85], whereas viscosity radius does not [86]. Experimentally this is clearly not the case [23,24]. The majority of polymer types elute congruently in terms of their viscosity radii R_η, including the flexible and bent rod spectrin with spherical viruses in the present study (Table III). There are only two well established systems, schizophyllan and DNA, where the universal size parameter R_{SEC} seems to be larger than R_η but smaller than $L/2$ [23,28]. For DNA $R_{SEC} \approx 1.15R_\eta$ based on data from a single eluent. A recent claim that even proteins and pullulan do not co-elute [29] is at variance with numerous previous assessments regarding universal calibration of solid spheres and flexible chain polymers (reviewed in ref. 23), including work by the same group [28]. The admittedly unpleasant uncertainty regarding the principles of the SEC mecha-

nism cannot negate useful correlations of a more limited nature. Thus, comparison of solid spherical native proteins and viruses with nearly ideal flexible chains of the denatured proteins in terms of viscosity radii R_η is not nearly as problematic as generalization to all possible structures would be. Universal calibration in terms of viscosity radii R_η may be an empirical coincidence, but available theory also is insufficient: (1) real porous matrices are hardly ideal random and isotropic by the obvious need for ingress and egress of solutes; (2) pore walls are not plane but curved; (3) alignment of asymmetric units is energetically favoured; and (4) excess frictional drag may perturb chain–polymer configurations (a detailed account on the theory is in preparation).

Comparison of native proteins and viruses, which are more or less compact spheres, and of polypeptides denatured by GuHCl, which are charged random coils, may improve our perspectives of universal calibration, but matters are complicated. GuHCl is a chaotropic agent that reportedly affects the structure of gel matrices. Our data support earlier evidence from Eriksson and Hjertén [16] that cross-linked agaroses tend to change pore size on exposure to GuHCl. More remarkable is the reported congruent universal calibration on Sepharose, a different type of cross-linked agarose [18].

Horiike *et al.* [14] have previously established universal calibration of silicate TSK-SW with the GuHCl system and we have now extended this observation to TSK-PW. It therefore seems that universal calibration between solid spheres and charged coils holds. The deviation on Superose-6 then is explained by solvent-induced changes of the matrix itself. This does not contradict theory. Universal calibration may still hold within one given eluent. In fact, Superose yields reproducible GuHCl data that may be analysed directly but not compared with those for other solvents. Clearly, non-rigid gels may not be used for universal calibration amongst different eluents. The notion that uncharged polymer coils, such as pullulan, do deviate from solid spheres remains to be examined in more detail. For example, the intermediate case of proteins denatured in urea deserves critical observation.

Ionic strength dependence of elution

A surprisingly linear correlation between total apparent elution radius R and $I^{-1/2}$ has been observed previously for lower ionic strength in the case of repulsive interactions [23,25,26]. If this is extrapolated to high ionic strength, significant calibration differences are to be expected between $I = 100$ mM and 6 M GuHCl. That is, increasing salt would continue to shift calibration graphs to larger volumes, *i.e.*, apparently smaller sizes. This is not the case. At high ionic strength the mentioned linearity in $I^{-1/2}$ breaks down and this has been verified experimentally for native conditions. It is also expected from theory. When the diffuse double layer shrinks below a certain size, other forces, such as hydration, take over to dominate the interfacial radius contribution R_{IF}. This effect might be enhanced by the fact that at increasing ionic strength the surface potential ψ_s may cease to be maximally saturated and constant but diminishes. The actual break point depends on the magnitude of the electrostatic interaction and thus some matrices may require 200 or even 500 mM salt to match 6 M GuHCl in a dual solvent experiment, whereas others may suffice with 60 mM salt.

Non-ideal effects

Polyelectrolyte adsorption is related to an effect known as hydrophobic interaction chromatography and, if it occurs, increases with increasing salt concentration. No retarded elution has been observed with 6 M GuHCl solutions, but a compensatory change of the TSK-PW matrix structure cannot be excluded in principle. Adsorption certainly is unable to explain the GuHCl data on Superose, nor can it explain the small ionic strength difference of TMV on TSK-6000PW under non-denaturing conditions.

Denaturant gradient chromatography

GuHCl gradient chromatography is used to study details of the denaturation of proteins [31–34]. A most interesting aspect of this work is a gradual shift towards smaller elution volumes, *i.e.*, larger sizes, well before and possibly also after the sharp cooperative transition curve between the native and denatured conformation. This effect, which seems to be general, is best

demonstrated in the data for lysozyme [31] and ribonuclease [33]. Native proteins apparently enlarge their size in spite of retaining their native conformation, as judged by unchanged circular dichroism spectra. One obvious explanation is that the matrix changes its structure gradually to produce extreme points such as ones in Fig. 2 for Superose-6. Unfortunately, the workers involved did not perform a universal calibration to test this situation directly for their conditions. Convincing evidence for such a gradual shift was obtained, however, on TSK-SW [31,33], which presumably is resistant to a change in matrix structure [14]. Hence different explanations must be sought. The effect may be related to interfacial repulsion, *i.e.*, the solvation shell enlarges with preferential adsorption of bulky guanidinium ions. This may partly compensate for residual ionic strength differences. This suggestion is amenable to testing by direct force methods [87,88] with moderately increasing amounts of GuHCl well before denaturation takes place.

Proteins in GuHCl

GuHCl dissociates all known protein aggregates and induces an almost ideal random coil structure to the monomeric polypeptide chain. The size of the coil is therefore directly related to the linear sequence length. Carbohydrates, introducing branch points, would then be expected to decrease the observed size, *i.e.*, molecular masses calculated from eqn. 2 should attain an intermediate value between the total molecular mass and that for the plain polypeptide alone. However, carbohydrates do expand the chain and deviations from total molecular mass are only observed for high carbohydrate contents [9,11,16]. For the same reason, otherwise cross-linked chains may give erroneous results. Hence proteins need to be alkylated or studied under reducing conditions to break all disulphide bonds. Unreduced proteins in GuHCl have substantially smaller radii whose exact value is sequence dependent. As a representative case, consider bovine serum albumin whose unreduced GuHCl state is $[\eta] = 24.8$ ml g^{-1} instead of 50.1 ml g^{-1} for the reduced linear form [19]. Chemically cross-linked proteins are similarly expected to deviate. It was therefore very interesting to observe that our mildly cross-linked myosin preparation almost behaved like an ideal linear coil. Good results critically depend on the cross-linking conditions, however, and the procedure can hardly be recommended for general usage.

For small peptides the conventional calibration within the GuHCl system is obviously to be preferred. Using only one solvent throughout reduces the risks and uncertainties. Our analysis demonstrates that accuracy is better in a single solvent measurement. Actually, one may even calibrate directly in terms of molecular mass. For large peptides, where standards are rare or difficult to acquire, the procedure of universal calibration in two solvents on a selected rigid matrix is the method of choice. It should be mentioned that membrane proteins may also be studied if the lipid is first removed with acetone [89].

Other chaotropic agents

For chromatography GuHCl is currently the denaturant of choice to determine chain molecular masses, as denaturation by urea is frequently incomplete and the SDS–protein system supposedly violates universal calibration by eluting retarded (reviewed in ref. 23). A recent publication, however, insinuates that previous hydrodynamic constants, on which the latter judgment was based, are wrong [19]. Further studies of the SDS–protein system will be required. GuHCl chromatography also works with large polypeptides where SDS-PAGE fails (as with titin).

Accuracy of measurement

The accuracy of measurement has been reported for native proteins on Sephadex [90,91], Sepharose [92] and Sephacryl [92,93]. Differences between R_η and R_{SEC} are normally small and may indicate systematic bias due to interfacial effects. Large differences were found for membrane proteins in detergent solution on Sepharose [92], Sephacryl [92], Bio-Rad agarose [18], TSK-SW [94] and TSK-PW [94]. These figures, however, were based on R_s instead of R_η, which is not known in these cases, and the real bias may be comparable to those for other native proteins [23]. Generally, the detailed values depend on the method of calibration [93]

but the trend is typical for a given matrix. Different matrices may, however, exhibit different trends. Thyroglobulin, for example, has a similar R_{SEC} value on Superose-6 (Table V) ($R_{SEC} = 8.65$ nm) compared with $R_\eta = 8.6$ nm but a lower value on Sephacryl ($R_{SEC} = 7.93$ nm) [93]. Note, however, that this comparison may be biased by the reference standards studied in each instance. Similarly, ovalbumin has repeatedly been reported to elute prematurely ($R_{SEC} = 2.9$ nm on Sephadex [90] or even $R_{SEC} = 3.0$ nm [95]) compared with $R_\eta = 2.83$ nm. However, one report gives $R_{SEC} = 2.75$ nm on Sephacryl [93]. It is a challenging task for the future to single out and interpret systematic bias contained in this type of data. For now, let it suffice to say that errors in GuHCl and under native conditions are of comparable magnitude. As has been shown in the Results section, the accuracy of matching R_η by R_{SEC} is better than 5% in single solvent and better than 10% in dual solvent experiments.

Nebulin

Nebulin has not been isolated in native form. Most purification protocols used detergents such as SDS [38,46–48] or urea [49]. Final purification was mostly by SEC on Sephacryl S-500. The size of nebulin has been estimated so far only by SDS-PAGE and assigned values ranging from 500 000 to 900 000 [36,39,43,46,47]. The lack of well characterized standards in this size region is one reason for this large uncertainty. However, the size of nebulin is also species specific [46]. Here we describe a preparation method based on GuHCl and SEC. Nebulin is so large that all contaminants are easily removed. The subsequent analytical run on a different SEC matrix, TSK-6000PW, is straightforward and yielded a molecular mass of 560 000 for chicken pectoralis muscle. The most recent estimate by SDS-PAGE is 650 000 for this species. It is amongst the smallest types of nebulin [46].

Titin

Titin has been characterized by a variety of methods. Here we found a molecular mass for the monomeric polypeptide chain of titin T-II of 2 000 000 for the chicken type. Previously reported molecular masses exhibit wide variations (Table I), which reflects methodological limitations. The main problem is the lack of adequate calibration standards. The discrepancy in the SDS-PAGE data is an artifact of myosin cross-linking and differences in size assignment for the cross-link ladder. The previous SEC study in GuHCl may have had similar problems unless it merely relied on extrapolation of the calibration graph with resulted in the same detrimental effect. Measurement of native titin T-II is complicated by aggregation, which was not recognized initially and lead to overestimates of the molecular mass. Sedimentation equilibrium studies in 6 *M* GuHCl, on the other hand, were conducted with a mixture of titin T-I and T-II, which again give values larger than expected for pure titin T-II. All things considered, our molecular mass of 2 000 000 for titin T-II is consistent with available information (Table I). Titin originating from either T-II_A or T-II_B eluted identically in 4 *M* GuHCl. Our molecular mass revises the mass per unit length of 2700 ± 900 nm^{-1} [45] to 2200 nm^{-1}.

An interesting and possibly important facet of the present study is the close similarity of titin T-II denatured in 6 *M* GuHCl with native titin T-II_B in 600 m*M* salt. Here $R_\eta = R_{SEC} = 53$ nm, whereas native titin T-II_B has been characterized on the same column as $R_\eta = R_{SEC} = 48$ nm (Table I) [42]. First, native titin T-II_B is clearly a monomer. Using a molecular mass of 2 000 000 and *s*- value of 12.5 S with a partial specific volume of 0.727 yields $R_s = 38$ nm. The same value is calculated from the data of Maruyama *et al.* [39] for an aggregate mixture with a molecular mass of 2 700 000 and $s = 17$ S (see above). This gives strong support for our lower molecular mass value and demonstrates that Maruyama *et al.* studied a mixture of lateral aggregates. Early micrographs of titin molecules showed flexible, very long and heterogeneous strings [39–41]. Using improved specimen orientation methods before metal shadowing, titin molecules may be uniformly oriented [42], which facilitates length measurements but does not correspond to the structure in solution.

For proteins in GuHCl, experimental *s* values [58] may be analysed similarly to intrinsic vis-

cosities (eqn. 2) and the resulting correlation between diffusional Stokes radius (nm) and molecular mass is [62]

$$R_s = 2.32_0 \cdot 10^{-2} M^{0.511} \quad (3)$$

Hence one may calculate for $R_\eta = 53$ nm that titin T-II in 6 *M* GuHCl has a Stokes radius of $R_s = 38$ nm. In conclusion, native titin T-II_B is highly flexible, close to a random coil and very similar in structure to its 6 *M* GuHCl counterpart. Native titin nonetheless has a defined secondary structure as judged by circular dichroism [96]. It contains β-strands but also "random" elements. In solution titin forms elastic coils that may be stretched out to 900-nm long rods during preparation for electron microscopy [42].

CONCLUSIONS

This study represents a practical application of chromatographic technique, but at the same time it maps features relevant to a mechanism of the SEC process which remains to be identified.

At high ionic strength calibration no longer changes with $I^{-1/2}$ and rather becomes congruent for various conditions. It is therefore possible to create a combined universal calibration for several different solvents, provided that the matrix is rigid and does not change in structure with changes in solvent. The latter has to be established for every case. If conditions of rigidity are fulfilled, native assemblies may be used to establish a high-molecular-mass calibration for 6 *M* GuHCl. In this manner it was possible for the first time to characterize two ultra-large polypeptides, titin and nebulin, by SEC in 6 *M* GuHCl. Their resultant molecular masses are 560 000 for nebulin and 2 000 000 for titin T-II. Native titin T-II monomers assume a conformation in solution that is very similar to that of their denatured counterpart. Error analysis demonstrates that a dual solvent approach, which was necessary in the present study, is inherently less accurate than studies using a single solvent. Whenever possible a single solvent design should be chosen.

REFERENCES

1 C. Tanford, *Adv. Protein Chem.*, 23 (1968) 121.
2 P.F. Davison, *Science*, 161 (1968) 906.
3 W.W. Fish, K.G. Mann and C. Tanford, *J. Biol. Chem.*, 244 (1969) 4989.
4 W.W. Fish, J.A. Reynolds and C. Tanford, *J. Biol. Chem.*, 245 (1970) 5166.
5 K.G. Mann and W.W. Fish, *Methods Enzymol.*, 26 (1972) 28.
6 A.A. Ansari and R.G. Mage, *J. Chromatogr.*, 140 (1977) 98.
7 N. Ui, *Anal. Biochem.*, 97 (1979) 65.
8 Y. Kato, K. Komiya, H. Sasaki and T. Hashimoto, *J. Chromatogr.*, 193 (1980) 458.
9 B.S. Leach, J.F. Collawn Jr. and W.W. Fish, *Biochemistry*, 19 (1980) 5741.
10 T. Imamura, K. Konishi, M. Yokoyama and K. Konishi, *J. Liq. Chromatogr.*, 4 (1981) 613.
11 N. Ui, *J. Chromatogr.*, 215 (1981) 289.
12 C. Lazure, M. Dennis, J. Rochemont, N.G. Seidah and M. Chrétien, *Anal. Biochem.*, 125 (1982) 406.
13 H. Tojo, K. Horiike, K. Shiga, Y. Nishina, R. Miura, H. Watari and T. Yamano, *J. Biochem.*, 92 (1982) 1741.
14 K. Horiike, H. Tojo, T. Yamano and M. Nozaki, *J. Biochem.*, 93 (1983) 99.
15 W.O. Richter, B. Jacob and P. Schwandt, *Anal. Biochem.*, 133 (1983) 288.
16 K.-O. Eriksson and S. Hjertén, *J. Pharm. Biomed. Anal.*, 4 (1986) 63.
17 G.P. Kurzban and K. Wang, *Biophys. J.*, 51 (1987) 323a.
18 M. LeMaire, A. Viel and J.V. Møller, *Anal. Biochem.*, 177 (1989) 50.
19 N. Chikazumi and T. Ohta, *J. Liq. Chromatogr.*, 14 (1991) 403.
20 J.C. Lee and S.N. Timasheff, *Methods Enzymol.*, 61 (1979) 49.
21 Z. Grubisic, P. Rempp and H. Benoit, *J. Polym. Sci., Part B*, 5 (1967) 753.
22 W.W. Fish, *Methods Membrane Biol.*, 4 (1975) 189.
23 M. Potschka, *Macromolecules*, 24 (1991) 5023.
24 M. Potschka, *Anal. Biochem.*, 162 (1987) 47.
25 M. Potschka, *J. Chromatogr.*, 441 (1988) 239.
26 M. Potschka, R. Nave, K. Weber and N. Geisler, *Eur. J. Biochem.*, 190 (1990) 503.
27 M. Potschka, *J. Chromatogr.*, 587 (1991) 276.
28 P.L. Dubin and J.M. Principi, *Macromolecules*, 22 (1989) 1891.
29 P.L. Dubin, J.I. Kaplan, B.S. Tian and M. Mehta, *J. Chromatogr.*, 515 (1990) 37.
30 C. Tanford, *Physical Chemistry of Macromolecules*, Wiley, New York, 1967, p. 345.
31 S. Endo, Y. Saito and A. Wada, *Anal. Biochem.*, 131 (1983) 108.
32 M. Herold and K. Kirschner, *Biochemistry*, 29 (1990) 1907.

33 M. Herold, *Hewlett-Packard Application Note*, No. 12-5952-1428 (1990).
34 M. Herold and B. Leister, *J. Chromatogr.*, 539 (1991) 383.
35 K. Maruyama, *Int. Rev. Cytol.*, 104 (1986) 81.
36 K. Wang, *Cell Muscle Motility*, 6 (1985) 315.
37 J. Trinick, *Current Opinion Cell Biol.*, 3 (1991) 112.
38 D.O. Fürst, M. Osborn, R. Nave and K. Weber, *J. Cell Biol.*, 106 (1988) 1563.
39 K. Maruyama, S. Kimura, H. Yoshidomi, H. Sawada and M. Kikuchi, *J. Biochem.*, 95 (1984) 1423.
40 J. Trinick, P. Knight and A. Whiting, *J. Mol. Biol.*, 180 (1984) 331.
41 K. Wang, R. Ramirez-Mitchell and D. Palter, *Proc. Natl. Acad. Sci. U.S.A.*, 81 (1984) 3685.
42 R. Nave, D.O. Fürst and K. Weber, *J. Cell Biol.*, 109 (1989) 2177.
43 K. Wang, J. McClure and A. Tu, *Proc. Natl. Acad. Sci. U.S.A.*, 79 (1979) 3698.
44 K. Wang, *Methods Enzymol.*, 85 (1982) 264.
45 J.F. Hainfeld, J.S. Wall and K. Wang, *FEBS Lett.*, 234 (1988) 145.
46 M. Kruger, J. Wright and K. Wang, *J. Cell Biol.*, 115 (1991) 97.
47 K. Wang and C.L. Williamson, *Proc. Natl. Acad. Sci. U.S.A.*, 77 (1980) 3254.
48 K. Wang and J. Wright, *J. Cell Biol.*, 107 (1988) 2199.
49 R. Nave, D.O. Fürst and K. Weber, *FEBS Lett.*, 269 (1990) 163.
50 H.G. Barth and F.J. Carlin, Jr., *J. Liq. Chromatogr.*, 7 (1984) 1717.
51 M. Potschka, M.H.J. Koch, M.L. Adams and T.M. Schuster, *Biochemistry*, 27 (1988) 8481.
52 P. Knight and G. Offer, *Biochem. J.*, 175 (1978) 1023.
53 J.J. O'Malley and J.L. Weaver, *Biochemistry*, 11 (1972) 3527.
54 F. Ahmad and A. Salahuddin, *Int. J. Pept. Protein Res.*, 7 (1975) 417.
55 W.W. Kielley and W.F. Harrington, *Biochim. Biophys. Acta*, 41 (1960) 401.
56 J.M. Creeth and C.G. Knight, *Biochim. Biophys. Acta*, 102 (1965) 549.
57 E.F. Woods, S. Himmelfarb and W.F. Harrington, *J. Biol. Chem.*, 238 (1963) 2374.
58 C. Tanford, K. Kawahara and S. Lapanje, *J. Am. Chem. Soc.*, 89 (1967) 729.
59 W.F. Harrington and G.M. Karr, *J. Mol. Biol.*, 13 (1965) 885.
60 B. De Crombrugghe, R. Pitt-Rivers and H. Edelhoch, *J. Biol. Chem.*, 241 (1966) 2766.
61 J. Olander, M.F. Emerson and A. Holtzer, *J. Am. Chem. Soc.*, 89 (1967) 3058.
62 M. Potschka, *Landolt Börnstein, Neue Serie*, Vol. VII/2, Springer, Berlin, in preparation.
63 J.T. Edsall, in H. Neurath and K. Bailey (Editors), *The Proteins*, Vol. 1B, Academic Press, New York, 1953, p. 549.
64 R.C. Williams and R.L. Steere, *J. Am. Chem. Soc.*, 73 (1951) 2057.
65 C.E. Hall, *J. Am. Chem. Soc.*, 80 (1958) 2556.
66 T. Sigurgeirson and W.M. Stanley, *Phytopathology*, 32 (1947) 26.
67 G. Schramm and W. Wiedemann, *Z. Naturforsch., Teil B*, 6 (1951) 379.
68 M.A. Lauffer, *J. Am. Chem. Soc.*, 66 (1944) 1188.
69 G. Schramm and G. Bergold, *Z. Naturforsch., Teil B*, 2 (1947) 108.
70 M.A. Lauffer, *J. Biol. Chem.*, 151 (1943) 627.
71 H. Boedtker and N.S. Simmons, *J. Am. Chem. Soc.*, 80 (1958) 2550.
72 G. Oster, P.M. Doty and B.H. Zimm, *J. Am. Chem. Soc.*, 69 (1947) 1193.
73 R.W.G. Wyckoof, *J. Biol. Chem.*, 124 (1938) 585.
74 I. Watanabe and Y. Kawade, *Bull. Chem. Soc. Jpn.*, 26 (1953) 294.
75 H. Triebel, H. Venner and W. Kayser, *Z. Naturforsch., Teil B*, 16 (1961) 368.
76 H.K. Schachman, *J. Am. Chem. Soc.*, 73 (1951) 4808.
77 H.K. Schachman and W.J. Kauzmann, *J. Phys. Colloid Chem.*, 53 (1949) 150.
78 H.K. Schachman, *J. Am. Chem. Soc.*, 69 (1947) 1841.
79 T.M. Schuster, R.B. Scheele, M.L. Adams, S.J. Shire, J.J. Steckert and M. Potschka, *Biophys. J.*, 32 (1980) 313.
80 R.L. Steere, *Science*, 140 (1963) 1089.
81 H.Z. Cummins, F.D. Carlson, T.J. Herbert and G. Woods, *Biophys. J.*, 9 (1969) 518.
82 H. Neurath and A.M. Saum, *J. Biol. Chem.*, 126 (1938) 435.
83 K. Ohta, K. Yamaguchi, N. Jikumaru and K. Kawahara, *J. Chromatogr.*, 350 (1985) 292.
84 E. Kaufmann, N. Geisler and K. Weber, *FEBS Lett.*, 170 (1984) 81.
85 J.C. Giddings, E. Kucera, C.P. Russell and M.N. Myers, *J. Phys. Chem.*, 72 (1968) 4397.
86 E.F. Casassa, *Macromolecules*, 9 (1976) 182.
87 J.N. Israelachvili, *Intermolecular and Surface Forces*, Academic Press, London, 1985.
88 V.A. Parsegian, R.P. Rand and D.C. Rau, in S.A. Safran and N.A. Clark (Editors), *Physics of Complex and Supermolecular Fluids*, Wiley, New York, 1987, p. 115.
89 R.C. Montelaro, N. Lohrey, B. Parekh, E.W. Blakeney and C.J. Issel, *J. Virol.*, 42 (1982) 1029.
90 H.S. Warshaw and G.K. Ackers, *Anal. Biochem.*, 42 (1971) 405.
91 L.M. Siegel and K.J. Monty, *Biochim. Biophys. Acta*, 112 (1966) 346.
92 M. LeMaire, E. Rivas and J.V. Møller, *Anal. Biochem.*, 106 (1980) 12.
93 F. Cabré, E.I. Canela and M.A. Canela, *J. Chromatogr.*, 472 (1989) 347.
94 M. LeMaire, L.P. Aggerbeck, C. Monteilhet, J.P. Andersen and J.V. Møller, *Anal. Biochem.*, 154 (1986) 525.
95 C. Tanford, Y. Nozaki, J.A. Reynolds and S. Makino, *Biochemistry*, 13 (1974) 2369.

96 K. Maruyama, Y. Itoh and F. Arisaka, *FEBS Lett.*, 202 (1986) 353.
97 G.P. Kurzban and K. Wang, *Biochem. Biophys. Res. Commun.*, 150 (1988) 1155.
98 F.J. Castellino and R. Barker, *Biochemistry*, 7 (1968) 2207.
99 K.C. Aune, *Ph.D. Thesis*, Duke University, Durham, NC, 1968.
100 M.J. Voll, E. Apella and R.G. Martin, *J. Biol. Chem.*, 242 (1967) 1760.
101 A.H. Reisner, J. Rowe and H.M. Macindoe, *Biochim. Biophys. Acta*, 188 (1969) 196.
102 K.G. Mann, W.W. Fish, A.C. Cox and C. Tanford, *Biochemistry*, 9 (1970) 1348.
103 F.K. Stevenson and P.W. Kent, *Biochem. J.*, 116 (1970) 791.
104 N. Sharon, *Annu. Rev. Biochem.*, 35 (1966) 485.
105 S.M. Jones and R.C. Williams, Jr., *J. Biol. Chem.*, 257 (1982) 9902.

Journal of Chromatography A, 654 (1993) 247–254
Elsevier Science Publishers B.V., Amsterdam

CHROM. 25 529

Determination of aflatoxins by reversed-phase high-performance liquid chromatography with post-column in-line photochemical derivatization and fluorescence detection

Henry Joshua*

Merck Research Laboratories, P.O. Box 2000, Rahway, NJ 07065 (USA)

(First received May 4th, 1993; revised manuscript received August 26th, 1993)

ABSTRACT

Post-column in-line photochemical derivatization permits fluorescence detection of all four common aflatoxins B_1, B_2, G_1 and G_2. Chromatographic evidence indicates that the photolysis causes the hydration of the non-fluorescent B_1 and G_1 components to the B_{2a} and G_{2a} components respectively. Analysis of naturally contaminated corn samples show no interfering peaks and permits the determination of 1 and 0.25 ppb (w/w) of B_1 and B_2, respectively.

INTRODUCTION

Aflatoxins are a major concern as toxic, carcinogenic and mutagenic contaminants in feeds and foods [1] and are closely monitored by commercial and governmental bodies [2]. The four major aflatoxins produced by the fungi *Aspergillus flavus* and *Aspergillus parasiticus* are B_1, B_2, G_1 and G_2 (Fig. 1). The B_1 component is usually predominant [3] and is also the most toxic on a mass basis [1]. The determination of aflatoxins in food products by chromatography has recently been reviewed [4]. Reversed-phase HPLC affords separation of the components using C_{18} columns and water–acetonitrile–methanol as mobile phase. Whereas UV detection at 365 nm affords peaks for all four components, fluorescence detection (365 nm excitation, >415 nm emission) is more selective and has greater sensitivity for the B_2 and G_2 components. Sensitivity for components B_1 and G_1, however, is quite poor due to the quenching of their fluorescence by eluents used in both normal- and reversed-phase HPLC. Two basic approaches have been used to increase the fluorescence detectability of the B_1 and G_1 components in HPLC: (a) methods to decrease the quenching of fluorescence by modifying the eluent and/or the detector and (b) pre- or post-column derivatization to compounds whose fluorescence is not quenched.

Methods of reducing fluorescence quenching include, for normal-phase HPLC, switching from chloroform, dichloromethane or methanol as major components of the eluent to a mobile phase consisting mainly of toluene [5] and packing the fluorescence flow cell with silica gel [6].

For reversed-phase HPLC the addition of cyclodextrins to the mobile phase causes a decrease in the quenching of fluorescence of B_1 and G_1 [7–9].

Pre-column derivatization includes the re-

* Present address: Aura Industries, Inc., P.O. Box 898, Staten Island, NY 10314, USA.

0021-9673/93/$06.00 © 1993 Elsevier Science Publishers B.V. All rights reserved

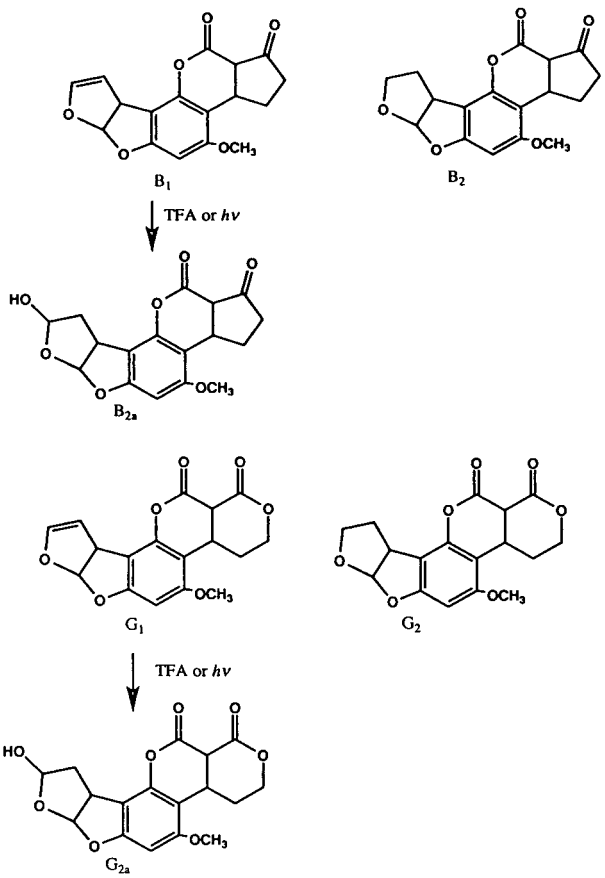

Fig. 1. Structure of the four common aflatoxins and the hydration products of B_1 and G_1.

action of B_1 and G_1 in aqueous trifluoroacetic acid (TFA) to form B_{2a} and G_{2a} (Fig. 1) whose fluorescence is not quenched under HPLC conditions [10,11]. Unfortunately, pre-column derivatization requires chemical manipulations which are time consuming, involve aggressive reagents and are difficult to automate. The reactions are not always complete and side reactions occur. Furthermore, the derivatives are usually more polar than the starting components and consequently elute earlier in reversed-phase chromatography with retention times which are similar to many polar compounds unrelated to the aflatoxins.

Similarly, B_1 and G_1 form non-quenched derivatives when reacted with iodine. A post-column application of this procedure requires the mixing of the column effluent with a stream of water saturated with iodine followed by the reaction of the flowing mixture in a heated capillary reactor [12]. The disadvantages of this procedure include the requirement to prepare the iodine solution daily, the necessity for two pumps, dilution of the eluent stream, the need to thermostat the reactor coil and insufficient day-to-day reproducibility [13]. Post-column split flow iodine addition from a solid-phase iodine reservoir to derivatize aflatoxins was reported requiring only one pump [14].

Post-column derivatization of aflatoxins with electrochemically generated bromine also produces compounds which are well detected by fluorescence detectors but requires a KOBRA electrochemical cell [13].

Post-column photochemical derivatization procedures have been reported to successfully enhance the sensitivity and selectivity of response of many analytes by a variety of detectors [15,16].

The application of photochemical derivatization for the determination of aflatoxins by HPLC with fluorescence detection has not been reported to our knowledge. We report the use of post-column photochemical derivatization to increase the fluorescence response of aflatoxins B_1 and G_1. Coupling post-column photochemical derivatization with fluorescence detection thus permits the sensitive detection of all four common aflatoxins with the advantages of simplicity, linearity of response and reproducibility without requiring chemical reagents, additional pumps or electrochemical cells. We also present chromatographic evidence which suggests that the initial photolysis reaction product of G_1 is G_{2a} (Fig. 1). It is highly probable that similarly photolysis of B_1 generates B_{2a}.

Application of this method to the analysis of naturally contaminated corn samples shows no interfering peaks for the B_1 component based on the comparison of chromatograms with and without photolysis. B_1 and B_2 can be determined at 1 and 0.25 ppb (w/w), respectively.

EXPERIMENTAL

Apparatus

The chromatographic equipment consisted of a SP 8700 XR pump, SP 4200 computing inte-

grator, SP 8780 autosampler, Spectra FOCUS rapid scanning UV detector and Spectra-Physics WINNER software (Spectra-Physics Analytical, San Jose, CA, USA). Further a Kratos FS 970 LC fluorometer set for 365 nm excitation and >415 nm emission, 0.2 μA range and 6 s time constant a Microsorb-MV 25 cm × 4.6 mm I.D. C_{18} column (Rainin, Woburn, MA, USA) thermostated at 40°C with a CJB-14 column jacket and a "PHRED" photochemical reactor with low-pressure mercury lamp were used. Knitted reactor coils: KRC 5-25, 5 m × 0.25 mm, KRC 10-25, 10 m × 0.25 mm; KRC 15-25, 15 m × 0.25 mm I.D.; KRC 5-50, 5 m × 0.5 mm; KRC 10-50, 10 m × 0.5 mm I.D.; KRC 15-50, 15 m × 0.5 mm I.D. (AURA Industries, Staten Island, NY, USA). The lengths and I.D. dimensions for these coils are nominal and before knitting. The calculated void volumes based on these values differ from those observed for the knitted coils (see text).

The flow-rate of eluent was 1.0 ml/min and 20-μl full loop injections were made. The eluent composition was water–acetonitrile–methanol (63:22:15) or where noted aqueous 0.1% TFA–acetonitrile–methanol (63:22:15).

Chemicals and solvents

An aflatoxin mixture containing components B_1 and G_1 at 1 μg/ml and B_2 and G_2 at 0.3 μg/ml in methanol (aflatoxin mixture M, cat. No. 4-6303) was purchased from Supelco, Bellefonte, PA, USA). Aflatoxins G_{2a} (cat. No. A-9151), B_1 (cat. No. A-6636), B_2 (cat. No. A-9887), G_1 (cat. No. A-0138) and G_2 (cat. No. A-0263) were purchased from Sigma, St. Louis, MO, USA). Solvents were HPLC-grade Omnisolv, EM Science, Gibbstown, NJ, USA). Water was purified through a Milli-RO4 and Milli-Q water purification system (Millipore, Milford, MA, USA).

The aflatoxin mixture was serially diluted with methanol to give B_1, G_1, and B_2, G_2 concentrations of 400, 120; 200, 60; 100, 30; and 50, 15 ng/ml. For the study of fluorescence response as a function of UV irradiation time 20-μl injections of the solution containing B_1 and G_1 at 200 ng/ml and B_2 and G_2 at 60 ng/ml was used.

The dried purified extracts of three naturally contaminated corn samples, prepared according to Wilson and Romer [17], supplied by Romer Labs. (Union, MO, USA), were each taken up in 1 ml of methanol. Each extract represented 4 g of corn. A knitted reactor coil of 15 m × 0.25 mm I.D. was used in the determination of these samples.

RESULTS AND DISCUSSION

Fluorescence response after photoirradiation

Preliminary to the photoirradiation–fluorescence experiments, a commercial mixture of aflatoxins was chromatographed using a UV detector. A 20-μl injection of a solution containing B_1 and G_1 at 1 μg/ml and the B_2 and G_2 components at 0.3 μg/ml with detection at 360 nm gave the chromatogram shown in Fig. 2.

A 15 m × 0.25 mm I.D. knitted reactor coil was attached to a polished support plate, positioned in the bottom of the photochemical reactor housing and the UV lamp assembly placed on top of the coil (Fig. 3). One end of the knitted reactor coil was attached to the outlet of the column and the other end to the flow cell of the fluorescence detector. The residence time in the coil is defined as the void volume in ml divided by the flow-rate in ml/min. The irradiation time is equivalent to the residence time when the UV light is on. The determination of the void volumes is discussed subsequently. A 20-μl injection of the aflatoxin mixture containing B_1 and G_1 at 200 ng/ml and B_2 and G_2 at 60 ng/ml with the "PHRED" light off gave the chromatogram shown in Fig. 4a, while the same injection made with the "PHRED" light on gave the chromatogram shown in Fig. 4b.

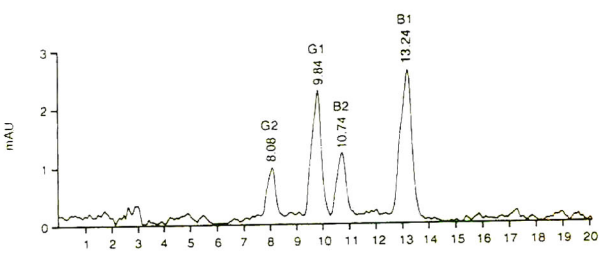

Fig. 2. Chromatogram of aflatoxins with UV detection at 360 nm, using a reversed-phase C_{18} column at 40°C and eluent consisting of water–acetonitrile–methanol (63:22:15) at 1 ml/min. The peaks at 8.08, 9.84, 10.74 and 13.24 min correspond to G_2, G_1, B_2 and B_1 respectively.

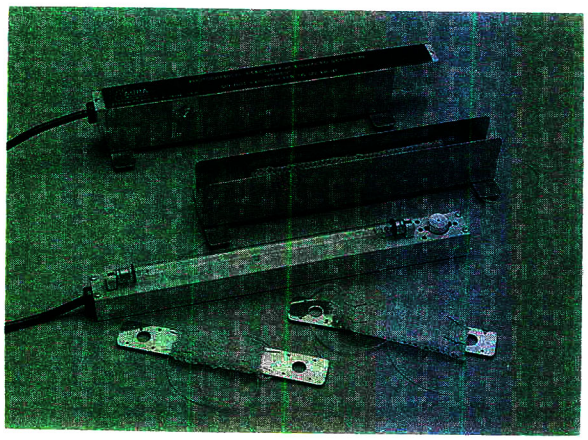

Fig. 3. Photochemical reactor components from front to rear, knitted reactor coils attached to polished support plates, UV lamp attached to lamp fixture, reactor housing with reactor coil placed inside and assembled photochemical reactor.

In Fig. 4a (light off) components G_2 (9.52 min) and B_2 (12.36 min) give significant peaks. In contrast components G_1 (*ca.* 11.4 min) and B_1 (*ca.* 15.0 min) are barely discernable. In Fig. 4b (light on), however, all four components show significant well resolved peaks. The UV irradiation consequently modified the B_1 and G_1 components to fluorescent entities.

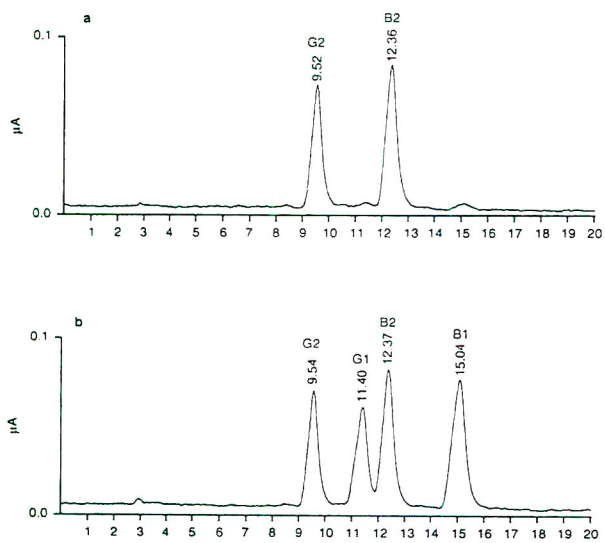

Fig. 4. Chromatogram with fluorescence detection of aflatoxins B_1, B_2, G_1 and G_2, using photochemical reactor with (a) light off and (b) light on. Time scale in min.

Linearity of fluorescence response

The linearity of response was studied with a 15 m × 0.5 mm I.D. knitted reactor coil in the reactor housing and injecting 20-μl samples of the serially diluted aflatoxin solutions starting with one containing B_1 and G_1 at 400 ng/ml and B_2 and G_2 at 120 ng/mol. The peak areas for the four components at the indicated concentrations are plotted in Fig. 5. Linear least squares analysis of the data points yields the intercept, slopes, the coefficient of determination (R^2) and the relative response (peak area/ng/ml). They are listed in Table I. No deviation from linearity was observed within the range studied for any of the four components.

Fluorescence response as a function of UV irradiation time

The irradiation time for each of the coils was determined by subtracting the retention time for G_2 with the column connected directly to the fluorescence detector from the retention time observed for G_2 with a knitted reactor coil interposed between the column and the detector. The retention time differences were also determined for B_2. The retention time differences for each KRC obtained for the G_2 and B_2 components as well as the average of these differences are collected in Table II. As a com-

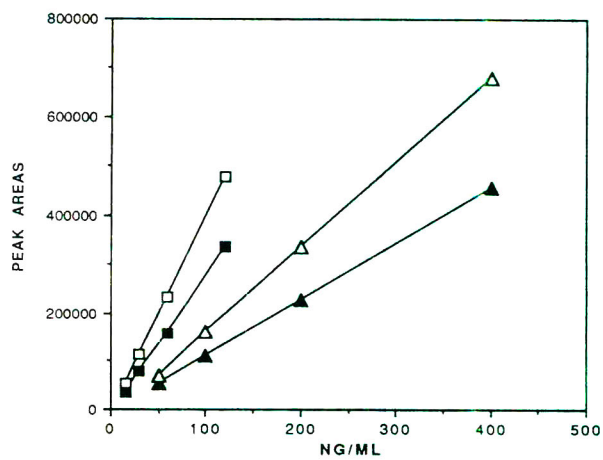

Fig. 5. Fluorescence response of aflatoxins using post-column in-line photolysis. KRC 15-50, light on, 20-μl injections. ■ = G_2; ▲ = G_1; □ = B_2; △ = B_1.

TABLE I

LINEARITY OF RESPONSE AND RELATIVE RESPONSE FOR AFLATOXINS G_2, G_1, B_2 AND B_1

Component	Intercept	Slope	R^2	Relative response
G_2	−8416.3	2858.6	1.000	0.708
G_1	−3107.8	1151.0	1.000	0.285
B_2	−6468.3	4036.7	1.000	1.00
B_1	−12401.4	1735.4	1.000	0.430

parison, Table II also lists the nominal dimension values for the coils before knitting.

Fig. 6a plots the peak areas obtained from B_2 and G_2 for identical 1.2-ng injections as a function of irradiation time in knitted reactor coils of 0.25 and 0.5 mm I.D. The response is essentially constant. In Fig. 6b the peak areas for 4-ng injections of B_1 and G_1 are similarly plotted as a function of UV irradiation time in knitted reactor coils of 0.25 and 0.5 mm I.D. There is a considerable and consistent increase in fluorescence response with irradiation time up to 1.8 min. A smaller increase between 1.8 and 3.1 min indicates that an equilibrium has been reached or that the original photolysis product(s) decomposes further to less fluorescing compounds. Experiments indicating the fate of the photolysis product(s) will be presented below.

The relative B_1/B_2 and G_1/G_2 fluorescence response normalized for equal-mass injections as a function of irradiation time is plotted in Fig. 7. The calculated B_1/B_2 and G_1/G_2 relative response values at 1.8 min are 0.39 and 0.38, respectively and at 3.1 min they are 0.43 and 0.43, respectively. The similarity in response indicates similar photolysis reactions and products for both B and G sets of components. The relative response factors listed above for the post-column photochemical irradiation derivatization can be compared to the B_1/B_2 relative response factors extracted from reports on post-column derivatizations with electrochemically generated bromine [13,18]. Fig. 3a of ref. 13 shows a B_1/B_2 fluorescence response ratio of *ca.* 0.5 for pure standards. Fig. 1b of ref. 18 shows a chromatogram of a maize sample spiked with

TABLE II

NOMINAL DIMENSIONS AND RESIDENCE TIME AT A FLOW-RATE OF 1 ml/min IN KNITTED REACTOR COILS

Coil	Length[b] (m)	I.D.[b] (mm × 100)	Volume[b] (ml)	RTG_2[c] (min)	ΔRTG_2[d] (min)	RTB_2[e] (min)	ΔRTB_2[f] (min)	AVEΔRT[g] (min)
[a]	0.5	25		8.39		11.15		
1	5	25	0.25	8.74	0.35	11.50	0.35	0.35
2	10	25	0.50	9.33	0.94	12.11	0.96	0.95
3	15	25	0.75	9.54	1.15	12.37	1.22	1.185
4	5	50	1.0	9.12	0.73	11.76	0.61	0.67
5	10	50	2.0	10.20	1.81	12.89	1.74	1.775
6	15	50	3.0	11.55	3.16	14.30	3.15	3.155

[a] Column connected directly to fluorescent detector with stainless-steel capillary.
[b] Nominal values before knitting of coil.
[c] Retention time of G_2.
[d] Difference in retention time for G_2 due to insertion of coil.
[e] Retention time of B_2.
[f] Difference in retention time for B_2 due to insertion of coil.
[g] Average of the differences in retention times due to the insertion of coil for G_2 and B_2.

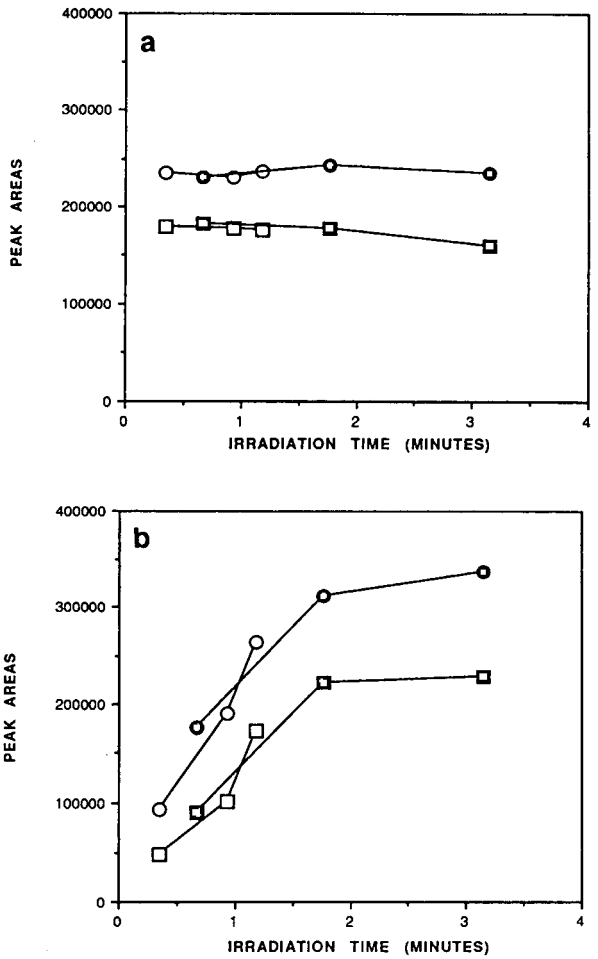

Fig. 6. Aflatoxin peak areas as a function of irradiation time in reactor coils of 0.25 mm (open symbols) and 0.5 mm I.D. (closed symbols). (a) B_2 (circles) and G_2 (squares); (b) B_1 (circles) and G_1 (squares).

aflatoxins. The B_1/B_2 relative fluorescence response calculated from peak heights after normalization for mass of injected components was *ca.* 0.40.

Characterization of photolysis product

The conversion of B_1 and G_1 on silica gel thin-layer plates by irradiation with UV light to new fluorescent more polar compounds was reported in 1967 [19]. A number of subsequent articles have also reported the photoactivation of B_1 [20–24].

For this study 500 μl of a solution containing

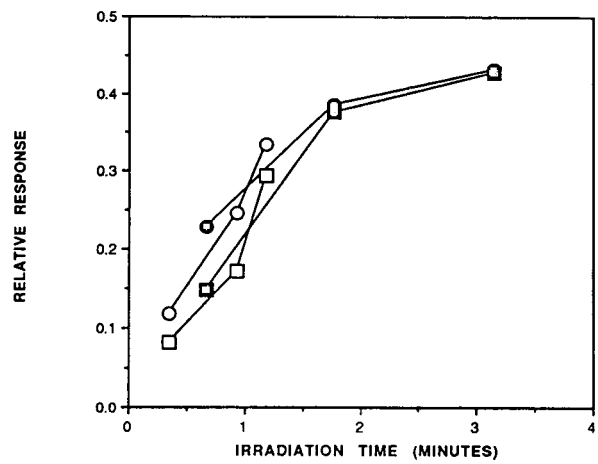

Fig. 7. Relative B_1/B_2 (circles) and G_1/G_2 (squares) fluorescence response as a function of irradiation time. Open symbols, 0.25 mm coils; closed symbols, 0.50 mm coils.

250 μg G_1/ml in methanol was injected directly to a 15 m × 0.5 mm I.D. long irradiated knitted reactor coil using a manual injection valve. The pump, eluent composition and flow rate conditions for the analytical HPLC analysis were used to cause the photolysis in a flow injection mode. The photolysis reaction mix obtained by the 3.15 min irradiation of G_1 in the flow injection mode was collected and analyzed by analytical HPLC using the same 15 m × 0.5 mm I.D. coil in the photochemical reactor. The chromatogram (Fig. 8) shows a peak for G_{2a} (8.01 min), residual G_1 (13.53 min) and an unknown (14.48 min). The retention time of a G_{2a} standard under these conditions was 8.01 min. The G_{2a}/G_1 peak area ratio is 0.69. In order to ascertain whether the G_{2a} and G_1 components interconvert under the photolysis conditions, the photolysis reaction mix obtained

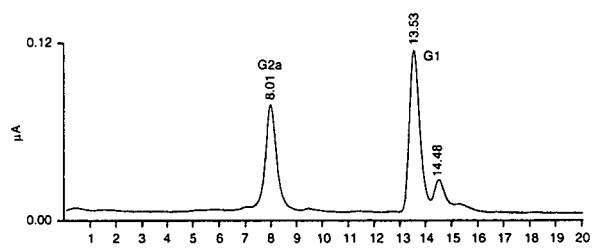

Fig. 8. Chromatogram of G_1 photolysis reaction mixture. G_{2a} retention time 8.01 min, residual G_1 at 13.53 min.

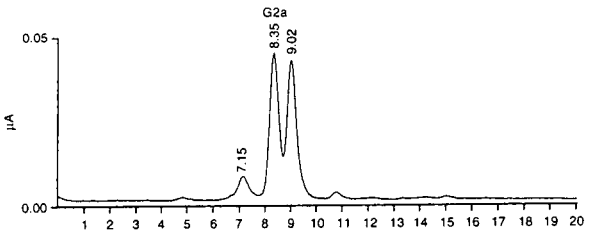

Fig. 9. Chromatogram of G_{2a} photolysis reaction mixture. Residual G_{2a} retention time 8.35 min.

by the 3.15 min irradiation of G_{2a} in a flow injection mode was analyzed as above. The chromatogram (Fig. 9) shows residual G_{2a} (8.35 min) and unknowns at 7.15, 9.02 and 10.8 min. However, no peak for G_1 was observed. It is highly probable that under the photolysis conditions B_1 undergoes the parallel reaction to B_{2a} (Fig. 1).

The effect of low pH on fluorescence response

The conversions of B_1 to B_{2a} in aqueous TFA is well established [10,11]. It was hoped therefore, that adding TFA to the eluent might increase the conversion of B_1 to B_{2a} and G_1 to G_{2a} during the photolysis. Using aqueous 0.1% TFA–acetonitrile–methanol (63:22:15) as eluent and the 15 m × 0.5 mm I.D. coil the relative peak areas normalized for mass of components injected was 0.790, 0.206, 1.000 and 0.259 for G_2, G_1, B_2 and B_1, respectively. The B_1/B_2 relative fluorescence response was lower using the eluent containing TFA than when the neutral eluent was used (Table I).

Analysis of naturally contaminated corn samples

The application of this method to "real life" samples of corn was demonstrated by the analysis of three naturally contaminated corn samples, which had been extracted and the extracts forced through Mycosep multifunctional cleanup columns [17], which allow aflatoxins to pass through while retaining interfering compounds. The samples A, B and C had nominal concentrations for B_1 of 15, 30 and 100 ppb. Using 20-μl injections, each representing 80 mg of corn, gave the chromatograms shown in Fig. 10A, B and C, respectively. Quantitation of the B_1 peaks and comparison with those obtained from B_1 standards indicated that samples A, B and C assayed at 23, 37 and 65 ppb, respectively. These values did not take into account possible sampling problems, losses in the extraction and cleanup processes, nor degradations in transit. However, a comparison of the chromatogram of sample C with the UV light of the photochemical reactor on (Fig. 10C) with the chromatogram of the same sample with the UV light off (Fig. 10D) shows that no naturally fluorescing compounds elute at the same retention time as B_1, and that the B_2 peak is unaffected by the photolysis.

Aflatoxins B_1 and B_2 concentrations of 1 and 0.25 ppb, respectively, can readily be determined since at these levels the signal-to-noise ratio is approximately three. However, increasing the milligrams of feed equivalence for each injection, by using larger injection volumes and/or higher equivalence of mass of feed per injection volume as well as the use of more sensitive fluorescence detectors would significantly increase the sensitivity of this method.

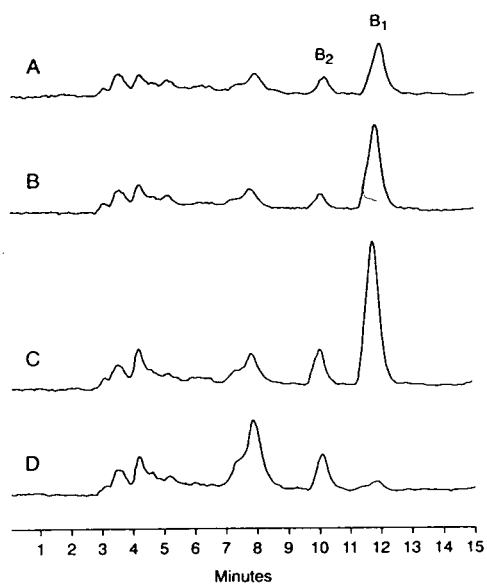

Fig. 10. Chromatograms of purified extracts of naturally contaminated corn samples with nominal B_1 concentrations of (A) 15, (B) 30 and (C) 100 ppb with photolysis light on. (D) Chromatogram of sample C with photolysis light off.

CONCLUSIONS

The HPLC analysis of aflatoxins using post-column photochemical UV irradiation and fluorescence detection is sensitive, simple and robust even for the G_1 and B_1 components whose fluorescence detectability is normally low or absent. This method obviates the need for pre- or post-column chemical derivatizations which require chemical reagents, pumps, heated reactors, electrochemical reagent generators and/or related apparatus. The demonstrated linearity of response over a wide range of concentrations is not affected by the number of photolysis products formed. No interfering peaks were observed in the analysis for B_1 in naturally contaminated corn samples.

ACKNOWLEDGEMENTS

Helpful suggestions by Mr. Edward Vecchione in the use of the Spectra-Physics instrumentation and software are very much appreciated. Mr. Tom Romer of Romer Labs. Inc. provided the purified extracts of naturally contaminated corn samples. They are gratefully acknowledged.

REFERENCES

1 W.O. Ellis, J.P. Smith, B.K. Simpson and J.H. Oldham, *Crit. Rev. Food Sci. Nutr.*, 30 (1991) 403.
2 H.P. van Egmond, *Food Addit. Contam.*, 6 (1989) 139.
3 S. Tabata, H. Kamimura, A. Ibe, H. Hashimoto, M. Iida, Y. Tamura and T. Nishima, *J. Assoc. Off. Anal. Chem.*, 76 (1993) 32.
4 M. Holcomb, D.M. Wilson, M.W. Truckess and H.C. Thompson, Jr., *J. Chromatogr.*, 624 (1992) 341.
5 M. Manabe, T. Goto and S. Masuura, *Agric. Biol. Chem.*, 43 (1978) 2003.
6 T. Panalaks and P.M. Scott, *J. Assoc. Off. Anal. Chem.*, 60 (1977) 583.
7 O.J. Francis, G.P. Kirschenheuter, Jr., G.M.G. Ware, A.S. Carman and S.S. Kuan, *J. Assoc. Off. Anal. Chem.*, 71 (1988) 725.
8 M.L. Vazquez, A. Cepeda, P. Prognon, G. Mahuzier and J. Blais, *Anal. Chim. Acta*, 255 (1991) 343.
9 M.L. Vazquez, C.M. Franco, A. Cepeda, P. Prognon and G. Mahuzier, *Anal. Chim. Acta*, 269 (1992) 239.
10 D.M. Takahashi, *J. Chromatogr.*, 131 (1977) 147.
11 H. Engelhardt and P. Maas, *J. Chromatogr.*, 31 (1993) 13.
12 M.J. Shepherd and J. Gilbert, *Food Addit. Contam.*, 1 (1984) 325.
13 W.Th. Kok, Th.C.H. van Neer, W.A. Traag and L.G.M.Th. Tuinstra, *J. Chromatogr.*, 367 (1986) 231.
14 H. Jansen, R. Jansen, U.A.Th. Brinkman and R.W. Frei, *Chromatographia*, 24 (1987) 555.
15 J.R. Poulsen and J.W. Birks, in J.W. Birks (Editor), *Chemiluminescence and Photochemical Reaction Detection in Chromatography*, VCH, New York, 1989, Ch. 6, pp. 149–230.
16 I.S. Lurie, D.A. Cooper and I.S. Krull, *J. Chromatogr.*, 629 (1993) 143.
17 T.J. Wilson and T.R. Romer, *J. Assoc. Off. Anal. Chem.*, 74 (1991) 651.
18 C. Dunne, M. Meaney, M. Smyth and L.G.M.Th. Tuinstra, *J. Chromatogr.*, 629 (1993) 229.
19 P.J. Andrellos, A.C. Beckwith and R.M. Eppley, *J. Assoc. Off. Anal. Chem.*, 50 (1967) 346.
20 J.C. Shieh and P.S. Song, *Cancer Res.*, 40 (1980) 698.
21 G. Buchi, K.W. Fowler and A.M. Nadzan, *J. Am. Chem. Soc.*, 104 (1982) 544.
22 K. Nagaya, B.H. Way, R.M. Tran and P.S. Song, *Cancer Lett.*, 18 (1983) 191.
23 B.L. Sergeyev, S.P. Bogovsky, R.Kh. Tanner, T.I. Veidebaum and I.N. Shevchuk, *Eksp. Onkol.*, 11 (1989) 76.
24 A.A. Stark and D.F. Liberman, *Mutat. Res.*, 247 (1991) 77.

Journal of Chromatography A, 654 (1993) 255–260
Elsevier Science Publishers B.V., Amsterdam

CHROM. 25 502

Normal-phase high-performance liquid chromatographic separation of procyanidins from cacao beans and grape seeds

J. Rigaud*, M.T. Escribano-Bailon☆, C. Prieur, J.-M. Souquet and V. Cheynier

Institut National de la Recherche Agronomique, Institut des Produits de la Vigne, Laboratoire des Polymères et des Techniques Physico-Chimiques, 2 Place Viala, 34060 Montpellier Cedex (France)

(First received June 10th, 1993; revised manuscript received August 11th, 1993)

ABSTRACT

An HPLC method using a normal-phase silica column and a gradient of dichloromethane–methanol–formic acid–water mixtures as the eluent was developed to separate procyanidins on a molecular mass basis, without derivatization. It was successfully applied to the analysis of procyanidin extracts from cacao beans and grape seeds. The monomers and major dimers were resolved as discrete peaks. Oligomeric and polymeric components were eluted in order of increasing degree of polymerization, as confirmed by determining the average molecular mass of successive fractions collected from the normal-phase column using gel permeation chromatography, after acetylation.

INTRODUCTION

Proanthocyanidins (*i.e.*, condensed tannins) form a class of compounds that are both ubiquitous and very important owing to their chemical properties. Their tendency to link with proteins is responsible for the astringency of many foods and drinks [1], haze formation in beer [2] and the poor digestibility of fodder legumes [3]. In addition, the oligomers are bitter [1] and show toxicity to methane bacteria [4]. Their pharmaceutical effects are interesting because they act beneficially on the circulatory system [5] and are efficient free radical scavengers [6,7]. All these properties largely depend on their structures and particularly on their degree of polymerization. As a consequence, many methods have been developed to evaluate oligomeric and polymeric ratios.

Among these methods, counter-current chromatography allows the isolation of groups of constituents differing in their chain length [8]. Chromatography on Sephadex LH-20 [9] or Fractogel [10] columns permits the separation of oligomeric fractions, but beyond the tetrameric forms elution requires acetone so that UV monitoring becomes impossible. Gel permeation of the acetylated derivatives makes it possible to obtain a mass profile [11] but requires fairly tedious derivatization procedures that do not allow good recoveries of the samples. Another procedure is to separate procyanidins according to their affinities for proteins [12], but this may be relatively specific and not strictly related to the molecular mass.

Good separations based on molecular mass were achieved with a silica phase but, as it was used in TLC, the resolution was limited to oligomers up to the heptameric forms [13]. When used in HPLC, silica yielded only two rough

* Corresponding author.
☆ Present address: Departamento de Quimica Analitica, Nutricion y Bromatologia, Universidad de Salamanca, Avda. del Campo Charro s/n, 37007 Salamanca, Spain.

0021-9673/93/$06.00 © 1993 Elsevier Science Publishers B.V. All rights reserved

fractions, one containing oligomers and the other polymers [14]. Another polar HPLC column, containing a cyano-bonded silica phase, permitted the separation of peracetylated derivatives [15] or native procyanidins [16]. In the latter instance, many oligomeric groups were distinguishable. However, no individual compound could be separated. In contrast, individual resolution of monomers and many small oligomers was achieved by reversed-phase HPLC [17,18] but the elution order appeared unrelated to the degree of polymerization. However, polymeric forms were separated from the oligomers and eluted towards the end of the chromatogram as a broad, unresolved peak [19,20].

The purpose of this investigation was to develop a chromatographic method to separate oligomeric and polymeric procyanidins on a molecular mass basis. The method had to be suitable both for analytical purposes and for quantitative isolation of procyanidin fractions. Therefore, a normal-phase HPLC method was adapted from the TLC method described by Lea [13]. In particular, the original elution system was modified so as to render it convenient both for UV detection and for the recovery of the eluted compounds.

EXPERIMENTAL

Chemicals

All chromatographic solvents were of HPLC grade, purchased from Merck (Darmstadt, Germany) or Prolabo (Paris, France). Acetic anhydride and pyridine were purchased from Labosi (Paris, France) and gallic acid, (+)-catechin and (−)-epicatechin from Sigma (St. Louis, MO, USA). Epicatechin gallate and procyanidin dimers and trimers were isolated from grape seeds in our laboratory and epicatechin tetramer was prepared from cacao beans by Dr. E. Cros (IRCC, Montpellier, France). Polystyrene standards were purchased from Interchim (Montluçon, France).

Extraction

The cacao procyanidin extract, kindly provided by Dr. E. Cros, had been obtained from lyophilized beans by the following procedure: washing with pentane (lipid removal), extraction with 70% methanol, filtration, evaporation and dissolution in 60% acetone, salting out with NaCl, concentration of the organic layer, addition of water, washing with chloroform to remove caffeine and theobromine and extraction with ethyl acetate. After concentration, the resulting extract is brownish red owing to the presence of anthocyanins.

Grape seeds were obtained from frozen berries of *Vitis vinifera* var. Tannat, harvested at commercial maturity. They were ground under liquid nitrogen, extracted with 60% acetone and centrifuged. The acetone supernatant was then evaporated to dryness under vacuum, the residue was dissolved in methanol and the solution was centrifuged to obtain a crude extract of procyanidins.

HPLC conditions

The HPLC apparatus was a Millipore–Waters (Milford, MA, USA) system composed of a U6K injector, a Model 660 gradient controller, two Model 510 pumps and a Model 990 photodiode array detector. The column was a LiChrospher Si 100 (particle size 5 μm; 250 × 4 mm I.D.) purchased from Merck, protected with a guard column (20 × 4 mm I.D.) packed with the same material. The solvents were dichloromethane–methanol–formic acid–water with volume ratios of (A) 5:43:1:1 and (B) 41:7:1:1. The elution conditions were as follows: flow-rate, 1 ml/min; oven temperature, 30°C; elution, linear gradients from 0 to 20% A in 30 min, from 20 to 50% A in 30 min and from 50 to 100% A in 5 min, followed by isocratic elution with 100% A for 5 min and re-equilibration of the column.

Gel permeation chromatography

Gel permeation chromatography (GPC) was performed on the fractions acetylated with acetic anhydride–pyridine as described by Williams *et al.* [11]. The GPC analyses were carried out on a Millipore–Waters system, using TSK G 2500 Hxl and TSK G 3000 Hxl columns (particle size 6 μm; 300 × 7.8 mm I.D.) purchased from Tosohaas (Philadelphia, PA, USA), connected in series. The acetylated compounds were eluted isocratically with tetrahydrofuran (flow-rate 1

ml/min; column temperature 30°C) and detected with a Waters M440 detector set at 254 nm. The GPC system was calibrated with eleven polystyrene standards (molecular mass 162–50 000).

Enzymatic hydrolysis

Enzymatic hydrolysis was performed by incubating the crude grape seed procyanidin extract in 0.1 *M* acetate buffer (pH 5.3) with tannase AJ (Gist Brocades, Seclin, France) for 30 min at 25°C. The ratio of procyanidins to tannase was close to 10 on a mass basis. Protein and salt were eliminated by percolating the mixture through a Sephadex LH-20 column and washing with water. Degalloylated procyanidins were then eluted with acetone–water (60:40), evaporated to dryness and the residue was dissolved in methanol. It was checked that application of the same purification process to the original crude extract extract did not modify its chromatographic profile.

Procyanidin identification

The main individual peaks were collected in several runs, pooled, gently evaporated to dryness, with addition of water to prevent hydrolysis due to formic acid concentration, and identified by micro-thiolysis as described previously [21] and/or enzymatic hydrolysis. The results were confirmed by reversed-phase HPLC [20] and co-injection of the procyanidin extract with pure compounds previously isolated and identified in our laboratory [20] on the normal-phase column.

RESULTS AND DISCUSSION

Fig. 1 shows the chromatogram of the cacao bean extract. The major components were identified as (−)-epicatechin and its C_4–C_8 linked oligomers up to the pentamer. This example illustrates the expected ability of the normal-phase HPLC system used to separate oligomeric procyanidins (at least in the epicatechin series) according to their degree of polymerization.

Fig. 2 presents the chromatograms obtained by injection of the grape seed extract on to the normal-phase HPLC system, (A) before and (B) after enzymatic hydrolysis. Identification of the major oligomers (listed in Table I) confirms that,

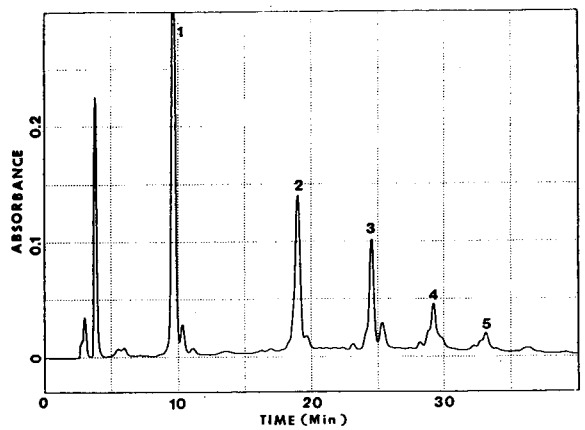

Fig. 1. HPLC analysis of a cacao bean procyanidin extract, monitored at 280 nm. Peaks: 1 = epicatechin; 2, 3, 4 and 5 = dimer, trimer, tetramer and pentamer, respectively, of the epicatechin series, tentatively identified by thiolysis.

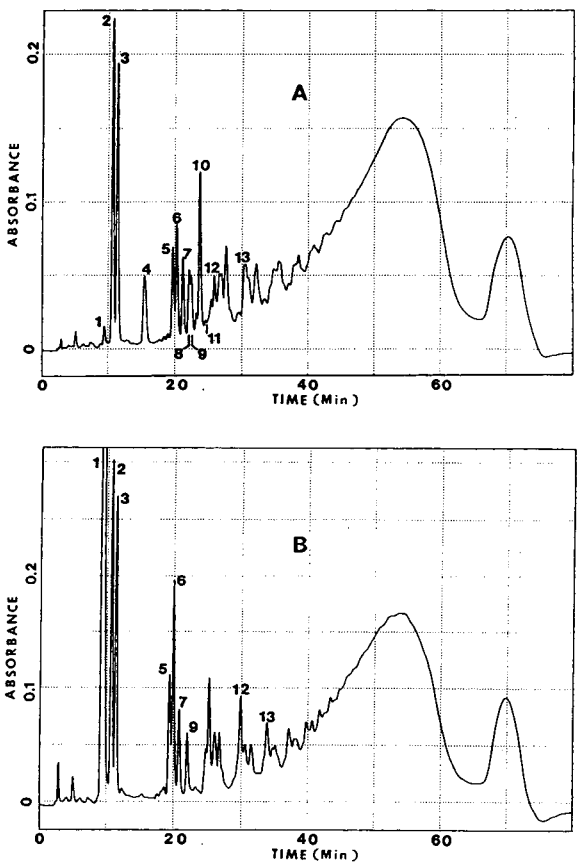

Fig. 2. HPLC analyses (monitored at 280 nm) of a grape seed procyanidin extract (A) before and (B) after hydrolysis with tannase. For identification of peaks, see Table I.

TABLE I

LIST OF IDENTIFIED COMPOUNDS

No.	Compound
1	Gallic acid
2	Epicatechin
3	Catechin
4	Epicatechin 3-O-gallate
5	Procyanidin B4 [catechin-(4$\alpha \rightarrow$8)-epicatechin]
6	Procyanidin B2 [epicatechin-(4$\beta \rightarrow$8)-epicatechin]
7	Procyanidin B3 [catechin-(4$\alpha \rightarrow$8)-catechin]
8	Procyanidin B4 3′-O-gallate [catechin-(4$\alpha \rightarrow$8)-epicatechin-3-O-gallate]
9	Procyanidin B1 [epicatechin-(4$\beta \rightarrow$8)-catechin]
10	Procyanidin B2 3-O-gallate [epicatechin-3-O-gallate-(4$\beta \rightarrow$8)-epicatechin]
11	Procyanidin B2 3,3′-di-O-gallate [epicatechin-3-O-gallate-(4$\beta \rightarrow$8)-epicatechin-3-O-gallate]
12	Procyanidin C1 [epicatechin-(4$\beta \rightarrow$8)-epicatechin-(4$\beta \rightarrow$8)-epicatechin]
13	Tetramer [epicatechin-(4$\beta \rightarrow$8)-epicatechin-(4$\beta \rightarrow$8)-epicatechin-(4$\beta \rightarrow$8)-epicatechin]

although the grape seed extract contained catechin oligomers and mixed catechin–epicatechin derivatives in addition to the epicatechin oligomers found in the cacao extract, they were eluted in successive groups corresponding to increasing degree of polymerization up to the tetramer series. Note that, when co-injected with the grape seed procyanidin extract, the C_4–C_6 linked procyanidin dimers B5 and B7 co-eluted with the corresponding C_4–C_8 linked procyanidins B2 and B1.

Hydrolysis with tannase (Fig. 2B) improved the resolution of these consecutive groups, suggesting that some galloylated compounds overlapped with the neighbouring fractions in the original sample. In fact, all identified galloylated compounds eluted further than the corresponding non-galloylated compounds. In particular, epicatechin 3-O-gallate (peak 4) eluted between monomers and dimers and B2 3′-O-gallate (peak 10) between dimers and trimers. Moreover, B2 3,3′-di-O-gallate (peak 11) almost co-eluted with the trimers, confirming that some overlapping took place as the complexity of the molecules, and especially the number of galloyl substituents, increased.

Fractions eluting further than the tetramers gradually fused into two broad, unresolved humps. This is probably due to the larger diversity of structures as the degree of polymerization increases, but it may also mean that larger galloylated procyanidin oligomers and polymers are more resistant to hydrolysis by tannase because of enzyme inhibition by tannins or steric hindrance.

In order to check the ability of the silica column to separate larger procyanidins according to their degree of polymerization, four fractions of the eluate were collected. All of them exhibited an absorption maximum near 280 nm and gave a positive response when heated with butanol–HCl as described by Bate-Smith [22], confirming that they were mostly composed of tannins. After elimination of the dichloromethane and methanol by rotary evaporation under vacuum, each fraction was submitted to Sephadex LH-20 chromatography to remove formic acid and avoid acid hydrolysis during concentration. The procyanidin fractions were recovered from the Sephadex LH-20 column by elution with acetone–water (60:40). After evaporation to dryness and acetylation, they were analysed by GPC and their average molecular masses were determined by comparison with polystyrene standards. The results obtained for each fraction are presented in Table II along with the calculated average degree of polymerization and elution time in normal-phase HPLC.

TABLE II

CHARACTERIZATION OF PROCYANIDIN FRACTIONS

Parameter	Elution time on normal-phase column (min)			
	30–40	40–50	50–65	65–75
Average molecular mass of acetylated fractions[a]	1900	3750	7200	9150
Average degree of condensation	3.8	7.5	14.4	18.3

[a] Determined by GPC.

As expected, the degree of polymerization increased with increasing retention time, starting from *ca.* 4 for the fraction eluting at 30 min. The complexity of the polymeric group is responsible for the broad peak at 55 min. The second broad peak eluting near 70 min corresponds to the largest compounds detected. Note that, for the first fraction collected, the average molecular mass determined by GPC was slightly lower than expected. This may be due to partial hydrolysis of the compounds during concentration prior to acetylation or to contamination of the fraction by lower molecular mass galloylated compounds.

CONCLUSIONS

The use of a normal-phase silica HPLC column is a good way to achieve elution of procyanidins according to their degree of polymerization. The technique developed permits the separation and determination of oligomeric and polymeric procyanidins from grape seeds. It also allows monomers and many oligomers to be determined individually. The procedure is simple and, as it does not require derivatization of the samples, is suitable for the quantitative isolation of tannin fractions differing in their degree of polymerization. In addition, the amounts of the various procyanidin groups can be determined from their respective peak areas. Therefore, the method should be of help in understanding the role of the different types of procyanidins and monitoring their changes during wine making during wine making and ageing. Finally, it may presumably be extended to procyanidins from other plant sources, although this might require some adaptation if prodelphinidins or other proanthocyanidins are also present.

REFERENCES

1 A.G.H. Lea and G.M. Arnold, *J. Sci. Food Agric.*, 29 (1978) 478–483.
2 J.W. Gramshaw, *J. Inst. Brew.*, 75 (1969) 61–83.
3 L.Y. Foo, W.T. Jones, L.J. Porter and V.M. Williams, *Phytochemistry*, 21 (1982) 933–935.
4 J.A. Fields, S. Kortekaas and G. Lettinga, *Biol. Wastes*, 29 (1989) 241–262.
5 J. Masquelier, in *C.R. Symposium Int. "L'Alimentation et la Consommation de Vin", Verona, Italy, 1982*, pp. 147–155.
6 S. Uchida, R. Edamatsu, M. Miramatsu, A. Mori, G. Nonaka, I. Nishioka, M. Miwa and M. Ozaki, *Med. Sci. Res.*, 91 (1987) 831–832.
7 J.M. Ricardo da Silva, N. Darmon, Y. Fernandez and S. Mitjavila, *J. Agric. Food Chem.*, 39 (1991) 1549–1552.
8 L.J. Putman and L.G. Buttler, *J. Chromatogr.*, 318 (1985) 85–93.
9 A.G.H. Lea and C.F. Timberlake, *J. Sci. Food Agric.*, 25 (1974) 1537–1545.
10 G. Derdelinckx and J. Jerumanis, *J. Chromatogr.*, 285 (1984) 231–244.
11 V.M. Williams, L.J. Porter and R.W. Hemingway, *Phytochemistry*, 22 (1983) 569–572.
12 H.I. Oh and J.E. Hoff, *J. Food Sci.*, 44 (1979) 87–96.
13 A.G.H. Lea, *J. Sci. Food Agric.*, 29 (1978) 471–477.
14 C.W. Glennie, W.Z. Kaluza and P.J. Van Niekerk, *J. Agric. Food Chem.*, 29 (1981) 965–968.
15 M.V. Piretti and P. Doghieri, *J. Chromatogr.*, 514 (1990) 334–342.
16 E.L. Wilson, *J. Sci. Food Agric.*, 32 (1981) 257–264.

17 P. Mulkay, R. Touillaux and J. Jerumanis, *Cerevisiae*, 1 (1981) 29–31.
18 K. Kantz and V.L. Singleton, *Am. J. Enol. Vitic.*, 41 (1990), 223–228.
19 L.J. Putman and L.G. Buttler, *J. Agric. Food Chem.*, 37 (1989) 943–946.
20 J.M. Ricardo da Silva, J. Rigaud, V. Cheynier, A. Cheminat and M. Moutounet, *Phytochemistry*, 30 (1991) 1259–1264.
21 J. Rigaud, J. Perez-Ilzarbe, J.M. Ricardo da Silva, V. Cheynier, *J. Chromatogr.*, 540 (1991) 401–405.
22 E.C. Bate-Smith, *J. Exp. Bot.*, 4 (1953) 1–9.

Journal of Chromatography A, 654 (1993) 261–268
Elsevier Science Publishers B.V., Amsterdam

CHROM. 25 436

Speciation of inorganic and organotin compounds in biological samples by liquid chromatography with inductively coupled plasma mass spectrometric detection☆

Uma T. Kumar, John G. Dorsey and Joseph A. Caruso*

Department of Chemistry, University of Cincinnati, Cincinnati, OH 45221-0172 (USA)

E. Hywel Evans

Department of Environmental Sciences, University of Plymouth, Plymouth PL4 8AA (UK)

(First received February 23rd, 1993; revised manuscript received July 6th, 1993)

ABSTRACT

This paper describes the effect of inorganic tin chloride on the separation of trimethyl-, tributyl- and triphenyltinchlorides by reversed-phase ion-pair high-performance liquid chromatography with detection by inductively coupled plasma mass spectrometry. The detection limits are 1.6 pg, 1.5 pg and 2.3 pg as tin for trimethyltin, tributyltin and triphenyltin, respectively. The relative standard deviation for ten injections of 20 ng of the tin compounds was less than 5%. Inorganic tin was held strongly on the columns used, to a greater extent on the silica column compared to the polymer column. Extraction and determination of tributyltin and triphenyltin as chlorides in fish tissue (certified reference material) and tuna fish (grocery store) were performed. The recovery study from fish tissue showed an efficiency of over 90% for both tributyltin and triphenyltin and over 60% recovery for spiked tuna.

INTRODUCTION

Speciation of an element is the determination of the individual physico-chemical forms of that element which together make up its total concentration in a sample. Variation in the elemental species can dramatically change their bioavailability or toxicity. Therefore speciation information at subnanogram levels is essential.

Organotin compounds have numerous applications [1–4], for example, mono- and diorganotins are used to stabilize poly(vinyl chloride) (PVC) polymers. Triorganotins are used as biocides, catalysts, wood preservatives, fire retardants and reducing agents, as well as in the pharmaceutical, ceramic and glass industries. Tin compounds have also been used in the production of cans for food storage. These organotin compounds are of high environmental and toxicological concern, since they are released into the environment [5,6]. A large fraction of the total organotin compounds used as biocides and algicides in antifouling paints have directly entered into the aquatic environment. For example, coastal water

* Corresponding author.

☆ Presented in part at the *Pittsburgh Conference on Analytical Chemistry and Applied Spectroscopy, Chicago, IL, March 4–8, 1991*, paper 1093.

0021-9673/93/$06.00 © 1993 Elsevier Science Publishers B.V. All rights reserved

pollution is one of the most serious environmental problems in Japan. Tributyltin and triphenyltin have been used as antifouling paints for fish nets and ship hulls. Pollution by triphenyltin is a more serious problem than pollution by tributyltin, since it accumulates in the lipophilic tissues in the fish. Also, the speciation of tin in natural waters is important because of the large amount of tin mining and the increased use of toxic organotin compounds such as tri(*n*-butyl)tin oxide and tri(*n*-butyl)tin acetate in antifouling paints.

Several approaches to organotin speciation have been suggested [7,8]. One of the more promising approaches is to couple the separatory power of chromatography with the selectivity and sensitivity of atomic spectrometry. Gas and liquid chromatography are suitable techniques for the analysis of complex samples. Although gas chromatography (GC) has been coupled to atomic spectrometry for organotin speciation [7], it is limited to volatile and thermally stable organometallic compounds. The use of high-performance liquid chromatography (HPLC) considerably expands the type of chemical and physical species that may be studied. The separation of ions and non-volatile organotin species, in addition to volatile species is possible using several LC configurations [8].

Atomic spectrometry offers the possibility of selectively detecting a wide range of metals and non-metals. The use of detectors responsive only to selected elements in a multi-component mixture reduces the constraints placed on the chromatographic step, since only those components in the mixture which contain the element of interest will be detected. Among the various atomic spectrometric techniques, plasma detectors have evolved into a dominant source for trace metal speciation. Inductively coupled plasma mass spectrometry (ICP-MS) is a sensitive technique and has been investigated as a detector for HPLC [9–18]. HPLC–ICP-MS offers the sensitivity necessary for trace metal speciation in real samples [16], and the on-line detection capability required to enable optimization of the separation and routine operation. ICP-MS can detect chromatographic eluents at subnanogram to picogram levels under the optimal conditions.

Previously, in this laboratory, Suyani *et al.* [18] have investigated the separation of three organotin compounds: trimethyltin chloride, tributyltin chloride and triphenyltin acetate by ion-pair reversed-phase HPLC on a Spherisorb ODS-2 C_{18} column. They observed relatively high background, about 3300 counts per second (cps), after several injections of organotin mixture. This suggested an accumulation of tin compounds on the column probably because of the equilibration between ion-pairing agent and the column packing material.

This paper describes the use of a PRP-1 column for the organotin separation. The more stable polymer-based column accepts a wide range of pH values giving greater flexibility in developing chromatographic conditions. The composition of the PRP-1 particle is more homogeneous from the surface to the center, thus exposure of active sites, which are chemically different, is reduced.

In this study, three alkyltin compounds are separated using reversed-phase ion-pair chromatography on PRP-1 column. Also presented, is the effect of inorganic tin on the organotin separation and the effect on background after repeated injections of organic and inorganic tin. The analytical figures of merit obtained by using the PRP-1 column are compared to those obtained using a Spherisorb ODS-2 column [18]. The accuracy of the method was determined by speciating organotin compounds that were extracted from fish tissue (certified reference material) and tuna fish.

EXPERIMENTAL

Instrumentation

The HPLC system consisted of a Model 2350 pump, a Model 2360 gradient programmer (Isco, Lincoln, NE, USA) and a Model 7010 injector with 200-μl sample loop (Rheodyne). A PlasmaQuad (PQ I, VG Elemental, Winsford, Cheshire, UK) ICP-MS was used. A forward power of 1500 W was used with an argon coolant flow of 16 l/min, auxiliary flow of 1 l/min and nebulizer gas flow of 0.66 l/min of argon mixed with about 1% of oxygen to prevent carbon

accumulation on the sampler. A double-pass Scott-type spray chamber was used, jacketed, and cooled to − 20°C. Cooling is necessary to remove organic solvent vapor which causes quenching of the plasma. The tin major isotope at m/z 120 (32.37% abundance) was monitored.

Reagents

Organotin compounds, trimethyltin chloride (TMT), tributyltin chloride (TBT) and triphenyltin chloride (TPT) were obtained from Alfa products (Ward Hill, MA, USA) and used without further purification. An inorganic tin chloride standard solution was obtained from Aldrich (St. Louis, MO, USA). Stock solutions (1000 μg/g as tin) were prepared in HPLC-grade methanol and working solutions were prepared daily using methanol for dilutions. HPLC-grade methanol (Fisher Scientific), deionized distilled water (Barnstead, 18 MΩ), reagent-grade glacial acetic acid (Fisher Scientific) and certified A.C.S ammonium acetate (Fisher Scientific) were used to prepare the mobile phase.

Biological samples

Fish tissue (certified reference material No. 11) was obtained from National Institute for Environmental Studies, Japan Environmental Agency. The tuna fish was from canned tuna obtained at a local grocery store. Tuna was dried in the oven and homogenized before the extraction procedure.

Chromatographic separations and conditions

The two columns that were employed for ion-pairing reversed-phase chromatography were: (1) Spherisorb ODS-2 (C_{18}) (Phase Separations), 250 mm × 4.6 mm I.D with 5 μm particle size (Alltech, Deerfield, IL, USA). (2) PRP-1 column (Anspec, Ann Arbor, MI, USA) 150 mm × 4.1 mm I.D with 5 μm particle size. The ion-pairing agent used was sodium pentane sulfonate (PIC-B5, Eastman Kodak Company, Rochester, NY, USA). For the Spherisorb ODS-2 C_{18} column, a mobile phase of methanol–water–acetic acid (80:19:1) was used at a pH of 3. All the mobile phases, for both columns, contained 0.004 *M* sodium pentane sulfonate. Mobile phases with the PRP-1 column were adjusted to the pH by using 1% acetate which was composed of ammonium acetate and acetic acid in a ratio that would give the desired pH. For example, mobile phase containing 94% methanol and 5% water had 0.046 *M* acetic acid and 0.012 *M* of ammonium acetate to yield a pH of 6. The mobile phase flow-rate for all the studies was 1 ml/min.

Extraction of tributyltin and triphenyltin

Tributyltin and triphenyltin were extracted from the samples following the procedure described by Tsuda *et al.* [19]. About 2.5 g of sample was placed in a separatory funnel and extracted with 12.5 ml of ethyl acetate for 30 min after adding 25 ml of deionised water (Barnstead, 18 MΩ), 3.75 g of sodium chloride and 2.5 ml of 6 *M* HCl. The mixture was then centrifuged for 5 min. The organic layer was evaporated nearly to dryness at low pressure and rotation at 40°C. The residue was then dissolved in 5 ml of methanol. A 200 μl volume of sample was injected into the liquid chromatograph for analysis.

RESULTS AND DISCUSSION

Initial studies were performed to find the optimal chromatographic conditions for the PRP-1 column. The effect of changing the pH and the methanol concentration of the mobile phase on the organotin (TMT-Cl + TBT-Cl + TPT-Cl) separation, with 500 ng g^{-1} inorganic tin also present was studied. At 94% methanol concentration of the mobile phase,the pH was varied from 3 to 6. As the pH increased, from 3 to 5, there was an increase in resolution between the organotin compounds but there was no base-line resolution between inorganic tin and trimethyltin. Whereas, at pH 6, a base-line resolution between TMT-Cl and the inorganic tin chloride, was observed. This is shown in Fig. 1. A shorter analysis time was observed with the PRP-1 column which yielded a complete separation within 6 min.

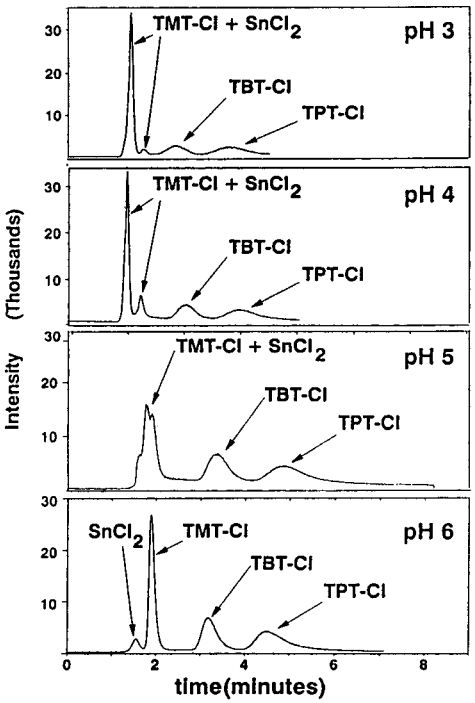

Fig. 1. The effect of pH on tin separation (500 ng g^{-1} inorganic tin chloride + 100 ng g^{-1} of organotin compounds) on PRP-1 column with mobile phase containing 94% methanol, 5% water, 1% acetate (*e.g.* for pH = 6, 0.046 *M* acetic acid and 0.012 *M* ammonium acetate) and 0.004 *M* sodium pentane sulfonate. Flow-rate = 1 ml/min.

Effect of inorganic tin on organotin separation

This study was done on both the silica-based column and the polymer-based column. Co-injection of the inorganic tin with organotin compounds for the silica-based column is shown in Fig. 2. Inorganic tin was retained on the column and did not affect the organotin separation, unless a concentration higher than 1 $\mu g\ g^{-1}$ of inorganic tin chloride was co-injected. Co-injection of inorganic tin chloride with organotins for the PRP-1 column is shown in Fig. 3. Inorganic tin eluted from the column, though not in a quantitative manner since some tin was retained even when using the PRP-1 column.

The above observations indicate that there was less retention of inorganic tin on the PRP-1 column than on the silica-based column. These observations also suggest that the silica-based column acted as an internal guard column, retaining the inorganic tin, and also acted as a

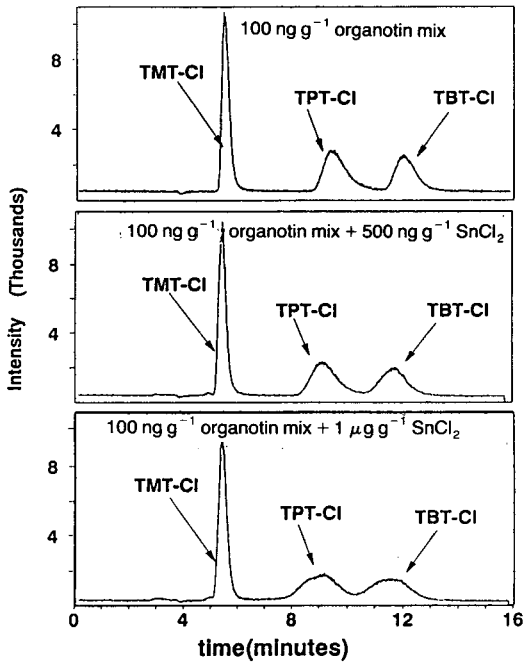

Fig. 2. The effect of inorganic tin on organotin separation with ODS-2 silica-based column, mobile phase containing 80% methanol, 19% water, 1% acetic acid (pH = 3) and 0.004 *M* sodium pentane sulfonate. Flow-rate = 1 ml/min.

chromatographic column by separating the organotins. An elevated background was observed with silica-based column after several injections of tin compounds which necessitated frequent reconditioning of the column by running the mobile phase for several hours.

Effect of organic and inorganic tins on background

The tin background intensities with the PRP-1 column and the silica-based column after ten 10 $\mu g\ g^{-1}$ injections of inorganic tin chloride and the organotin mixture (TMT-Cl + TBT-Cl + TPT-Cl) was studied. For the PRP-1 column, the background was monitored after the ten injections, including a 6-min period between each injection, which is the normal analysis time for the tin compounds. Similarly, for the silica-based column, there was a period of 13 min between each injection, which was the normal time for the tin compounds to elute. The base-line intensity of the mobile phase which was directly

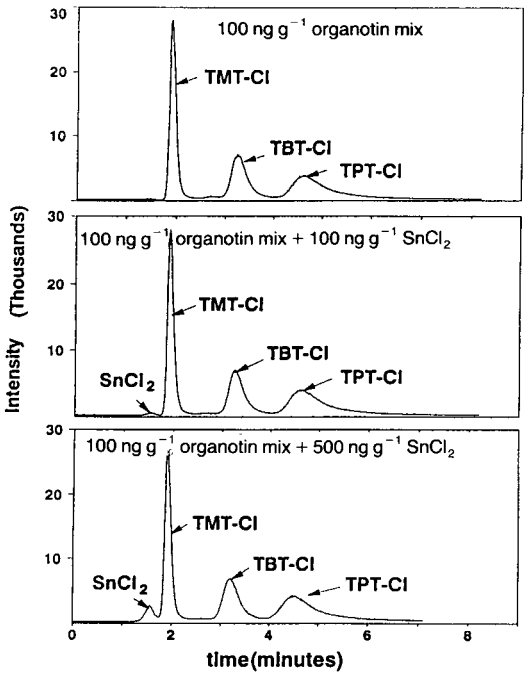

Fig. 3. The effect of inorganic tin on organotin separation with PRP-1 column, mobile phase containing 94% methanol, 5% water, 1% acetate (0.046 *M* acetic acid and 0.012 *M* ammonium acetate) and 0.004 *M* sodium pentane sulfonate. pH = 6. Flow-rate = 1 ml/min.

nebulized into the plasma without passing it through the column was observed to be approximately 50 cps. A tin bleed off the column was seen after repeated injections of both organic and inorganic tin. It was observed that organotins are retained less on the column than the inorganic tin chloride which is evident from their signal intensities. The intensity of the background was only in the hundreds of cps after the series of inorganic tin injections, whereas, the intensity was in thousands of cps (1500–3000 for both the columns) after the series of organotin injections of the mixture containing TMT-Cl, TBT-Cl and TPT-Cl. Inorganic tin was held strongly on both the columns, but to a greater extent on the silica-based column (300–400) compared to the PRP-1 column (600–700). It was also observed that organotins washed off with the mobile phase within 30–45 min whereas inorganic tin bleeds off the column with the mobile phase within 2 to 3 hours.

Analytical figures of merit

Detection limits. Detection limits for the organotin compounds with the PRP-1 column are presented in Table I. These are at the picogram level as compared to the nanogram level obtained by Suyani *et al.* [18] using a silica-based column and an earlier version of the plasma mass spectrometer.

Precision and linear dynamic range. Reproducibilities of peak areas were determined using ten replicate injections of 20 ng analyte as tin. The results are also listed in Table I, which are presented as relative standard deviations and are comparable with the work of Suyani *et al.* [18].

The linear dynamic range was 3 orders of magnitude for TMT-Cl and TBT-Cl, 2.5 orders of magnitude for TPT-Cl. These are again compared to the work of Suyani *et al.* [18] in Table II. Correlation coefficients obtained by using peak area measurements are also reported.

Detection of tributyltin and triphenyltin in biological samples

The chromatographic separation method described above was then applied to detect tributyltin and triphenyltin in fish tissue and tuna fish. The elution profile for organotins in fish tissue is shown in Fig. 4. The chromatogram indicates that there are no interfering peaks throughout the elution. The recovery study of

TABLE I

DETECTION LIMITS AND REPRODUCIBILITY OF PEAK AREA

	Detection limit[a]		Reproducibility of peak area[b]	
	PRP-1 (pg)	ODS-2[c] (ng)	PRP-1	ODS-2[c]
TMT-Cl	1.6	0.4	3.4	7.2
TBT-Cl	1.5	0.7	3.8	5.8
TPT-Cl	2.3	–	4.5	–
TPhT[d]	–	1.0	–	6.3

[a] Detection limit = $\frac{3 \times \text{standard deviation of background}}{\text{slope of calibration curve.}}$

[b] Relative standard deviation (%).

[c] Suyani *et al.* [18].

[d] Triphenyltin acetate.

TABLE II

SLOPE AND CORRELATION COEFFICIENTS FOR CALIBRATION PLOTS

	Slope[a]		LDR[b] (order of magnitude)		Correlation[c] coefficient	
	PRP-1	ODS-2[d]	PRP-1	ODS-2[d]	PRP-1	ODS-2[d]
TMT-Cl	0.9689	0.9872	3	2	0.9997	0.9999
TBT-Cl	0.9447	1.0251	3	2	0.9999	0.9999
TPT-Cl	1.0528	–	2.5	–	0.9999	–

[a] Obtained from log (integrated area) *vs.* log (concentration) plot.
[b] LDR = linear dynamic range.
[c] Obtained from integrated area *vs.* concentration plot.
[d] Suyani *et al.* [18].

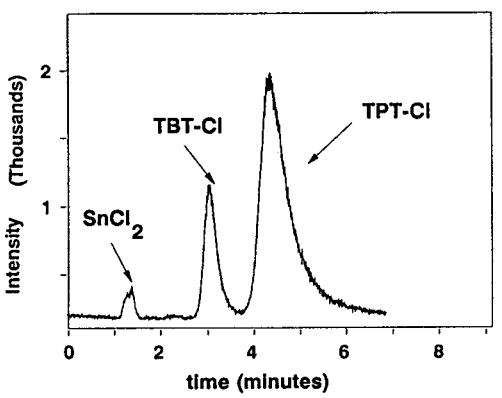

Fig. 4. Chromatogram of tin compounds from the fish tissue (certified reference material) extract. Mobile phase: 94% methanol, 5% water, 1% acetate (0.046 *M* acetic acid and 0.012 *M* ammonium acetate), 0.004 *M* sodium pentane sulfonate. pH = 6. Flow-rate = 1 ml/min.

these compounds shows good recovery of over 90% for both tributyltin and triphenyltin. The precision of the extraction method was evaluated by replicate analysis of the sample, which is shown in Table III.

This method was also used to analyze the amount of organotins in tuna fish. The elution profile for tins in tuna fish is shown in Fig. 5. An appreciable amount of inorganic tin was seen to be present in the tuna fish sample which might arise from the container, having a soldered seam, used to preserve the canned tuna. The amount of tributyltin and triphenyltin were estimated to be about 29.8 (± 1.2) ng g^{-1} and 21.5 (± 5.6) ng g^{-1}, respectively in 2.5 g of the dried tuna sample. Fig. 6. shows the chromatogram from the tuna fish extract which was spiked with 100 ng g^{-1} of TBT-Cl and TPT-Cl. The percent

TABLE III

RECOVERY OF TRIBUTYLTIN AND TRIPHENYLTIN FROM BIOLOGICAL SAMPLES (MEAN ± STANDARD DEVIATION, $n = 3$)

	Fish tissue (certified reference material)			Tuna fish (local grocery store)		
	Certified value ($\mu g\, g^{-1}$)	Amount detected ($\mu g\, g^{-1}$)	Recovery (%)	Amount spiked (ng g^{-1})	Amount detected (ng g^{-1})	Recovery (%)
TBT-Cl	1.3	1.2	94 ± 4.4	100	65.3	65.3 ± 1.7
TPT-Cl	6.3	6.2	99 ± 4.4	100	63.8	63.8 ± 4.9

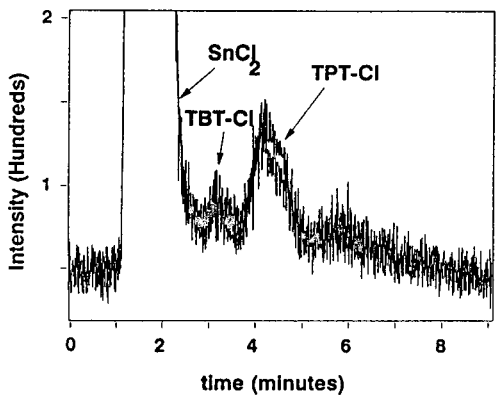

Fig. 5. Chromatogram (PRP-1 column) of tin compounds from the tuna fish (grocery store) extract. Mobile phase: 94% methanol, 5% water, 1% acetate (0.046 *M* acetic acid and 0.012 *M* ammonium acetate), 0.004 *M* sodium pentane sulfonate. pH = 6. Flow-rate = 1 ml/min.

recoveries for spikes of TBT-Cl and TPT-Cl compounds in tuna fish subjected to extraction conditions is also included in Table III.

CONCLUSIONS

Good separation between inorganic and organotin compounds was achieved at pH 6 using a PRP-1 column. Elution time for the analysis of tin compounds is reduced to about 6 min as compared to 13 min with the use of a silica-based column. Inorganic tin retains more on the silica-based column than on the polymer-based column. Thus, for a mixture of compounds having inorganic tin concentrations less than 1 μg g^{-1}, silica-based column acts as both a guard column by retaining inorganic tin, and as an analytical column by separating the organotin compounds. Whereas, the polymer-based column can be used to separate lower concentrations of inorganic tin from organotin compounds. Tin bleed off the column is observed for both columns after several injections of the tin compounds. Also, the organotins wash off the column faster than the inorganic tin. The detection limits were improved to the picogram level with the use of a PRP-1 column as compared to those of the silica-based column. This method of analysis was applied to detect tributyltin and triphenyltin compounds extracted from fish tissue (certified reference material) and tuna fish obtained from a local grocery store.

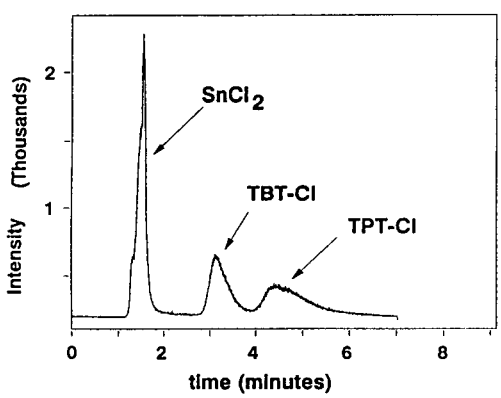

Fig. 6. Chromatogram (PRP-1 column) of tin compounds from tuna fish (grocery store) extract which was spiked with 100 ng g^{-1} of TBT-Cl and TPT-Cl. Mobile phase: 94% methanol, 5% water, 1% acetate (0.046 *M* acetic acid and 0.012 *M* ammonium acetate), 0.004 *M* sodium pentane sulfonate. pH = 6. Flow-rate = 1 ml/min.

ACKNOWLEDGEMENTS

The authors are greatful to the National Institute of Environmental Health Sciences for support through research grants ES-03221 and ES-04908. We acknowledge the NIH-BRS Shared Instruments Grant for providing the VG PlasmaQuad through grant number S10RR02714. J.A.C. and U.T.K. are thankful to Dr. Victoria McGuffin for suggesting the use of a polymer-based column as an alternative to silica-based column. A special thanks to Nohora Vela and Jeffrey Giglio for helping with the manuscript.

REFERENCES

1 T.M. Florence, *Talanta*, 29 (1982) 345.
2 J.J. Zuckerman, R.P. Reisdorf, H.V. Ellis and R.R. Wilkinson, in F.C. Brinckman and J.M. Bellama (Editors), *Organometals and organometalloids: Occurrence and fate in the environment* (*ACS Symposium Series*, No. 82), American Chemical Society, Washington, DC, 1978, p. 388.
3 S.P. Blunden, L.A. Hobbs and P.J. Smith, in H.J.M. Bowen (Editor), *Environmental chemistry*, The Royal Society of Chemistry, London, 1982, p. 49.
4 A.G. Davies and P.J. Smith, in *Advances in inorganic chemistry and radiochemistry*, Vol. 23, Academic Press, New York, 1980, pp. 1–77.
5 R.J. Maguire, *Appl. Organomet. Chem.*, 1 (1987) 475.

6 E.A. Clark, R.M. Sterritt and J.N. Lester, *Environ. Sci. Technol.*, 22 (1988) 600.
7 L. Ebdon, S. Hill and R.W. Ward, *Analyst*, 111 (1986) 1113.
8 L. Ebdon, S. Hill and R.W. Ward, *Analyst*, 112 (1987) 1.
9 W. Niasamaneepong, M. Ibrahim, T.W. Gilbert and J.A. Caruso, *J. Chromatogr. Sci.*, 22 (1984) 473–477.
10 M. Ibrahim, T.W. Gilbert and J.A. Caruso, *J. Chromatogr. Sci.*, 22 (1984) 111–115.
11 J.J. Thomson and R.S. Houk, *Anal. Chem.*, 58 (1986) 2541.
12 S. Branch, L. Ebdon, S. Hill and P. O'Neil, *Anal. Proceed.*, 26 (1989) 401.
13 J.W. McLaren, K.W.M. Siu, J.W. Lam, S.N. Willie, P.S. Maxwell, A. Palepu, M. Koether and S.S. Berman, *Fresenius' J. Anal. Chem.*, 337 (1990) 721.
14 B. Sheppard, D. Heitkemper, K. Wolnik and J.A. Caruso, *Analyst*, 117 (1992) 971.
15 H. Suyani, D. Heitkemper, J. Creed and J.A. Caruso, *Appl. Spectrosc.*, 43 (1989) 962–967.
16 D. Heitkemper, J. Creed and J. Caruso, *J. Anal. At. Spectrom.*, 4 (1989) 279.
17 A. Al-Rashdan, D. Heitkemper and J. Caruso, *J. Chromatogr. Sci.*, 29 (1991) 98–102.
18 H. Suyani, J. Creed, T. Davidson and J. Caruso, *J. Chromatogr. Sci.*, 27 (1989) 139.
19 T. Tsuda, H. Nakanishi, S. Aoki and J. Takebayashi, *J. Chromatogr.*, 387 (1987) 361–370.

Journal of Chromatography A, 654 (1993) 269–277
Elsevier Science Publishers B.V., Amsterdam

CHROM. 25 515

Characterization of an element-specific detector for combined gas chromatography–atomic emission detection

András Gelencsér, János Szépvölgyi and József Hlavay*

Department of Analytical Chemistry, University of Veszprém, P.O. Box 158, 8201 Veszprém (Hungary)

(First received May 28th, 1993; revised manuscript received August 12th, 1993)

ABSTRACT

An element-specific detector using a capacitively coupled plasma developed recently for gas chromatography was characterized according to the accepted terms of gas chromatographic detectors. The most important detector parameters, sensitivity, linearity, limit of detection, linear range and selectivity, were determined for channels of four elements, carbon, chlorine, bromine and sulphur, with a view to potential applications. The parameters obtained were compared, as permitted by the different mechanisms of operation, with some common gas chromatographic detectors of similar application. The characteristics of the detector were evaluated independently of application.

INTRODUCTION

Element-selective chromatographic detectors play an important role in separation science for compound identification. Element-selective detection methods commonly used in gas chromatography (GC) are nitrogen–phosphorus detection (NPD), flame photometric detection (FPD), which is selective for sulphur and phosphorus, and Hall electrolytic conductivity detection (HECD), which is selective for halogens, nitrogen or sulphur [1]. Three types of atomic spectrometry have been applied for GC detection: atomic absorption, flame emission and atomic plasma emission spectrometry. Atomic emission detectors have just recently been introduced to GC [2,3]. Their application as GC detectors is based on the fact that a multitude of elements, C, H, D, O, N, S, P and the halogens, give intense emission signals in the plasma, thus making the detector perfectly suited for the analysis of organic compounds.

For GC detection, microwave-induced plasmas are generally used. The molecules entering the plasma are atomized and the atoms are excited at high temperature, emitting at given emission lines which represent their characteristic spectra. By measuring the signal at a given emission line, a signal proportional to the concentration of the given element can be obtained irrespective of the type of molecule.

The element-specific detector was developed by Anton Paar (Graz, Austria) [4]. In contrast to other atomic emission GC detectors, it utilizes a capacitively coupled, stabilized plasma which is made up from helium plasma gas and oxygen dopant gas in a water-cooled fused-silica discharge tube. Helium is used as the plasma gas because it gives a simpler background spectrum, provides higher excitation energy and yields a broader linear range than does argon. For the four elements studied (C, Cl, Br and S), oxygen

* Corresponding author.

0021-9673/93/$06.00 © 1993 Elsevier Science Publishers B.V. All rights reserved

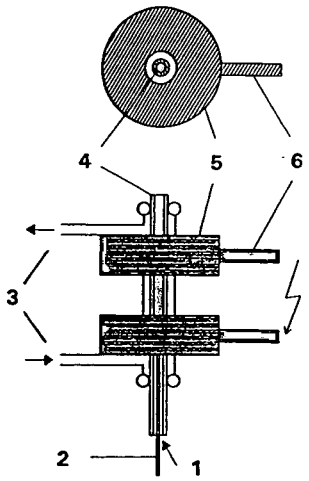

Fig. 1. ESD torch design. 1 = Plasma gas in; 2 = chromatographic column; 3 = water cooling; 4 = discharge tube; 5 = annular electrode; 6 = HF contact.

was the most suitable dopant gas. The scheme of the discharge tube is depicted in Fig. 1.

The discharge tube is held in the plasma generator unit mounted on the detector position of the gas chromatograph. The light emitted is directed through fibre optics to the spectrometer, where light is resolved by interference filters and detected by photodiodes in four separate units for the four elements. The aim of this paper was to determine the fundamental detector parameters for the individual channels, to make a broad comparison of the parameters with those of the corresponding common GC detectors and to evaluate the characteristics of the detector independently of application.

Basic parameters of gas chromatographic detectors

There has been continuing debate in the literature about the interpretation of certain parameters of gas chromatographic detectors. Apart from the different mechanisms of operation and their consequences, it aggravates the difficulties in comparing the performances of different detectors independently of application. Therefore, the most critical detector parameters are briefly addressed below.

Linearity of detectors is often defined in the literature with linear coordinates. Detectors are classified as linear and non-linear. As non-linear behaviour may either result from the operating principle of the detector or the electronics, the calibration graph should always be plotted with logarithmic coordinates. Linearity is defined as the proportionality constant between the logarithm of the signal and the logarithm of the amount eluted.

Limit of detection has been a subject of much controversy. For this paper, the considerations given in ref. 5 were accepted.

The selectivity for an element-specific detector can be quantified as the amount of a given element that yields a chromatographic peak on the channel of another element or disturbs its baseline to such an extent that determination of a co-eluting compound on that channel is no longer feasible. In the former instance, the degree of interference may also be expressed by the selectivity ratio as defined in ref. 5.

EXPERIMENTAL

Chemicals

n-hexane was obtained from Carlo Erba, *n*-decane from Fluka, *tert.*-pentanethiol and *n*-hexanethiol from Polyscience, bromobenzene, carbon tetrachloride and chlorobenzene from Supelco and tetrachloroethylene, bromoform and 2-bromochlorobenzene from Aldrich. All the chemicals were used as received without further purification.

For the determination of the fundamental detector parameters, four model solutions of different concentrations were prepared with *n*-decane as internal standard at a concentration of 0.9 μmol/ml. The concentrations of the compounds in the model solutions are listed in Table I. For the determination of C:X mole ratios, carbon tetrachloride, bromoform, bromobenzene and chlorobenzene were applied at concentrations of 1.35, 1.43, 1.15 and 1.10 μmol/ml, respectively (solution 1) and in a tenfold dilution of solution 1 (solution 2). All solutions were thoroughly homogenized in an ultrasonic bath. Peak areas were considered as signals after normalization by the signal of the internal standard. For preparation of the calibration graph, nine measurements were carried out. The ex-

TABLE I

AMOUNTS OF THE COMPOUNDS IN 1 ml OF THE MODEL SOLUTIONS

Compound	Solution 1 (μmol)	Solution 2 (μmol)	Solution 3 (μmol)	Solution 4 (μmol)
tert.-Pentanethiol	9.20	0.84	91.3	11.1
n-Hexanethiol	8.08	0.78	80.0	9.7
Tetrachloroethylene	8.81	0.80	87.2	10.6
Bromoform	11.45	1.04	113.4	13.7
1-Bromochlorobenzene	7.27	0.66	72.0	8.7

perimental conditions were kept at their optimum values, except when the dependence of sensitivity values on experimental parameters was determined.

Instrumental conditions

The gas chromatograph used was a Carlo Erba MEGA 5300, equipped with a split/splitless injector (temperature 250°C). The column was SPB-20 (30 m × 0.32 mm I.D., 0.25 μm film thickness) (Supelco) and the carrier gas was helium (T55, Messer Griesheim). The column was held at 40°C for 2 min, then programmed to 220°C at 10°C/min and held at 220°C for 5 min. The detector was an element-specific detector (Anton Paar) with a stabilized capacitive plasma (generator frequency 27.12 MHz; plasma power 150 W). The selected emission lines were 940.6, 837.6, 827.4 and 921.4 nm for carbon, chlorine, bromine and sulphur, respectively.

RESULTS AND DISCUSSION

The sensitivity, linearity, linear range, limit of detection and selectivity found for each channel are summarized in Table II.

Sensitivity

If the amounts of the elements entering the detector are measured in picomoles and the signal is expressed in peak- area units, the sensitivities listed in Table II are obtained for the channels. As can be seen, the sensitivities of the different channels are very similar. This phenomenon may be surprising in the light of the fact that the four elements have different plasma-chemical behaviours and the emission intensities of the measuring lines and the efficiencies of the filters are different. The sensitivities of the channels are dependent on the experimental parameters, particularly on the flow-rate of the plasma and dopant gases. It can be considered that a change in the flow-rate of the gases affects the local thermal equilibrium of the plasma and hence the number of atoms excited.

Linearity

The data in Table II clearly indicate that the carbon, chlorine and bromine channels can be considered as linear detectors but the sulphur channel shows non-linear behaviour. On the basis of the operating principle of the detector, linear behaviour would also be expected for this

TABLE II

FUNDAMENTAL DETECTOR PARAMETERS OF THE CHANNELS

Parameter	Carbon	Chlorine	Bromine	Sulphur
Sensitivity	3.32	3.41	3.06	2.77
Linearity	1.0	1.0	1.0	1.4
Linear range	4.0	4.5	4.6	4.2
Limit of detection (pg/s)	7	14	25	6

channel, so the result indicates that the reaction producing the excited S atoms is not a simple first-order reaction. As sulphur tends to participate in a series of bimolecular reactions in flames [6], the reaction leading to the excited S atoms may also be fairly complex in the plasma. The observed phenomenon, however, calls for further investigations.

Linear range

As can be seen from the data in Table 2, the values for the channels are fairly similar to each other. It is more informative, however, to compare these values with those of GC detectors of similar application.

The outstanding figure for flame ionization detection (FID, 10^7) [7] exceeds the linear range of the carbon channel of the element-specific detector. This is not surprising, however, as FID is unsurpassed among GC detection methods in terms of its linear range. The comparison of the linear ranges of the chlorine and bromine channels with that of ECD is not so straightforward. In ECD the linear range is strongly dependent on the mode of operation (constant-current or constant-frequency mode). In the constant-current mode this value can be as high as 10^4–10^5, similar to those of the Cl and Br channels, with a concomitant decrease in sensitivity and the disadvantage that for compounds with ultrafast electron attachment rate constants ($2.8 \cdot 10^{-7}$–$4.6 \cdot 10^{-7}$ ml/molecule·s; Cl_4, SF_6, $CFCl_3$, CH_3I) the detector shows non-linear response behaviour. In the constant-frequency mode the linear range of ECD is not more than 100 [6].

The linear range of the sulphur channel of the element-specific detector can be compared with that of the flame photometric detector which has values between 500 and 1000 depending on the structure of the functional group containing the sulphur atom [7].

An additional comment on the comparison of the linear ranges of the different detectors is worthy of note. For a conventional GC detector the value is usually given with integers, as it is strongly dependent on the type of compound being analysed. For the element-specific detector, however, the response is proportional only to the number of atoms of a given element irrespective of the type of substance, hence the second digit may also be significant.

Limit of detection

Although in theory the element-specific detector is a mass flow-sensitive GC detector, in contrast to the electron-capture detector, which has a concentration dependent response, direct comparison of the detection limits is feasible. In practice, calibration and the subsequent quantitative analysis are always carried out under constant, optimized experimental conditions. In this case the limits of detection can be expressed in mass/time or number of moles/time units for both types of detector. A chromatographic peak given by 14 pg/s of chlorine on the chlorine channel is depicted in Fig. 2.

Each of these values is worth comparing with those given a common GC detector or similar application, taking into account the differences in the mechanisms of their operation. The limit of detection of the carbon channel of the element-specific detector is of the same order of magnitude as that for FID (2–5 pg/s). As a consequence of the operating principle of the FID instrument, its response is proportional to the number of "effective" carbon atoms capable of hydrogenation. The signal is the largest for hydrocarbons, truly proportional to the number of carbon atoms, whereas compounds containing

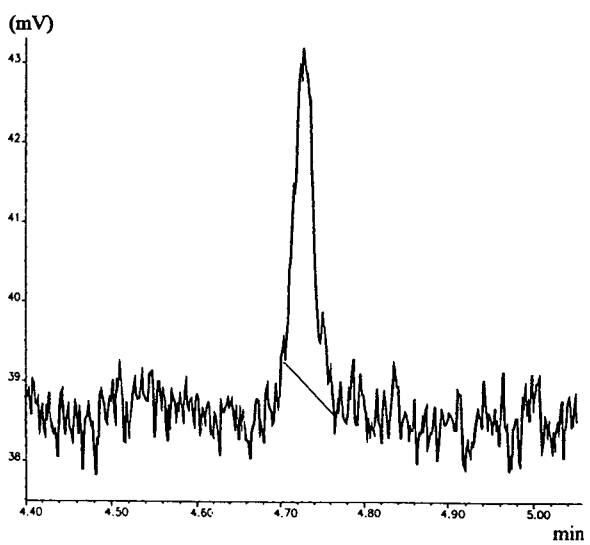

Fig. 2. Signal for 14 pg/s of chlorine on the chlorine channel.

nitrogen, sulphur or halogens yield smaller responses depending on the character of the heteroatom and the electron affinity of the combustion products. The effective carbon number can be estimated from the contributions of carbon atoms and other elements. The detection limit in FID is most often given for members of the *n*-alkanes (*e.g.*, *n*-butane), for which direct comparison with that of the carbon channel is feasible.

The detection limits of the chlorine and bromine channels of the element-specific detector can be compared with that for ECD. The fundamentally different operation principle and selectivity of the electron-capture detector (the latter covers six orders of magnitude) and the differences between their operation modes and the strong dependence on experimental parameters make this comparison ambiguous. The detection limit in ECD is most often quoted for lindane (hexachlorocyclohexane) (50 fg/s). The detection limit obtained for the chlorine channel can be re-calculated for this compound, yielding a value of 20 pg/s. In this respect the element-specific detector can only be competitive with ECD for compounds containing one (or two) chlorine or bromine atom(s).

The detection limit of the sulphur channel can be compared with that in flame photometric detection (FPD). The value obtained for the element-specific detector is normally lower than those reported for FPD (5–50 pg/s). The response for FPD, however, depends slightly on the substance to be determined.

Selectivity

For the definition of selectivity, the cross-interactions of the different channels should be considered in the form of a matrix. Quantification of these effects, however, is hampered by the fact that the disturbance on a given channel may reflect the contributions of all the atoms in the detector and not only of those giving signals on the other channels.

Therefore, the selectivity of the different channels of the element-specific detector, in fact the only one among the parameters of the detector, depends on the type of interfering substance, hence its determination is mostly linked to a particular application.

The most important effect among the cross-interactions is the effect of hydrocarbons on each of the selective channels. During the elution of the solvent peak, especially when a larger sample volume is injected at a low splitting ratio, the change in the physical conditions of the plasma is noticeable with concomitant disturbances on the selective channels. This region of the chromatogram is best avoided by optimizing the conditions of separation and selecting a suitable programme for the detector.

Apart from the peak of the solvent, hydrocarbons have little effect on the other channels with the exception of the sulphur channel. During the elution of 11 nmol/s carbon atom a distinct chromatographic peak appears on the sulphur channel, giving a selectivity ratio of 550. This value is poor compared with the similar parameter in FPD (10^4–10^5) and raises serious doubts about the applicability of this channel for more complex samples.

In addition, considerable cross-effects can be observed between the selective channels of the element-specific detector; 1.5 nmol/s of chlorine atom (in tetrachloroethylene) yielded a chromatographic peak on the bromine channel, whereas 1.1 nmol/s of bromine atom (in bromoform) gave a peak on the chlorine channel. Above these critical amounts the selectivity ratios for chlorine/bromine and bromine/chlorine were *ca.* 600 and 400, respectively. Sulphur gave a signal on the chlorine channel in amounts as low as 400 pmol/s with a selectivity ratio of 800. These cross-effects are illustrated in Fig. 3.

The carbon channel shows the elution of *n*-hexanethiol (6.9 min) and bromoform (7.1 min) with baseline resolution. The amounts of carbon atoms entering the detector were 7.13 and 1.68 nmol, respectively. Their effects on the chlorine channel clearly reflect that pseudo-peaks primarily result from the effects of the sulphur and bromine atoms. The ratio of the two pseudo-peaks can be accounted for by the amounts of the two elements and the corresponding selectivity ratios. These phenomena may be interpreted as follows. First, there may be some overlap between the emission lines of different

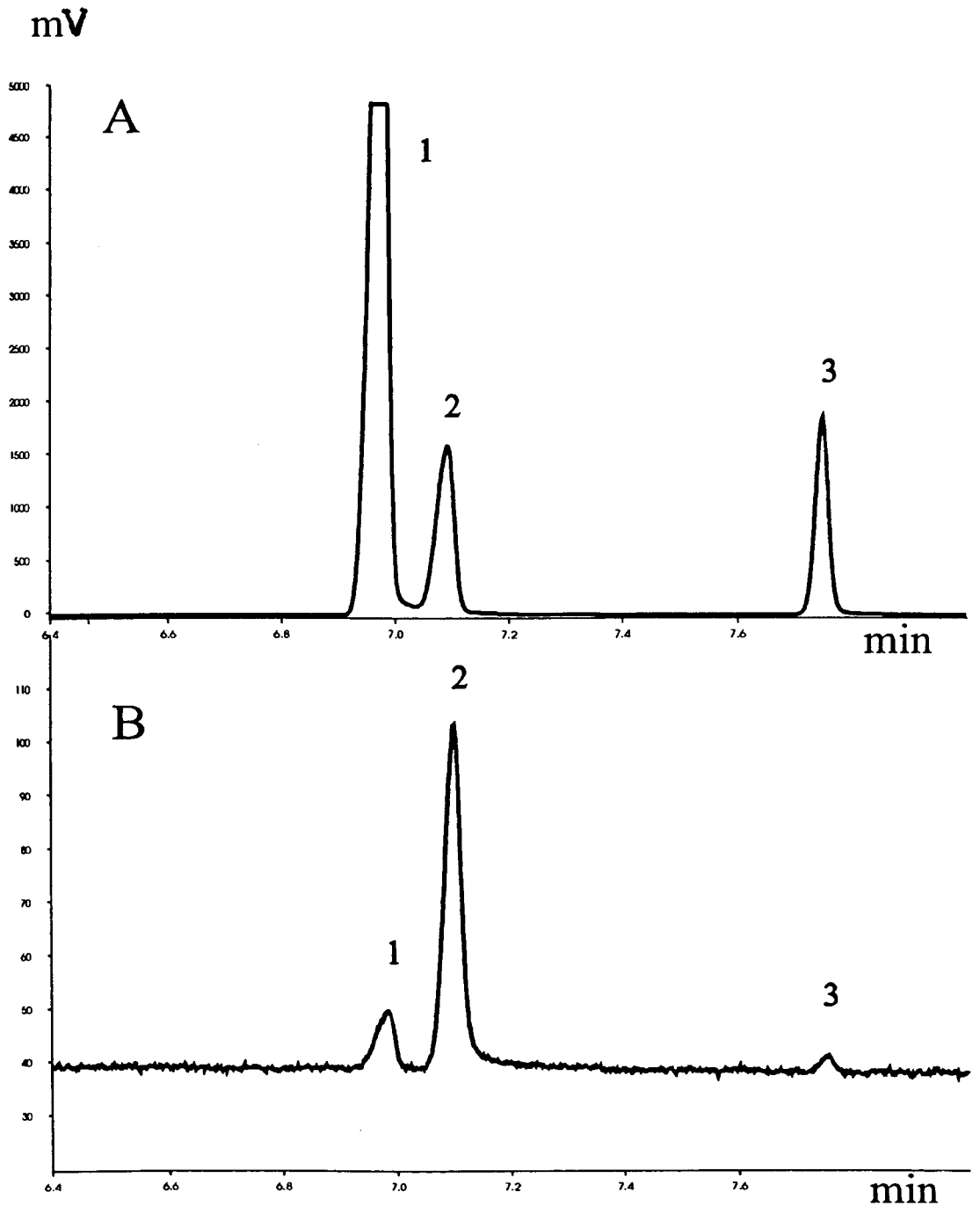

Fig. 3. Effect of sulphur and bromine on the chlorine channel. (A) Carbon channel; (B) chlorine channel. Peaks: 1 = *tert.*-pentanethiol; 2 = bromoform; 3 = *n*-decane.

elements. For example, chlorine gives an emission line at 827.4 nm whereas the bromine signal is measured at 827.2 nm. Similarly, bromine gives an emission line at 836.2 nm in the vicinity of the selected line for chlorine (837.2 nm). Second, some cross-effects may be experienced through a change in the chemical conditions in the plasma. The evaluation of these effects, however, is fairly academic. On a high-resolution fused-silica capillary column, two compounds containing different heteroatoms can probably be separated from each other. From practical considerations, only the selectivity with respect to hydrocarbons is of importance, which is normally good for the selective channels except the sulphur channel.

Advantages of the element-specific detector in qualitative and quantitative analyses

One of the most important advantages of the element-specific detector is that the detector is capable of the truly simultaneous acquisition of four virtually independent chromatograms without splitting of the flow. Therefore, the amount of information supplied by the detector is unsurpassed among conventional GC detectors. The fact that the signal is proportional to the amount of the element gives the detector unique selectivity and helps in the identification of the compounds. From the signal of the different channels the mole ratios of the elements can be calculated, allowing the determination of molecular formulae and increasing the probability of positive identification of the unknown compounds.

Experimental C:X mole ratios were calculated for four halogenated compounds at two concentration levels (see Experimental). The number of moles were determined from the corresponding calibration graphs and their ratios were calculated. The results are given in Table III. Although the values found are different from the theoretical values, they can still be related to the correct integers. The departures from the theoretical values can partly be explained by the fact that calibration graphs for the elements chlorine and carbon were established using compounds not included in Table III. In addition, the fact that the ratios are closer to the theoretical values at higher concentrations may imply that the amounts in solution 2 are fairly close to the lower end of the calibration graph, introducing a larger bias to the determination of mole ratios.

TABLE III

EXPERIMENTAL C:X MOLE RATIOS AT TWO CONCENTRATION LEVELS

Compound	Solution 2	Solution 1
Carbon tetrachloride	1:3.83	1:3.91
Tribromomethane	1:3.07	1:3.03
Bromobenzene	5.78:1	5.81:1
Chlorobenzene	6.11:1	5.99:1

As, in theory, the signal of each channel is directly proportional to the amount of the element and independent of the structure of the compounds, a single standard for each element should be appropriate for determining the concentration of any compounds containing the given element. This assumption was tested with a model solution containing four halogenated compounds. The concentrations were determined using the previously established calibration graphs. The results of the single standard measurements are given in Table IV.

The results are in fairly good agreement with the true concentrations except for 2-bromochlorobenzene (on both the chlorine and bromine channels), where the interferences between chlorine and bromine (as discussed with respect to the selectivity of the detector) can be held responsible for the observed bias. The good accuracy of the single standard measurements implies that there is no need to run calibration samples in order to determine the response factors of the individual compounds. This is a great advantage over the conventional GC detectors where the determination of response factors in a separate set of calibration experiments for each compound to be quantified is essential.

The parameters of the detector allocate the potential field of application where its advantages can be fully exploited. In laboratories where samples of changing character are frequently encountered, the element-specific detector may be superior to conventional GC detec-

TABLE IV

RESULTS OF QUANTIFICATION WITH A SINGLE STANDARD PER CHANNEL

Compound	Concentration found (μg/l)[a]	True concentration (μg/l)
Carbon tetrachloride	457 ± 23	470
Tribromomethane	1261 ± 49	1320
2-Bromochlorobenzene[b]	2031 ± 198	1615
2-Bromochlorobenzene[c]	2124 ± 182	1615
Chlorobenzene	752 ± 15	740

[a] Mean ± standard deviation ($n = 6$).
[b] Determined on bromine channel.
[c] Determined on the chlorine channel.

tors as it may considerably reduce the efforts required for the preparation of calibration solutions and their measurements and evaluation.

In addition, the element-specific detection can be simultaneously operated as a universal or selective detector. It is uniquely versatile, responding quickly to incoming samples requiring different types of detectors without instrumental modification or extensive calibration measurements. All these facets can be achieved without any compromise in quantitative analysis within the framework allocated by the parameters of the detector.

CONCLUSIONS

The most important parameters of GC detectors were determined for the four channels (C, Cl, Br, S) of the element-specific detector. Each parameter of the channels was compared with the performance of a common GC detector of similar application with regard to the basic differences in the operational mechanisms.

The sensitivities were found to be nearly identical for all channels. The values were dependent on the flow-rates of the plasma and dopant gases. The responses of the carbon, chlorine and bromine channels were linear whereas the sulphur channel showed non-linear characteristics, its linearity parameter being 1.4. This finding calls for further investigation. The linear ranges for all channels covered 4–5 orders of magnitude. The values were worse than the corresponding parameter for FID but generally exceeded the values for other selective detection methods (ECD, FPD).

For detection limits the standard classification of GC detectors were neglected (mass flow- or concentration-sensitive detectors) and limits of detection were determined at the optimum experimental parameters. The detection limit of the carbon channel (7 pg/s) was similar to that of FID. For the chlorine and bromine channels (14 and 25 pg/s, respectively) these parameters were generally worse than those of ECD. The detection limit obtained for the sulphur channel was usually lower than that of FPD. The selectivities of the channels towards hydrocarbons were exceptionally good for the chlorine and bromine channels whereas it was poor for the sulphur channel, limiting its applicability in the case of complex samples. In contrast, there were considerable cross-effects between the selective channels. The selectivity ratios varied between 400 and 1600, but these effects are rather academic.

The fact that the detector is capable of acquiring four different, universal and selective chromatograms at the same time considerably increases the probability of positive identification of analyte compounds. As the signal on each channel is directly proportional to the amount of the given element, the concentration of any compound can be determined with a single standard without the need to determine response factors in separate calibration measurements.

The element-specific detector is a versatile

instrument for laboratories encountering a flow of samples requiring different types of detectors even with a single gas chromatograph.

ACKNOWLEDGEMENTS

The authors are grateful to Anton Paar, and especially to Dr. Friedrich Santner and Professor Günter Knapp, for supplying the element-specific detector. Financial support of this project by OTKA (2561) is gratefully acknowledged.

REFERENCES

1 P.C. Uden, *Trends Anal. Chem.*, 6 (1987) 238–246.
2 J.J. Sullivan and B.D. Quimby, *Anal. Chem.*, 62 (1990) 1034–1043.
3 B.D. Quimby and J.J. Sullivan, *Anal. Chem.*, 62 (1990) 1027–1034.
4 B. Platzer, E. Leitner, G. Knapp, A. Schalk and A. Grillo, Am. Lab., 22 (1990) 12–17.
5 J. Sevcík, *Detectors in Gas Chromatography*, Elsevier, Amsterdam, 1976.
6 C.F. Poole and S.K. Poole, *Chromatography Today*, Elsevier, Amsterdam, 1991.
7 G. Schomburg, *Gas Chromatography*, VCH, Weinheim, 1990.

Journal of Chromatography A, 654 (1993) 279–285
Elsevier Science Publishers B.V., Amsterdam

CHROM. 25 518

Simple device for permeation removal of water vapour from purge gases in the determination of volatile organic compounds in aqueous samples

Wacław Janicki, Lidia Wolska, Waldemar Wardencki* and Jacek Namieśnik

Department of Analytical Chemistry, Chemical Faculty, Technical University of Gdańsk, Narutowicz Str. 11/12, 80-952 Gdańsk (Poland)

(First received June 2nd, 1993; revised manuscript received August 16th, 1993)

ABSTRACT

A commercially available Nafion tube (a perfluorinated ion-exchange resin membrane separator) inserted in a plastic container filled with 5A molecular sieve was tested on dry water-saturated gas streams containing common volatile pollutants of aqueous environmental samples after a purging cycle. The proposed device was shown to remove water vapour effectively from humidified gas streams (>90%) even under continuous operation for more than 10 days. The results showed that the system is compatible with the tested compounds (aliphatic and aromatic hydrocarbons, chlorinated hydrocarbons and some sulphur compounds) because these compounds are practically unaffected on passing through the Nafion dryer tube. The losses of most compounds at the μg/kg level are less than 5%. Therefore, the proposed device is suitable for the removal of water vapour from purging streams and can be used in the determination of these volatile organic compounds in aqueous samples using the purge-and-trap technique.

INTRODUCTION

Volatile organic compounds (VOCs) are an important class of water pollutants. The determination of trace amounts of VOCs in water is often carried out by gas chromatography (GC), usually after a preconcentration step [1–3]. Various methods are used for preconcentration, but the purge-and-trap (PT) technique is the most preferred, especially for the determination of purgeable priority pollutants listed by the US Environmental Protection Agency (EPA) [4–6].

In the first step of the PT technique, the analytes are stripped from the aqueous phase. In the next, the swept analytes can be either (1) adsorbed on a thermally desorbable sorbent bed (especially one containing Tenax) [7], (2) retained in a cold trap (cryotrapping) [8], (3) cryofocused on the head of the column [9] or (4) transferred to a capillary column maintained at a cryogenic temperature (whole-column cryotrapping) [10,11]. Finally, the solutes trapped in different ways, after liberation, are separated on a column and detected.

The main disadvantage of the PT technique is the purging of significant amounts of water vapour along with the analytes. This ubiquitous presence of water can cause many problems, mainly during the focusing of the analytes and their chromatographic analysis. The same problem is encountered during the determination of trace amounts of VOCs in air samples, but the content of water is considerably lower.

The main problems caused by the presence of water in streams of gases in the mentioned procedures are as follows: decrease of the adsorption capacity of the sorbent used for the

* Corresponding author.

0021-9673/93/$06.00 © 1993 Elsevier Science Publishers B.V. All rights reserved

concentration of VOCs owing to co-adsorption of water; condensation of water along with the analytes on the walls of the tubes connecting the purge device with the sorbent trap or GC injection port; plugging of traps and GC columns at sub-zero temperatures [10,12]; degradation of the performance of retention gaps or GC columns [13,14]; and variations of retention times and responses of the compounds that elute near water [15,16].

Several procedures have been used to avoid these adverse effects: using a hydrophobic sorbent [16]; heating the connection tubes [17]; the use of desiccants such as $Mg(ClO_4)_2$ [18–20], Ascarite [21], K_2CO_3 [22], $CaSO_4$, $Ba(ClO_4)_2$ and Na_2SO_4 [23,24]; removal of water by reaction in a precolumn filled with triethyl orthoformate or 2,2-dimethoxypropane [25]; adsorptive removal of water by silica gel [26] or molecular sieves 3A, 4A and 5A [27]; removal of water by passing the moist streams through a short column of glass beads (condenser) at −10°C [8,9]; and permeation removal of water by using membrane tubes [27–31].

The last procedure, based on the use of perfluorosulphonic acid membranes made of Nafion tubes produced by DuPont, has two important advantages over conventional bed desiccants, namely a small dead volume and a small pressure drop.

A commercially available Nafion drier (a perfluorinated ion-exchange resin) has proved to be an efficient membrane separator. The exceptional performance of these membranes derives from the chemical, mechanical and thermal stabilities provided by a perfluorinated backbone and the ion-exchange properties supplied by the pendant sulphonate groups. In the salt form, Nafion has the following repeat structure [32]:

$$-(CF_2CF_2)_mCF_2CF-$$
$$(OCF_2CF)_mOCF_2CF_2SO_3^- X^+$$
$$CF_3$$

where m is small and X^+ is an exchangeable cation.

Some previous applications of Nafion tube dryers have helped to define the conditions under which they can be used [27,30,33]. In most of these applications Nafion was used to remove water from ambient air samples. Coutant and Keigley [34] used Nafion in the direct injection of water samples of considerable volume. To our knowledge, no previous systematic investigations have been reported on drying of gases after purging volatiles from water samples containing typical environmental pollutants. In such cases the conditions are more drastic because saturation of the sample streams with water vapour occurs.

The purpose of this work was to test the compatibility of common volatile pollutants of water (aliphatic and aromatic hydrocarbons, organosulphur compounds and halogenated hydrocarbons) with Nafion to show its suitability for drying water-saturated gases in the PT–GC technique.

EXPERIMENTAL

Efficiency of the Nafion tube for drying of gas streams after the purging step

Nafion used in all experiments was obtained from Perma Pure Products (Toms River, NJ, USA) as tubing of 0.33 mm I.D. and 0.51 mm O.D., wall thickness 0.089 mm and internal volume 0.099 cm^2 m^{-1}.

Initial studies to determine the water removal efficiency under approximately ambient conditions from gas streams in the PT technique were conducted in a system consisting of the following components: (1) an argon reservoir; (2) a 20-cm^3 laboratory-made purge vessel with a medium pore size frit; (3) interchangeably, (a) a fused-silica capillary (system A), (b) a 1.2-m Nafion tube inserted in an empty clear plastic cylinder (system B) and (c) a 1.2-m Nafion tube inserted in the cylinder with molecular sieve type 5A (system C); and (4) a scrubber filled with magnesium perchlorate.

Argon was delivered to the purge vessel through a frit and was bubbled through 10 cm^3 of water for 10 min at a flow-rate of 30 cm^3 min^{-1}. It can be assumed that under these conditions the gas stream leaving the purge is saturated with water vapour (>90%). The efficiency of each system was determined from the mass increase of

the scrubber. The average mass increase in case 3a was 5.97 mg, which corresponds to complete saturation of gas with water vapour at ambient temperature (18.7 μg of water in 1 cm^3 of gas) and is the expected value. In case 3b, this increase was 3.11 mg and in case 3c, in which the humidity outside the Nafion tube due to the presence of molecular sieve was close to 0%, the mass of the scrubber was virtually unchanged (0.1 mg).

Effect of the Nafion dryer on the recovery of the selected volatile organic compounds

Preparation of solutions. Stock standard solutions of trichloromethane, tetrachloromethane, dichlorobromomethane, chlorobenzene, *n*-propanethiol and *tert.*-butanethiol were prepared in methanol and those of 1,7-octadiene, 1-octene, thiophene, diethyl sulphide, styrene, benzene, toluene, nonane and decane in dimethyl sulphoxide (DMSO). The concentrations of the analytes ranged from *ca.* 0.1 to 1 g kg^{-1}. Model aqueous solutions at the μg kg^{-1} level were prepared in measuring flasks (100 cm^3) by injecting 3–10 μl of stock solutions with a microsyringe. A 10-cm^3 volume of the model solution of each compound was taken for the recovery tests under different sampling procedures.

Purge-and-trap conditions. A general view of the laboratory-made PT system is shown in Fig. 1. The device consists of (1) a 20-cm^3 laboratory-made purge vessel; (2) optionally, a 1.2-m Nafion dryer inserted in the cylinder with molecular sieve type 5A (*ca.* 2–3-mm beads); (3) a six-port rotary valve; and (4) a trap with an appropriate sorbent.

For experiments with trichloromethane, tetrachloromethane and dichlorobromomethane the trap was filled with 30 mg of Carbosieve III S and 80 mg of Tenax TA. For all other compounds only 80 mg of Tenax TA were used. The purge gas, argon, was passed through the system (Fig. 1A) at a flow-rate of 30 cm^3 min^{-1} for 15 min for thiophene and diethyl sulphide, for 5 min for *n*-propanethiol and *tert.*-butanethiol and for 10 min for the remaining compounds. After that time, the flow was stopped and heating of the trap was started. When the trap reached a temperature of 170°C the carrier gas was directed to the trap (Fig. 1B) and desorbed analytes at 250°C [17] were passed to the chromatographic column.

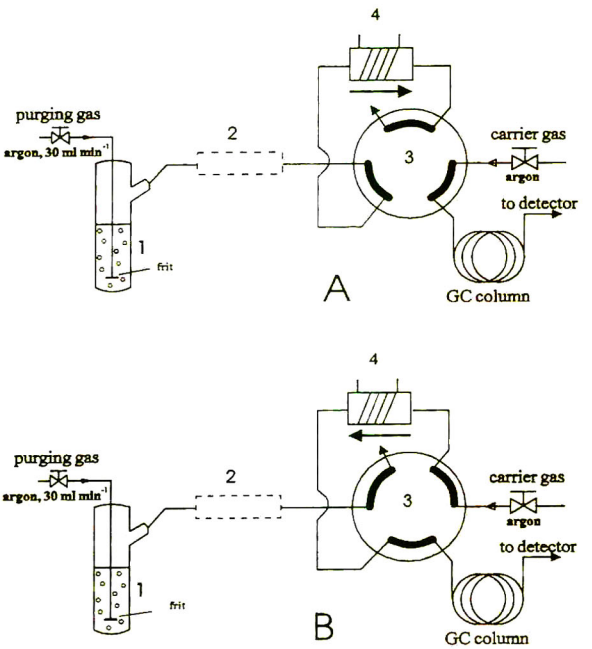

Fig. 1. Experimental apparatus assembly: 1 = purging vessel with frit; 2 = 1.2-m Nafion dryer embedded in 5A molecular sieve desiccant; 3 = six-port rotary valve; 4 = heated sorbent trap. (A) Purge and trap step; (B) desorption step.

Chromatographic conditions. Analyses for trichloromethane, tetrachloromethane and dichlorobenzene were performed using a Hewlett-Packard Model 5890 II gas chromatograph equipped with a 30-m DB-1 capillary column and an electron-capture detector. The temperature programme was initially 70°C for 4 min, increased at 10°C min^{-1} to 110°C and held at the final temperature for 7 min.

The remaining compounds were measured using a Hewlett-Packard Model 5830 A gas chromatograph equipped with the packed columns and a flame ionization detector. Benzene, toluene, nonane, decane, thiophene and dimethyl sulphide were separated on 2 m × 0.3 mm I.D. column packed with Dexil 300. The temperature programme was initially 80°C for 1 min, increased at 4°C min^{-1} to 120°C and held at the final temperature for 1 min. For the separation of the remaining compounds a 3 m × 0.3 mm

I.D. column packed with DC-550 was used. The column temperature was 50°C for propanethiol and *tert.*-butanethiol, 70°C for 1,7-octadiene, 80°C for chlorobenzene and 105°C for styrene.

RESULTS AND DISCUSSION

To prevent column plugging and chromatographic interference by water, the purge gas should be dried before reaching the column. The proposed systems should remove water vapour and not affect the analyte compounds.

Preliminary experiments showed that the proposed device, a Nafion tube inserted in a plastic container filled with 5A molecular sieve, effectively removes water from water-saturated gas streams after a purging step. Fig. 2 compares the water-removal efficiencies for the different systems used. The effectiveness of water removal with the tested systems was calculated on the basis of the mass increase of the scrubber containing magnesium perchlorate. A virtually unchanged mass of the scrubber (Table I) after passing the purge gas stream through the proposed system (A) indicates that water is nearly completely removed. From Fig. 3, it is clear that the effectiveness of the water removal remains almost constant for as long as 10 days of continuous operation.

In a second series of experiments, the effect of the system used on the recovery of common volatile pollutants of aqueous environmental samples after passing through the proposed device was tested. Fig. 4 illustrates the recoveries of the tested compounds at the ppb level (expressed as the area of corresponding peaks) with and without the use of a Nafion tube. The tests were conducted for two different concentrations of the tested compounds and the results are averages of 5–11 measurements. Table II shows the differences in the recoveries of the investigated compounds with and without a Nafion tube. It can be seen that there is essentially no sample loss (generally <5%) when a Nafion tube containing molecular sieve was connected in-line. These results agree generally with data reported previously [27,30,33]. According to these reports, most inorganic gases, hydrocarbons, esters, chlorinated hydrocarbons and some sulphur compounds were unaffected when a Nafion tube was used for drying air samples. In our study, only the recoveries of octadienes and tetrachloromethane, especially at very low concentrations, are affected by the Nafion tube. The losses of these compounds are about 10%. This may be partially explained by the slightly polar character of some of these compounds. From previous reports it is known that Nafion removes polar compounds such as alcohols, amines, some ethers and esters [27,35]. It has also been reported that Nafion rearranged several monoterpenes and removed several oxygenated compounds [30]. However, this limitation may not be critical for polar compounds in the PT technique because this gas extraction technique is generally unsuitable for such compounds. If analyses for polar compounds are intended, more tests

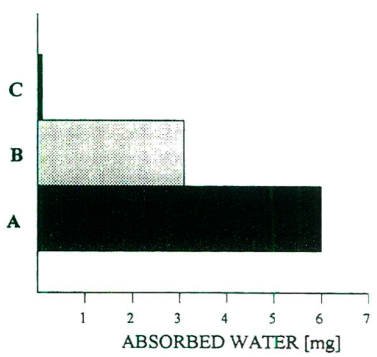

Fig. 2. Comparison of water-removal efficiencies of different drying systems: (A) without a Nafion tube; (B) with a Nafion tube; (C) with a Nafion tube inserted in 5A molecular sieve.

TABLE I

WATER REMOVAL FROM WATER-SATURATED GAS STREAM BY THE DIFFERENT SYSTEMS USED

System	Mass increase of scrubber (mg)	Standard deviation (mg) ($n = 3$)
(A) Without a Nafion tube	6.0	0.44
(B) With a 1.2-m Nafion dryer	3.1	0.13
(C) With a 1.2-m Nafion dryer inserted in 5A molecular sieve	0.1	0.16

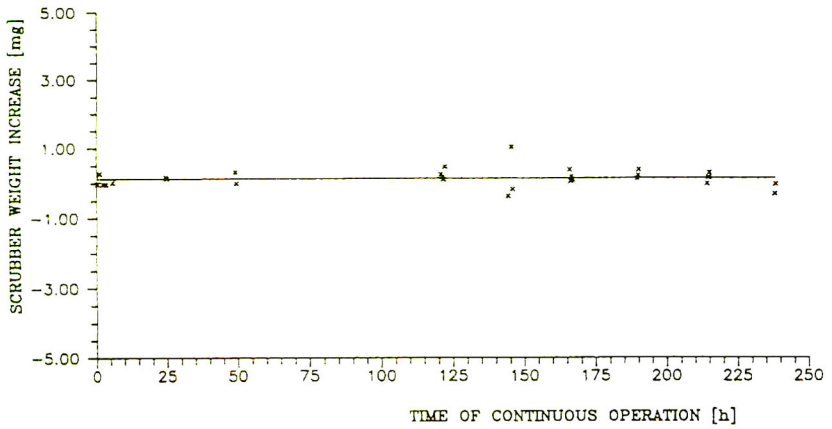

Fig. 3. Efficiency of water removal as a function of time.

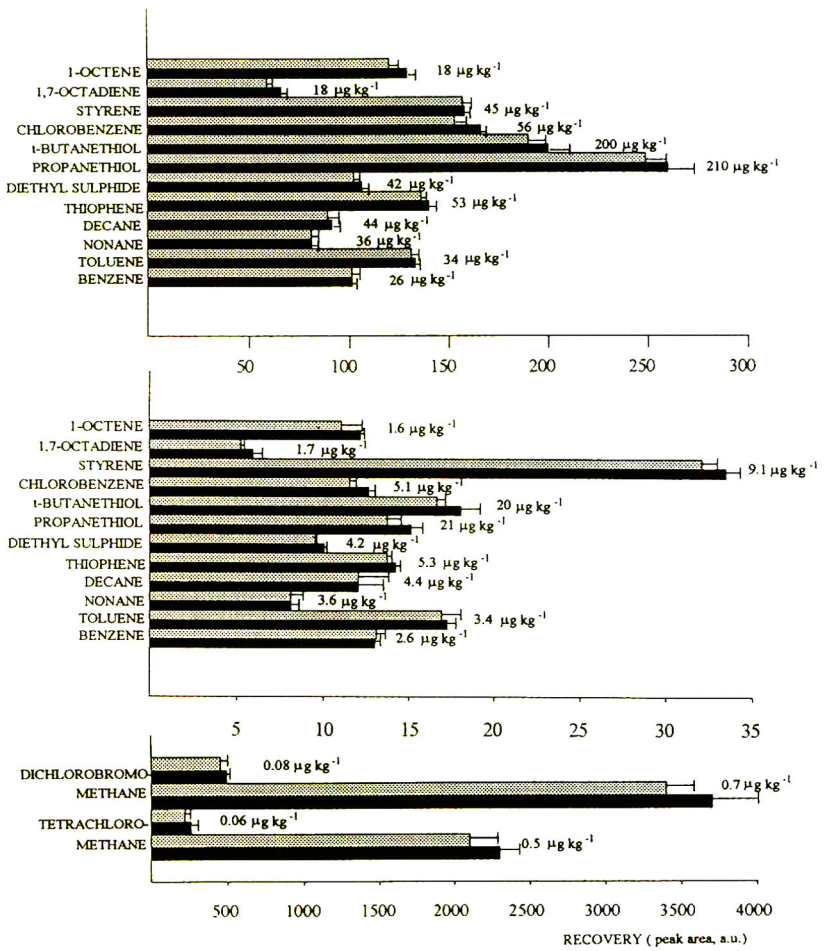

Fig. 4. Recovery of tested compounds with different sampling procedures. Black boxes, sampling directly after purging without a Nafion dryer; dotted boxes, sampling through Nafion dryer. ⊢⊣ = Standard deviation. a.u. denotes arbitrary area units of integration.

TABLE II

RECOVERIES OF TESTED COMPOUNDS WITH AND WITHOUT A NAFION DRYER

Compound	Concentration ($\mu g\ kg^{-1}$)	Deviation[a] (%)	Compound	Concentration ($\mu g\ kg^{-1}$)	Deviation[a] (%)
Benzene	26	0.0	*tert.*-Butanethiol	200	−5.0
	2.6	0.8		20	−7.8
Toluene	34	−1.5	Chlorobenzene	56	−7.8
	3.4	−1.7		5.1	−8.7
Nonane	36	0.0	Styrene	45	−1.6
	3.6	0.0		9.1	−4.2
Decane	44	−2.2	1,7-Octadiene	18	−10.6
	4.4	0.0		1.7	−11.9
Thiophene	53	−2.9	1-Octene	18	−7.0
	5.3	−3.5		1.6	−9.1
Diethyl sulphide	42	−3.8	Tetrachloromethane	0.5	−8.7
	4.2	−5.0		0.06	−15.4
Propanethiol	210	−4.2	Dichlorobromomethane	0.7	−8.1
	21	−9.3		0.08	−8.2

[a] Difference between recovery of purged compound with and without use of a Nafion dryer, expressed in %.

should be made to establish the suitability of a Nafion dryer.

CONCLUSIONS

It was found that a Nafion tube inserted in a plastic container with 5A molecular sieve is suitable for drying water-saturated gas streams leaving the purge vessel during analyses for many common volatile pollutants of water using the PT technique. Water is quantitatively removed from the humidified gas stream and the analyte compounds are virtually unaffected. The proposed device is much cheaper and technically simpler than commercially available equipment such as glass-bead dryers and permeation dryers with a countercurrent flow of dry gas.

ACKNOWLEDGEMENT

This research was supported by the Polish Scientific Committee, grant 40489203.

REFERENCES

1 I. Liška, J. Krupčik and P.A. Leclerq, *J. High Resolut. Chromatogr.*, 12 (1989) 577.
2 F.I. Onuska, *J. High Resolut. Chromatogr.*, 12 (1989) 4.
3 J. Namieśnik, T. Górecki, M. Biziuk and L. Torres, *Anal. Chim. Acta*, 237 (1990) 1.
4 *Federal Register Rules and Regulations*, Vol. 49, No. 209, Oct. 26, 1984, *EPA Method 624 —Purgeables*, pp. 141–152.
5 *Determination of Volatile Organic Compounds According to EPA Method 524.2; Bulletin No. 503562*, Chrompack, Middelburg, 1992.
6 M.R. Driss and M. Bougerra, *Int. J. Environ. Anal. Chem.*, 45 (1991) 193.
7 M.E. Rosen and J.F. Pankow, *J. Chromatogr.*, 537 (1991) 21.
8 M.F. Pankow, *Environ. Sci. Technol.*, 25 (1991) 123.
9 A. Zlatkis, H.A. Lichtenstein and A. Tishbee, *Chromatographia*, 6 (1973) 67.
10 J.F. Pankow, *J. High Resolut. Chromatogr. Chromatogr. Commun.*, 10 (1987) 409.
11 J.F. Pankow and M.E. Rosen, *Environ. Sci. Technol.*, 22 (1988) 98.
12 L. Lepine and J.F. Archambault, *Anal. Chem.*, 64 (1992) 810.
13 J.J. Vreuls, R.T. Ghijsen, G.J. de Jong and U.A.Th. Brinkman, *J. Chromatogr.*, 625 (1992) 237.
14 W.F. Burns, D.T. Tingey and R.C. Evans, *J. High Resolut. Chromatogr. Chromatogr. Commun.*, 5 (1982) 504.
15 H.J. Schaeffer, *J. High Resolut. Chromatogr.*, 12 (1989) 69.
16 J.F. Pankow, M.P. Ligocki, M.E. Rosen, L.M. Sabelle and K.M. Hart, *Anal. Chem.*, 60 (1988) 40.
17 W. Janicki, B. Zygmunt, L. Wolska, W. Chrzanowski and W. Wardencki, *Chem. Anal. (Warsaw)*, 37 (1992) 599.
18 K. Bachmann and J. Polzer, *J. Chromatogr.*, 481 (1990) 373.

19 J. Novak, J. Zlaticky, V. Kubella and J. Mostecki, *J. Chromatogr.*, 76 (1973) 45.
20 P.V. Doskey, *J. High Resolut. Chromatogr.*, 14 (1991) 724.
21 E. Kozłowski and J. Namieśnik, *Microchim. Acta*, II (1972) 435.
22 S.E. Maljaars and M.W.F. Nielen, *Int. J. Environ. Anal. Chem.*, 39 (1988) 333.
23 J.H. Raymer and E.D. Pellizzari, *Int. J. Environ. Anal. Chem.*, 43 (1991) 151.
24 A. Tangerman, *J. Chromatogr.*, 366 (1986) 205.
25 J. Chen and J.S. Fritz, *Anal. Chem.*, 63 (1991) 2016.
26 S.W. Klamm and G.W. Scheil, *Environ. Sci. Technol.*, 23 (1989) 1420.
27 B.B. Baker, Jr., *Am. Ind. Hyg. Assoc.*, 35 (1974) 735.
28 B.E. Foulger and P.G. Simmonds, *Anal. Chem.*, 51 (1979) 1089.
29 R.D. Cox and R.F. Earp, *Anal. Chem.*, 54 (1982) 2265.
30 W.F. Burns, D.T. Tingey, R.C. Evans and E.H. Bates, *J. Chromatogr.*, 269 (1983) 1.
31 W.A. McClenny, J.D. Pleil, M.W. Holdren and R.N. Smith, *Anal. Chem.*, 56 (1984) 2947.
32 A.S.R. Lowry and K.A. Mauritz, *J. Am. Chem. Soc.*, 102 (1980) 4665.
33 U. Hofmann, R. Hofmann and J. Kesselmeier, *Atmos. Environ.*, 13 (1992) 2445.
34 R.W. Coutant and G.W. Keigley, *Anal. Chem.*, 60 (1988) 2536.
35 N.T. Campbell, G.A. Bere, T.J. Blasko and R.H. Groth, *J. Air Pollut. Control Assoc.*, 32 (1972) 533.

Journal of Chromatography A, 654 (1993) 287–298
Elsevier Science Publishers B.V., Amsterdam

CHROM. 25 508

On-line liquid backflush of an uncoated precolumn for automated gas chromatographic analysis of complex mixtures

Gunnar Hagman and Johan Roeraade*

Royal Institute of Technology, Department of Analytical Chemistry, S-100 44 Stockholm (Sweden)

(First received July 12th, 1993; revised manuscript received August 13th, 1993)

ABSTRACT

A fully automated system for the GC analysis of samples containing non-volatile material, consisting of a double-oven on-line liquid backflush system, was constructed and evaluated. An uncoated precolumn is mounted in the first oven and the analytical column is housed in the second oven. It is possible to backflush the precolumn with both gases and liquids, *via* low-volume three-way connectors, while the analysis is proceeding in the coated column. The different events are controlled pneumatically by off-line valves, situated outside the GC ovens. The performance of the system was evaluated by repetitive injections of sample solutions containing crude oil, olive oil and shoe polish. It is shown that refocusing of high-boiling solutes from contaminated precolumns is enhanced when a faster temperature ramp of the precolumn is utilized. It is also shown that the useful lifetime of the precolumn is significantly extended by the on-line solvent rinsing of the precolumn.

INTRODUCTION

The performance of automated GC analyses of complex mixtures is often gradually impaired owing to the accumulation of non-volatile material in the injector or in the column entrance. Trace analysis, using the retention gap technique, is particularly sensitive in this respect as the uncoated precolumn tolerates only a very limited amount of non-volatile material [1,2]. When this limit is exceeded, extra-column band broadening and/or peak splitting occur.

In order to avoid this problem, an off-line sample clean-up is often employed. Techniques such as liquid–liquid or solid-phase extraction are, however, labour demanding, time consuming and not as reproducible as direct introduction of the sample. In this respect, on-line coupled LC–GC is a better approach [3]. A separation on the basis of polarity may remove the non-volatile components present in the sample as long as these do not co-elute with the volatile solutes of interest. Size-exclusion chromatography can also be employed when the resolution between the high- and low-molecular-mass fractions is sufficient [4–7]. Problems such as adsorption of sample material on the LC column and contamination of the LC column should, however, be taken into consideration.

Continuous monitoring of trace components, to perform large series of routine laboratory analyses or on-line measurements in industrial processes should produce reliable results during long periods of time, preferably without supervision. At present, capillary GC is not capable of fulfilling these criteria when the sample contains non-volatile compounds. Recently, we presented the principle of a GC technique which could be a remedy for this problem [8]. A double-oven GC system was utilized where an uncoated precolumn was independently temperature pro-

* Corresponding author.

0021-9673/93/$06.00 © 1993 Elsevier Science Publishers B.V. All rights reserved

grammed from the column and subsequently backflushed with a solvent during the analysis. By employing a faster temperature ramp for the precolumn than for the analytical column, the solutes that are spread over the precolumn reach the entrance of the analytical column while it is at a lower temperature than in the traditional retention gap set-up [9–11]. Consequently, a more effective solute focusing effect is obtained while the presence of non-volatile material becomes less critical. An additional liquid backflush of the retention gap removes most of the non-volatile material and restores the system performance between each analysis.

The performance of this technique was demonstrated with a system where the uncoated precolumn and the analytical column were isolated by an in-line valve [8]. In this paper, a computer-controlled, fully automated GC system that utilizes pneumatic (Deans) switching [12–15], which eliminates the need for in-line valves, is presented.

EXPERIMENTAL

Equipment

A schematic diagram of the experimental set-up is shown in Fig. 1. Two gas chromatographs (Varian Model 3700) were utilized with an uncoated precolumn [8 m × 0.32 mm I.D., deactivated with diphenyl-trimethyldisilazane (DPTMDS)] mounted in the first oven and an analytical column [30 m × 0.25 mm I.D., coated with 0.25 μm DB-5 (J&W Scientific)] housed in the second oven. Three-way press-fit connectors were prepared by fusing three borosilicate glass press-fit connectors together, guided by 0.25 mm I.D. bare fused-silica tubes as described elsewhere [16].

V_1–V_6 were Valco rotary valves of the CW and NW series, pneumatically actuated by digital valve interface units. The sample loop and the solvent loops were filled from glass reservoirs pressurized *via* three-way solenoid valves (Model 339; Asco Controls). The system was fully auto-

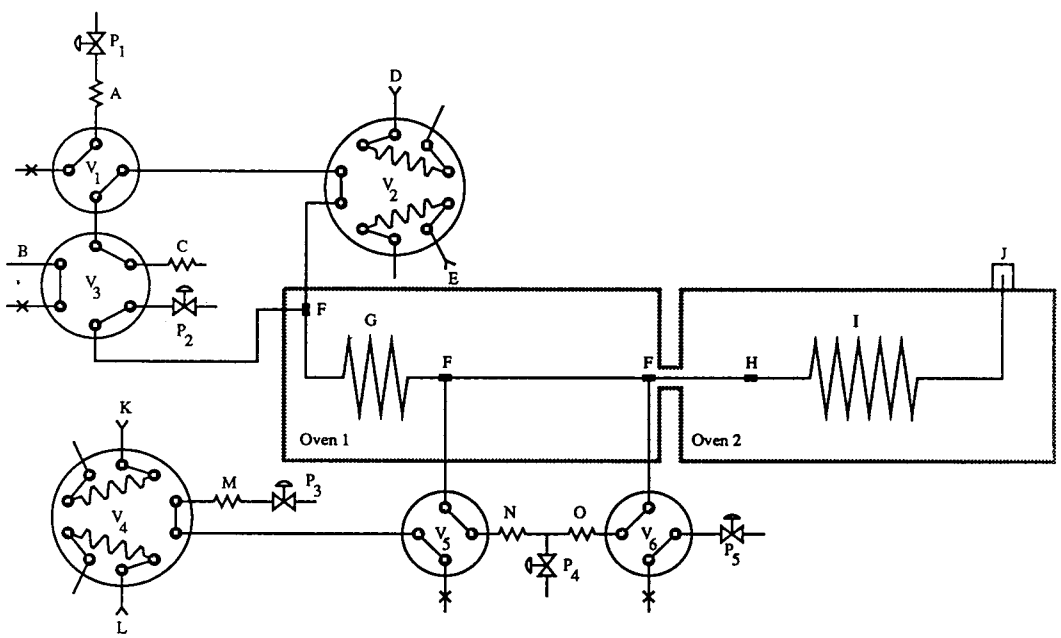

Fig. 1. Schematic diagram of the experimental set-up. A = Restrictor (1 m × 52 μm I.D.); B = waste outlet; C = restrictor (60 cm × 52 μm I.D.); D = wash loop (10 μl) inlet; E = sample loop (10 μl) inlet; F = three-way press-fit connector; G = uncoated precolumn; H = press-fit connector; I = analytical column; J = flame ionization detector; K = backflush solvent loop (500 μl) inlet; L = backflush solvent loop (500 μl) inlet; M = restrictor (60 cm × 52 μm I.D.); N = restrictor (1 m × 52 μm I.D.); O = restrictor (1 m × 52 μm I.D.); P_1–P_5 = pressure regulators; V_1–V_6 = GC switching valves.

mated from a personal computer equipped with a relay driver card (PC-36/A 8255; ELFA) and a electromechanical relay adapter unit (PC-38; ELFA). The different events were time controlled by contact closures of the relays with a computer program written in Pascal.

Pressure regulator P_2 provides the carrier gas pressure during injection and the sample refocusing stage and P_5 provides the carrier gas pressure in the backflush mode. P_1 (and restrictor A) serves to inject the sample at a controlled rate and was set at a higher pressure than P_2. P_3 (and restrictor M) controls the rate of backflush solvent introduction and was set at a higher pressure than P_5. P_4 provides a small purge flow to the three-way press-fit connectors *via* restrictors N and O to avoid dead volumes in the connector legs and was set at a higher pressure than P_2 and P_5. Restrictor C ensures a backflush purge flow of the cold part of the transfer line from valve V_2 to avoid slow release of residual solvent from the transfer line and the valve after sample transfer.

Procedure

The operating sequence of the system is outlined below.

(1) In the load position (where the valves V_1–V_6 are in the positions shown in Fig. 1) the sample loop, the wash loop and the liquid backflush loops are filled with sample, wash solvent and backflush solvents, respectively.

(2) The sample and the wash solvent are transferred to the uncoated precolumn by switching valves V_1 and V_2 (Fig. 2A).

(3) When the sample transfer is completed, valves V_1 and V_2 are switched back to the initial position. Remaining solvent residues in the cold transfer line are thereby backflushed with gas.

(4) During evaporation of the solvent, isothermal conditions are employed. Subsequently, ovens 1 and 2 are temperature programmed independently of each other, until a desired fraction of the sample is refocused and transferred from the uncoated precolumn to the column.

(5) By switching valves V_3 and V_6 (Fig. 2B) the uncoated precolumn is backflushed with gas. Meanwhile, the separation is proceeding in the analytical column. Before the liquid backflush procedure is initiated, the temperature in oven 1 is lowered below the boiling point of the backflush solvents.

(6) The uncoated precolumn is rinsed with the backflush solvents by switching valves V_4 and V_5 (Fig. 2C).

(7) Valves V_4 and V_5 are switched back to the initial position when the liquid backflush cycle is completed. The solvent residues in the uncoated precolumn are removed by increasing the temperature of oven 1.

(8) When the analysis is completed, valves V_3 and V_6 are switched back to the initial position. After lowering the temperatures of the ovens the system is ready for the next sample.

RESULTS AND DISCUSSION

System considerations

Two-dimensional GC is performed either with an in-line rotary valve between the columns or by pneumatic switching actuated from external valves (*e.g.*, [17,18]). In-line rotary valves are easy to operate and the columns are mechanically separated from each other. However, frequently adsorption of sample solutes on non-glass surfaces of the valve is experienced and the large thermal mass of the valve causes thermal lagging compared with the oven temperature. These disadvantages are eliminated with pneumatic switching where the sample stream is directed between the columns by balancing the inlet pressures of the first and second columns *via* inert three-way connectors with a low thermal mass.

In this work we chose to construct a backflush system based on pneumatic switching. Apart from the reasons mentioned above, the main cause of abandoning our previous set-up [8], where an in-line rotary valve was utilized, was the occurrence of disturbances of the baseline after the solvent peak. When large volumes of liquid samples were injected, part of the solvent was trapped in the valve and slowly released as a large hump after the solvent peak. The solvent probably penetrated into the plastics of the rotor and/or the Vespel ferrule of the valve.

In the present set-up, the vaporized sample is

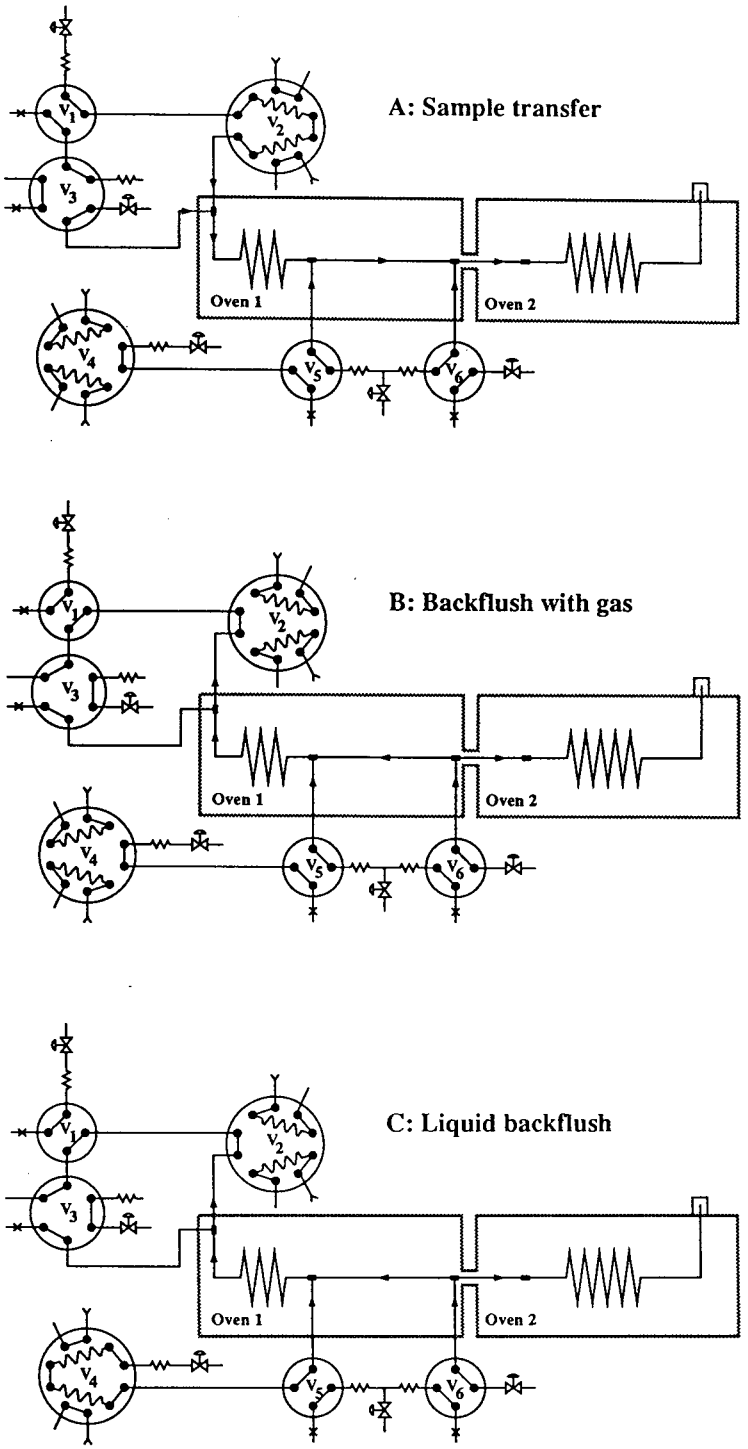

Fig. 2. Operational steps of the liquid backflush system. (A) The sample is transferred to the uncoated precolumn; (B) the retention gap is backflushed with gas; (C) on-line liquid backflush of the precolumn while the analysis is proceeding in the analytical column.

only in contact with glass surfaces and the disorders mentioned above are absent. Balancing the pressures of a pneumatic system used for heart cutting is a delicate operation. Pressure balancing a Deans switch designed for backflushing with gas is, however, not critical [12]. When a desired fraction is transferred from the precolumn to the column (Fig. 2A), the inlet to the first column is simply opened to the atmosphere while the three-way connector between the columns is pressurized (Fig. 2B).

During the stage when the backflush solvents are transferred to the precolumn (Fig. 2C), the liquid causes a restriction of the precolumn and the gas velocity in the tubing between the two three-way connectors is slowed down. This velocity should not approach the diffusion velocity of the vapour of the solvent, otherwise solvent vapour will enter the analytical column. With the present set-up it was possible to introduce 500 μl of chloroform followed by 500 μl of hexane at a maximum speed of 7 μl/s ($P_3 = 4.1$ bar), using an inlet pressure of $P_5 = 1.3$ bar between the columns, without disturbing the flame ionization detector. When liquid samples are injected from valves, situated outside the oven, part of the transfer line between the valve and the column is not oven thermostated. It is preferable to keep this part as short as possible and also to backflush this transfer line with gas, in order to avoid solvent tailing caused by slowly released solvent residues from the cold part of the transfer line and the valve [19]. This solvent tailing is especially pronounced when solvents with a relatively high boiling point compared with ambient temperature are utilized.

A small part of the high-boiling solutes of the sample will remain in the cold part of the transfer line despite the backflushing with gas. This material can cause a memory effect during consecutive analyses, as it is likely that deposited solutes from the previous sample are released by the solvent of the next sample [20]. This has serious consequences when the samples have large concentration differences. With the liquid backflush system the cold part of the transfer line is rinsed with pure solvents, between each analysis, which removes the deposited solutes and the memory effects are thereby avoided.

In a repeatability test, R.S.D. values for absolute area counts of the order of 0.5% were obtained for twelve consecutive injections of even-numbered *n*-alkanes (C_{10}–C_{22}) diluted in hexane.

Direct injection of an olive oil sample

The high content of triglycerides in vegetable oils is known to contaminate GC inlets, causing problems in analysis of trace components. Methods for analyses of fats and oils by GC usually require laborious clean-up procedures such as saponification, extraction and sometimes also a preseparation by thin-layer or liquid chromatography [21]. A comparatively rapid and reproducible on-line coupled LC–GC method has been described and applied to the analysis of olive oils [21–23]. The triglycerides and other disturbing components were removed by LC prior to determination of sterols and wax esters by capillary GC.

Our prime interest with this sample was not to design a method for the determination of the quality of the olive oil, but to investigate how the liquid backflush system would perform with direct injections of a sample containing a large amount of high-boiling material. A 10-μl volume of a 1% solution of an olive oil followed by 10 μl of solvent wash were directly injected on to the precolumn with the same temperature programme (5°C/min) for the precolumn and the column. A very distorted chromatogram was obtained, as shown in Fig. 3A. The trace components of the sample interact with the high-boiling matrix during refocusing in the retention gap. This interaction leads to a slow transfer of the solutes from the precolumn to the column and extra-column band broadening occurs.

Changing the temperature program for the precolumn to 20°C/min while the temperature ramp of the column remained at 5°C/min dramatically improved the quality of the analysis (Fig. 3B). The high-boiling trace solutes are now transported at a much faster speed through the precolumn and band focusing is improved. Fig. 3C shows a chromatogram of the same sample after 100 consecutive analyses, using an on-line liquid backflush with 500 μl of chloroform and 500 μl of hexane during each analysis. As can be

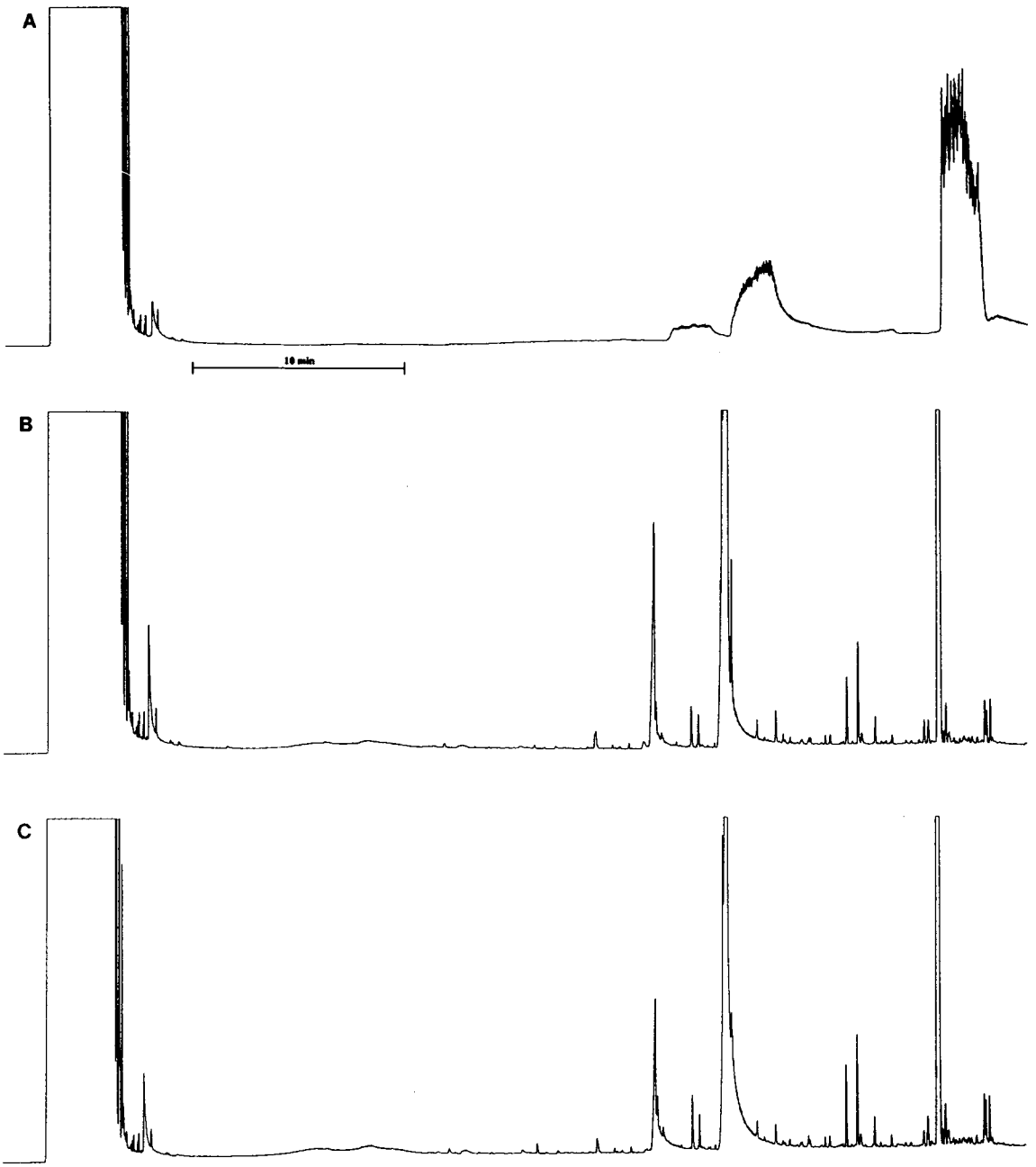

Fig. 3. Chromatograms of olive oil [1% (v/v) in hexane]. (A) Initial temperature 60°C. The same temperature programme (5°C/min) was employed for the uncoated precolumn and the column. (B) The retention gap was temperature programmed at 20°C/min (to 170°C) and the column at 5°C/min (to 300°C). (C) After 100 consecutive injections. Conditions as in (B) and a liquid backflush with 500 μl of chloroform and 500 μl of hexane during each analysis.

seen, the performance is still similar to the original one.

The activity level of the retention gap was tested with injections of an *n*-alkane standard solution (with the same temperature ramp for the precolumn and the column) before, during

and after the experimental series. Depending on the amount of non-volatile material present in the retention gap, extra-column band broadening was observed. These experiments showed that most of the non-volatile material was removed by the solvent rinsing procedure. After 100

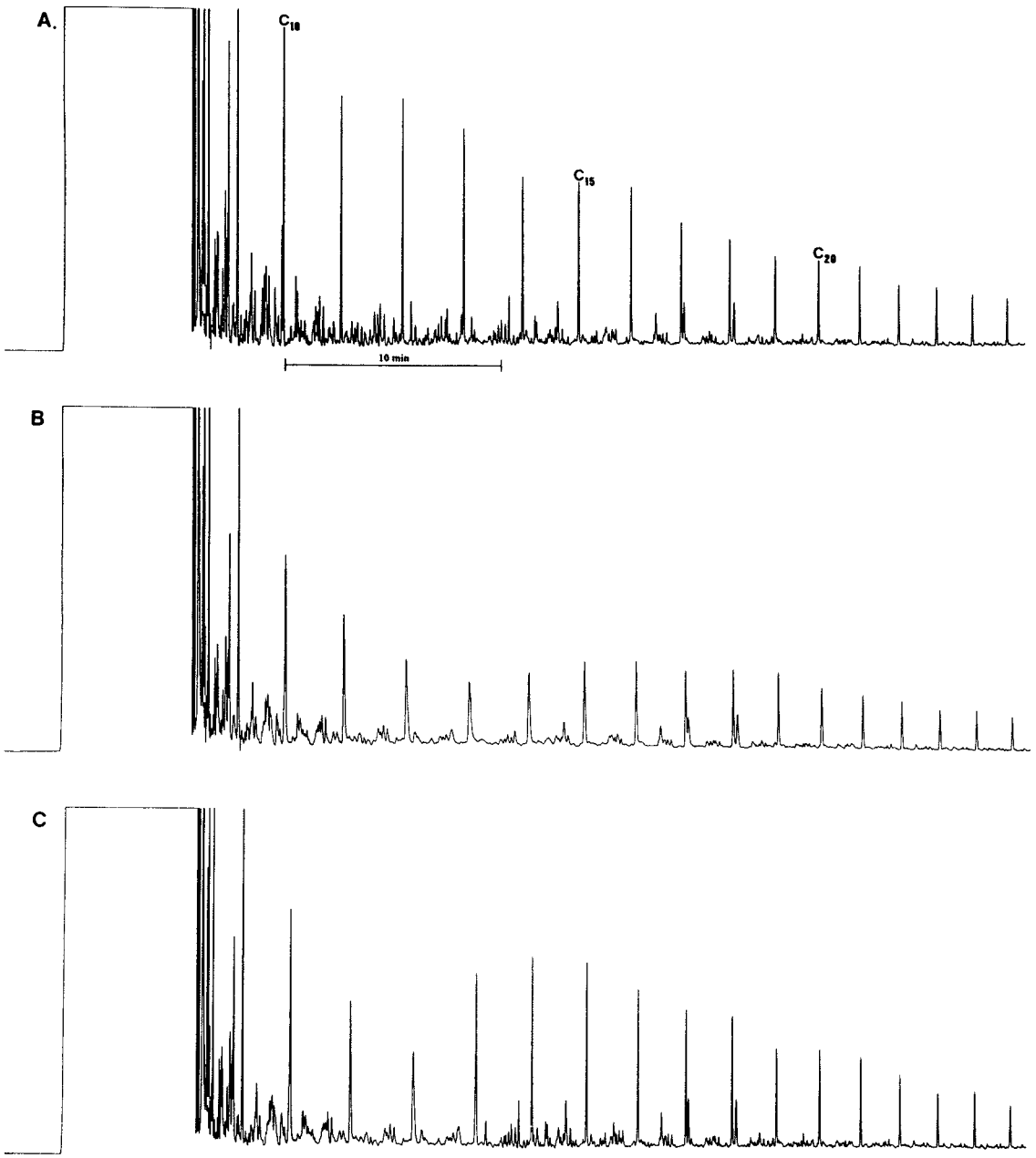

Fig. 4. Chromatograms of an Arabian light crude oil (100 μg/ml in chloroform). Influence of the temperature ramp of the precolumn on the system performance. (A) First injection; the uncoated precolumn and the analytical column were temperature programmed at 5°C/min (to 180 and 310°C, respectively). (B) After 100 injections; temperature programmes as in (A). (C) After 100 injections, where the uncoated precolumn was temperature programmed at 40°C/min and the column at 5°C/min.

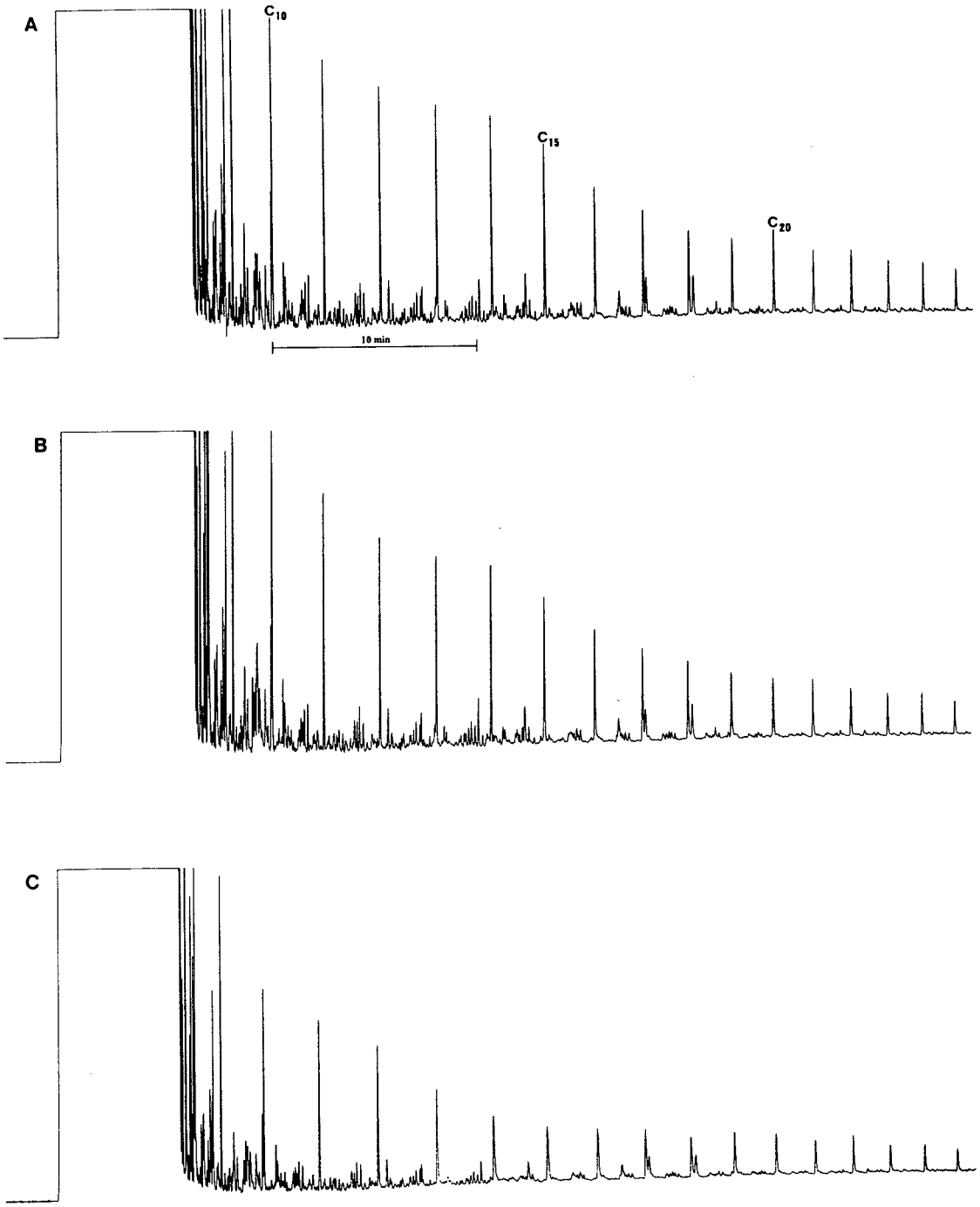

Fig. 5. Chromatograms of an Arabian light crude oil (100 μg/ml in chloroform). Influence of the liquid backflush on the long-term performance. (A) After 100 injections; (B) after 200 injections; (C) after 350 injections. Initial temperature, 60°C. The uncoated precolumn and the analytical column were temperature programmed at 5°C/min (to 180 and 310°C, respectively). A liquid backflush with 500 μl of hexane and 500 μl of chloroform was carried out during each analysis.

consecutive olive oil analyses with the liquid backflush procedure, the activity level of the retention gap was lower than after a single injection of the olive oil sample without a liquid backflush.

Another advantage of the double-oven system is that the final temperature of the uncoated precolumn and the coated column can be separately controlled. As the solutes of the sample are transported through the retention gap at a much lower temperature than the temperature when they start to migrate through the column, there is a risk that the column will become contaminated with non-elutable high-molecular-mass compounds if the final temperature of the precolumn is the same as that for the column. Contamination of the column with large amounts of triglycerides can be especially problematic in this respect as the volatility of these compounds is of a level where it can be difficult to elute them from the column. Transfer of these compounds to the column can be avoided by using a suitable lower final temperature of the precolumn than for the column.

Long-term analysis of an Arabian light crude oil

Capillary GC analysis of crude oils by on-column injection employing a short retention gap has been shown to suffer from a rapid decrease in separation power after a number of sample injections owing to the accumulation of non-volatile constituents [24]. In Fig. 4A, a chromatogram of an Arabian light crude oil, diluted 100 μg/ml in chloroform, is shown. When this sample was repeatedly injected, a gradual decrease in the chromatographic performance was experienced. Fig. 4B shows a chromatogram of the same sample after 100 consecutive injections. As can be seen, the peaks have become broad and much of the original resolution is lost. The analysis was performed without a liquid backflush using the same rate of temperature programming (5°C/min) for the uncoated precolumn and the analytical column.

In a following experiment, the precolumn was temperature programmed at 40°C/min while the temperature ramp of the column was kept at 5°C/min. The effect of the faster temperature ramp of the precolumn is shown in Fig. 4C. The resolution between the solutes that elutes after tridecane is restored, because the high-boiling solutes that are spread over the retention gap are transported to the column and cold trapped much faster when the precolumn is rapidly heated. Consequently, a higher retentive power of the precolumn caused by residual non-volatile material can be tolerated. The more volatile solutes, however, are reconcentrated by the solvent effect and by phase soaking [2], and these solute peaks remain broadened, despite the faster temperature programme of the precolumn. An attempt to restore the peak shapes also for these compounds was made by rinsing the precolumn with ethanol, chloroform and hexane. The efficiency was slightly improved but it was not possible to obtain the original performance. We believe that the prime cause of this is polymerization of the residual material.

The retention gap was exchanged and the same sample was again repeatedly injected. A liquid backflush with 500 μl of hexane and 500 μl of chloroform was now included during each analysis in order to remove the non-volatile material as fast as possible to minimize the risk of accumulation of polymerized residue. The useful lifetime of the retention gap was extended. The chromatographic efficiency was hardly affected during the first 100 injections, as can be seen in Fig. 5A, even though the same rate of temperature programming (5°C/min) was employed for the precolumn and the column. After 200 injections a slight decrease in the separation power became noticeable (Fig. 5B) and after 350 injections the decrease in efficiency was no longer acceptable (Fig. 5C). For the higher boiling solutes it was possible to restore the performance by using a faster temperature ramp of the precolumn, as described in the earlier experiment.

The retention gap was backflushed with a number of different solvents (acetone, carbon disulphide, chloroform, dichlormethane, diethyl ether, dimethyl sulphoxide, ethanol, hexane and isobutyl methyl ketone) in an attempt to dissolve the residue. The performance of the system was not restored, however. Finally, the retention gap

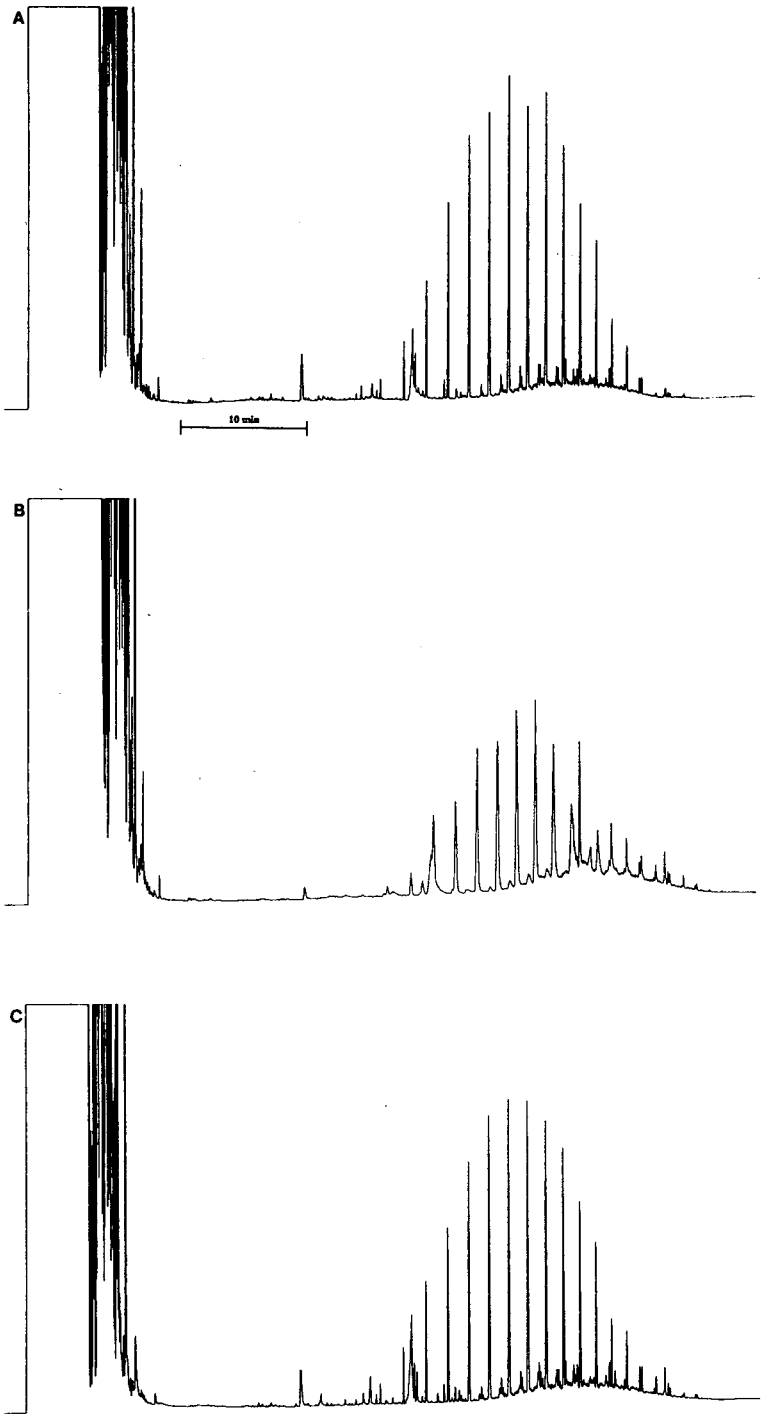

Fig. 6. Chromatograms of shoe polish diluted in chloroform (500 μg/ml). (A) First injection. Retention gap and column temperature programmed at 5°C/min (to 170 and 300°C, respectively). (B) After 50 consecutive injections; conditions as in (A). (C) After 250 consecutive injections. Uncoated precolumn temperature programmed at 20°C/min and column at 5°C/min, liquid backflush with 500 μl of hexane and 500 μl of chloroform between every 25 injections.

was resilylated and rinsed on-line without any improvement.

Repetitive injections of a shoe polish solution

In another example, shoe polish diluted in chloroform (500 μg/ml) was filtered through a 0.5-μm Teflon filter and injected into the system. Fig. 6 shows the first chromatogram and a chromatogram after 50 consecutive injections without a liquid backflush and with the same rate of temperature programming for the precolumn and the column. As can be seen, a considerable decrease in separation power occurred. The performance was to a large extent restored after rinsing the precolumn with hexane and chloroform, but the original low activity level of the precolumn was not completely re-established. When the precolumn was temperature programmed at a faster rate than the column, chromatograms comparable to those from the first injection were obtained. As the solutes have a high boiling point and are reconcentrated by stationary phase focusing, some increase in activity level of the retention gap is tolerable, provided that an independently temperature programmed retention gap is used.

We continued to inject the sample with the faster temperature ramp (20°C/min) of the precolumn and executed a liquid backflush between every 25 injections. In Fig. 6C, a chromatogram after 250 consecutive injections is shown. The performance is still comparable to that in the first run.

CONCLUSIONS

Samples that contain non-volatile material contaminate uncoated precolumns, which rapidly affects the performance of the GC analysis. The useful lifetime of the retention gap is extended when a combination of a faster temperature programme for the uncoated precolumn than for the column and a liquid backflush of the precolumn are employed.

The main obstacle to dissolving the non-volatile material from the retention gap is polymerization of the residue. In this respect it is advantageous to remove the non-volatile constituents from the uncoated precolumn as fast as possible after injection and reconcentration of the solutes of interest. Working conditions have to be established for each application where backflush solvents of different polarity have to be tested. The final temperature of the precolumn should be kept at the lowest level that allows reconcentration of the solutes, also in order to minimize the risk of polymerization of the residue.

Sample solutes that are reconcentrated by the solvent effect interact with the residues in the uncoated precolumn, causing broadened peaks. If, however, the sample solutes of interest have a relatively high boiling point compared with the solvent, a faster rate of temperature programming for the uncoated precolumn than for the column can be employed and these solutes are effectively refocused by cold trapping. When combined with a liquid backflush procedure that dissolves most of the non-volatile residue, a large number of samples can be analysed.

Column fouling caused by high-boiling solutes which, owing to the large difference in phase ratio, migrate through the uncoated precolumn but not through the coated column, can be avoided by keeping the final temperature of the precolumn oven below the final temperature of the second oven.

ACKNOWLEDGEMENTS

This work was supported financially by the Swedish National Board for Industrial and Technical Development and the Swedish Natural Science Research Council.

REFERENCES

1 K. Grob, Jr., *J. Chromatogr.*, 287 (1984) 1.
2 K. Grob, *On-Column Injection in Capillary GC*, Hüthig, Heidelberg, 1987.
3 K. Grob, *On-Line Coupled LC–GC*, Hüthig, Heidelberg, 1991.
4 C.V. Philip and R.G. Anthony, *J. Chromatogr. Sci.*, 24 (1986) 438.
5 M. Ghijs, J. van Dijck, C. Dewaele, M. Verstappe, M. Verzele and P. Sandra, in P. Sandra and G. Redant (Editors), *10th International Symposium on Capillary Chromatography*, Hüthig, Heidelberg, 1989, p. 726.
6 H.J. Cortes, B.M. Bell, C.D. Pfeiffer and J.D. Graham, *J. Microcol. Sep.*, 1 (1989) 278.

7 J. Blomberg, P.J. Schoenmakers and N. van den Hoed, in P. Sandra (Editor), *15th International Symposium on Capillary Chromatography*, Hüthig, Heidelberg, 1993, p. 837.
8 G. Hagman and J. Roeraade, in P. Sandra and M.L. Lee (Editors), *Proceedings of the 14th International Symposium on Capillary Chromatography*, Foundation for the ISCC, Miami, FL, 1992, p. 231; *J. High Resolut. Chromatogr.*, 16 (1993) 445.
9 E.C. Goosens, D. de Jong, J.H.M. van den Berg, G.J. de Jong and U.A.Th. Brinkman, *J. Chromatogr.*, 552 (1991) 489.
10 G. Hagman and J. Roeraade, in P. Sandra and M.L. Lee (Editors), *Proceedings of the 14th International Symposium on Capillary Chromatography*, Foundation for the ISCC, Miami, FL, 1992, p. 224; *J. Microcol. Sep.*, 5 (1993) 341.
11 J.F. Hiller, T. McCabe and P.L. Morabito, *J. High Resolut. Chromatogr.*, 16 (1993) 5.
12 D.R. Deans, *J. Chromatogr.*, 18 (1965) 477.
13 D.R. Deans, *Chromatographia*, 1 (1968) 18.
14 G. Schomburg, H. Husmann and F. Weeke, *J. Chromatogr.*, 112 (1975) 205.
15 D.R. Deans, *J. Chromatogr.*, 203 (1981) 19.
16 A. D'Amato, C. Bicchi and M. Galli, *J. High Resolut. Chromatogr.*, 12 (1989) 349.
17 W. Bertsch, *J. High Resolut. Chromatogr. Chromatogr. Commun.*, 1 (1978) 85, 187 and 289.
18 K. Himberg, E. Sippola and M.-L. Riekkola, *J. Microcol. Sep.*, 1 (1989) 271.
19 K. Grob, Jr., and J.-M. Stoll, *J. High Resolut. Chromatogr. Chromatogr. Commun.*, 9 (1986) 518.
20 G. Hagman and J. Roeraade, *J. High Resolut. Chromatogr.*, 13 (1990) 461.
21 K. Grob, M. Lanfranchi and C. Mariani, *J. Chromatogr.*, 471 (1989) 397.
22 K. Grob and T. Läubli, *J. High Resolut. Chromatogr. Chromatogr. Commun.*, 9 (1986) 593.
23 K. Grob and M. Lanfranchi, *J. High Resolut. Chromatogr.*, 12 (1989) 624.
24 I.M. Castro and R.A. Neto, *J. High Resolut. Chromatogr.*, 13 (1990) 302.

Journal of Chromatography A, 654 (1993) 299–302
Elsevier Science Publishers B.V., Amsterdam

CHROM. 25 301

Short Communication

High-performance liquid chromatographic method for the determination of bisoprolol and potential impurities

Nelly N. Agapova*

National Drug Institute, Bul. "Ianko Sakasov" 26, Sofia (Bulgaria)

Elissaveta Vasileva

Chemical Pharmaceutical Research Institute, Sofia (Bulgaria)

(First received February 1st, 1993; revised manuscript received May 5th, 1993)

ABSTRACT

An HPLC method capable of determining bisoprolol in bulk substance in the presence of its synthetic intermediates, which are potential impurities, is described. To choose the optimum conditions the behaviour of the compounds on octadecylsilica columns with acetonitrile–phosphate buffer mobile phases was studied. The influence of the acetonitrile and buffer concentrations and the pH of the mobile phase on retention was investigated. The results indicate that hydrophobic and silanophilic interactions contribute to the retention of the compounds.

INTRODUCTION

Bisoprolol, (±)-1-[4-(isopropylethoxy)methylphenoxy] - 3 - isopropylamino - 2 - propanol, is a highly selective β-adrenoceptor antagonist lacking intrinsic sympathomimetic activity with low anaesthetic potency [1–4]. A previously reported technique employing high-performance liquid chromatography (HPLC) [5,6] has been restricted to the determination of bisoprolol in biological samples. Bisoprolol is not described in any of the Pharmacopoeias and there are no official methods for the determination of chromatographic purity and assay of the compound.

This paper describes an HPLC method for the separation and determination of bisoprolol and potential impurities in drug substances.

EXPERIMENTAL

Chemicals

The molecular formulae of bisoprolol hemifumarate and potential impurities are shown in Fig. 1. They were all synthesized at the Chemical Pharmaceutical Research Institute (Sofia, Bulgaria) and had a purity of >98%, as determined by HPLC at 226 nm. Their identities were established by mass and NMR spectrometry. The organic solvents were of HPLC grade and all the reagents were of analytical-reagent grade.

* Corresponding author.

0021-9673/93/$06.00 © 1993 Elsevier Science Publishers B.V. All rights reserved

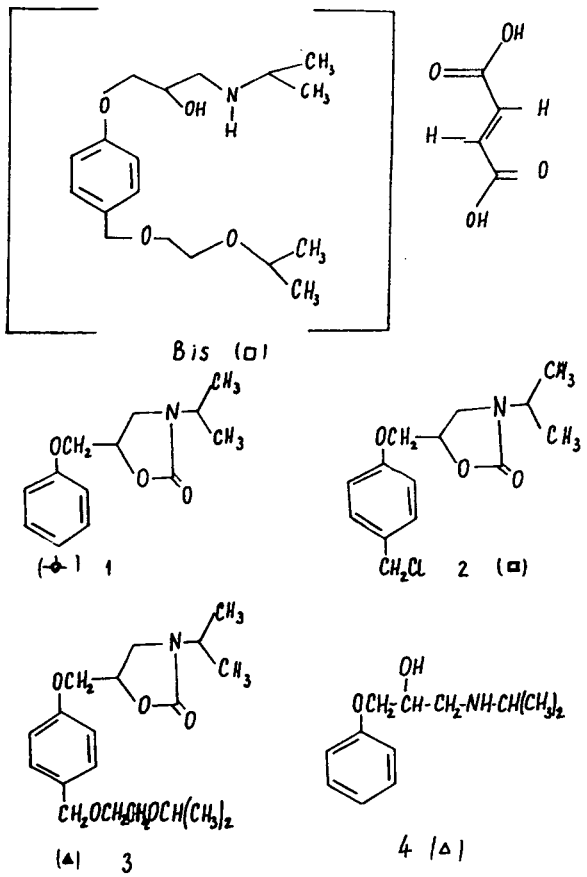

Fig. 1. Structures of bisoprolol fumarate (Bis) and conceivable impurities (**1–4**). The symbols are those used in Figs. 2 and 3. Amines are indicated by open symbols.

Equipment

The HPLC equipment consisted of a Perkin-Elmer (Norwalk, CT, USA) Series 3B chromatograph linked to a Perkin-Elmer LC 75 spectrophotometric detector with autocontrol and a Waters (Milford, MA, USA) Model 740 Data Module. The UV detector was set at 226 nm. A Rheodyne (Cotati, CA, USA) Model 7120 injection valve (20-μl sample loop) was used. Prepacked LiChrosorb RP-18 columns (25 cm × 4 mm I.D.), particle size 10 μm, were obtained from Merck (Darmstadt, Germany). A Radelkis (Budapest, Hungary) Model OP-211/1 pH meter equipped with a glass electrode and a calomel reference electrode was used.

Mobile phase

The mobile phases were prepared from acetonitrile and aqueous phosphate buffer. Acetonitrile and buffer solutions were filtered, mixed in the desired volume ratios and degassed ultrasonically. The pH value stated was measured in the buffer before mixing in the final eluent. The buffer was prepared from diammonium hydrogenphosphate [$(NH_4)_2HPO_4$] by adding 5 *M* orthophosphoric acid to give the desired pH, followed by dilution to the final concentration with water. The flow-rate was maintained at 1.5 ml/min. The retention time of an unretained compound, t_0, was determined using potassium nitrate.

Preparation of solutions

For the determination of chromatographic purity, about 50 mg of bisoprolol fumarate were transferred into a 50-ml volumetric flask and dissolved in and diluted to volume with the mobile phase.

For the assay, a standard solution was prepared by transferring about 25 mg of bisoprolol fumarate reference standard into a 100 ml volumetric flask and dissolving it in and diluting to volume with the mobile phase. A sample solution was prepared in the same way but using a bisoprolol fumarate sample instead of the reference standard.

RESULTS AND DISCUSSION

The influence of the mobile phase conditions (concentrations of the organic solvent and buffer and pH) on retention was studied.

Effect of acetonitrile content in the mobile phase

Fig. 2 illustrates the effect of the acetonitrile concentration in the mobile phase on the capacity factors (k') of the components investigated. It is clear that 50% acetonitrile is the optimum concentration. The elution order is advantageous for the determination of minor components in the presence of a large excess of bisoprolol. A comparison of the retention behaviours indicates that the capacity factors of compounds containing oxazolidin in the molecule (**1**, **2** and **3**) depend more strongly than those of components

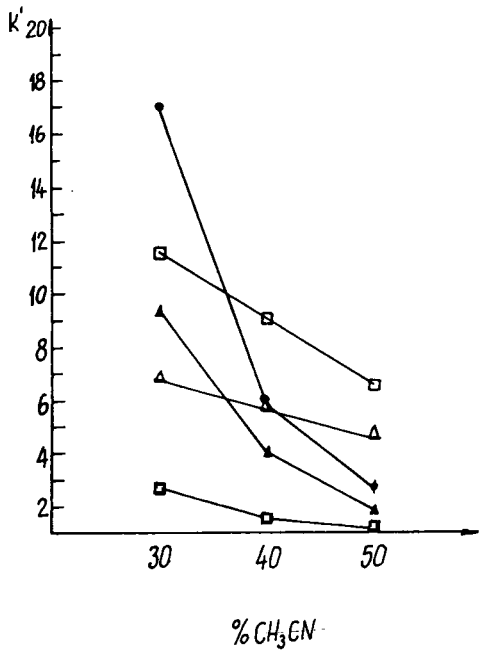

Fig. 2. Effect of acetonitrile content in the mobile phase on k'. Column, LiChrosorb RP-18, 10 μm; mobile phase, mixtures of acetonitrile and 0.050 M ammonium phosphate buffer (pH 7.0); flow-rate 1.5 ml/min. Symbols as in Fig. 1.

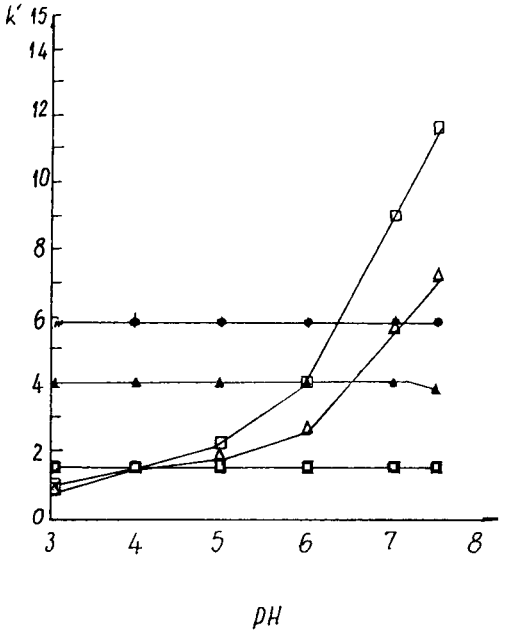

Fig. 3. pH dependence of k'. Mobile phase, acetonitrile–0.050 M ammonium phosphate buffer (4:6). Symbols as in Fig. 1.

containing a secondary amino group (bisoprolol and **4**) on the acetonitrile content of the mobile phase.

The difference in selectivity between acetonitrile and tetrahydrofuran (THF) was investigated using mixtures with different proportions of the two solvents in the mobile phase. Bisoprolol showed a decrease in retention time and tailing, but no effect on selectivity was observed and the elution order of all the compounds was maintained.

Effect of pH of the mobile phase

Fig. 3 shows the dependence of k' of the compounds investigated when using 40% acetonitrile as the mobile phase and 0.05 M ammonium phosphate buffer solution. The effect of pH on k' differs for the different compounds. A strong dependence of k' on pH was found for bisoprolol and **4**, which have secondary amino groups. At lower pH the proportion of protonated species increased and the retention of bisoprolol and **4** decreased. At pH 7.0 the retention of bisoprolol and **4** increased. This is due mostly to ionic interactions between ionized silanol groups and protonated bases. Compounds **1–3** do not have such ionizable moieties like bisoprolol and **4** in the pH range studied and pH had no effect on their retention. The pH dependence of k' was used for the separation of bisoprolol and **1–4**. It can be seen that a changed elution order of bisoprolol and **3** was obtained when the pH was increased from 3 to 7. pH 7.0 was chosen because one of the essential considerations is the order of elution of the separated peaks.

Effect of buffer concentration in the mobile phase

Capacity factors were determined for bisoprolol and **1–4** using mobile phases consisting of 40% of acetonitrile and 60% of an aqueous solution of diammonium hydrogenphosphate of concentrations 0.025, 0.050, 0.075 and 0.100 M.

The pH of the buffer was maintained at 7.0. An increased concentration of NH_4^+ cations led to decreased retention owing to ion exchange of protonated bases, whereas the retention of the other compounds was unaffected.

Based on the reported results, an HPLC method is recommended, that gives complete separation of bisoprolol from its related compounds. The chromatographic conditions are summarized in Fig. 4, which shows a typical chromatogram for a mixture of all five compounds.

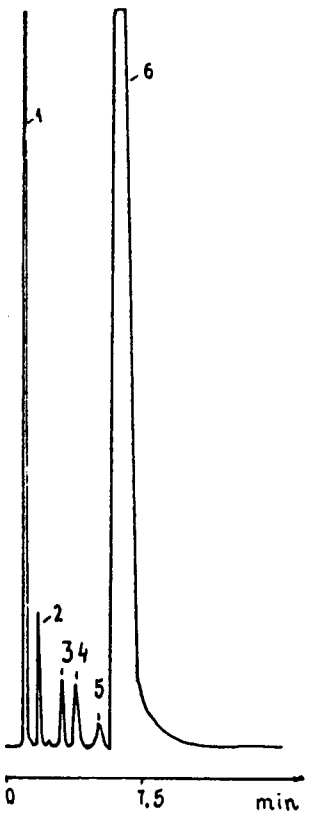

Fig. 4. Separation of 20 μg of bisoprolol fumarate and 40 ng each of the other solutes by use of the recommended method. Mobile phase, acetonitrile–0.050 *M* ammonium phosphate buffer (pH 7.0) (1:1); flow-rate, 1.5 ml/min; column, LiChrosorb RP-18, 10 μm (250 × 4.6 mm I.D.); UV detection at 226 nm (0.16 a.u.f.s.). Peaks: 1 = fumaric acid; 2 = **2**; 3 = **1**; 4 = **3**; 5 = **4**; 6 = bisoprolol.

To test the linearity of the assay procedure, a series of five standard solutions of known concentration with volumes from 1 to 10 μl injected were analysed. The regression coefficient of the linearity test was 0.9996. The precision of the system was determined by making five replicate injections of a bisoprolol standard solution. The relative standard deviation (R.S.D.) of the peak-area measurements was 0.3%. The precision of the method was determined by analysing the same sample of bisoprolol on six different days, with two replicate determinations on each day. The R.S.D. was 0.7%. To test the column-to-column variability, the results were checked on a similar, second column from the same manufacturer.

Detection limits, expressed as the amount of substance injected corresponding to a peak height equal to three times the noise, were in the range 5–20 ng for all solutes.

REFERENCES

1 A.S. Manalan, H.R. Besch and A.M. Watanale, *Circ. Res.*, 49 (1981) 326.
2 H.J. Schliep and J. Harting, *J. Cardiovasc. Pharmacol.*, 6 (1984) 1156.
3 A.E. Tatersfield, D.J. Cragg and R.J. Bacon, *Br. J. Clin. Pharmacol.*, 18 (1984) 343.
4 B. Kramer, J. Balser, K. Stubbing, G. Kramerand and W. Kuber, *J. Cardiovasc. Pharmacol.*, 8 (1986) 546.
5 K.U. Buhring and A. Garbe, *J. Chromatogr.*, 382 (1986) 215.
6 J.M. Poirier, M. Perez, G. Cheymol and P. Jailon, *J. Chromatogr.*, 426 (1988) 431.
7 W.R. Melander, J. Stoveken and Cs. Horváth, *J. Chromatogr.*, 185 (1979) 111.

Journal of Chromatography A, 654 (1993) 303–308
Elsevier Science Publishers B.V., Amsterdam

CHROM. 25 487

Short Communication

Chromatographic resolution of racemic α-halocarboxylic acids and O-substituted α-hydroxycarboxylic acids via diastereomeric N-acyloxazolidinones

Choong Eui Song*, Sang Gi Lee, Kyo Chul Lee and In O Kim

Organic Chemistry Research Laboratory III, Korea Institute of Science and Technology, P.O. Box 131, Cheongryang, Seoul (South Korea)

Jong Hwa Jeong

Department of Chemistry, Kyungpook National University, Taegu 702-701 (South Korea)

(Received June 26th, 1993)

ABSTRACT

Diastereomeric pairs of N-acyloxazolidinones, derived from (4*R*,5*S*)-4-methyl-5-phenyl-2-oxazolidinone (as a chiral derivatizing agent) and racemic α-halocarboxylic acids or O-substituted α-hydroxycarboxylic acids, were separated chromatographically on a large preparative scale and showed appreciable degrees of NMR-shift difference. The origins of the chromatographic separability of these diastereomers are discussed.

INTRODUCTION

Optically active α-halocarboxylic acids and α-hydroxycarboxylic acids are important chiral building blocks in the synthesis of many biologically active substances. The enantiomeric forms of α-halocarboxylic acids and O-substituted α-hydroxycarboxylic acids are generally prepared via either classical resolution with alkaloids or enzymes [1–5] or enantioselective synthesis using a chiral auxiliary [6–13]. In this paper we report that chiral oxazolidinones can be used as efficient chiral derivatizing agents for the chromatographic resolution of α-halocarboxylic acids and O-substituted α-hydroxycarboxylic acids via diastereomeric N-acyloxazolidinones. It has already been reported that chiral oxazolidinones as chiral derivatizing agents can be used to resolve amines [14].

EXPERIMENTAL

Apparatus

Preparative liquid chromatography was performed using a column of Merck Kieselgel 60 (70–230 mesh). All melting points were determined on a Thomas Hoover capillary melting point apparatus and were uncorrected. ^{1}H NMR

* Corresponding author.

0021-9673/93/$06.00 © 1993 Elsevier Science Publishers B.V. All rights reserved

spectra were obtained on a Varian Gemini 300 spectrometer. All chemical shift values are reported on the δ scale with respect to internal tetramethylsilane. Microanalyses were determined with a Perkin-Elmer Model 240 DS elemental analyser. An Enraf-Nonius CAD-4 diffractometer with graphite-monochromated Mo Kα radiation ($\lambda = 0.71073$ Å) was used for the measurement of diffraction intensities. All calculations for X-ray structures were carried out using an MVAX-3900 computer.

Reagents

(4*R*,5*S*)- 4 -Methyl- 5 -phenyl- 2 -oxazolidinone was prepared as described in the literature [15,16]. 2-Bromopropionyl bromide, 2-chloropropionyl chloride, (±)-2-bromobutyryl bromide, (±)-2 bromohexanoyl bromide, 2-bromophenylacetic acid, DL-2-phenoxypropionic acid and (±)-2-bromo-3-methylbutyric acid were purchased from Aldrich and used as received.

*N-2-Bromopropionyl-(4S,5R)-4-methyl-5-phenyl-2-oxazolidinone (**2a**)*

To 48.13 g (271 mmol) of (4*R*,5*S*)-4-methyl-5-phenyl-2-oxazolidinone dissolved in 450 ml of dry tetrahydrofuran (THF), 108.5 ml of *n*-butyllithium (2.5 *M* THF solution) were added at −10°C. The solution obtained was added to 28.4 ml (271 mmol) of racemic 2-bromopropionyl bromide (in 150 ml of dry THF) at −30°C. After 30 min, the reaction mixture was poured into ammonium chloride solution. The aqueous mixture was extracted with ethyl acetate and dried with anhydrous sodium sulphate. The solvent was removed at reduced pressure and then the diastereomeric mixture was separated by column chromatography [silica gel (70–230 mesh, 60 Å), eluent *n*-hexane–ethyl acetate (7:1)].

First eluted: N-[(2S)-2-bromopropionyl]-(4R,5S)- 4 -methyl- 5 -phenyl- 2- oxazolidinone. M.p. 90°C. ^{1}H NMR (300 MHz, $CDCl_3$): δ 0.94 [*d*, $J = 6.6$ Hz, 3H, –NCH(CH_3)–], 1.86 [d, $J = 6.7$ Hz, 3H, CH_3CH(Br)–], 4.77 ["p" from qd, $J = 6.7$ Hz, 1H, –NCH(CH_3)CHO–], 5.76 [q, $J = 6.7$ Hz, 1H, CH_3CH(Br)–], 5.76 [d, $J = 6.7$ Hz, 1H, –NCH(CH_3)CHO–], 7.2–7.5 (m, 5H, C_6H_5–). Analysis: calculated for $C_{13}H_{14}BrNO_3$, C 50.0, H 4.5, N 4.5; found, C 50.1, H4.5, N 4.3%.

Second eluted: N-[(2R)-2-bromopropionyl]-(4R,5S)- 4 -methyl- 5 -phenyl- 2 -oxazolidinone. M.p. 98°C. ^{1}H NMR (300 MHz, $CDCl_3$): δ 0.91 [d, $J = 6.6$ Hz, 3H, –NCH(CH_3)–], 1.86 [d, $J = 6.7$ Hz, 3H, CH_3CH(Br)–], 4.84 ["p" from qd, $J = 6.7$ Hz, –NCH(CH_3)CHO–], 5.70 [q, $J = 6.7$ Hz, 1H, CH_3CH(Br)–], 5.73 [d, $J = 6.7$ Hz, 1H, –NCH(CH_3)CHO–], 7.2–7.5 (m, 5H, C_6H_5–). Analysis: calculated for $C_{13}H_{14}BrNO_3$, C 50.0, H 4.5, N 4.5; found, C 50.1, H 4.5, N 4.3%.

*N-2-Chloropropionyl-(4R,5S)-4-methyl-5-phenyl-2-oxazolidinone (**2b**)*

First eluted: N-[(2S)-2-chloropropionyl]-(4R,5S)- 4 -methyl- 5 -phenyl- 2 -oxazolidinone. M.p. 102°C. ^{1}H NMR (300 MHz, $CDCl_3$): δ 0.93 [d, $J = 7.0$ Hz, 3H, –NCH(CH_3)–], 1.72 [d, $J = 6.6$ Hz, 3H, CH_3CH(Cl)–], 4.78 ["p" from qd, $J = 6.7$ Hz, 1H, –NCH(CH_3)CHO–], 5.70 [q, $J = 6.6$ Hz, 1H, CH_3CH(Cl)–], 5.76 [d, $J = 7$ Hz, 1H, –NCH(CH_3)CHO–], 7.2–7.6 (m, 5H, C_6H_5–). Analysis: calculated for $C_{13}H_{14}ClNO_3$, C 58.33, H 5.27, N 5.23; found, C58.4, H5.21, N 5.00%.

Second eluted: N-[(2R)-2-chloropropionyl]-(4R,5S)- 4 -methyl- 5 -phenyl- 2 -oxazolidinone. M.p. 95°C. ^{1}H NMR (300 MHz, $CDCl_3$): δ 0.92 [d, $J = 7.0$ Hz, 3H, –NCH(CH_3)–], 1.72 [d, $J = 6.7$ Hz, 3H, CH_3CH(Cl)–], 4.81 ["p" from qd, $J = 6.7$ Hz, 1H, –NCH(CH_3)CHO–], 5.70 [q, $J = 6.6$ Hz, 1H, CH_3CH(Cl)–], 5.72 [d, $J = 6.8$ Hz, 1H, –NCH(CH_3)CHO–], 7.2–7.6 (m, 5H, C_6H_5–). Analysis: calculated for $C_{13}H_{14}ClNO_3$, C 58.33, H 5.27, N 5.23; found, C 58.4, H 5.23, N 5.07%.

*N-2-Bromobutanoyl-(4R,5S)-4-methyl-5-phenyl-2-oxazolidinone (**2c**)*

First eluted: N-[(2S)-2-bromobutanoyl]-(4R,5S)- 4 -methyl- 5 -phenyl- 2 -oxazolidinone. M.p. 69°C. ^{1}H NMR (300 MHz, $CDCl_3$): δ 0.94 [d, $J = 6.6$ Hz, 3H, –NCH(CH_3)–], 1.06 [t, $J = 6.7$ Hz, 3H, CH_3CH_2CH(Br)–], 2.11 [m, 2H, CH_3CH_2CH(Br)–], 4.81 ["p" from qd, $J = 6.7$

Hz, 1H, –NCH(CH_3)CHO–], 5.61 [t, J = 6.6 Hz, 1H, CH_3CH_2CH(Br)–], 5.77 [d, J = 6.7 Hz, 1H, –NCH(CH_3)CHO–], 7.2–7.5 (m, 5H, C_6H_5–). Analysis: calculated for $C_{14}H_{16}BrNO_3$, C 51.5, H 4.9, N 4.3; found, C 51.3, H 4.9, N 4.1%.

Second eluted: N-[(2R)-2-bromobutanoyl]-(4R,5S)- 4 -methyl- 5 -phenyl- 2 -oxazolidinone. M.p. 94°C. ^{1}H NMR (300 MHz, $CDCl_3$): δ 0.90 [d, J = 6.6 Hz, 3H, –NCH(CH_3)–], 1.06 [t, J = 6.7 Hz, 3H, CH_3CH_2CH(Br)–], 2.11 [m, 2H, CH_3CH_2CH(Br)–], 4.83 ["p" from qd, J = 6.7 Hz, 1H, –NCH(CH_3)CHO–], 5.54 [t, J = 6.6 Hz, 1H, CH_3CH_2CH(Br)–], 5.70 [d, J = 6.7 Hz, 1H, –NCH(CH_3)CHO–], 7.2–7.5 (m, 5H, C_6H_5–). Analysis: calculated for $C_{14}H_{16}BrNO_3$, C 51.5, H 4.9, N 4.3; found, C 51.3, H 5.0, N 4.3%.

N-2-Bromo-3-methylbutanoyl-(4R,5S)-4-methyl-5-phenyl-2-oxazolidinone ***(2d)***

First eluted: N-[(2S)-2-bromo-3-methylbutanoyl]-(4R,5S)- 4 -methyl- 5 -phenyl- 2 -oxazolidinone. ^{1}H NMR (300 MHz, $CDCl_3$): δ 0.94 [d, J = 6.7 Hz, 3H, –NCH(CH_3)–] 1.05 [d, J = 6.6 Hz, 3H, $(CH_3)_2CH$–], 1.15 [d, J = 6.7 Hz, 3H, $(CH_3)_2CH$–], 2.35 [sym.m, 1H, $(CH_3)_2CH$–], 4.82 ["p" from qd, J = 6.7 Hz, 1H, –NCH(CH_3)CH(C_6H_5)–], 5.56 [d, J = 6.6 Hz, 1H, $(CH_3)_2CHCH$(Br)–], 5.75 [d, J = 6.8 Hz, 1H, –NCH(CH_3)CH(C_6H_5)–], 7.2–7.6 (m, 5H, –C_6H_5–].

Second eluted: N-[(2R)-2-bromo-3-methylbutanoyl]-(4R,5S)- 4 -methyl- 5 -phenyl- 2 -oxazolidinone. ^{1}H NMR (300 MHz, $CDCl_3$): δ 0.91 [d, J = 6.8 Hz, 3H, –NCH(CH_3)–] 1.06 [d, J = 6.6 Hz, 3H, $(CH_3)_2CH$–], 1.15 [d, J = 6.6 Hz, 3H, $(CH_3)_2CH$–], 2.37 [m, 1H $(CH_3)_2CH$–], 4.84 ["p" from qd, J = 6.8 Hz, 1H, –NCH(CH_3)CH(C_6H_5)–], 5.49 [d, J = 6.6 Hz, 1H, $(CH_3)_2CHCH$(Br)–], 5.71 [d, J = 6.7 Hz, 1H, –NCH(CH_3)CH(C_6H_5)–], 7.2–7.6 [m, 5H, C_6H_5–].

N-2-Bromohexanoyl-(4R,5S)-4-methyl-5-phenyl-2-oxazolidinone ***(2e)***

First eluted: N-[(2S)-2-bromohexanoyl]-(4R,5S)- 4 -methyl- 5 -phenyl- 2 -oxazolidinone. M.p. 110°C. ^{1}H NMR (300 MHz, $CDCl_3$): δ 0.94 [br d, 6H, CH_3CH_2– and –NCH(CH_3)–], 1.3–1.6 (m, 4H, $CH_3CH_2CH_2$–), 1.9–2.2 [m, 2H, –CH_2CH(Br)–], 4.80 ["p" from qd, J = 6.7 Hz, 1H, –NCH(CH_3)CH(C_6H_5)–], 5.67 [t, J = 7.1 Hz, 1H, –CH_2CH(Br)–], 5.75 [d, J = 7.1 Hz, 1H, –NCH(CH_3)CH(C_6H_5)–], 7.2–7.6 (m, 5H, C_6H_5–). Analysis: calculated for $C_{16}H_{20}BrNO_3$, C 54.25, H 5.69, N 3.95; found, C 54.3, H 5.65, N 3.90%.

Second eluted: N-[(2R)-2-bromohexanoyl]-(4R,5S)- 4 -methyl- 5 -phenyl- 2 -oxazolidinone. M.p. 89°C. ^{1}H NMR (300 MHz, $CDCl_3$): δ 0.91 [br d, 6H, CH_3CH_2– and –NCH(CH_3)–], 1.2–1.6 (m, 4H, $CH_3CH_2CH_2$–), 1.9–2.2 [m, 2H, –CH_2CH(Br)–], 4.80 ["p" from qd, J = 6.7 Hz, 1H, –NCH(CH_3)CH(C_6H_5)–], 5.67 [t, J = 7.1 Hz, 1H, –CH_2CH(Br)–], 5.75 [d, J = 7.1 Hz, 1H, –NCH(CH_3)CH(C_6H_5)–], 7.2–7.6 (m, 5H, C_6H_5–). Analysis: calculated for $C_{16}H_{20}BrNO_3$, C 54.25, H 5.69, N 3.95; found, C 54.3, H 5.65, N 3.90%.

N-2-Bromophenylacetyl-(4R,5S)-4-methyl-5-phenyl-2-oxazolidinone ***(2f)***

First eluted: N-[(2S)-bromophenylacetyl-(4R,5S)-4-methyl-5-phenyl-2-oxazolidinone. ^{1}H NMR (300 MHz, $CDCl_3$): δ 0.83 [d, J = 7.4 Hz, 3H, –NCH(CH_3)–], 4.87 ["p" from qd, J = 6.8 Hz, 1H, –NCH(CH_3)CH(C_6H_5)–], 5.76 [d, J = 7.0 Hz, 1H, –NCH(CH_3)CH(C_6H_5)–], 6.88 [s, 1H, C_6H_5CH(Br)–], 7.2–7.7 [m, 10H, C_6H_5CH(Br) and –NCH(CH_3)CH(C_6H_5)–].

Second eluted: N-[(2R)-bromophenylacetyl-(4R,5S)-4-methyl-5-phenyl-2-oxazolidinone. ^{1}H NMR (300 MHz, $CDCl_3$): δ 0.79 [d, J = 7.2 Hz, 3H, –NCH(CH_3)–], 4.87 ["p" from qd, J = 6.6 Hz, 1H, –NCH(CH_3)CH(C_6H_5)–], 5.74 [d, J = 6.8 Hz, 1H, –NCH(CH_3)CH(C_6H_5)–], 6.81 [s, 1H, C_6H_5CH(Br)–], 7.2–7.7 [m, 10H, C_6H_5CH(Br) and –NCH(CH_3)CH(C_6H_5)–].

N-2-Phenoxypropionyl-(4R,5S)-4-methyl-5-phenyl-2-oxazolidinone ***(2g)***

First eluted: N-[(2S)-2-phenoxypropionyl]-(4R,5S)-4-methyl-5-phenyl-2-oxazolidinone. ^{1}H NMR (300 MHz, $CDCl_3$): δ 0.91 [d, J = 6.6 Hz, 3H, –NCH(CH_3)–], 1.67 [d, J = 6.6 Hz, 3H,

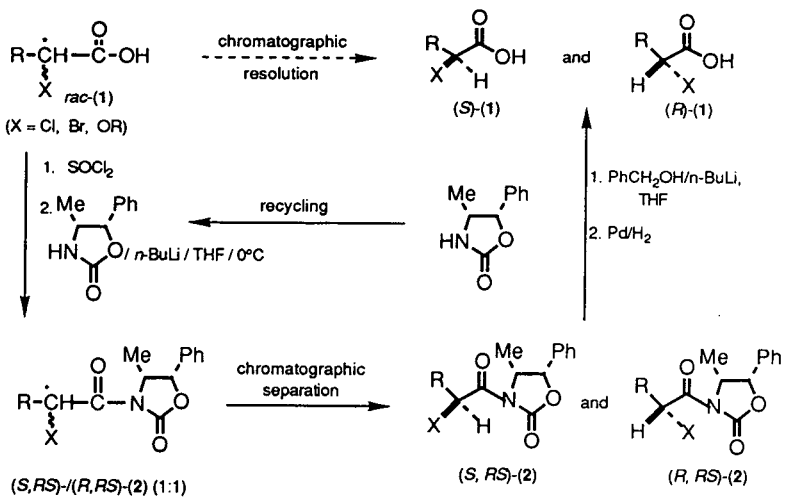

Fig. 1. Chromatographic resolution of α-halo acids and O-substituted α-hydroxy acids.

$CH_3CH(OC_6H_5)$–], 4.80 ["p" from qd, $J = 6.6$ Hz, 1H, –$NCH(CH_3)CH(C_6H_5)$–], 5.77 [d, $J = 6.6$ Hz, 1H, –$NCH(CH_3)CH(C_6H_5)$–], 6.03 [q, $J = 6.6$ Hz, 1H, $CH_3CH(OC_6H_5)$–], 6.8–7.6 [m, 10H, $-OC_6H_5$ and –$NCH(CH_3)CH(C_6H_5)$–].

Second eluted: N-[(2R)-2-phenoxypropionyl]-(4R,5S)-4-methyl-5-phenyl-2-oxazolidinone. ^1H NMR (300 MHz, $CDCl_3$): δ 0.91 [d, $J = 6.6$ Hz, 3H, –$NCH(CH_3)$–], 1.67 [d, $J = 6.6$ Hz, 3H, $CH_3CH(OC_6H_5)$–], 4.83 ["p" from qd, $J = 6.7$

TABLE I

NMR AND CHROMATOGRAPHIC PROPERTIES OF DIASTEREOMERIC N-ACYLOXAZOLIDINONES

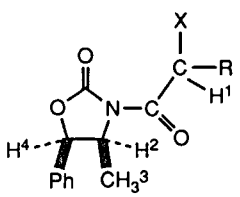

Compound	R	X	α[a]	Chemical shift[b] (ppm)								Configuration of acid[d]
				δ_1	$\Delta\delta_1$[c]	δ_2	$\Delta\delta_2$[c]	δ_3	$\Delta\delta_3$[c]	δ_4	$\Delta\delta_4$[c]	
2a	CH_3	Br	2.60	5.75	0.05	4.77	−0.07	0.94	0.03	5.76	0.03	*S*
2b	CH_3	Cl	2.24	5.76	0.04	4.78	−0.03	0.93	0.01	5.70	0	*S*
2c	Et	Br	1.78	5.77	0.07	4.81	−0.02	0.94	0.04	5.61	0.07	*S*
2d	*i*-Pr	Br	1.64	5.75	0.04	4.82	−0.02	0.94	0.03	5.56	0.07	*S*
2e	*n*-Bu	Br	1.40	5.75	0.05	4.80	−0.04	0.94	0.03	5.67	0.05	*S*
2f	Ph	Br	1.13	6.88	0.07	4.87	0	0.83	0.04	5.76	0.02	*S*
2g	CH_3	OPh	1.85	6.03	0.07	4.78	−0.03	0.91	0	5.77	0.01	*S*

[a] These non-optimized separations were achieved by normal preparative liquid chromatography using silica gel (70–230 mesh, 60 Å) as stationary phase and eluting with ethyl acetate–hexane (1:7).

[b] Chemical shifts (δ) are given for high R_f diastereomer in parts per million, downfield of Me_4Si.

[c] $\Delta\delta = \delta_{\text{high } R_f} - \delta_{\text{low } R_f}$.

[d] Configuration is that of the high R_f diastereomer.

Hz, 1H, $-NCH(CH_3)CH(C_6H_5)-$], 5.76 [d, J = 6.8 Hz, 1H, $-NCH(CH_3)CH(C_6H_5)-$], 5.96 [q, J = 6.7 Hz, 1H, $CH_3CH(OC_6H_5)-$], 6.8–7.6 [m, 10H, $-OC_6H_5$ and $-NCH(CH_3)CH(C_6H_5)-$].

RESULTS AND DISCUSSION

As depicted in Fig. 1, the diastereomeric N-acyloxazolidinones **2** were prepared in quantitative yield by lithiation of (4*R*,5*S*)-4-methyl-5-phenyl-2-oxazolidinone (*n*-butyllithium, 2.5 *M* THF) and subsequent reaction with racemic α-halocarboxylic acid chlorides or O-substituted α-hydroxycarboxylic acid chlorides. Each diastereomer was easily separated chromatographically on a large scale. As is shown in Table I, in the case of the typical examples **2a**, **2b** and **2c**, chromatographic separation factors of $\alpha = 1.8–2.6$ are achieved under preparative conditions. The pure diastereomer were cleaved by esterification and subsequent hydrolysis by the well known procedure to yield enantiomerically pure (*R*)- and (*S*)-acids [17]. Further, the consistent elution orders (the [*S*, (*R*,*S*)]-diastereomer always elutes first) can be used to indicate the absolute configuration of acids.

The chemical shift difference ($\Delta\delta$) of the diastereomer is also appreciable (Table I). This permits the NMR determination of enantiomeric purity and absolute configuration for α-halocarboxylic acids and O-substituted α-hydroxycarboxylic acids. Especially the single decoupling operation can make the integration easy.

One plausible explanation for this high degree of chromatographic separability and NMR shift difference could be associated with the conformational rigidity of diastereomers **2**. As can be seen from the X-ray structure of the second-eluted diastereomer of **2a**, (*R*,*RS*)-**2a** (Fig. 2). the eight atoms C(1), C(3), O(1), N, C(4), C(6), O(2) and O(3) form a plane (defined by the equation $0.8715x - 0.4305y - 0.2347z = 0.5589$), since none of these atoms is displaced by more than 0.134(7) Å. Further, the intramolecular contact distances of Br–O(1) and Br–O(2) are 3.476(6) and 3.420(6) Å, respectively, which are very close to the sums of their Van der Waals radii (sum of Van der Waals radius of Br and O = 3.3–3.5 Å). These facts resulted from the steric hindrance between Br and O(2), and then the C(1)–C(3) single bond cannot rotate easily. Hence this diastereomer is conformationally rigid. This conformational rigidity causes a difference in polarity and confers a high degree of chromatographic separability and NMR shift difference on diastereomers. In Table II, relevant intramolecular contact distances are given.

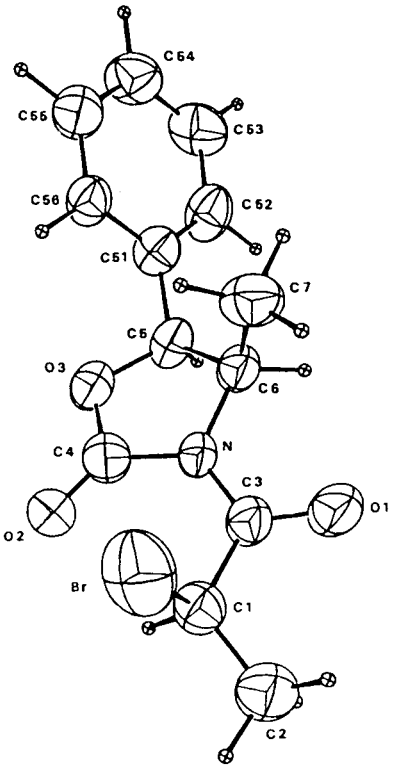

Fig. 2. X-ray structure of (*R*, *RS*)-**2a**.

In conclusion, we found that chiral oxazolidinones are valuable derivatizing agents for the chromatographic resolution of α-halocarbox-

TABLE II

INTRAMOLECULAR CONTACT DISTANCES (Å) FOR (*R*, *RS*)-**2a**

Br–O(1)	3.476(6)	Br–O(2)	3.420(6)
Br–N	3.370(5)	Br–C(4)	3.638(8)
C(2)–O(1)	2.79(1)	C(2)–N	3.76(1)
C(7)–O(1)	3.20(1)	C(1)–O(2)	2.894(9)

ylic acids and O-substituted α-hydroxycarboxylic acids.

ACKNOWLEDGEMENT

This research was supported financially by the Ministry of Science and Technology in Korea.

REFERENCES

1 B. Cambou and A.M. Klibanov, *Appl. Biochem. Biotechnol.*, 9 (1984) 255.
2 G. Kirchner, M.P. Scollar and A.M. Klibanov, *J. Am. Chem. Soc.*, 107 (1985) 7072.
3 K. Motosugi, N. Esaki and K. Soda, *Biotechnol. Bioeng.*, 26 (1984) 805.
4 A.M. Klibanov and G. Kirchner, *US Pat.*, 4 601 987 (1986).
5 B. Cambou and A.M. Klibanov, *Biotechnol. Bioeng.*, 26 (1984) 1449.
6 D.A. Evans, M.M. Morresey and R.L. Dorrow, *J. Am. Chem. Soc.*, 107 (1985) 4346.
7 D.A. Evans, J.A. Ellman and R.L. Dorrow, *Tetrahedron Lett.*, 28 (1987) 1123.
8 W. Oppolzer and P. Dudfield, *Tetrahedron Lett.*, 26 (1985) 5037.
9 W. Oppolzer and R. Moretti, *Helv. Chim. Acta*, 69 (1986) 1923.
10 W. Oppolzer and P. Dudfield, *Helv. Chim. Acta*, 68 (1985) 216.
11 G. Helmchen and R. Wierzchowski, *Angew. Chem., Int. Ed. Engl.*, 23 (1984) 60.
12 T.R. Kelley and A. Arvanitis, *Tetrahedron Lett.*, 25 (1984) 39.
13 M. Enomoto, Y. Ito, T. Katsuki and M. Yamaguchi, *Tetrahedron Lett.*, 26 (1984) 1343.
14 W.H. Pirkle and K.A. Simmons, *J. Org. Chem.*, 48 (1983) 2520.
15 M.S. Newman and A. Kutner, *J. Am. Chem. Soc.*, 73 (1951) 4199.
16 D.A. Evans, J. Bartroli and T.L. Shih, *J. Am. Chem. Soc.*, 103 (1981) 2127.
17 D.A. Evans, M.D. Ennis and D.J. Marthre, *J. Am. Chem. Soc.*, 104 (1982) 1737.

Journal of Chromatography A, 654 (1993) 309–314
Elsevier Science Publishers B.V., Amsterdam

CHROM. 25 513

Short Communication

Separation of polypropylene glycol 1200 and polybutylene glycol 1000 by reversed-phase high-performance liquid chromatography on a C_{18} stationary phase with different organic modifiers and detection by evaporative light scattering

Klaus Rissler*, Ulf Fuchslueger and Hans-Jörg Grether

Polymers Division, Ciba-Geigy Ltd., K-401.208, CH-4002 Basle (Switzerland)

(First received April 19th, 1993; revised manuscript received July 16th, 1993)

ABSTRACT

The separation of polypropylene glycol 1200 (PPG 1200) and polybutylene glycol 1000 (PBG 1000) was investigated by reversed-phase high-performance liquid chromatography on octadecylsilyl silica gel (C_{18}) with aprotic (acetonitrile) and protic (methanol, ethanol, 2-propanol) organic modifiers. Detector responses were monitored by means of evaporative light scattering. It was shown that the retentions of all oligomers of PPG 1200 decrease in the order methanol > acetonitrile > ethanol > 2-propanol. A biphasic elution pattern was observed with the more hydrophobic PBG 1000 and the retentions of low-molecular-mass homologues decreased in the order methanol > ethanol > acetonitrile > 2-propanol, whereas those of medium- and high-molecular-mass oligomers decreased in the order acetonitrile ≫ methanol > ethanol > 2-propanol. Participation of substantial solvophobic solute–solvent influences was hypothesized but the different mobile phase effects of the protic modifiers may also need to be taken into account. The former effect may be explained by interactions between the alkyl chains of ethanol and 2-propanol with the hydrophobic tetramethylene backbone of PBG 1000, which further enhances the solubility increase elicited by hydrogen bond formation between the hydroxyl groups of the organic solvent and the ether oxygens of the analyte. The latter effect may particularly be assumed in the case of methanol, where the methyl group seems to be too small to undergo efficient hydrophobic interactions with non-polar sites of the analyte.

INTRODUCTION

Polyethers and their α,ω-O-alkylated or arylated derivatives have a broad application range in many different fields of chemistry. In particular, polyethylene glycol (PEG) plays a major role in both industrial and biotechnical applications, whereas polypropylene glycol (PPG) and polybutylene glycol (PBG) play an important role in polymer chemistry as flexibilizers and tougheners in formulated systems [1–3]. In many applications PPGs are first reacted with diisocyanates to form isocyanate prepolymers, which are subsequently converted into polyurethanes [4,5].

Different chromatographic methods have been successfully used for the characterization of

* Corresponding author.

0021-9673/93/$06.00 © 1993 Elsevier Science Publishers B.V. All rights reserved

polyether mixtures, *e.g.*, gas chromatography (GC), gel permeation chromatography/size-exclusion chromatography (GPC/SEC), thin-layer chromatography (TLC), reversed-phase high-performance liquid chromatography (RP-HPLC) and supercritical fluid chromatography (SFC). GC yields an optimum resolution of polyethers but unfortunately its use is restricted to low-molecular-mass samples, whereas GC/SEC covers the whole molecular mass range but is associated with poor peak resolution. TLC can be used at least up to the intermediate molecular mass range but exhibits substantially less resolution in comparison with HPLC. SFC is a very promising new technique, but it is still restricted to a small number of suitable mobile phases. Therefore, HPLC may still be regarded as the most efficient technique for the separation of polyethers owing to the large number of experimental alternatives, *i.e.*, the wide availability of both mobile and stationary phases. Additionally, in combination with evaporative light scattering detection (ELSD), the monitoring of UV-inactive components is achieved with high sensitivity.

It should be taken into account that polyethers of technical quality generally consist of a large number of oligomers often yielding a distinct chromatographic pattern, which, in turn, can be used to identify the type of polyether within a formulated system by its "fingerprint".

In a previous paper, we treated the separation of polyethers, such as PEG 1000, PPG 1200 and PBG 1000, on different stationary phases with either acetonitrile or methanol as mobile phase modifier [6]. Methanol proved to be superior to acetonitrile especially for the elution of medium- to high-molecular-mass oligomers [6]. Its marked improvement of the elution power was attributed to solute solvation by hydrogen bonding with polyether oxygens and, as a consequence, retention seems to be essentially governed by its hydrophilic properties. The question arises of whether a "solvophobic solvation" effect of the alcoholic modifier on solute retention (*i.e.*, depending on the length of the alkyl chain and thus attributable to an increase in lipophilicity in the order methanol < ethanol < 2-propanol) will be synergistic with the effect of hydrogen bonding. On the other hand, mobile phase effects influencing desorption of the solute as a function of increasing elution strength in the order methanol < ethanol < 2-propanol has additionally to be considered. For this reason we have applied gradient RP-HPLC with PPG 1200 and PBG 1000 as model components on octadecylsilyl silica gel (C_{18}) with methanol, ethanol and 2-propanol as organic modifiers. Acetonitrile is used as a "reference" solvent, because it is not able to release medium- to high-molecular-mass homologues from the hydrophobic stationary phase, as shown recently [6].

EXPERIMENTAL

Reagents and solvents

Polypropylene glycol 1200 ("pract." quality) was purchased from Fluka (Buchs, Switzerland) and polybutylene glycol 1000 (technical quality) from BASF (Ludwigshafen, Germany). Acetonitrile, methanol and 2-propanol (all of HPLC quality) were from Fluka and ethanol was purchased from Merck (Darmstadt, Germany). Water for use in HPLC was purified with a Milli-Q reagent water system from Millipore–Waters (Milford, MA, USA).

Analytical equipment

The HPLC apparatus consisted of a combined-type SP 8100 system of an HPLC pump and autosampler and a PC 1000 data acquisition unit, all obtained from Spectra-Physics (San Jose, CA, USA). For ELSD a Sedex 45 apparatus from Sedere (Vitry sur Seine, France) equipped with a 20-W iodine lamp was used.

Chromatographic separation and detection

Separation of polyethers was performed on a Nucleosil $5C_{18}$ column (125 × 4.6 mm I.D., 5 μm particle size) from Macherey–Nagel (Oensingen, Switzerland). The gradient profile used is shown in Table I and chromatography was performed at ambient temperature (*ca.* 22°C) at a flow-rate of 1.5 ml/min. Polyether samples (2%, w/v) were dissolved in methanol and 10-μl aliquots were injected. For detection by means of ELSD the nebulization chamber was heated to 40°C and the nitrogen flow-rate was adjusted

TABLE I

GRADIENT PROGRAMME FOR THE ELUTION OF POLYETHER SAMPLES

Time (min)	Organic solvent (%)	Water (%)
0	20	80
40	100	0
75	100	0
76	20	80
90	20	80

to 4.5 l/min, corresponding to an inlet pressure of 200 kPa.

RESULTS AND DISCUSSION

On the basis of our experience in polyether analysis as described recently [6], we used signal monitoring by ELSD. Alternatively, tagging of a chromophoric agent to the α,ω-dihydroxy groups will permit UV detection in the usual wavelength range [7]. However, the increase in hydrophobicity of both polyethers through derivatization makes long elution times necessary, especially for PBG 1000.

The retention of PPG 1200 (a polyether of intermediate polarity) decreases substantially in the order methanol > acetonitrile > ethanol > 2-propanol (Fig. 1a–d). When compared with the peak resolution R_s obtained with acetonitrile (Fig. 1a), a significant "levelling" effect is observed with the protic solvents, resulting in fairly poor R_s values (Fig. 1b–d). With methanol the marked time delay in the onset of oligomer elution and the concomitant "compression" of peaks attributable to high-molecular-mass constituents to within a period of a few minutes when compared with acetonitrile can be explained by its decreased elution power for the low-molecular-mass homologues and to a concomitant relative increase in desorption of oligomers of higher molecular mass, presumably owing to their better solubility in the mobile phase by means of hydrogen bond formation between the hydroxy groups and polyether oxygens [6]. The further decrease in solute retention with ethanol and 2-propanol compared with methanol may be attributed to (i) stronger desorption as a consequence of a more efficient displacement of solute from the non-polar stationary phase by the more hydrophobic modifiers and/or (ii) an effect of "hydrocarbon (tetramethylene) backbone solvation" mediated by the alkyl groups of ethanol and 2-propanol, *i.e.*, a solvophobic solute–solvent effect.

In general, separation of the more hydrophobic PBG 1000 yields similar retention characteristics (Fig. 2a–d). Nevertheless, some peculiarities with respect to PPG 1200 are observed. The elution power of acetonitrile seems at first sight to be superior to that of methanol and ethanol, but it is evident that only a minor part of PBG 1000 oligomers was eluted on a C_{18} matrix. Therefore, the aprotic solvent proves to be the eluent of choice at least for the low-molecular-mass PBGs yielding optimum resolution of homologues. With methanol, more than twice the number of well resolved oligomers are eluted compared with acetonitrile but the complete release of the total amount of sample is only effected with ethanol and 2-propanol (Fig. 2c and d). In contrast, only oligomers with apparently low and medium molecular mass are well resolved by the use of ethanol and 2-propanol. It is conspicuous that a substantial discrimination between oligomers with different molecular mass takes place in particular at the change from methanol to ethanol and 2-propanol (see Fig. 2b–d). Further, retention of low-molecular-mass oligomers seems to be differently affected with ethanol and 2-propanol (Fig. 2c and d). This observation can be ascribed to a heterogenous distribution of oligomers in the PBG 1000 sample. We cannot give a reasonable explanation of these surprising mobile phase influences. Nevertheless a possible influence of the column pressure on retention and selectivity [8–11] of PBG 1000 with 2-propanol as the modifier may probably be ruled out. This view is supported by the observation that a consecutive temperature increase in 10°C intervals from room temperature to 70°C did neither essentially influence retention of oligomers nor the chromatographic pattern (results not shown).

Replacement of acetonitrile with methanol (Fig. 2b) effects a stronger retention of low-molecular-mass homologues, whereas sample

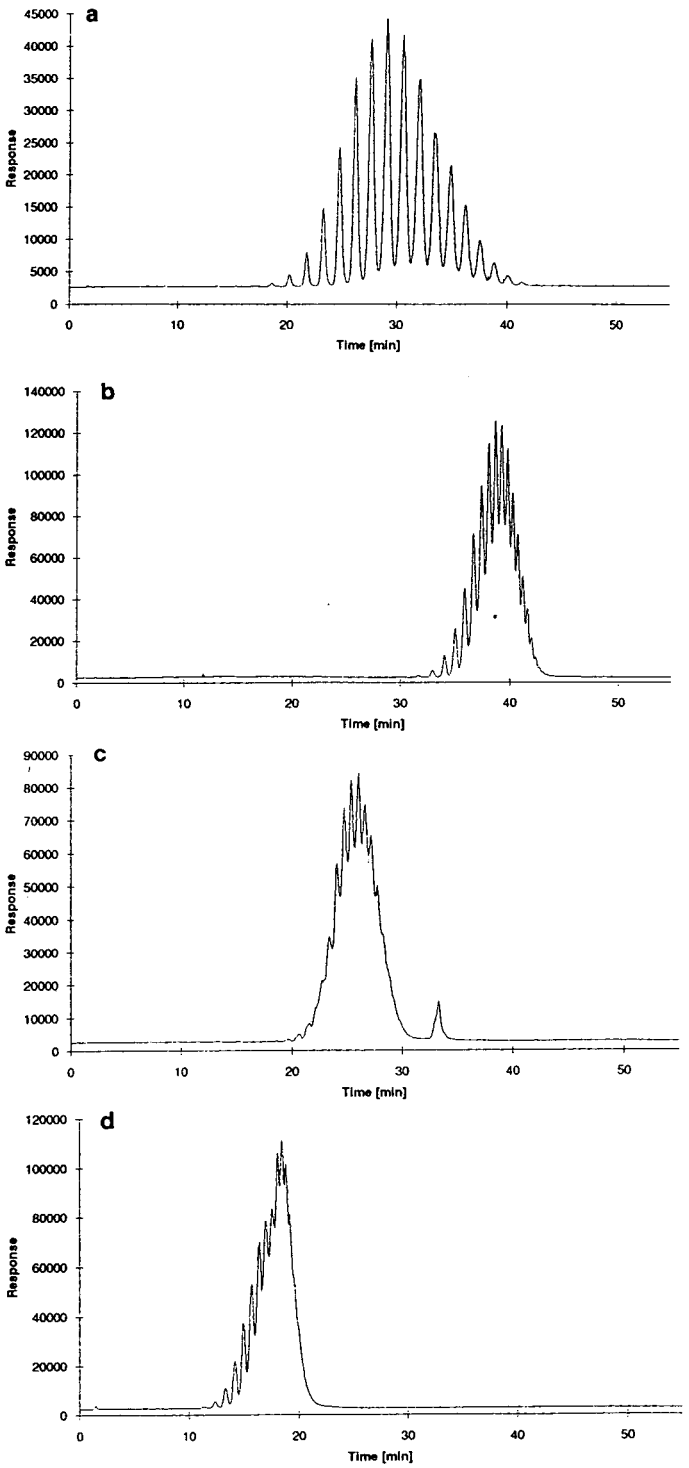

Fig. 1. HPLC of PBG 1000 on a C_{18} column with (a) acetonitrile, (b) methanol, (c) ethanol and (d) 2-propanol as the organic modifier.

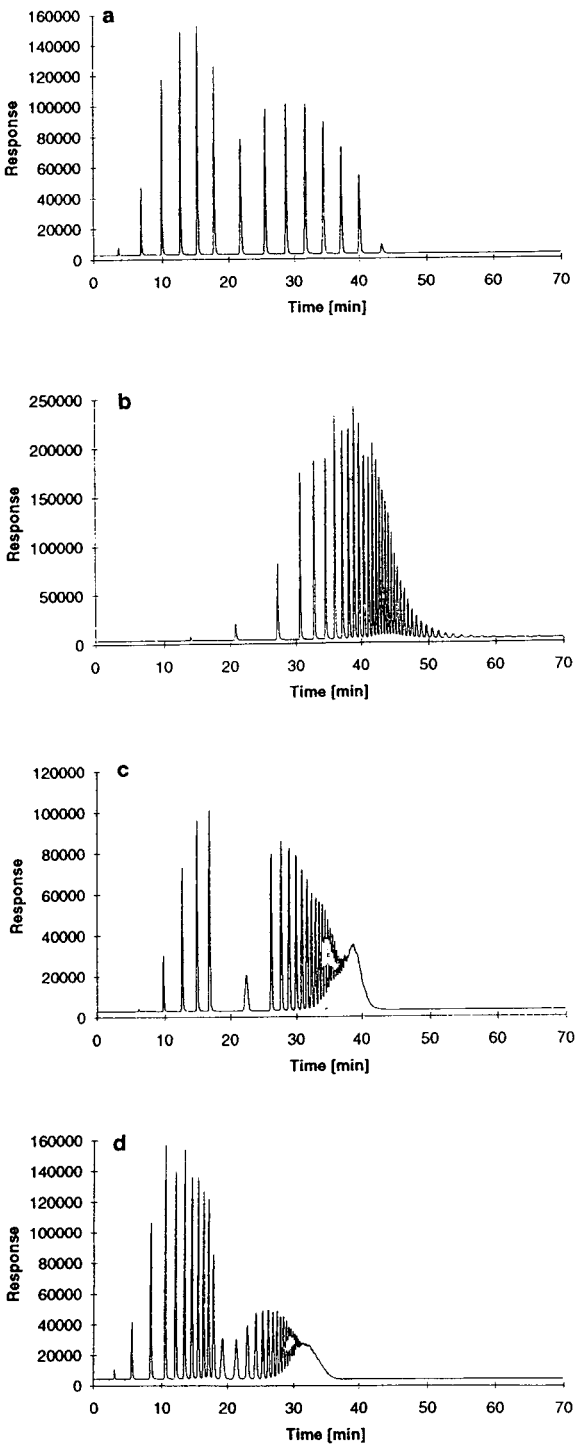

Fig. 2. HPLC of PBG 1000 on a C_{18} column with (a) acetonitrile, (b) methanol, (c) ethanol and (d) 2-propanol as the organic modifier.

constituents of higher mass are eluted either more rapidly or more quantitatively (see ref. 6). It may be assumed that low-molecular-mass oligomers are sufficiently soluble in acetonitrile and, owing to its superior elution power, are eluted more rapidly than with methanol and ethanol. Although more than twice the number of oligomers are released with methanol, its beneficial effect on the solubility of PBG 1000, at least on a C_{18} column, is not sufficient enough for their quantitative elution. Concerning the large increase in elution power elicited by ethanol, we suggest a substantial participation of solvophobic (*i.e.*, solubility-enhancing) interactions between the lipophilic side-chain of ethanol and 2-propanol ($+CH_2-$ and $+CH_3CH-$ *versus* methanol) in the order 2-propanol > ethanol > methanol and the hydrophobic tetramethylene backbone of PBG 1000, which, in turn, may be responsible for the increase in desorption. This hypothetical view is supported by the fact that the retention of high-molecular-mass components (eluting at high concentrations of the modifier) is obviously much more affected than that of low-molecular-mass sample constituents and yields substantial "signal compression" (Fig. 2c and d). It may be assumed that low-molecular-mass oligomers, their solubilities being approximately identical in all four organic solvents, are less affected and elute nearly in the range of the modifier's elution power. Nevertheless a contribution of a mobile phase effect to retention should also be considered. This means that the increase in elution power in the order methanol < ethanol < 2-propanol (*i.e.*, depending on the modifier's hydrophobicity) may be ascribed to the better sorption of the alcohols on the stationary phase and thus increased desorption of the analyte in the same direction. However, the large discrepancies in retention between methanol and ethanol may be interpreted as supporting our hypothesis. This point of view is further corroborated by (i) the strongly increasing "signal compression" of high- compared with low-molecular-mass PBG 1000 oligomers in the order methanol < ethanol < 2-propanol and (ii) the different effects of ethanol and 2-propanol on the retention of low- and medium-molecular-mass oligomers compared with metha-

nol, which cannot be explained by stronger desorption alone. In this respect we hypothesize an additional solvophobic solute–solvent interaction in addition to also a reasonably substantial "mobile phase" influence mentioned above, which superimposes the effect of hydrogen bond formation. As an appropriate means of obtaining a more quantitative estimate of the extent of solovophobic solute–solvent interactions compared with a "mobile phase" effect based on increased desorption from the stationary phase, measurement of the heats of solubility of both analytes in the different modifiers would be feasible.

According to our previous investigations with different stationary phases [6], silanophilic solute–matrix interactions [12–15] do not seem to play a significant role. Hence the elution power of the protic solvents *versus* acetonitrile probably cannot be attributed to their better ability to cleave hydrogen bonds between polyether oxygens and residual silanols of the stationary phase [12].

It will further be of interest if the trend observed within the series of C_1, C_2 and C_3 alcohols continues with butanol. However, the expected back-pressure of the HPLC column will prevent its use at least at room temperature. It is notable that the column back-pressure of aqueous solutions of the three alcoholic modifiers reaches a maximum value at *ca.* 40–70% (v/v) of organic solvent (depending on the modifier used), which with 2-propanol markedly exceeds 300 bar. For this reason, at least for C_4 alcohols, column heating is necessary and thus micro-HPLC at elevated temperature will offer an attractive alternative for the use of alcohols with more than four carbon atoms and alcohols of the ethylene glycol or diethylene glycol type. In addition, it may be of great importance to evaluate the possible influence of column temperature on the retention of hydrophobic polyethers, by means of which more insight into the separation mechanism should be possible. This aim will only be achieved, however, by testing more than three homologous alcohols as used in our study, which, in turn, also raises the question of sufficient miscibility of, *e.g.*, C_4–C_6 alcohols and water even at elevated temperature.

CONCLUSIONS

From the chromatograms in Figs. 1a–d and 2a–d, it can be concluded that the separation efficiency of oligomers on the C_{18} matrix is substantially higher for PBG 1000 than PPG 1200, which, as a consequence, facilitates identification of PBG 1000 by the "fingerprint" pattern of its low- and medium-molecular-mass oligomers. This "pattern recognition" is even possible with the stronger modifiers ethanol and 2-propanol, which, however, do not or at least insufficiently resolve high-molecular-mass homologues. Although the R_s of PPG 1200 oligomers vanishes completely with both ethanol and 2-propanol it should be emphasized that discrimination of different PPG samples ranging from $M_r = 2000$ to more than 10 000 is still possible and allows a selective attribution within polyether mixtures compared with GPC (preliminary investigations, results not shown).

REFERENCES

1 K. Blinne and W. Möller, *Kunstst.-Plast. (Solothurn)*, 10 (1963) 1.
2 R. Schmid and R. Stierli, *Chimia*, 19 (1965) 359.
3 H. Möller and M. Schwab, *Kunststoffe*, 74 (1984) 4.
4 G.B. Guise and G.C. Smith, *J. Chromatogr.*, 247 (1982) 369.
5 D. Noël and P. van Gheluwe, *J. Chromatogr. Sci.*, 25 (1987) 231.
6 K. Rissler, H.-P. Künzi and H.-J. Grether, *J. Chromatogr.*, 635 (1993) 89.
7 A. Nozawa and T. Ohnuma, *J. Chromatogr.*, 187 (1980) 261.
8 D.C. Locke and D.E. Martire, *Anal. Chem.*, 39 (1967) 921.
9 B.A. Bidlingmeyer and L.B. Rogers, *Sep. Sci.*, 7 (1972) 131.
10 V.L. McGuffin and C.E. Evans, *J. Microcol. Sci.*, 3 (1991) 513.
11 G. Guiochon and M.J. Sepaniak, *J. Chromatogr.*, 606 (1992) 248.
12 K.E. Bij, Cs. Horváth, W.R. Melander and A. Nahum, *J. Chromatogr.*, 203 (1981) 65.
13 E.L. Weiser, A.W. Salotto, S.M. Flach and L.R. Snyder, *J. Chromatogr.*, 303 (1984) 1.
14 W.A. Moats and L. Leskinen, *J. Chromatogr.*, 386 (1987) 79.
15 G.C. Fernandez Otero and C.N. Carducci, *J. Liq. Chromatogr.*, 14 (1991) 1561.

Journal of Chromatography A, 654 (1993) 315–318
Elsevier Science Publishers B.V., Amsterdam

CHROM. 25 496

Short Communication

Analysis of fullerenes by reversed-phase high-performance liquid chromatography

John J. Harwood*

Department of Chemistry, Foster Hall, Tennessee Technological University, Cookeville, TN 38505 (USA)

Gleb Mamantov

Department of Chemistry, 575 Buehler Hall, University of Tennessee, Knoxville, TN 37996 (USA)

(First received June 21st, 1993; revised manuscript received August 11th, 1993)

ABSTRACT

Chromatographic separation of fullerenes was achieved with a conventional reversed-phase analytical system. A tetrahydrofuran–acetonitrile mobile phase (60:40) (1.0 ml/min) used with a 25 cm ODS column separates C_{60} and C_{70} with a resolution of 6.4 and an analysis time of 11.4 min. This method is convenient and offers sufficient resolving power to be applied to the analysis of a variety of fullerenes and fullerene reaction product mixtures. The mobile phase allows use of the sensitive ultraviolet absorbance bands of fullerenes in detection. The method is compared with other reversed-phase methods for analysis of fullerene mixtures.

INTRODUCTION

Efforts to develop chromatographic methods to separate fullerenes (C_{60} and C_{70}) have focused on developing preparatory methods which utilize mobile phase mixtures with high solubilities for the compounds, principally mixtures of hexane with methylene chloride, benzene or toluene [1–5]. Good preparatory separations of C_{60} and C_{70} have been obtained with stationary phases such as dinitroanalinopropyl silica [1], tripodal 2,4-dinitrophenyl ether octyl silica [2,3], phenylglycine chiral stationary phase [6] and polystyrene–divinylbenzene [7]. These stationary phases are not commonly used by chromatographers, and an analytical separation method utilizing conventional chromatographic stationary and mobile phases, especially using the common octadecylsilane (ODS) column, can be more useful to researchers interested in various aspects of the chemistry of the fullerenes.

C_{60} and C_{70} have been resolved on ODS columns with mobile phases of toluene with isopropanol or methanol [8–10]. Absorption by toluene prevents use of the sensitive ultraviolet absorbance region in detecting the eluates. Diack *et al.* [11] have obtained baseline resolution of C_{60} and C_{70} using hexane with an ODS column. Improvement of this separation to allow resolution of fullerene adducts or reaction mixture impurities is not straightforward due to

* Corresponding author.

0021-9673/93/$06.00 © 1993 Elsevier Science Publishers B.V. All rights reserved

the immiscibility of commonly used reversed-phase modifiers in hexane. Jinno *et al.* [9] have obtained better resolution with hexane using a monomeric ODS column (Develosil ODS-5). Reversed-phase chromatography of fullerenes using methylene chloride–acetonitrile mobile phase has been investigated [12,13]. This mobile phase produces good resolution of these and other fullerenes on both Whatman Partisil 5 analytical and Vydac 201TP510 preparatory columns. Methylene chloride is an inhalation irritant, a mutagen and an animal carcinogen [14], and as a chlorinated hydrocarbon disposal of this solvent is strictly regulated, hence its use should be avoided when possible.

We have found that excellent resolution of C_{60} and C_{70} can be obtained with ODS stationary phase and tetrahydrofuran (THF)–acetonitrile (ACN) mobile phase. This mobile phase sufficiently solubilizes C_{60} and C_{70} to allow injection of reasonable quantities of the compounds for analysis, and the ability to detect low concentrations of these and other fullerenes in reaction mixtures is enhanced as strong UV absorbance bands of the compounds can be monitored. Reversed-phase chromatography of C_{60} and C_{70} in methylene chloride with this mobile phase is compared with chromatography using hexane, isopropanol–toluene and other mobile phases.

MATERIALS AND METHODS

Chromatograms were obtained with a Perkin-Elmer Series 4 HPLC chromatograph equipped with a Hitachi 100-10 detector. A Phenomenex Spherex 5 C_{18} column (250 mm × 4.6 mm) was used in obtaining all chromatograms for which chromatographic parameters are reported. A Hewlett-Packard 1090M chromatograph equipped with a diode array UV–visible absorbance detector and a HP ODS Hypersil 5 μm column (200 mm × 4.6 mm) was also used.

Unretained time was determined by injection of 1 *M* sodium nitrate solution [15]. A mobile phase flow-rate of 1.0 ml/min was used throughout.

Absorbance of the compounds was monitored at 254 except in the case of the isopropanol–toluene mobile phases, with which absorbance was monitored at 330 nm. Identities of the C_{60} and C_{70} chromatographic peaks were confirmed by comparing spectra of the peaks obtained with the diode array detector with published UV–visible spectra [16].

A portion of a mixture of C_{60} and C_{70} (Mer Labs., Tucson, AZ, USA), was allowed to equilibrate at room temperature with methylene chloride in a sealed vial for several weeks, then filtered through a 0.5-μm pore diameter PTFE filter (Corning) prior to injection. All mobile phases were either ACS reagent grade or HPLC grade (Fisher Scientific).

RESULTS AND DISCUSSION

Tetrahydrofuran–acetonitrile

With the Spherex ODS column, a mobile phase mixture of THF–ACN (80:20, v/v) produces near-baseline resolution of C_{60} and C_{70}, with capacity factor (k') values of 0.47 and 0.62 for the two compounds, respectively. A 60:40 mixture of these solvents produces a resolution of 6.4, with k' values of 2.2 and 3.8 and plate numbers of 3300 and 5300 for C_{60} and C_{70}, respectively (Fig. 1a). (See Table I for a comparison of this and other reversed-phase separations of C_{60} and C_{70}.) Several unidentified mix-

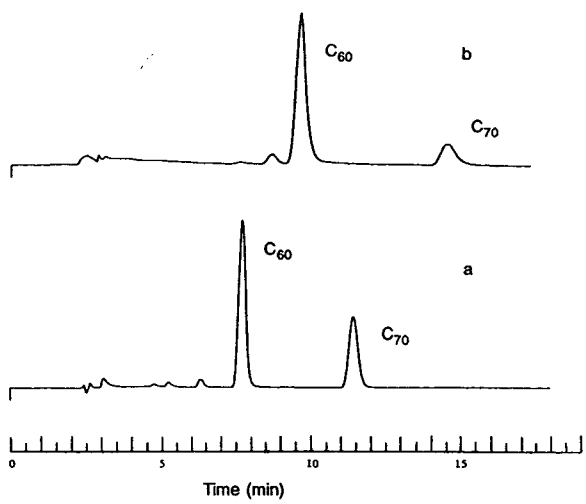

Fig. 1. Separation of C_{60} and C_{70} with an ODS column and (a) THF–ACN (60:40) (254 nm detection) and (b) isopropanol–toluene (75:25) (330 nm detection).

TABLE I

REVERSED-PHASE CHROMATOGRAPHIC SEPARATIONS OF C_{60} AND C_{70}

Resolution values are estimated from published chromatograms.

Mobile phase	Retention time of C_{70} (min)	Resolution[a]	Ref.
Isopropanol–toluene (60:40)	9.3	3.4	8
Isopropanol–toluene (75:25)	14.5	6.1	Present work
Hexane	5.6	1.7	11
Hexane (monomeric ODS)	9.2	5.1	9
Methylene chloride–ACN (67.5:32.5)	20	10	12
THF–ACN (60:40)	11.4	6.4	Present work

[a] Of C_{60} from C_{70}.

ture components eluted before C_{60} with the THF–ACN mixture.

Slight fronting of both the fullerene peaks is observed on injection of 35 μl of the methylene chloride sample. This fronting becomes more apparent with higher injection volumes, though similar retention times and reasonable peak profiles are obtained on injection of 75 μl sample.

A THF–ACN (50:50) mixture gives even greater resolution, 9.7, with no peak distortion at low injection volumes. Reproducible elution of the compounds is not obtained with a 40:60 mixture, probably reflecting diminished solubility of the compounds in this mixture.

Isopropanol–toluene

Isopropanol–toluene mobile phases are effective in resolving C_{60} and C_{70}. The 60:40 mobile phase mixture used by Meier and Selegue [8] produces a resolution of only 2.4 with our column, less than that reported for the Waters Novapak column. An isopropanol–toluene (75:25) mixture yields a resolution of 6.1, with k' values of 2.9 and 4.9 for C_{60} and C_{70}. This separation is not as efficient as that obtained with the THF–ACN (60:40) mixture, which produces narrower peaks and better resolution with an analysis time (for elution of C_{70}) of 12 min as compared with 15 min with the isopropanol–toluene mixture (Fig. 1b). As with the THF–ACN mobile phase, slight peak fronting is observed with the isopropanol–toluene (75:25) mixture on injection of 35 μl sample. Impurity peaks eluting before C_{60} are not as well resolved from C_{60} as those apparent in the THF–ACN chromatogram (Fig. 1a).

Other mobile phases

A resolution of 1.9, with k' values of 0.87 and 1.2 for C_{60} and C_{70}, is obtained with hexane mobile phase, in agreement with the results of Diack *et al.* [11].

A THF–water (80:20) mixture rapidly elutes and partially resolves C_{60} and C_{70}. Increasing water in the mixture to 30% separates the components, but produces pronounced peak splitting, indicating a lack of solubility of the compounds at the higher water content.

Baseline resolution of the two compounds is obtained with a THF–methanol (70:30) mobile phase. C_{60} and C_{70} are not eluted in a reproducible manner when the THF–methanol mixture ratio is adjusted to the same mixture polarity (P') [17] as the THF–ACN (60:40) mixture, a 34.5:65.5 mixture. Again, it is probable that the chromatographic failure is due to poor solubility of the compounds in the mixture.

CONCLUSIONS

Analysis of fullerenes can be achieved by conventional reverse phase chromatography with THF–ACN mobile phase. The efficiency of separation with this system, coupled with the good solubility of C_{60} and C_{70} in this mixture and the ability to detect the compounds utilizing strong absorbance bands in the ultraviolet spectral region, can facilitate analysis of mixtures of a variety of fullerenes and fullerene products.

ACKNOWLEDGEMENTS

This research was sponsored in part by the National Science Foundation Visiting Faculty Analytical Research Associate Program at the University of Tennessee at Knoxville. The C_{60}/C_{70} sample was supplied by R.N. Compton, UTK/Oak Ridge National Laboratory.

REFERENCES

1 C.M. Cox, S. Behal, M. Kisko, S.M. Gorun, M. Greaney, C.S. Hsu, E.B. Killin, J. Millar, J. Robbins, W. Robbins, R.D. Sherwood and P.J. Tindall, *J. Am. Chem. Soc.*, 113 (1991) 2940.
2 C.J. Welch and W.H. Pirkle, *J. Chromatogr.*, 609 (1992) 89.
3 L. Nondek and V. Kužílek, *Chromatographia*, 33 (1992) 344.
4 R. Baum, *Chem. Eng. News*, 70 No. 39 (1992) 43.
5 M. Pickett, Phenomenex, personal communication.
6 J.M. Hawkens, T.A. Lewis, S.D. Loren, A. Meyer, J.R. Heath, Y. Shibato and R.J. Saykally, *J. Org. Chem.*, 55 (1990) 6250.
7 D.L. Stalling, K.C. Kuo, C.Y. Guo and S. Saim, *J. Liq. Chromatogr.*, 16 (1993) 699.
8 M.S. Meier and J.P. Selegue, *J. Org. Chem.*, 57 (1992) 1924.
9 K. Jinno, T. Uemura, H. Nagashima and K. Itoh, *Chromatographia*, 35 (1993) 38.
10 F. Yan, Y. Liu and J. Ma, *Chin. Chem. Lett.*, 3 (1992) 903.
11 M. Diack, R.L. Hettich, R.N. Compton and G. Guiochon, *Anal. Chem.*, 64 (1992) 2143.
12 R.C. Klute, H.C. Dorn and H.M. McNair, *J. Chromatogr. Sci.*, 30 (1992) 438.
13 R. Ettl, I. Chao, F. Diederich and R.L. Whetten, *Nature*, 353 (1991) 149.
14 *Material Safety Data Sheet —Methylene Chloride*, Fisher Scientific, Chemical Division, Fair Lawn, NJ, 1989.
15 M.J.M. Wells and C.R. Clark, *Anal. Chem.*, 53 (1981) 1341.
16 H. Ajie, M.M. Alvarez, S.J. Anz, R.D. Beck, F. Diederich, K. Fostiropoulos, D.R. Huffman, W. Krätschmer, Y. Rubin, K.E. Schriver, D. Sensharma and R.L. Whetten, *J. Phys. Chem.*, 94 (1990) 8630.
17 J.L. Glajch, J.J. Kirkland and K.M. Squire, *J. Chromatogr.*, 199 (1980) 57.

Journal of Chromatography A, 654 (1993) 319–325
Elsevier Science Publishers B.V., Amsterdam

CHROM. 25 520

Short Communication

Gas chromatographic separation of pairs of isotopic molecules

Buchang Shi and Burtron H. Davis*

Center for Applied Energy Research, 3572 Iron Works Pike, Lexington, KY 40511 (USA)

(First received May 24th, 1993; revised manuscript received August 16th, 1993)

ABSTRACT

Nine pairs of isotopic (hydrogen/deuterium) molecules have been completely separated and quantitatively determined by gas chromatograph using a DB-5 column. All pairs exhibited an inverse isotope effect. The differences of enthalpy, entropy and free energy changes have been calculated for the chromatographic process. The data show that deuterium on the aliphatic part of a molecule makes more of a contribution to the inverse isotope effect than those on aromatic rings.

INTRODUCTION

The gas chromatographic (GC) separation of isotopically labeled molecules has been investigated during recent years [1–12]. Because this technique affords a convenient method to study isotope effects in solution and scale up might afford economically feasible separations of large amounts of material, studies on GC separation of isotopic molecules continue to receive widespread attention. A considerable amount of the literature studies on isotopic separations were conducted at relative low temperatures so that long times (sometimes more than 1 h) were required for the separations (see, *e.g.*, refs. 13–15). This has limited the utilization of this technique. Fortunately, the introduction of high-efficiency GC columns in recent years opens new opportunities for the analysis of isotopic labeled molecules [16]. We report here the separation of several pairs of isotopic molecules. Quantitative determination of each component was possible, and the analysis was accomplished in a few minutes.

EXPERIMENTAL

The DB-5 column, purchased from J & W Scientific, is a 60 m × 0.32 mm fused silica column. The liquid phase was 5% diphenyl, 95% dimethylsilicone. A Hewlett-Packard 5890 Series II gas chromatograph equipped with a flame ionization detector was utilized; this gas chromatograph interfaced with an HP5971A mass-selective detector that was operated under the control of a Vectra 05/165 computer using HPG1034B software. Helium was used as the carrier gas.

The deuterated compounds used in this work were purchased from Aldrich except for

* Corresponding author.

0021-9673/93/$06.00 © 1993 Elsevier Science Publishers B.V. All rights reserved

bibenzyl-$d_{7\text{-benzyl}}$ which was provided by Professor R.D. Guthrie (Department of Chemistry, University of Kentucky).

Experiments were performed to estimate the response of the flame ionization detector to these compounds. The ratio of the GC peak areas is the same as the ratio of the weights of the compounds within the range of the experiment error (1–2%).

Retention volumes have been corrected using the retention time of methane to determine the dead volume.

RESULTS AND DISCUSSION

The data in Table I show the time and the temperature needed for complete separation of pairs of isotopic molecules. At 25°C, benzene-d_6 and benzene-d_0 were completely separated in 7 min. Liberti *et al.* [14] reported a complete separation of benzene-d_6 and benzene-d_0 on both squalane and silicone oil columns; however, in these cases the times needed were 34 and 61 min, respectively. At 45°C, toluene-$d_{3\text{-methyl}}$, toluene-d_8 and toluene-d_0 can be separated completely and can be measured quantitatively. A very good separation of octane-d_{18} and octane-d_0 was obtained at 80°C in 5 min. The mixture of naphthalene-d_8 and naphthalene-d_0 was separated at 110°C in 12 min. At 160°C, bibenzyl-$d_{7\text{-benzyl}}$ and bibenzyl-d_0 were separated in 15 min, and could be determined quantitatively. At 60°C, ethylbenzene-d_{10}, ethylbenzene-$d_{5\text{-ethyl}}$ and ethylbenzene-d_0 were completely separated. Ethylbenzene-$d_{5\text{-ring}}$ labeled was separated from ethylbenzene-d_0 at 35°C within 20 min. Typical gas chromatograms for these compounds (Figs. 1–3) show that the heavier species always eluted first. This phenomena is an inverse isotope effect [2,10,13–17]. Intermolecular Van der Waals forces make the major contribution to the inverse isotope effect. These are operative in the condensed phase and result in a shift in the zero point energy (ZPE) when a molecule of interest is transferred from the gas to the condensed phase. Since the ZPE is isotope sensitive, this results in a thermodynamic isotope effect. The sign of the effect correlates with the fact that the Van der Waals' interaction causes a red shift in

TABLE I

TIME AND TEMPERATURE NEEDED FOR COMPLETE SEPARATION OF PAIRS OF ISOTOPICALLY LABELED MOLECULES USING THE DB-5 COLUMN

Isotopic pair	Temperature (°C)	Time (min)
Benzene-d_6/-d_0	25	7
Toluene-d_3/-d_0	45	8
Toluene-d_8/-d_0	50	7
Octane-d_{18}/-d_0	80	5
Naphthalene-d_8/-d_0	110	12
Bibenzyl-d_7/-d_0	160	15
Ethylbenzene-d_{10}/-d_0	60	10
Ethylbenzene-d_5-ethyl/-d_0	60	10
Ethylbenzene-d_5-ring/-d_0	35	21

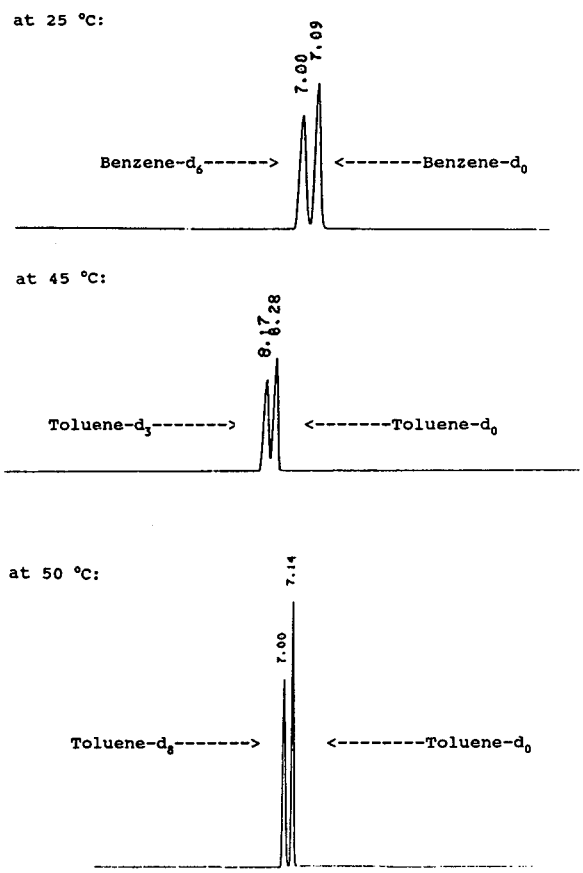

Fig. 1. Gas chromatograms of benzene-d_0/-d_6, toluene-d_0/-d_3 and toluene-d_0/-d_8 on DB-5 capillary column. Values at peaks indicate retention times in min (also in Figs. 2 and 3).

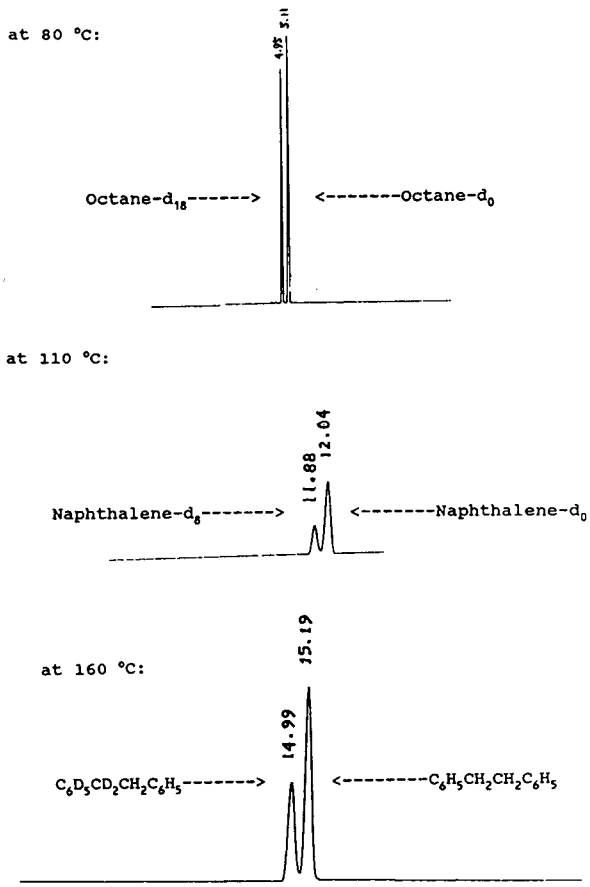

Fig. 2. Gas chromatograms of octane-d_0/-d_{18}, naphthalene-d_0/-d_8 and bibenzyl-d_0/-d_7 on DB-5 capillary column.

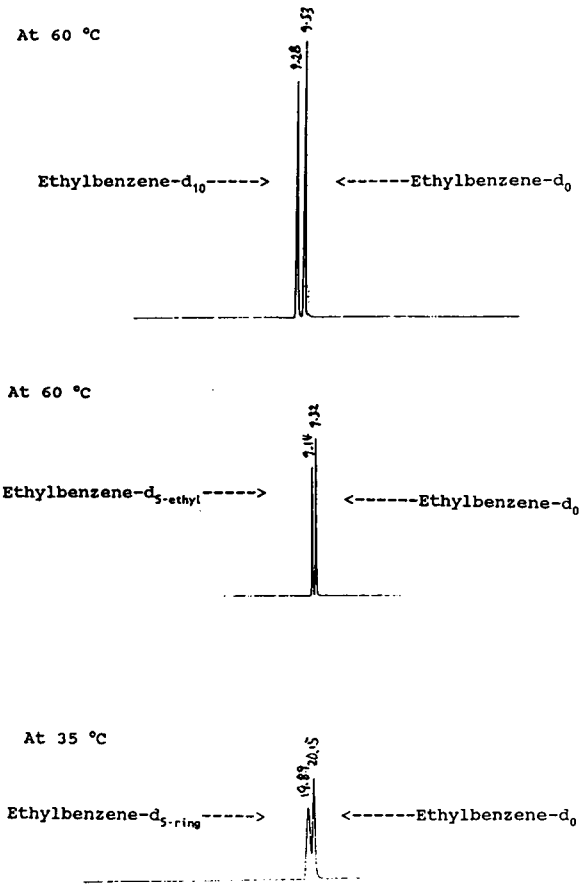

Fig. 3. Gas chromatograms of ethylbenzene-d_0/-d_{10}, -$d_{5\text{-ethyl}}$ and -$d_{5\text{-ring}}$ on DB-5 capillary column.

the carbon–hydrogen (or carbon–deuterium) vibrational modes [17,18].

To obtain the most favorable and the most convenient operating temperature, the separation factor has been measured over a fairly wide range (Fig. 4). For all of the systems studied except bibenzyl-d_7/-d_0, naphthalene-d_8/-d_0 and benzene-d_6/-d_0, the highest separation factors are observed around 300 K. The octane-d_{18}/-d_0 system has the highest separation factor and is very sensitive to temperature.

In Fig. 4, the logarithm of the ratio of the retention volumes obtained with a DB-5 column are plotted against the reciprocal of the absolute temperature. All of the isotopic mixtures show an inverse isotope effect and a relationship of the type $\log (V_R)_H/(V_R)_D = B/T + C$ describes the

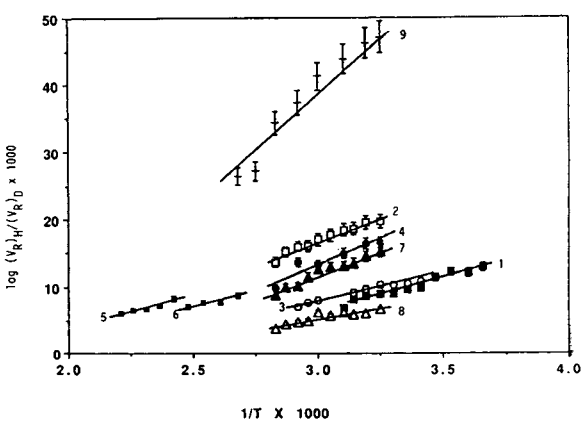

Fig. 4. Plot of the logarithms of the retention volumes *versus* $1/T$. 1 = $C_6H_5CH_3/C_6H_5CD_3$; 2 = ethylbenzene-d_0/-d_{10}; 3 = ethylbenzene-d_0/-$d_{5\text{-ring}}$; 4 = $C_6H_5CH_3/C_6H_5CD_3$; 5 = Bibenzyl-d_0/-d_7; 6 = C_8H_8/C_8D_8; 7 = ethylbenzene-d_0/-$d_{5\text{-ethyl}}$; 8 = C_6H_6/C_6D_6; 9 = octane-d_0/-d_{18}; D,d = deuterium.

variation of the separation factor with temperature [19]. The highest isotopic effect is shown by the pair octane-d_{18}/octane-d_0. The isotope effects of the pair of toluene-d_3/toluene-d_0 and toluene-d_8/toluene-d_0 are higher than that of benzene-d_6/benzene-d_0. However, the isotope effect for naphthalene-d_8/naphthalene-d_0 is about same as that of benzene-d_6/benzene-d_0. It can be concluded that the deuterium in the aliphatic part of the molecule plays a more important role in the GC separation than deuterium on the aromatic ring.

To obtain a relative measure of the impact of the aliphatic and the aromatic deuterium, the GC separations of ethylbenzene-d_{10}, ethylbenzene-$d_{5\text{-ethyl}}$, ethylbenzene-$d_{5\text{-ring}}$ and ethylbenzene-d_0 were measured (Fig. 4). The separation factor for the pair of ethylbenzene-d_0/ethylbenzene-$d_{5\text{-ethyl}}$ is much larger than that of ethylbenzene-d_0/ethylbenzene-$d_{5\text{-ring}}$. Also, the inverse isotope effect is additive. As can be seen from Fig. 5, the separation factor for the pair of ethylbenzene-d_0/ethylbenzene-d_{10} is the sum of the separation factors for the pairs of ethylbenzene-d_0/ethylbenzene-$d_{5\text{-ethyl}}$ and of ethylbenzene-d_0/ethylbenzene-$d_{5\text{-ring}}$.

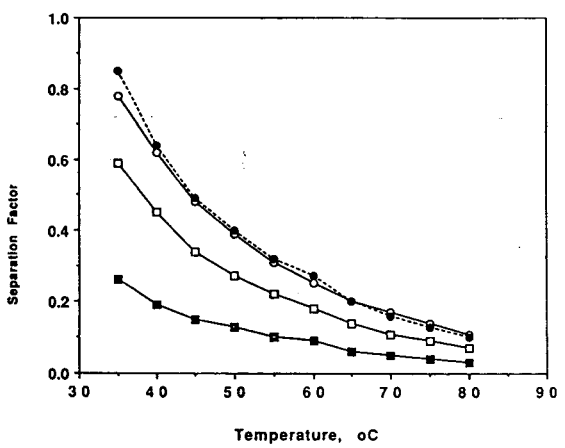

Fig. 5. Separation factors ($R_H - R_D$) for the pairs of ethylbenzene-d_0/ethylbenzene-$d_{5\text{-ring}}$ (■), ethylbenzene-d_0/ethylbenzene-$d_{5\text{-ethyl}}$ (□) and ethylbenzene-d_0/ethylbenzene-d_{10} (○). ---○ = represents the value calculated as the sum of the separation factor of ethylbenzene-d_0/ethylbenzene-$d_{5\text{-ring}}$ and ethylbenzene-d_0/ethylbenzene-$d_{5\text{-ethyl}}$. R_H and R_D refer to retention times of the compounds containing hydrogen and deuterium, respectively.

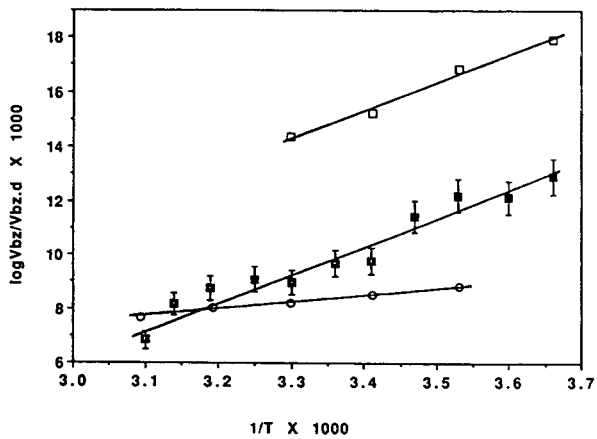

Fig. 6. Plot of the logarithms of the retention volumes *versus* $1/T$. ■ = DB-5 column; □ = squalane column; ○ = silicone oil 702. Vbz and Vbzd are retention volumes of benzene-d_0 and benzene-d_6, respectively.

The logarithm of the ratio of retention volumes for the benzene-d_6/benzene-d_0 pair are compared for squalane, silicone oil and DB-5 columns (Fig. 6). The squalane and the silicone oil data are from ref. 14. The greatest isotope effect was obtained on a squalane column; the isotope effect on DB-5 column is greater than that of the silicone oil column.

The data in Figs. 5 and 6 show that there is a reasonably linear relationship between the re-

TABLE II

DIFFERENCE IN ENTHALPY OF FOR THE PAIRS OF ISOTOPIC MOLECULES RELATED TO THE CHROMATOGRAPHIC PROCESS ON DB-5 COLUMN

1 cal = 4.14 J.

Pairs of isotopic molecules	$\Delta H_H - \Delta H_D$ (cal)
Benzene-d_6/-d_0	−45.8
Toluene-d_3-methyl/-d_0	−32.1
Toluene-d_8/-d_0	−67.6
Ethylbenzene-d_{10}/-d_0	−62.5
Ethylbenzene-d_5-ethyl/-d_0	−65.9
Ethylbenzene-d_5-ring/-d_0	−27.6
Naphthalene-d_8/-d_0	−34.9
Bibenzyl-d_7 [a]/-d_0	−42.2
Octane-d_{18}/-d_0	−175.8

[a] The structure of this compound is C_6D_5–CD_2–CH_2–C_6H_5.

tention volumes and the reciprocal of the temperature which can be expressed by eqn. 1:

$$\log (V_R)_H/(V_R)_D = -(\Delta H_H - \Delta H_D)/2.3RT + C \quad (1)$$

From the slope of each system on the graph, the enthalpy difference for the chromatographic process can be calculated; these results are given in Table II. The difference of entropy can be calculated by eqn. 2 and the difference in free energy by eqn. 3.

$$\Delta G_H - \Delta G_D = \Delta H_H - \Delta H_D - T(\Delta S_H - \Delta S_D) \quad (2)$$

$$\Delta G_H - \Delta G_D = -2.3RT \log(V_R)_H/(V_R)_D \quad (3)$$

The values of the difference in free energy and entropy are presented in Tables III and IV, respectively.

These fundamental thermodynamic data can be used to define the chromatographic process as well as the properties of compounds and the columns. The GC process should be considered

TABLE III

DIFFERENCE IN FREE ENERGY CHANGES [$-(\Delta G_H - \Delta G_D)$, cal] OBTAINED FROM RETENTION VOLUMES FOR PAIRS OF ISOTOPIC MOLECULES

Temperature (K)	Benzene[a]	Tol-CD_3[b]	Toluene-d_8[c]	EB-d_{10}[d]	EB-d_5-ethyl[e]	EB-d_5-ring[f]	Octane-d_{18}[g]	NP-d_8[h]	BB-d_7[i]
273	16.1	–	–	–	–	–	–	–	–
278	15.4	–	–	–	–	–	–	–	–
283	15.8	–	–	–	–	–	–	–	–
288	15.1	–	–	–	–	–	–	–	–
293	13.1	14.4	–	–	–	–	–	–	–
298	13.2	14.4	–	–	–	–	–	–	–
303	12.4	14.2	–	–	–	–	–	–	–
308	12.8	14.5	23.3	27.7	21.4	9.4	66.3	–	–
313	12.5	13.9	23.5	27.8	20.8	8.7	66.1	–	–
318	11.9	13.3	–	27.0	19.7	8.6	–	–	–
323	10.1	14.6	22.1	27.2	19.3	9.2	64.7	–	–
328	–	13.9	–	26.5	19.3	8.7	–	–	–
333	–	12.3	20.2	25.8	19.1	9.5	62.8	–	–
338	–	11.9	–	24.8	17.8	7.6	–	–	–
343	–	11.0	21.3	25.0	15.8	7.5	58.6	–	–
348	–	–	–	24.2	16.0	7.1	–	–	–
353	–	–	15.8	22.1	14.4	6.1	55.5	–	–
363	–	–	–	–	–	–	45.0	–	–
373	–	–	–	–	–	–	44.9	14.9	–
383	–	–	–	–	–	–	–	13.6	–
393	–	–	–	–	–	–	–	13.8	–
403	–	–	–	–	–	–	–	13.0	–
413	–	–	–	–	–	–	–	–	15.5
423	–	–	–	–	–	–	–	–	13.9
433	–	–	–	–	–	–	–	–	13.3
443	–	–	–	–	–	–	–	–	13.3
453	–	–	–	–	–	–	–	–	12.6

[a] Benzene-d_6/-d_0.
[b] Toluene-d_3-methyl/-d_0.
[c] Toluene-d_8/-d_0.
[d] Ethylbenzene-d_{10}/-d_0.
[e] Ethylbenzene-d_5-ethyl/-d_0.
[f] Ethylbenzene-d_5-ring/-d_0.
[g] Octane-d_{18}/-d_0.
[h] Naphthalene-d_8/-d_0.
[i] C_6D_5-CD_2CH_2-C_6H_5/-d_0.

TABLE IV

DIFFERENCE IN ENTROPY $[-(\Delta S_H - \Delta S_D) \times 10^2$, cal] OBTAINED FROM RETENTION VOLUMES FOR PAIRS OF ISOTOPIC MOLECULES

Temperature (K)	Benzene[a]	C_6H_5-CD_3 [b]	Toluene-d_8 [c]	EB-d_{10} [d]	EB-d_5-ethyl[e]	EB-d_5-ring[f]	Octane-d_{18} [g]	NP-d_8 [h]	BB-d_7 [i]
273	10.9	–	–	–	–	–	–	–	–
278	10.9	–	–	–	–	–	–	–	–
283	10.6	–	–	–	–	–	–	–	–
288	10.7	–	–	–	–	–	–	–	–
293	11.2	6.0	–	–	–	–	–	–	–
298	10.9	5.9	–	–	–	–	–	–	–
303	11.0	5.9	–	–	–	–	–	–	–
308	10.7	5.7	14.4	11.3	14.4	5.9	35.6	–	–
313	10.6	5.8	14.1	11.1	14.4	6.0	35.1	–	–
318	10.7	5.9	–	11.2	14.5	6.0	–	–	–
323	11.1	5.4	14.1	10.9	14.4	5.7	34.4	–	–
328	–	5.6	–	11.0	14.2	5.8	–	–	–
333	–	6.0	14.2	11.0	14.0	5.4	33.9	–	–
338	–	6.0	–	11.1	14.2	5.9	–	–	–
343	–	6.2	13.5	10.9	14.6	5.9	34.2	–	–
348	–	–	–	11.0	14.3	5.9	–	–	–
353	–	–	14.7	11.5	14.6	6.1	34.1	–	–
363	–	–	–	–	–	–	37.1	–	–
373	–	–	–	–	–	–	36.2	5.4	–
383	–	–	–	–	–	–	–	5.6	–
393	–	–	–	–	–	–	–	5.4	–
403	–	–	–	–	–	–	–	5.5	–
413	–	–	–	–	–	–	–	–	6.5
423	–	–	–	–	–	–	–	–	6.7
433	–	–	–	–	–	–	–	–	6.7
443	–	–	–	–	–	–	–	–	6.5
453	–	–	–	–	–	–	–	–	6.5

[a] Benzene-d_6/-d_0.
[b] Toluene-$d_{3\text{-methyl}}$/-d_0.
[c] Toluene-d_8/-d_0.
[d] Ethylbenzene-d_{10}/-d_0.
[e] Ethylbenzene-$d_{5\text{-ethyl}}$/-d_0.
[f] Ethylbenzene-$d_{5\text{-ring}}$/-d_0.
[g] Octane-d_{18}/-d_0.
[h] Naphthalene-d_8/-d_0.
[i] C_6D_5-CD_2CH_2-C_6H_5/-d_0.

to consist of two processes; one is due to the condensation evaporation process for each eluted component and the other is due to their mixing with the liquid partitioning material [7]. Of the two processes, the mixing process is assumed to be relatively isotope insensitive. This leaves the condensation-evaporation process as the important one [18].

CONCLUSIONS

Pairs of isotopic molecules have been completely separated and quantitatively determined by GC using a DB-5 column. An inverse isotope effect was obtained for all pairs of the isotopically labelled molecules. Very good separations were obtained at low temperatures with a short elution time. The differences of ΔG, ΔH and ΔS for a DB-5 column have been calculated. The data clearly show that deuterium on the aliphatic part of a molecule plays a more important role in determining the inverse isotope effect than those on the aromatic ring; this is shown by the fact that the vapor pressure isotope effect per D for the aromatics is less than that per D for aliphatics [10].

ACKNOWLEDGEMENT

Conversations with Professor W.A. Van Hook and his suggestions are especially appreciated.

REFERENCES

1 K. Wilzbach and R. Riesz, *Science*, 126 (1957) 748.
2 W.A. Van Hook, *Adv. Chem. Ser.*, No. 89 (1969) 99.
3 F. Bruner, G.P. Carboni and A. Liberti, *Anal. Chem.*, 38 (1966) 298.
4 F. Bruner and G.P. Cartoni, *J. Chromatogr.*, 18 (1965) 390.
5 F. Bruner, C. Canulli, A. Di Corcia and A. Liberti, *Nature Phys. Sci.*, 231 (1971) 175.
6 A. Di Corcia and A. Liberti, *Trans. Faraday Soc.*, 66 (1970) 967.
7 A. Liberti, G.P. Cartoni and F. Bruner, *J. Chromatogr.*, 12 (1963) 8.
8 W.A. Van Hook, *J. Phys. Chem.*, 71 (1967) 3270.
9 J.T. Phillips and W.A. Van Hook, *J. Phys. Chem.*, 71 (1967) 3276.
10 W.A. Van Hook and J.T. Phillips, *J. Phys. Chem.*, 70 (1966) 1515.
11 W.A. Van Hook and M.E. Kelly, *Anal. Chem.*, 37 (1965) 508.
12 W.A. Van Hook and J.T. Phillips, *J. Chromatogr.*, 30 (1967) 211.
13 M. Possanzini, A. Pela, A. Liberti and G.P. Cartoni, *J. Chromatogr.*, 38 (1968) 492.
14 A. Liberti, G.P. Cartoni and F. Bruner, *J. Chromatogr.*, 12 (1963) 8.
15 G.C. Goretti, A. Liberti and G. Nota, *J. Chromatogr.*, 34 (1968) 96.
16 M. Mohnke and J. Heybey, *J. Chromatogr.*, 417 (1989) 37.
17 G. Jancso and W.A. Van Hook, *Chem. Rev.*, 74 (1974) 689.
18 W.A. Van Hook, personal communication.
19 A. Di Corcia, D. Fritz and F. Bruner, *J. Chromatogr.*, 53 (1970) 135.

Author Index

Journal of Chromatography

Request for Manuscripts

Ralph Riggin and Gregory Davis will edit a special, thematic issue of the *Journal of Chromatography* entitled "**Analytical Biotechnology**". Both reviews and research articles will be included.

Topics such as the following will be covered:

- Sequencing
- Host Cell Protein Determination
- Peptide Mapping
- Electrophoretic Methods
- Capillary Electrophoresis/Electrokinetic Chromatography
- Protein Mass Spectrometry
- Glycoprotein Characterization
- High-Speed Separations
- Chromatographic Methods
- Residual DNA Determination
- Immunochemical Assays
- Moisture Determination

Potential authors of reviews should contact Roger Giese, Editor, prior to any submission. Address: Mugar Building Rm 122, Northeastern University, Boston, MA 02115, USA; tel.: (617) 373-3227; fax: (617) 373-8720.

The deadline for receipt of submissions is **April 30, 1994**. Manuscripts submitted after this date can still be published in the Journal, but then there is no guarantee that an accepted article will appear in this special, thematic issue. Four copies of the manuscript, citing this issue, should be submitted to the Editorial Office, Journal of Chromatography, P.O. Box 681, NL-1000 AR Amsterdam, The Netherlands. All manuscripts will be reviewed and acceptance will be based on the usual criteria for publishing in the *Journal of Chromatography*.

New Books in the Series
Journal of Chromatography Library

Volume 53

Hyphenated Techniques in Supercritical Fluid Chromatography and Extraction

edited by **K. Jinno**

This is the first book to focus on the latest developments in hyphenated techniques using supercritical fluids. The advantages of SFC in hyphenation with various detection modes, such as, FTIR, MS, MPD and ICP and others are clearly featured throughout the book. Special attention is paid to coupling of SFE with GC or SFC.

1992 x + 334 pages
Price: US $ 157.25 / Dfl. 275.00
ISBN 0-444-88794-6

Volume 52

Capillary Electrophoresis

Principles, Practice and Applications

by **S.F.Y. Li**

All aspects of CE, from the principles and technical aspects to the most important applications are covered in this volume. It is intended to meet the growing need for a thorough and balanced treatment of CE. The book will serve as a comprehensive reference work and can also be used as a textbook for advanced undergraduate and graduate courses. Both the experienced analyst and the newcomer will find the text useful.

1992 xxvi + 582 pages
Price: US $ 225.75 / Dfl. 395.00
ISBN 0-444-89433-0

"...anybody wanting to write a book on CE after this would look like a fool. Everything seems to be there, any detection system you have ever dreamed of, any capillary coating, enough electrolyte systems to saturate your wits, and more, and more.
...by far the most thorough book in the field yet to appear."
P.G. Righetti

Volume 51

Chromatography, 5th edition

Fundamentals and Applications of Chromatography and Related Differential Migration Methods

edited by **E. Heftmann**

Part A: Fundamentals and Techniques

Part A covers the theory and fundamentals of such methods as column and planar chromatography, countercurrent chromatography, field-flow fractionation, and electrophoresis. Affinity chromatography and supercritical-fluid chromatography are covered for the first time.

1992 xxxvi + 552 pages
Price: US $ 200.00 / Dfl. 350.00
ISBN 0-444-88236-7

Part B: Applications

Part B presents various applications of these methods. New developments in the analysis and separation of inorganic compounds, amino acids, peptides, proteins, lipids, carbohydrates, nucleic acids, their constituents and analogs, porphyrins, phenols, drugs and pesticides are reviewed and summarized. Important topics such as environmental analysis and the determination of synthetic polymers and fossil fuels, are covered for the first time.

1992 xxxii + 630 pages
Price: US $ 211.50 / Dfl. 370.00
ISBN 0-444-88237-5
Parts A & B
Set price: US $ 371.50 / Dfl. 650.00
ISBN 0-444-88404-1

ELSEVIER
SCIENCE PUBLISHERS

Volume 50

Liquid Chromatography in Biomedical Analysis

edited by **T. Hanai**

This book presents a guide for the analysis of biomedically important compounds using modern liquid chromatographic techniques. After a brief summary of basic liquid chromatographic methods and optimization strategies, the main part of the book focuses on the various classes of biomedically important compounds: amino acids, catecholamines, carbohydrates, fatty acids, nucleotides, porphyrins, prostaglandins and steroid hormones.

1991 xii + 296 pages
Price: US $ 154.25 / Dfl. 270.00
ISBN 0-444-87451-8

"...will be valuable for anyone involved in liquid chromatography. It is timely and highlights throughout the techniques that are most successful. This is not so much a book to put on the shelf of the specialist for reference purposes, but instead it is a book which is meant to be read by the general reader to obtain perspective and insights into this general area."
Trends in Analytical Chemistry

ORDER INFORMATION

For USA and Canada
ELSEVIER SCIENCE PUBLISHERS
Judy Weislogel
P.O. Box 945
Madison Square Station,
New York, NY 10160-0757
Tel: (212) 989 5800
Fax: (212) 633 3880

In all other countries
ELSEVIER SCIENCE PUBLISHERS
P.O. Box 211
1000 AE Amsterdam
The Netherlands
Tel: (+31-20) 5803 753
Fax: (+31-20) 5803 705

US$ prices are valid only for the USA & Canada and are subject to exchange rate fluctuations; in all other countries the Dutch guilder price (Dfl.) is definitive. Customers in the European Community should add the appropriate VAT rate applicable in their country to the price(s). Books are sent postfree if prepaid.

Organofluorine Compounds in Medicinal Chemistry and Biomedical Applications

Edited by **R. Filler, Y. Kobayashi** and **L.M. Yagupolskii**

Studies in Organic Chemistry Volume 48

An examination of the important role of fluorine in medicinal chemistry reveals that, in most cases, an organic compound needs be only lightly substituted with fluorine. Indeed, a single fluorine atom or a trifluoromethyl group, located in a key position of a bioactive molecule, can exert a profound pharmacological effect. Recently, developments in previously well-studied fields have been augmented by exciting reports in newer areas. The topics chosen by the authors are likely to be of broad interest and represent the work of established international leaders in their areas of research.

Keeping in mind the question *"what does fluorine provide that is so special?"*, the reader will find information on anticancer and antiviral agents and be brought up to date on volatile anesthetics and central nervous system agents, areas in which fluorine has played a pivotal role for almost forty years. Antibiotics receive special attention, with coverage of β-lactams and fluoroquinolone antibacterials. Newer applications of biologically-active fluorine compounds are reviewed, including cardiovascular drugs, fluoroamino acids and peptides, and the prostaglandins and leukotrienes of the arachidonic acid cascade. Biomedical applications, such as ^{18}F in positron emission tomography (PET) and fluorinated surfactants are exceptionally well covered. In the opening chapter, an overview of the field is given, including brief reports on areas not otherwise covered in the book, e.g. recent advances in antidiabetic and hypolipidemic agents.

Contents:

© 1993 394 pages Hardbound
Price: Dfl. 395.00 (US $ 225.75)
ISBN 0-444-89768-2

ELSEVIER
SCIENCE PUBLISHERS

ORDER INFORMATION

For USA and Canada
ELSEVIER SCIENCE PUBLISHERS
Judy Weislogel, P.O. Box 945
Madison Square Station
New York, NY 10160-0757
Fax: (212) 633 3880

In all other countries
ELSEVIER SCIENCE PUBLISHERS
P.O. Box 330
1000 AH Amsterdam
The Netherlands
Fax: (+31-20) 5862 845

US$ prices are valid only for the USA & Canada and are subject to exchange rate fluctuations; in all other countries the Dutch guilder price (Dfl.) is definitive. Customers in the European Community should add the appropriate VAT rate applicable in their country to the price(s). Books are sent postfree if prepaid.

PUBLICATION SCHEDULE FOR THE 1994 SUBSCRIPTION

Journal of Chromatography A and *Journal of Chromatography B: Biomedical Applications*

MONTH	O 1993	N 1993	D 1993	
Journal of Chromatography A	652/1 652/2 653/1	653/2 654/1 654/2 655/1	655/2 656/1 + 2 657/1 657/2	The publication schedule for further issues will be published later.
Bibliography Section				
Journal of Chromatography B: Biomedical Applications				

INFORMATION FOR AUTHORS

(Detailed *Instructions to Authors* were published in Vol. 609, pp. 437–443. A free reprint can be obtained by application to the publisher, Elsevier Science Publishers B.V., P.O. Box 330, 1000 AH Amsterdam, Netherlands.)

Types of Contributions. The following types of papers are published: Regular research papers (Full-length papers), Review articles, Short Communications and Discussions. Short Communications are usually descriptions of short investigations, or they can report minor technical improvements of previously published procedures; they reflect the same quality of research as Full-length papers, but should preferably not exceed five printed pages. Discussions (one or two pages) should explain, amplify, correct or otherwise comment substantively upon an article recently published in the journal. For Review articles, see inside front cover under Submission of Papers.

Submission. Every paper must be accompanied by a letter from the senior author, stating that he/she is submitting the paper for publication in the *Journal of Chromatography A* or *B*.

Manuscripts. Manuscripts should be typed in **double spacing** on consecutively numbered pages of uniform size. The manuscript should be preceded by a sheet of manuscript paper carrying the title of the paper and the name and full postal address of the person to whom the proofs are to be sent. As a rule, papers should be divided into sections, headed by a caption (*e.g.*, Abstract, Introduction, Experimental, Results, Discussion, etc.) All illustrations, photographs, tables, etc., should be on separate sheets.

Abstract. All articles should have an abstract of 50–100 words which clearly and briefly indicates what is new, different and significant. No references should be given.

Introduction. Every paper must have a concise introduction mentioning what has been done before on the topic described, and stating clearly what is new in the paper now submitted.

Experimental conditions should preferably be given on a *separate* sheet, headed "Conditions". These conditions will, if appropriate, be printed in a block, directly following the heading "Experimental".

Illustrations. The figures should be submitted in a form suitable for reproduction, drawn in Indian ink on drawing or tracing paper. Each illustration should have a legend, all the *legends* being typed (with double spacing) together on a *separate sheet*. If structures are given in the text, the original drawings should be supplied. Coloured illustrations are reproduced at the author's expense, the cost being determined by the number of pages and by the number of colours needed. The written permission of the author and publisher must be obtained for the use of any figure already published. Its source must be indicated in the legend.

References. References should be numbered in the order in which they are cited in the text, and listed in numerical sequence on a separate sheet at the end of the article. Please check a recent issue for the layout of the reference list. Abbreviations for the titles of journals should follow the system used by *Chemical Abstracts*. Articles not yet published should be given as "in press" (journal should be specified), "submitted for publication" (journal should be specified), "in preparation" or "personal communication".

Vols. 1–651 of the *Journal of Chromatography*; *Journal of Chromatography, Biomedical Applications* and *Journal of Chromatography, Symposium Volumes* should be cited as *J. Chromatogr.* From Vol. 652 on, *Journal of Chromatography A* (incl. Symposium Volumes) should be cited as *J. Chromatogr. A* and *Journal of Chromatography B: Biomedical Applications* as *J. Chromatogr. B.*

Dispatch. Before sending the manuscript to the Editor please check that the envelope contains four copies of the paper complete with references, legends and figures. One of the sets of figures must be the originals suitable for direct reproduction. Please also ensure that permission to publish has been obtained from your institute.

Proofs. One set of proofs will be sent to the author to be carefully checked for printer's errors. Corrections must be restricted to instances in which the proof is at variance with the manuscript. "Extra corrections" will be inserted at the author's expense.

Reprints. Fifty reprints will be supplied free of charge. Additional reprints can be ordered by the authors. An order form containing price quotations will be sent to the authors together with the proofs of their article.

Advertisements. The Editors of the journal accept no responsibility for the contents of the advertisements. Advertisement rates are available on request. Advertising orders and enquiries can be sent to the Advertising Manager, Elsevier Science Publishers B.V., Advertising Department, P.O. Box 211, 1000 AE Amsterdam, Netherlands; courier shipments to: Van de Sande Bakhuyzenstraat 4, 1061 AG Amsterdam, Netherlands; Tel. (+31-20) 515 3220/515 3222, Telefax (+31-20) 6833 041, Telex 16479 els vi nl. *UK*: T.G. Scott & Son Ltd., Tim Blake, Portland House, 21 Narborough Road, Cosby, Leics. LE9 5TA, UK; Tel. (+44-533) 753 333, Telefax (+44-533) 750 522. *USA and Canada*: Weston Media Associates, Daniel S. Lipner, P.O. Box 1110, Greens Farms, CT 06436-1110, USA; Tel. (+1-203) 261 2500, Telefax (+1-203) 261 0101.

Ovomucoid Bonded Column for Direct Chiral Separation

ULTRON ES-OVM

Narrow-Bore Column (2.0 I.D. x 150 mm) for Trace Analyses
Analytical Column (4.6 I.D., 6.0 I.D. x 150 mm) for Regular Analyses
Semi-Preparative Column (20.0 I.D. x 250 mm) for Preparative Separation

Analysis of Trace FLURBIPROFEN in Metabolite with NARROW-BORE COLUMN

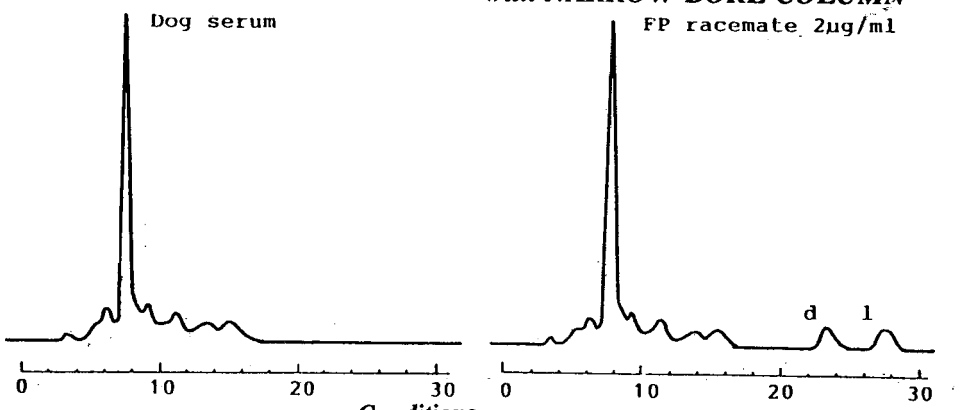

Conditions

Column: ULTRON ES-OVM(2.0I.D. x 150mm)
Mobile Phase: 20mMPhosphate Buffer(pH=3.0)/CH3CN =100/15
Flow Rate: 0.1ml/min
Temperature: 25°C
Injection: 5µl
Detection: UV- 247nm(0.05AUFS)

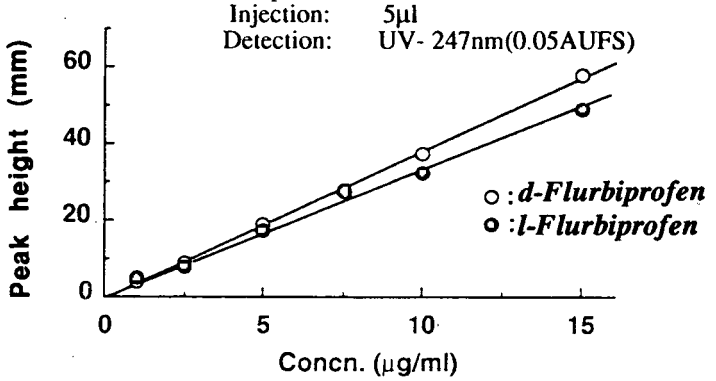

Calibration Curve for Each Enantiomer of Flurbiprofen

SHINWA CHEMICAL INDUSTRIES, LTD.

50 Kagekatsu-cho, Fushimi-ku, Kyoto 612, JAPAN
Phone:+81-75-621-2360 Fax:+81-75-602-2660

In the United States and Europe, please contact:

Rockland Technologies, Inc.

538 First State Boulevard, Newport, DE 19804, U.S.A.
Phone: 302-633-5880 Fax: 302-633-5893

This product is licenced by Eisai Co., Ltd.

14 S.H. 2536